EBM Experimental Biology and Medicine

Special Issue

Breakthroughs in Biomedical Research: Review/Minireview Issue

Issue Editor

Nicola Conran
University of Campinas, Brazil

ISBN 978-2-8325-7380-8
DOI 10.3389/978-2-8325-7380-8

frontiers | Publishing Partnerships

EBM Experimental Biology and Medicine

Breakthroughs in Biomedical Research: Review/Minireview Issue

ISSN 1535-3699
ISBN 978-2-8325-7380-8
DOI 10.3389/978-2-8325-7380-8

Table of contents

EBM Experimental Biology and Medicine

TYPE Review
PUBLISHED 19 February 2025
DOI 10.3389/ebm.2025.10444

OPEN ACCESS

*CORRESPONDENCE
Xincheng Yao,
xcy@uic.edu
Michael J. Heiferman,
mheif@uic.edu

RECEIVED 21 November 2024
ACCEPTED 04 February 2025
PUBLISHED 19 February 2025

CITATION
Dadzie AK, Iddir SP, Ganesh S, Ebrahimi B, Rahimi M, Abtahi M, Son T, Heiferman MJ and Yao X (2025) Artificial intelligence in the diagnosis of uveal melanoma: advances and applications. *Exp. Biol. Med.* 250:10444. doi: 10.3389/ebm.2025.10444

Artificial intelligence in the diagnosis of uveal melanoma: advances and applications

Albert K. Dadzie[1], Sabrina P. Iddir[2], Sanjay Ganesh[2], Behrouz Ebrahimi[1], Mojtaba Rahimi[1], Mansour Abtahi[1], Taeyoon Son[1], Michael J. Heiferman[2]* and Xincheng Yao[1,2]*

[1]Department of Biomedical Engineering, University of Illinois Chicago, Chicago, IL, United States, [2]Department of Ophthalmology and Visual Sciences, University of Illinois Chicago, Chicago, IL, United States

Abstract

Advancements in machine learning and deep learning have the potential to revolutionize the diagnosis of melanocytic choroidal tumors, including uveal melanoma, a potentially life-threatening eye cancer. Traditional machine learning methods rely heavily on manually selected image features, which can limit diagnostic accuracy and lead to variability in results. In contrast, deep learning models, particularly convolutional neural networks (CNNs), are capable of automatically analyzing medical images, identifying complex patterns, and enhancing diagnostic precision. This review evaluates recent studies that apply machine learning and deep learning approaches to classify uveal melanoma using imaging modalities such as fundus photography, optical coherence tomography (OCT), and ultrasound. The review critically examines each study's research design, methodology, and reported performance metrics, discussing strengths as well as limitations. While fundus photography is the predominant imaging modality being used in current research, integrating multiple imaging techniques, such as OCT and ultrasound, may enhance diagnostic accuracy by combining surface and structural information about the tumor. Key limitations across studies include small dataset sizes, limited external validation, and a reliance on single imaging modalities, all of which restrict model generalizability in clinical settings. Metrics such as accuracy, sensitivity, and area under the curve (AUC) indicate that deep learning models have the potential to outperform traditional methods, supporting their further development for integration into clinical workflows. Future research should aim to address current limitations by developing multimodal models that leverage larger, diverse datasets and rigorous validation, thereby paving the way for more comprehensive, reliable diagnostic tools in ocular oncology.

KEYWORDS

choroidal tumors, machine learning, deep learning, uveal melanoma, artificial intelligence, ocular oncology, convolutional neural networks

Impact statement

Machine learning and deep learning are reshaping oncology diagnostics, yet applications in uveal melanoma remain underexplored, particularly in using multimodal imaging to improve accuracy. This review highlights significant gaps in current research, such as the over-reliance on single imaging modalities and limited datasets, which restrict diagnostic precision, generalizability, and clinical utility. By identifying these limitations and proposing multimodal integration as a viable solution, this work advances the understanding of how diverse imaging data can be effectively leveraged for ocular tumor detection. This new perspective provides a foundation for developing robust, cross-validated models that could transform diagnostic practices, enabling early and reliable identification of uveal melanoma. The insights presented here set a clear direction for future research to refine and implement comprehensive, automated diagnostic tools in ocular oncology, enhancing clinical decision-making and patient outcomes.

Introduction

Melanocytic choroidal tumors encompass a spectrum of intraocular lesions that range from benign choroidal nevi to malignant melanomas. While choroidal nevi are common and typically asymptomatic, choroidal melanoma, though rare, are associated with a significant risk of metastasis and poor outcomes [1–5]. Early detection and accurate differentiation between these lesions are critical for management decisions and improving patient outcomes [6].

The diagnosis of melanocytic choroidal tumors is based on clinical examination and imaging techniques such as fundus photography, optical coherence tomography (OCT), and ultrasonography. Ophthalmologists assess features such as tumor size, thickness, and the presence of risk factors like subretinal fluid, orange pigment, and drusen to estimate the likelihood of malignancy [7, 8]. However, these diagnostic techniques are subject to inter-observer variability, and their sensitivity in detecting small melanomas, which can closely resemble benign nevi, is limited. In some cases, intraocular biopsies may be necessary to confirm the diagnosis, but these procedures carry some risks. This creates an unmet need for more objective, reproducible, and accurate diagnostic tools.

In recent years, artificial intelligence has emerged as a transformative technology in medical imaging. Machine learning, a subset of artificial intelligence, has shown great potential in automating diagnostic tasks that previously required expert interpretation. Deep learning, a further subset of machine learning, utilizes neural networks that can automatically learn and extract features from large datasets without the need for manual feature engineering. Convolutional neural networks (CNNs), in particular, have demonstrated impressive performance in image classification tasks across various medical fields, including ophthalmology [9–12].

This review aims to provide an overview of the current applications of artificial intelligence in the diagnosis of melanocytic choroidal tumors. It will discuss recent developments in artificial intelligence-based diagnostic models, the integration of multimodal imaging techniques, and the potential of these technologies to improve diagnostic accuracy and patient management. Furthermore, the review will address the limitations and challenges faced by machine learning applications in this field, as well as future directions for research and clinical translation.

Overview of melanocytic choroidal tumors

Melanocytic choroidal tumors represent a spectrum of similar appearing lesions located in the choroid, a vascular layer beneath the retina. These tumors can be broadly classified into benign choroidal nevi and malignant melanoma. The accurate differentiation between these two forms is crucial, as their management and prognosis differ dramatically.

Choroidal nevi

Choroidal nevi (Figures 1A1–3) are benign lesions that are more commonly found in the White population compared to other ethnic groups [13–15]. These nevi are typically asymptomatic and remain stable over time, often being discovered incidentally during routine eye exams [16]. However, while most nevi remain benign, a small percentage can undergo malignant transformation into melanoma [17]. The risk factors that suggest potential malignancy include greater lesion thickness, subretinal fluid, orange pigment, and the absence of overlying drusen [17–19].

Choroidal melanoma

Choroidal melanoma, the most common primary intraocular malignancy in adults, is a rare but aggressive disease with high metastatic potential (Figures 1B1–3) [20–22]. Approximately 50% of patients diagnosed with choroidal melanoma develop metastatic disease, with a high mortality rate once metastasis occurs [23, 24].

Choroidal melanomas are generally larger and thicker than nevi, and they often exhibit clinical features such as orange pigment, subretinal fluid, and low internal echogenicity. Advanced melanomas may also show a “mushroom” shape due to the tumor breaking through Bruch’s membrane [25]. Traditional diagnostic methods rely on clinical examinations,

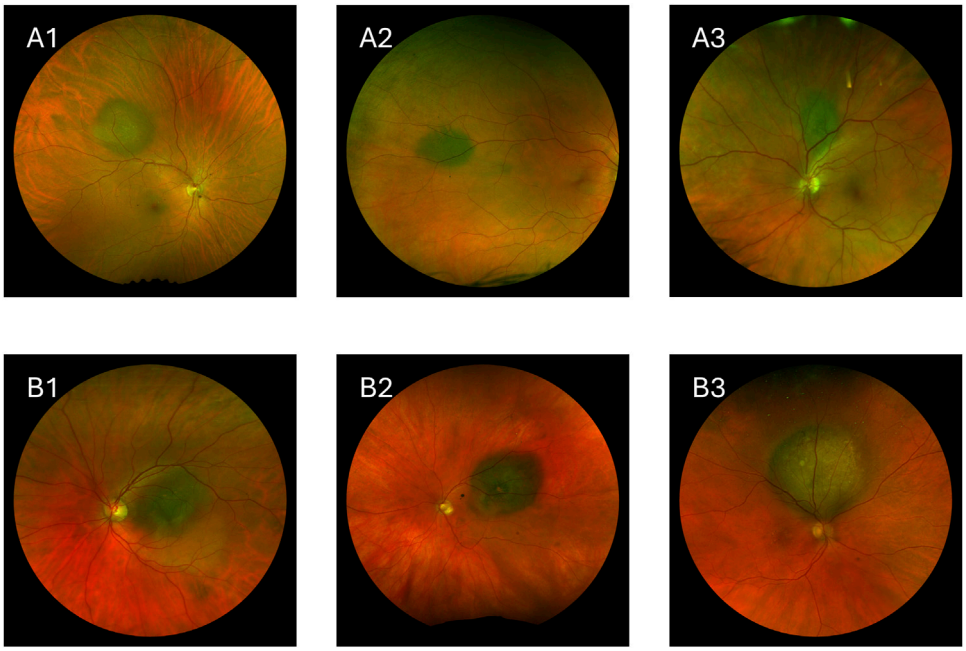

FIGURE 1
Images showing choroidal nevi and choroidal melanoma. **(A1–A3)** Choroidal nevi. **(B1–B3)** Choroidal melanoma.

imaging modalities, and tools like the MOLES algorithm [2] to identify these features, but distinguishing between benign and malignant lesions, especially in cases with overlapping features of nevi and melanoma, can be challenging [26]. However, patients referred to specialist ocular oncology centers may benefit from higher diagnostic accuracy due to the expertise and advanced diagnostic resources available. Figure 1 shows how visually similar benign and malignant lesions can be.

The need for improved diagnostic tools

One clinical challenge lies in identifying small choroidal melanomas that may closely resemble benign nevi in terms of clinical and imaging features. Misclassification can lead to either overtreatment or delayed treatment. Overtreatment exposes patients to unnecessary procedures such as radiation therapy, which carries risks of vision loss and other complications, while delayed treatment increases the risk of metastasis [27–29]. In some cases, intraocular biopsies may be necessary to confirm the diagnosis; however, these procedures carry risks such as hemorrhage, retinal detachment, and endophthalmitis [30, 31].

Given the clinical and imaging challenges, there is a critical need for more objective and precise diagnostic tools. This is where machine learning offers great promise. These advanced algorithms can process large datasets of imaging data to detect subtle features that may not be easily discernible by human experts, potentially revolutionizing the accuracy and efficiency of diagnosing melanocytic choroidal tumors.

Overview of artificial intelligence

Artificial intelligence refers to the ability of machines to mimic human intelligence, enabling them to perform tasks such as learning, problem-solving, and decision-making. Machine learning is a subset of artificial intelligence that enables computers to learn from data and make predictions or decisions without being explicitly programmed for every possible scenario. Machine learning algorithms build models based on patterns identified in training data, which can then be applied to new, unseen data for predictions. The key advantage of machine learning lies in its ability to adapt and improve over time as it processes more data, making it highly valuable for complex tasks like medical diagnosis. Over time, machine learning has evolved to include deep learning, a subfield of machine learning that leverages neural networks to model intricate relationships in data, particularly in fields like computer vision and natural language processing. Figure 2 illustrates the hierarchical relationship between artificial intelligence, machine learning, and deep learning. It highlights the key differences in processing workflows, showing that machine learning involves a manual feature extraction step, whereas deep learning integrates both feature extraction and classification within a single, automated framework.

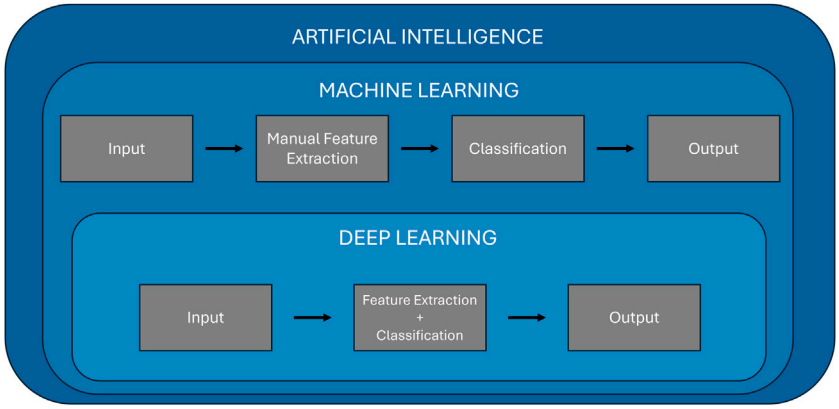

FIGURE 2
Relationship and differences between machine learning and deep learning.

Machine learning

Machine learning models can generally be classified into four primary categories: supervised learning, unsupervised learning, semi-supervised, and reinforcement learning. Supervised learning, the most common type, involves training models on labeled datasets, where each data point is associated with the correct output. Algorithms like support vector machines (SVMs), random forest, and K-nearest neighbors (KNNs) are widely used in supervised learning to perform tasks such as classification and regression. In contrast, unsupervised learning deals with unlabeled data, and the goal is to uncover hidden patterns within the data. Techniques like K-means clustering, and principal component analysis (PCA) are examples of unsupervised learning, which are useful for tasks like clustering and dimensionality reduction. Semi-supervised learning is a mix of supervised and unsupervised learning. It uses a small amount of labeled data along with a large amount of unlabeled data. This method is helpful when labeling data is difficult or expensive, like in healthcare. Finally, reinforcement learning is a method where a model learns by trial and error. It interacts with an environment, gets feedback through rewards or penalties, and uses this feedback to improve its actions over time. While these traditional machine learning approaches have shown significant success [32–35], they require manual feature extraction, as shown in Figure 2. This is where deep learning distinguishes itself.

Deep learning

Deep learning uses artificial neural networks with multiple layers to automatically extract and learn high-level features directly from raw data, such as images or signals, without requiring human intervention in the feature selection process (Figure 2). This makes deep learning particularly well-suited for tasks involving image recognition, speech processing, and natural language understanding. In the medical field, deep learning has revolutionized diagnostic applications by providing outstanding accuracy in analyzing medical images, such as MRI scans [36, 37], X-rays [38, 39], and retinal images [9, 40].

Deep learning networks, such as CNNs and recurrent neural networks (RNNs), have specific strengths tailored to different types of data. CNNs, for instance, are optimized for image data, employing layers that can automatically detect features such as edges, textures, and shapes in medical images. CNNs are extensively used in tasks like identifying tumors in medical scans [41–43] or detecting retinal abnormalities in ophthalmology [44–46]. On the other hand, RNNs excel at processing sequential data, making them useful for time-series data, such as monitoring disease progression or analyzing electrocardiogram (ECG) signals [47, 48].

Transfer Learning is an essential technique in deep learning that allows models to leverage knowledge gained from one task and apply it to a different but related task. This is particularly useful in medical imaging because large, labeled datasets are often difficult to obtain. A model pre-trained on a large dataset, such as ImageNet [49], learns general image features like edges and shapes. This pre-trained model can then be adapted to a new task, such as detecting tumors in retinal images, by fine-tuning its layers with a smaller dataset specific to the medical application. Transfer learning greatly reduces the amount of labeled data and training time needed while improving model performance in fields like ophthalmology, where data scarcity is a common challenge.

Evaluation metrics

To assess the performance of both machine learning and deep learning models, several evaluation metrics are commonly

used in medical diagnostics. These metrics include accuracy, sensitivity, specificity, F-1 score, and area under the curve (AUC). Explanations of these metrics are given below.

Accuracy: Accuracy measures the proportion of correctly predicted instances (both positive and negative) out of the total instances. It provides an overall measure of how often the model is correct.

$$Accuracy = \frac{TP + TN}{TP + TN + FP + FN}$$

Where TP = True Positives, TN = True Negatives, FP = False Positives, FN = False Negatives.

Sensitivity (Recall or True Positive Rate): Sensitivity measures the model's ability to correctly identify positive cases (correctly diagnosing a condition when it is present). It indicates how well the model captures actual positives in the dataset.

$$Sensitivity = \frac{TP}{TP + FN}$$

Specificity (True Negative Rate): Specificity measures the model's ability to correctly identify negative cases (correctly identifying when a condition is not present). Specificity focuses on correctly classifying the negatives and avoiding false positives.

$$Specificity = \frac{TN}{TN + FP}$$

Precision: Precision, also known as Positive Predictive Value, measures the proportion of true positive predictions out of all positive predictions made by the model. It's important when the cost of false positives is high.

$$Precision = \frac{TP}{TP + FP}$$

F-1 Score: The F-1 score is the harmonic mean of precision and sensitivity. It balances both false positives and false negatives and is particularly useful for imbalanced datasets.

$$F - 1\,Score = 2 \times \frac{Precision \times Sensitivity}{Precision + Sensitivity}$$

AUC: AUC is derived from the receiver operating characteristic (ROC) curve, which plots sensitivity against 1 - specificity. AUC gives an aggregate measure of model performance across all classification thresholds. A higher AUC indicates a better-performing model, with an AUC of 1.0 representing perfect classification.

Applications of artificial intelligence in choroidal tumor diagnosis

Machine learning and deep learning have recently been studied in the diagnosis of melanocytic choroidal tumors, particularly in differentiating between choroidal nevi and melanomas. These techniques have been applied to clinical datasets [50], pathologic specimens [51], and various imaging modalities, including fundus photography [52–56], OCT [50], and ultrasound imaging [57, 58], to enhance the accuracy and efficiency of diagnosing these tumors. Below, we discuss the use of both machine learning and deep learning models in the context of choroidal tumor diagnosis using ophthalmic imaging.

Machine learning

Machine learning models have been applied to manually extracted features from a variety of imaging modalities for the diagnosis of melanocytic choroidal tumors. Machine learning models typically rely on the manual extraction of key features, such as tumor thickness, subretinal fluid, orange pigment, the presence of drusen, ultrasonographic hollowness, and morphology of the tumor. These features are recognized as important risk factors for the potential malignant transformation of choroidal nevi into melanoma [18].

For example, Zabor et al. utilized logistic regression models to predict the malignancy of choroidal nevi based on features manually extracted from fundus photographs, OCT, and ultrasound [50]. Their model, which was developed using 123 patients and externally validated on a separate cohort of 240 patients, achieved an AUC of 0.861 in predicting small choroidal melanomas. From their study, their model identified tumor thickness, subretinal fluid, and orange pigmentation as significant risk factors associated with increased odds of malignancy. While these findings align with prior research emphasizing the importance of these features in distinguishing benign nevi from malignant melanomas [17, 19, 59], the performance of machine learning models is inherently limited by the quality and selection of features. The inclusion of external validation in this study is a notable strength, ensuring that the model can generalize to different clinical settings. Additionally, the authors created an online prediction tool to facilitate the real-world application of their machine learning model in clinical practice.

In another study, Jegelevicius et al. employed a decision tree model using features extracted from ultrasound imaging for the differential diagnosis of intraocular tumors [58]. Their results indicated that features such as tumor thickness, base width, and tumor shape were considered important for tumor classification. The decision tree model achieved a diagnostic error rate of 6.7%, demonstrating its potential as a decision-support tool for clinicians. However, as with other machine learning approaches, the reliance on manually extracted features and the inherent limitation of focusing only on predefined criteria restricts its scalability and generalizability.

One of the primary limitations of traditional machine learning in this context is its dependence on human-driven

feature extraction. While features like tumor size or subretinal fluid are easily identifiable and quantifiable, these models struggle to detect more complex patterns that may be key to differentiating between benign and malignant lesions. As a result, machine learning models can be less effective for tumor diagnosis compared to deep learning models, which can automatically learn and extract intricate hierarchical features from raw imaging data.

Deep learning

Deep learning has made substantial progress in diagnosing choroidal tumors, primarily through the use of CNNs. The power of CNNs lies in their ability to automatically learn features from raw images without the need for manual feature extraction, making them ideal for analyzing medical images, particularly in diagnosing ocular conditions such as uveal melanoma.

Shakeri et al. demonstrated the efficacy of CNNs in the detection of uveal melanoma using fundus images [60]. They employed pre-trained models like DenseNet121, DenseNet169, Inception-V3, and Xception, using transfer learning to fine-tune the models on the fundus images. Their best-performing model, DenseNet169, achieved an accuracy of 89%.

Similarly, Ganguly et al. achieved similar results using a custom CNN model trained on fundus images. Their model achieved an accuracy of 92%, an F1-score of 0.93, and a precision of 0.97 [54]. However, the relatively small dataset of 170 images used in the study presents concerns about overfitting, where the model may perform well on training data but struggle to generalize to new, unseen data.

Additionally, Hoffmann et al. utilized ResNet50 to distinguish choroidal melanoma from choroidal nevi using fundus images [55]. They reported an accuracy of 90.9% and F1 score of 0.91, and an AUC of 0.99, showcasing the high potential of deep learning models in automating tumor differentiation tasks. Furthermore, they showed that deep learning models can be used to estimate the likelihood of malignancy in melanocytic choroidal tumors.

In another study, Dadzie et al. focused on enhancing deep learning performance through color fusion strategies [56]. By employing the DenseNet121 architecture on ultra-widefield retinal images, they examined how combining color channels (red, green, and blue) affect tumor classification accuracy. Their results showed that the intermediate fusion provided the best classification accuracy, outperforming early and late fusion strategies with an accuracy of 92.2%, an F1 score of 0.88, and an AUC of 0.98. This study highlighted the importance of leveraging different color channels in fundus images to maximize the potential of deep learning models in tumor classification. The integration of multiple color channels enables these models to exploit more detailed color and texture information, further refining their classification capabilities. While color fusion is a novel approach, the study did not address the computational cost of using different fusion strategies which is an important consideration for clinical deployment.

In a recent study by Sabazade et al, they tackled a critical challenge in deep learning for choroidal melanoma diagnosis by ensuring model generalizability through a multicenter approach [52]. They used a custom U-Net architecture that achieved an average F1- score of 0.77 and an average AUC of 0.89 for the test dataset. On external validation dataset, the model achieved an F1-score of 0.71 and an AUC of 0.88. Notably, accuracy was not reported in this study. By incorporating datasets from various centers and imaging devices, they reduced the risk of bias often seen in single-center studies and improved the model's robustness. The inclusion of external validation was a crucial step toward real-world applicability, as it demonstrated the model's ability to generalize beyond the original training dataset. However, despite addressing generalizability, the study relied on relatively smaller datasets, which can still pose a risk of overfitting.

Addressing the issue of small datasets, another recent study by Jackson et. al employed over 25,000 ultra-widefield retinal images for deep learning classification of choroidal melanoma and nevus [53]. Using a transfer learning approach, they employed the RETFound, a foundation self-supervised deep learning model [61]. Their model achieved an accuracy of 83%, an F1 score of 0.84, and an AUC of 0.90. While the study demonstrates a promising solution to data scarcity, the lack of external validation limits its immediate clinical applicability, as model performance across different populations and imaging devices remains uncertain.

The studies reported above collectively demonstrate the powerful role that deep learning models play in the detection and classification of choroidal melanoma using fundus images. However, several limitations remain across the studies, such as the use of small datasets, the lack of external validation, and the reliance on a single imaging modality. However, recent studies have made progress in addressing these issues [52, 53], but further research is needed to explore the integration of multimodal imaging, which could offer a more comprehensive diagnostic approach. Table 1 offers a detailed comparison of the methodologies and results across these studies, providing a clear overview of how different architectures and approaches enhance tumor differentiation. The models presented in Table 1 represent the best-performing models reported in each study.

While fundus photography has been extensively used in deep learning applications for classifying melanocytic choroidal tumors, other imaging modalities, such as OCT and ultrasound, have not been widely employed for this purpose. This gap presents an opportunity for future research to explore the application of deep learning to these imaging modalities, which could enhance early detection and diagnosis of uveal

TABLE 1 Comparison between studies that used deep learning for the classification of Choroidal Nevus and Melanoma.

Study	Model used	Imaging modality	Number of Images			Performance metrics					
			Control	Melanoma	Nevus	Accuracy	Sensitivity	Specificity	Precision	F1-Score	AUC
Ganguly et al. [54]	Custom model	Standard images	NA	110	60	0.92	0.90	0.95	0.97	0.93	NA
Hoffman et al. [55]	ResNet50	UWF and standard images	NA	422	340	0.91	0.90	0.91	0.91	0.91	0.99
Dadzie et al. [56]	DenseNet121	UWF images	360	157	281	0.92	0.81	0.98	0.96	0.88	0.95
Sabazade et al. [52]	Custom model	UWF and standard images	NA	219	583	NA	1.00	0.74	NA	0.77	0.89
Jackson et al. [53]	RETFound	UWF images	1,192	18,510	8,671	0.83	0.79	0.87	0.89	0.84	0.90

UWF, Ultra-widefield; NA, not available.

melanoma by integrating structural information from OCT and ultrasound with surface-level data from fundus photography.

Challenges and limitations

The application of artificial intelligence in diagnosing choroidal melanoma has shown considerable promise, demonstrating the potential for enhanced diagnostic accuracy and efficiency. However, translating these advancements from research settings into routine clinical practice is accompanied by significant challenges and limitations. As machine learning and deep learning models evolve, understanding and addressing the obstacles that limit their clinical integration becomes critical, particularly for supporting downstream diagnosis and aiding non-specialists. These challenges encompass a range of issues, from the quality and availability of data to the interpretability of model outputs and the adaptability of machine learning systems within clinical workflows.

Effective implementation of artificial intelligence tools in healthcare requires not only technological advancements but also a nuanced understanding of clinical requirements and patient variability. Machine learning and deep learning models must be rigorously validated, reliable across diverse patient populations and imaging techniques, and transparent in their decision-making processes. Given the known differences in the incidence of choroidal nevi and choroidal melanoma across racial and ethnic groups, datasets used to train these models are often disproportionately composed of images from populations with higher disease prevalence, primarily White individuals. This imbalance can introduce bias, potentially limiting the model's applicability to underrepresented populations. Addressing these aspects is essential to achieving widespread clinical adoption and ensuring that artificial intelligence technologies fulfill their potential to improve patient outcomes. The following sections outline key challenges and limitations, providing insights into areas that require further research and refinement to support the successful deployment of machine learning in ocular oncology. Table 2 summarizes the main challenges and limitations in applying machine learning to uveal melanoma diagnosis, along with potential solutions to address each issue.

Data availability and quality

One of the most significant challenges in developing effective machine learning and deep learning models for the diagnosis of melanocytic choroidal tumors is the availability and quality of data. Uveal melanoma is a rare condition, making it difficult to acquire large, diverse datasets that are essential for training robust machine learning models. The rarity of the condition results in relatively small datasets, which can lead to overfitting in models. This issue is especially problematic in deep learning, where large-scale datasets are crucial for capturing complex patterns in medical images and achieving high performance. A recent study by Jackson et al. has begun addressing this issue by utilizing large datasets with over 25,000 images [53].

Another issue related to data limitations is the lack of diversity in the available datasets. Often times, datasets are collected from a single institution or geographic region, limiting the model's exposure to different patient demographics, imaging conditions, and equipment variations. A model trained on data from a specific population may not perform well when applied to a different demographic, leading to bias in predictions and unequal outcomes across patient populations. Potential solutions to these limitations include

TABLE 2 Challenges and potential solutions for integrating machine learning in uveal melanoma diagnosis.

Challenge	Description	Implication	Potential solutions
Data Availability	Uveal melanoma is rare, making it difficult to acquire large datasets for training robust models	Limited dataset size restricts model accuracy, leads to overfitting, and reduces model generalizability	Data-sharing collaborations; multimodal image training to optimize models using available data; synthetic data generation
Dataset Diversity	Many datasets are from single institutions or regions, limiting diversity in patient demographics and imaging conditions	Models trained on specific populations may not perform well across different demographics, leading to bias in predictions	Multicenter collaborations; access to data from clinical trials; external validation to ensure generalizability
Ground Truth Labeling	While standardized systems like MOLES and histopathological analysis exist, their adoption varies globally, posing challenges for consistent ground truth labeling	Lack of standardization in labeling can affect model accuracy and interpretability. Model design may not align with the intended clinical use	Broader adoption of standardized systems and expert consensus on defining ground truths can improve consistency in labeling across studies. Additionally, intraocular biopsy results, when available, can provide more definitive labels
Model Interpretability	Deep learning models often have opaque decision-making processes, making it difficult to understand exactly which features drive predictions. While techniques like CAMs, including Grad-CAM highlight regions used by the model, they do not reveal the specific features influencing the decision	Lack of transparency limits clinician trust and makes clinical integration difficult	Techniques such as CAMs and SHAP provide visual and feature-level explanations. Further improvement of these methods can enhance model transparency, build clinician trust, and support clinical integration
Clinical Integration	Machine learning tools often function as stand-alone systems, lacking integration with EHRs and imaging platforms	Increase workload for healthcare providers, as they may need to navigate multiple platforms to incorporate machine learning insights with traditional methods	Development of interoperable systems that integrate directly with EHRs and imaging systems for seamless workflow
Ethical Considerations	Use of machine learning algorithms for life-altering decisions like diagnosis and treatment raises ethical concerns	High-stakes medical decisions by machine learning must meet rigorous standards, as errors can seriously impact patient health	Rigorous validation of machine learning outputs with clinical ground truths and use as a decision support tool rather than for sole decision-making

GAN, generative adversarial network; CAM, class activation mapping; Grad-CAM, Gradient-weighted Class Activation Mapping; SHAP, Shapely Additive exPlanations; EHR, electronic health records.

data-sharing collaborations between institutions and leveraging images being collected for the increasing number of prospective multi-center clinical trials being conducted for uveal melanoma. Another promising avenue for addressing the issue of data scarcity is the use of synthetic data. Generative adversarial networks (GANs) and diffusion models have emerged as tools for generating synthetic medical images that mimic real-world data [62–65]. These synthetic datasets can be used to augment existing data, allowing deep learning models to train on larger and more diverse datasets. However, synthetic data may raise concerns about trust, as models trained on artificially generated images could be perceived as less reliable for real-world clinical applications. Therefore, proper validation on real-world data is essential to build clinician and patient confidence in these models.

Ground truth labeling and standardization

Another challenge regarding the dataset involves ground truth labeling. There are no universally accepted criteria for the definition of choroidal nevi and melanoma, which is why some cases are called indeterminate until the tumor is observed to be stable in size, grow during the observation period, or occasionally biopsied. Most often, the diagnosis of choroidal melanoma is clinical, but more careful definitions should be chosen for the indeterminate cases. Choroidal nevi versus melanomas can be defined by its clinical appearance, its pathological appearance (when tissue is available), or its metastatic potential and disease-specific mortality when long-term follow-up is available. The labels for ground truths in machine learning and deep learning studies should be chosen carefully to reflect the dataset available for that study. Alternative labels may include the tumor size, clinical characteristics, genetic profile, tumor growth rate over time, or the management decision chosen by the clinician. The type of machine learning project and clinical goal of the study should determine the ground truth labels being chosen, and care should be taken to prevent conclusions about an artificial intelligence model that exceeds the scope of the available data. Potential solutions to this challenge include expert committees to standardize the definitions and labels being used for machine learning studies in ocular oncology. Additionally, the MOLES scoring system, which is widely used in clinical practice for risk stratification of choroidal nevi, could serve as a standardized framework for developing ground truth labels in artificial intelligence studies. Labels agnostic of management decisions, such as calling the same lesion indeterminate when it would be observed versus a

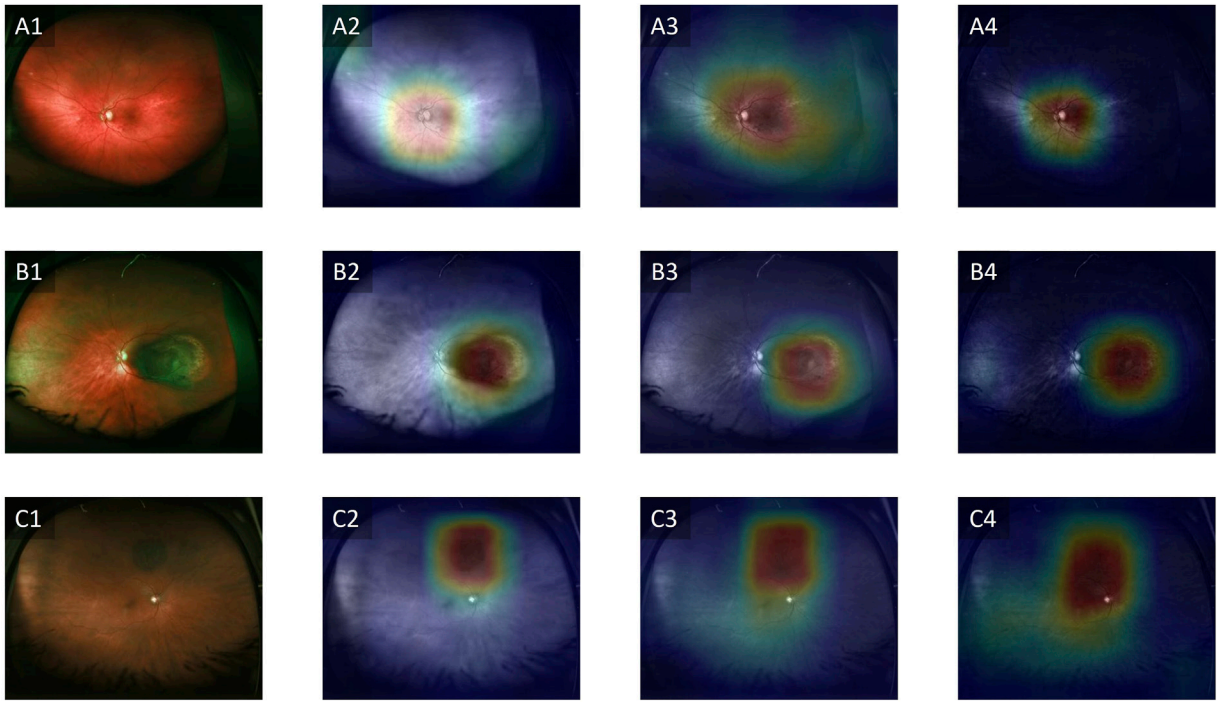

FIGURE 3
Grad-CAM showing regions relevant for classification. **(A1–A4)** Control, **(B1–B4)** Choroidal melanoma, **(C1–C4)** Choroidal nevus. Column 1 represents the original images, column 2 represents the red channels, column 3 represents the green channels and column 4 represents the blue channels. Adapted from [67].

small melanoma when it would be treated, can also improve the generalizability of the study when opinions on management differ.

Model interpretability

Another significant challenge in the adoption of machine learning and deep learning models in the diagnosis of melanocytic choroidal tumors is the lack of interpretability. While deep learning models have shown exceptional performance in classifying uveal melanoma and other ocular conditions, their decision-making process remains largely opaque. This is often referred to as the black box nature of deep learning. This lack of transparency often makes these models difficult to trust and integrate into clinical practice, as clinicians typically need to understand the reasoning behind a model's prediction to confidently use it for patient care.

To address the black-box issue in deep learning, researchers have developed several techniques to enhance the interpretability of these models in medical imaging. These methods provide insights into how the model makes predictions and identifies which parts of the image are most influential in the decision-making process. A commonly used method is Gradient-weighted Class Activation Mapping (Grad-CAM), which generates heatmaps overlaid on the original image to show which regions contributed the most to the model's classification [66]. Grad-CAM works by leveraging the gradients of a target class flowing into the final convolutional layer of a neural network, which produces a localization map highlighting the important regions in the image [66]. Clinicians can cross-reference the model's focus areas with their own knowledge of disease markers, ensuring that the model is not relying on irrelevant features. Another advantage of improved interpretability is the potential for clinicians to learn new insights into image evaluation. Experts can potentially learn new clinical or imaging features from machine learning models, to improve our understanding of how best to interpret imaging to diagnose melanocytic tumors. Figure 3 illustrates an example of Grad-CAM heatmap overlaid on different color channels of ultra-widefield retinal images to show regions considered most relevant for classification of choroidal nevus and melanoma. Figure 4 also shows the areas in ultrasound images that are considered crucial for deep learning models to make a classification decision.

Integration into clinical workflow

Another key challenge in the adoption of deep learning and machine learning models for the diagnosis of melanocytic

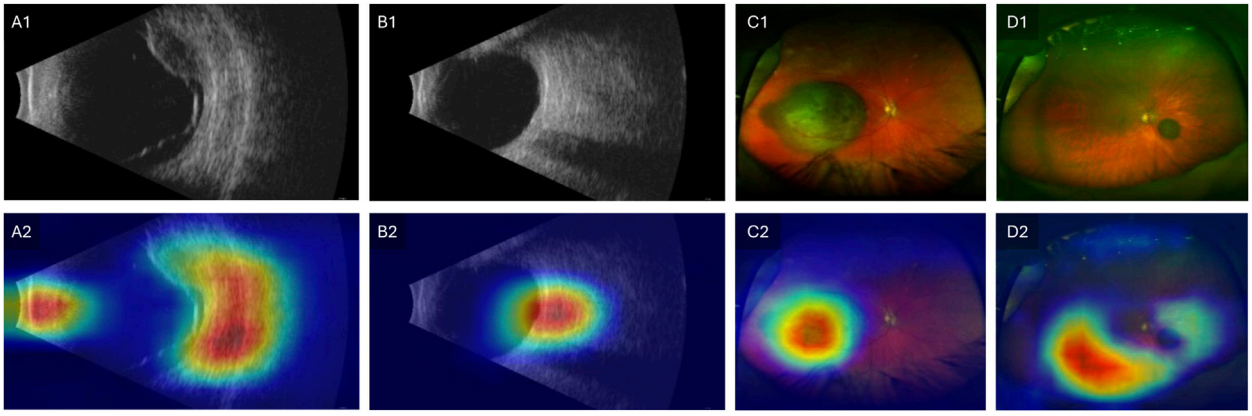

FIGURE 4
Grad-CAM showing regions relevant for classification. Row 1 shows original images and Row 2 shows the Grad-CAM heatmaps overlaid on the original images. **(A1–A2)** Ultrasound image of choroidal melanoma. **(B1–B2)** Ultrasound image of choroidal nevus. **(C1–C2)** Ultra-widefield retinal image of choroidal melanoma. **(D1–D2)** Ultra-widefield retinal image of choroidal nevus. Modified with permission from [57].

choroidal is their integration into existing clinical workflows. While these models have demonstrated impressive accuracy in research settings, translating them into real-world clinical practice remains difficult. Many machine learning tools function as stand-alone systems that do not seamlessly integrate with existing electronic health records (EHRs) or imaging systems, causing potential disruptions in established processes. This lack of interoperability can increase the workload for healthcare providers, who may need to navigate between multiple platforms to interpret machine learning results alongside traditional diagnostic methods. However, tools like the online calculator developed by Zabor et al. demonstrate how these models could be applied in practice [50]. Although the current version requires manual input, future versions could be integrated directly into clinical workflows, automatically extracting data from existing databases and providing instant results.

Ethical considerations

Another challenge in the clinical application of artificial intelligence in the diagnosis of uveal melanoma is the degree to which physicians will rely on machine learning algorithms. In cases of indeterminate choroidal tumors, diagnosis using histopathologic examination has been reported to be upwards of 90% accuracy [68, 69]. This level of accuracy will likely be surpassed by machine learning algorithms using multimodal data, depending on the quality of labels and choice of ground truth for the diagnosis of uveal melanoma. However, the ethical implications of using a computer algorithm to make vision and life-threatening decisions raise the standard for the required accuracy and quality of validation for this clinical use. In the near term, machine learning and deep learning algorithms may be used as clinical tools, such as for screening and triaging by optometrists and comprehensive ophthalmologists, or aid in management decisions along with clinical data, imaging, genetics, and biopsy results when deemed necessary. These tools are likely to be more beneficial in non-specialist community centers, where diagnostic accuracy may be lower, rather than in specialist ocular oncology centers, where experienced clinicians already achieve high diagnostic accuracy. The latter use as a tool for ocular oncologists will become more useful as long-term follow-up data is available to validate algorithm outputs prospectively with clinically meaningful ground truths, including tumor growth rate, histopathologic findings, metastatic risk, and disease-specific mortality.

Discussion

The application of artificial intelligence to diagnose melanocytic choroidal tumors represents a promising advancement in ocular oncology. Machine learning methods rely on manual examination of imaging features, which introduces variability and often limits diagnostic accuracy. Deep learning models, especially CNNs, address some of these limitations by automating feature extraction and analysis, improving diagnostic reliability and potentially enhancing patient outcomes.

Studies have predominantly utilized fundus photography as the primary imaging modality for developing and validating machine learning models. Pre-trained CNN architectures and

custom-built CNNs have already achieved accuracy metrics surpassing 90%, demonstrating the effectiveness of these models in capturing key image features. Despite these promising findings, models trained exclusively on fundus photography have inherent limitations. Fundus images provide a surface-level view, which may not capture critical information such as tumor depth and structural details. In contrast, OCT and ultrasound are capable of capturing deeper, three-dimensional characteristics of tumors, offering a more comprehensive understanding of tumor morphology.

By combining these different modalities, deep learning models can access a richer and more diverse set of features, enabling more accurate diagnosis and improving the ability to detect subtle signs of malignancy. Multimodal imaging has shown considerable success in ophthalmology, particularly in the diagnosis and management of conditions like diabetic retinopathy [70, 71], age-related macular degeneration (AMD) [72, 73], and glaucoma [74, 75]. However, despite the demonstrated success of multimodal imaging in diagnosing retinal diseases, its application to choroidal tumors has been limited. The use of multi-modal imaging for choroidal tumors has the potential to significantly enhance diagnostic accuracy by merging surface-level information from fundus photography with cross-sectional structural details provided by OCT and internal characteristics captured through ultrasound. Each modality offers unique advantages: fundus photography captures surface features like lesion color and margins, OCT provides detailed tumor thickness and subretinal fluid information, and ultrasound allows for the assessment of thicker tumor depth and internal echogenicity.

Such multimodal approaches hold wide-ranging clinical applications, including screening, referral triaging, risk assessment, detailed tumor characterization for clinical trials, surveillance, planning of radiation therapy, and monitoring for local recurrence after treatment. Multimodal imaging thus represents a promising frontier for research and innovation in ocular oncology, supporting the continued refinement of machine learning and deep learning tools in diagnosing and managing uveal melanoma.

Moreover, issues related to data availability and quality remain a major hurdle. Uveal melanoma is a rare condition, and the lack of large, diverse datasets increases the risk of model overfitting and reduces generalizability. Recent efforts to mitigate these issues include multicenter collaborations and external validation, which have demonstrated improved model robustness across different populations and imaging conditions [52]. Another significant challenge lies in clinical integration. While machine learning and deep learning models have achieved impressive results in research environments, real-world deployment requires seamless integration with electronic health records and imaging systems. This integration is crucial for reducing the workload on clinicians and ensuring that artificial-intelligence-generated insights can be readily incorporated into routine clinical workflows. Tools such as online prediction calculators have shown promise in this regard, but further work is needed to automate data input and output processes [50].

Conclusion

Artificial intelligence has the potential to improve the diagnostic approach to melanocytic choroidal tumors, offering significant improvements in accuracy and efficiency. However, challenges related to data availability, ground truth labeling, model interpretability, and clinical integration must be addressed to fully realize the potential of these tools in everyday clinical practice. Future directions such as the use of collaborative networks of institutions, multimodal imaging integration, and improved interpretability methods are key to overcoming current limitations. As these technologies continue to evolve, they are expected to play an increasingly important role in uveal melanoma diagnosis and treatment, leading to earlier detection, more accurate diagnoses, and ultimately better patient outcomes. Possible clinical applications encompass screening, referral triage, diagnosis, risk assessment, tumor localization and morphological analysis for clinical trials, active surveillance, radiation planning, and monitoring for post-treatment recurrence. Several critical areas require further exploration and development to fully realize the potential of these technologies. With continued refinement and targeted solutions to current limitations, machine learning and deep learning diagnostic tools could become integral to ophthalmic practice, empowering clinicians to make more accurate and informed decisions.

Author contributions

AD, MH, and XY contributed to the conceptualization, drafting and revision of the manuscript. AD, SI, SG, BE, MR, MA, TS, MH, and XY contributed to reviewing and editing. MH and XY contributed to the supervision. All authors contributed to the article and approved the submitted version.

Funding

The author(s) declare financial support was received for the research, authorship, and/or publication of this article. This work was supported by the National Eye Institute (R01 EY023522, R01 EY029673, R01 EY030101, R01 EY030842, P30EY001792, and K12 EY021475), Research to Prevent Blindness, Richard and Loan Hill Endowment, and Melanoma Research Foundation.

Conflict of interest

The author(s) declared no potential conflicts of interest with respect to the research, authorship, and/or publication of this article.

Generative AI statement

The author(s) declare that no Generative AI was used in the creation of this manuscript.

References

1. Chien JL, Sioufi K, Surakiatchanukul T, Shields JA, Shields CL. Choroidal nevus: a review of prevalence, features, genetics, risks, and outcomes. *Curr Opin Ophthalmol* (2017) **28**(3):228–37. doi:10.1097/icu.0000000000000361

2. Al Harby L, Sagoo MS, O'Day R, Hay G, Arora AK, Keane PA, et al. Distinguishing choroidal nevi from melanomas using the MOLES algorithm: evaluation in an ocular nevus clinic. *Ocul Oncol Pathol* (2021) **7**(4):294–302. doi:10.1159/000511363

3. Soliman N, Mamdouh D, Elkordi A. Choroidal melanoma: a mini review. *Medicines (Basel)* (2023) **10**(1):11. doi:10.3390/medicines10010011

4. Rossi E, Croce M, Reggiani F, Schinzari G, Ambrosio M, Gangemi R, et al. Uveal melanoma metastasis. *Cancers (Basel)* (2021) **13**(22):5684. doi:10.3390/cancers13225684

5. Rantala ES, Hernberg MM, Piperno-Neumann S, Grossniklaus HE, Kivelä TT. Metastatic uveal melanoma: the final frontier. *Prog Retin Eye Res* (2022) **90**:101041. doi:10.1016/j.preteyeres.2022.101041

6. Damato EM, Damato BE. Detection and time to treatment of uveal melanoma in the United Kingdom: an evaluation of 2384 patients. *Ophthalmology* (2012) **119**(8):1582–9. doi:10.1016/j.ophtha.2012.01.048

7. Kaliki S, Shields CL. Uveal melanoma: relatively rare but deadly cancer. *Eye (Lond)* (2017) **31**(2):241–57. doi:10.1038/eye.2016.275

8. Qureshi MB, Lentz PC, Xu TT, White LJ, Olsen TW, Pulido JS, et al. Choroidal nevus features associated with subspecialty referral. *Ophthalmol Retina* (2023) **7**(12):1097–108. doi:10.1016/j.oret.2023.07.022

9. Ebrahimi B, Le D, Abtahi M, Dadzie AK, Lim JI, Chan RVP, et al. Optimizing the OCTA layer fusion option for deep learning classification of diabetic retinopathy. *Biomed Opt Express* (2023) **14**(9):4713–24. doi:10.1364/boe.495999

10. Le D, Alam M, Yao CK, Lim JI, Hsieh YT, Chan RVP, et al. Transfer learning for automated OCTA detection of diabetic retinopathy. *Translational Vis Sci and Technology* (2020) **9**(2):35. doi:10.1167/tvst.9.2.35

11. Alam M, Le D, Lim JI, Chan RV, Yao X. Supervised machine learning based multi-task artificial intelligence classification of retinopathies. *J Clin Med* (2019) **8**(6):872. doi:10.3390/jcm8060872

12. Alam M, Thapa D, Lim JI, Cao D, Yao X. Computer-aided classification of sickle cell retinopathy using quantitative features in optical coherence tomography angiography. *Biomed Opt Express* (2017) **8**(9):4206–16. doi:10.1364/boe.8.004206

13. Sumich P, Mitchell P, Wang JJ. Choroidal nevi in a white population: the blue mountains eye study. *Arch Ophthalmol* (1998) **116**(5):645–50. doi:10.1001/archopht.116.5.645

14. Ng CH, Wang JJ, Mitchell P, Amirul Islam FM, Wong T. Prevalence and characteristics of choroidal nevi in an Asian vs white population. *Arch Ophthalmol* (2009) **127**(3):314–9. doi:10.1001/archophthalmol.2008.625

15. Greenstein MB, Myers CE, Meuer SM, Klein BE, Cotch MF, Wong TY, et al. Prevalence and characteristics of choroidal nevi: the multi-ethnic study of atherosclerosis. *Ophthalmology* (2011) **118**(12):2468–73. doi:10.1016/j.ophtha.2011.05.007

16. Shields CL, Furuta M, Mashayekhi A, Berman EL, Zahler JD, Hoberman DM, et al. Visual acuity in 3422 consecutive eyes with choroidal nevus. *Arch Ophthalmol* (2007) **125**(11):1501–7. doi:10.1001/archopht.125.11.1501

17. Shields CL, Dalvin LA, Ancona-Lezama D, Yu MD, Di Nicola M, Williams BK, et al. Choroidal nevus imaging features in 3,806 cases and risk factors for transformation into melanoma in 2,355 cases: the 2020 taylor R. Smith and victor T. Curtin lecture. *Retina* (2019) **39**(10):1840–51. doi:10.1097/iae.0000000000002440

18. Dalvin LA, Shields CL, Ancona-Lezama DA, Yu MD, Di Nicola M, Williams Jr BK, et al. Combination of multimodal imaging features predictive of choroidal nevus transformation into melanoma. *Br J Ophthalmol* (2019) **103**(10):1441–7. doi:10.1136/bjophthalmol-2018-312967

19. Shields CL, Furuta M, Berman EL, Zahler JD, Hoberman DM, Dinh DH, et al. Choroidal nevus transformation into melanoma: analysis of 2514 consecutive cases. *Arch Ophthalmol* (2009) **127**(8):981–7. doi:10.1001/archophthalmol.2009.151

20. Margo CE. The collaborative ocular melanoma study: an overview. *Cancer Control* (2004) **11**(5):304–9. doi:10.1177/107327480401100504

21. Singh AD, Turell ME, Topham AK. Uveal melanoma: trends in incidence, treatment, and survival. *Ophthalmology* (2011) **118**(9):1881–5. doi:10.1016/j.ophtha.2011.01.040

22. Agarwala SS, Eggermont AMM, O'Day S, Zager JS. Metastatic melanoma to the liver: a contemporary and comprehensive review of surgical, systemic, and regional therapeutic options. *Cancer* (2014) **120**(6):781–9. doi:10.1002/cncr.28480

23. Damato B. Ocular treatment of choroidal melanoma in relation to the prevention of metastatic death–a personal view. *Prog Retin Eye Res* (2018) **66**:187–99. doi:10.1016/j.preteyeres.2018.03.004

24. Damato B, Eleuteri A, Taktak AF, Coupland SE. Estimating prognosis for survival after treatment of choroidal melanoma. *Prog Retin Eye Res* (2011) **30**(5):285–95. doi:10.1016/j.preteyeres.2011.05.003

25. Roelofs KA, O'Day R, Al Harby L, Arora AK, Cohen VM, Sagoo MS, et al. The MOLES system for planning management of melanocytic choroidal tumors: is it safe? *Cancers* (2020) **12**(5):1311. doi:10.3390/cancers12051311

26. Khan J, Damato BE. Accuracy of choroidal melanoma diagnosis by general ophthalmologists: a prospective study. *Eye (Lond)* (2007) **21**(5):595–7. doi:10.1038/sj.eye.6702276

27. Zemba M, Dumitrescu OM, Gheorghe AG, Radu M, Ionescu MA, Vatafu A, et al. Ocular complications of radiotherapy in uveal melanoma. *Cancers (Basel)* (2023) **15**(2):333. doi:10.3390/cancers15020333

28. Banou L, Tsani Z, Arvanitogiannis K, Pavlaki M, Dastiridou A, Androudi S. Radiotherapy in uveal melanoma: a review of ocular complications. *Curr Oncol* (2023) **30**(7):6374–96. doi:10.3390/curroncol30070470

29. Stålhammar G. Delays between uveal melanoma diagnosis and treatment increase the risk of metastatic death. *Ophthalmology* (2024) **131**(9):1094–104. doi:10.1016/j.ophtha.2023.11.021

30. Singh AD, Medina CA, Singh N, Aronow ME, Biscotti CV, Triozzi PL. Fine-needle aspiration biopsy of uveal melanoma: outcomes and complications. *Br J Ophthalmol* (2016) **100**(4):456–62. doi:10.1136/bjophthalmol-2015-306921

31. Frizziero L, Midena E, Trainiti S, Londei D, Bonaldi L, Bini S, et al. Uveal melanoma biopsy: a review. *Cancers (Basel)* (2019) **11**(8):1075. doi:10.3390/cancers11081075

32. Kim SJ, Cho KJ, Oh S. Development of machine learning models for diagnosis of glaucoma. *PLoS One* (2017) **12**(5):e0177726. doi:10.1371/journal.pone.0177726

33. Miron M, Culea-Florescu A, Moldovanu S. Diabetic retinopathy image classification using machine learning and local binary patterns features. In: *2023 8th international symposium on electrical and electronics engineering (ISEEE)*. IEEE (2023).

34. Pragathi P, Nagaraja Rao A. An effective integrated machine learning approach for detecting diabetic retinopathy. *Open Computer Sci* (2022) **12**(1):83–91. doi:10.1515/comp-2020-0222

35. Hardas M, Mathur S, Bhaskar A, Kalla M. Retinal fundus image classification for diabetic retinopathy using SVM predictions. *Phys Eng Sci Med* (2022) **45**(3):781–91. doi:10.1007/s13246-022-01143-1

36. Liu S, Zheng H, Feng Y, Li W. Prostate cancer diagnosis using deep learning with 3D multiparametric MRI. In: *Medical imaging 2017: computer-aided diagnosis* (2017). SPIE.

37. Zhang N, Yang G, Gao Z, Xu C, Zhang Y, Shi R, et al. Deep learning for diagnosis of chronic myocardial infarction on nonenhanced cardiac cine MRI. *Radiology* (2019) **291**(3):606–17. doi:10.1148/radiol.2019182304

38. Khan AI, Shah JL, Bhat MM. CoroNet: a deep neural network for detection and diagnosis of COVID-19 from chest x-ray images. *Computer Methods Programs Biomed* (2020) **196**:105581. doi:10.1016/j.cmpb.2020.105581

39. Ayan E, Ünver HM. Diagnosis of pneumonia from chest X-ray images using deep learning. In: *2019 Scientific meeting on electrical-electronics and biomedical engineering and computer science (EBBT)*. Istanbul, Turkey: Ieee (2019).

40. Kim KM, Heo TY, Kim A, Kim J, Han KJ, Yun J, et al. Development of a fundus image-based deep learning diagnostic tool for various retinal diseases. *J Personalized Med* (2021) **11**(5):321. doi:10.3390/jpm11050321

41. Dipu NM, Shohan SA, Salam K. Deep learning based brain tumor detection and classification. In: *2021 International conference on intelligent technologies (CONIT)*. IEEE (2021).

42. Vankdothu R, Hameed MA, Fatima H. A brain tumor identification and classification using deep learning based on CNN-lstm method. *Comput Electr Eng* (2022) **101**:107960. doi:10.1016/j.compeleceng.2022.107960

43. Quon JL, Bala W, Chen L, Wright J, Kim L, Han M, et al. Deep learning for pediatric posterior fossa tumor detection and classification: a multi-institutional study. *AJNR Am J Neuroradiol* (2020) **41**(9):1718–25. doi:10.3174/ajnr.a6704

44. Schwartz R, Khalid H, Liakopoulos S, Ouyang Y, de Vente C, González-Gonzalo C, et al. A deep learning framework for the detection and quantification of reticular pseudodrusen and drusen on optical coherence tomography. *Translational Vis Sci and Technology* (2022) **11**(12):3. doi:10.1167/tvst.11.12.3

45. Li Z, Guo C, Nie D, Lin D, Cui T, Zhu Y, et al. Automated detection of retinal exudates and drusen in ultra-widefield fundus images based on deep learning. *Eye (Lond)* (2022) **36**(8):1681–6. doi:10.1038/s41433-021-01715-7

46. Pham QTM, Ahn S, Song SJ, Shin J. Automatic drusen segmentation for age-related macular degeneration in fundus images using deep learning. *Electronics* (2020) **9**(10):1617. doi:10.3390/electronics9101617

47. Lynn HM, Pan SB, Kim P. A deep bidirectional GRU network model for biometric electrocardiogram classification based on recurrent neural networks. *IEEE Access* (2019) **7**:145395–405. doi:10.1109/access.2019.2939947

48. Schwab P, Scebba G, Zhang J, Delai M, Karlen W. Beat by beat: classifying cardiac arrhythmias with recurrent neural networks. In: *2017 computing in cardiology (CinC)*. IEEE (2017).

49. Deng J, Dong W, Socher R, Li L, Li K, Fei-Fei L. Imagenet: a large-scale hierarchical image database. In: *2009 IEEE conference on computer vision and pattern recognition*. Miami, FL: Ieee (2009).

50. Zabor EC, Raval V, Luo S, Pelayes DE, Singh AD. A prediction model to discriminate small choroidal melanoma from choroidal nevus. *Ocul Oncol Pathol* (2022) **8**(1):71–8. doi:10.1159/000521541

51. Wan Q, Ren X, Wei R, Yue S, Wang L, Yin H, et al. Deep learning classification of uveal melanoma based on histopathological images and identification of a novel indicator for prognosis of patients. *Biol Proced Online* (2023) **25**(1):15. doi:10.1186/s12575-023-00207-0

52. Sabazade S, Lumia Michalski MA, Bartoszek J, Fili M, Holmström M, Stålhammar G. Development and validation of a deep learning algorithm for differentiation of choroidal nevi from small melanoma in fundus photographs. *Ophthalmol Sci* (2025) **5**(1):100613. doi:10.1016/j.xops.2024.100613

53. Jackson M, Kalirai H, Hussain RN, Heimann H, Zheng Y, Coupland SE. Differentiating choroidal melanomas and nevi using a self-supervised deep learning model applied to clinical fundoscopy images. *Ophthalmol Sci* (2025) **5**(2):100647. doi:10.1016/j.xops.2024.100647

54. Ganguly B, Biswas S, Ghosh S, Maiti S, Bodhak S. A deep learning framework for eye melanoma detection employing convolutional neural network. In: *2019 international conference on computer, electrical and communication engineering (ICCECE)*. IEEE (2019).

55. Hoffmann L, Runkel CB, Künzel S, Kabiri P, Rübsam A, Bonaventura T, et al. Using deep learning to distinguish highly malignant uveal melanoma from benign choroidal nevi. *J Clin Med* (2024) **13**(14):4141. doi:10.3390/jcm13144141

56. Dadzie AK, Iddir SP, Abtahi M, Ebrahimi B, Le D, Ganesh S, et al. Colour fusion effect on deep learning classification of uveal melanoma. *Eye* (2024) **38**: 2781–7. doi:10.1038/s41433-024-03148-4

57. Iddir SP, Love J, Ma JS, Bryan JM, Ganesh S, Heiferman MJ, et al. Predicting malignant transformation of choroidal nevi using machine learning. *Res Sq* (2023). doi:10.21203/rs.3.rs-3778562/v1

58. Jegelevičius D, Lukoševičius A, Paunksnis A, Barzdžiukas V. Application of data mining technique for diagnosis of posterior uveal melanoma. *Informatica* (2002) **13**(4):455–64. doi:10.3233/INF-2002-13406

59. Chin K, Finger PT. Autofluorescence characteristics of suspicious choroidal nevi. *Optom - J Am Optometric Assoc* (2009) **80**(3):126–30. doi:10.1016/j.optm.2008.07.018

60. Shakeri E, Mohammed E, Crump T, Weis E, Shields CL, Ferenczy SR. Deep learning-based detection and classification of uveal melanoma using convolutional neural networks and SHAP analysis. In: *2023 IEEE 24th international conference on information reuse and integration for data science (IRI)*. IEEE (2023).

61. Zhou Y, Chia MA, Wagner SK, Ayhan MS, Williamson DJ, Struyven RR, et al. A foundation model for generalizable disease detection from retinal images. *Nature* (2023) **622**(7981):156–63. doi:10.1038/s41586-023-06555-x

62. Salini Y, HariKiran J. Deepfakes on retinal images using GAN. *Int J Adv Computer Sci Appl* (2022) **13**(8). doi:10.14569/ijacsa.2022.0130880

63. Andreini P, Ciano G, Bonechi S, Graziani C, Lachi V, Mecocci A, et al. A two-stage GAN for high-resolution retinal image generation and segmentation. *Electronics* (2021) **11**(1):60. doi:10.3390/electronics11010060

64. Biswas S, Rohdin J, Drahanský M. Synthetic retinal images from unconditional GANs. In: *2019 41st annual international conference of the IEEE engineering in medicine and biology society (EMBC)*. IEEE (2019).

65. Bellemo V, Burlina P, Yong L, Wong TY, Wei Ting DS. Generative adversarial networks (GANs) for retinal fundus image synthesis. In: *Computer vision–ACCV 2018 workshops: 14th asian conference on computer vision, perth, Australia, december 2–6, 2018, revised selected papers 14*. Springer (2019).

66. Selvaraju RR, Cogswell M, Das A, Vedantam R, Parikh P, Batra D. Grad-cam: visual explanations from deep networks via gradient-based localization. In: *Proceedings of the IEEE international conference on computer vision* (2017).

67. Yao X, Dadzie A, Iddir S, Abtahi M, Ebrahimi B, Le D, et al. Color fusion effect on deep learning classification of uveal melanoma. *Res Square* (2023). doi:10.21203/rs.3.rs-3399214/v1

68. Bechrakis NE, Foerster MH, Bornfeld N. Biopsy in indeterminate intraocular tumors. *Ophthalmology* (2002) **109**(2):235–42. doi:10.1016/s0161-6420(01)00931-9

69. Kvanta A, Seregard S, Kopp ED, All-Ericsson C, Landau I, Berglin L. Choroidal biopsies for intraocular tumors of indeterminate origin. *Am J Ophthalmol* (2005) **140**(6):1002–6. doi:10.1016/j.ajo.2005.06.025

70. Hua C-H, Kim K, Huynh-The T, You JI, Yu SY, Le-Tien T, et al. Convolutional network with twofold feature augmentation for diabetic retinopathy recognition from multi-modal images. *IEEE J Biomed Health Inform* (2021) **25**(7):2686–97. doi:10.1109/jbhi.2020.3041848

71. Li X, Zhou Y, Wang J, Lin H, Zhao J, Ding D, et al. Multi-modal multi-instance learning for retinal disease recognition. In: *Proceedings of the 29th ACM international conference on multimedia* (2021).

72. Wang W, Li X, Xu Z, Yu W, Zhao J, Ding D, et al. Learning two-stream CNN for multi-modal age-related macular degeneration categorization. *IEEE J Biomed Health Inform* (2022) **26**(8):4111–22. doi:10.1109/jbhi.2022.3171523

73. Chen M, Jin K, Yan Y, Liu X, Huang X, Gao Z, et al. Automated diagnosis of age-related macular degeneration using multi-modal vertical plane feature fusion via deep learning. *Med Phys* (2022) **49**(4):2324–33. doi:10.1002/mp.15541

74. Wu J, Fang H, Li F, Fu H, Lin F, Li J, et al. GAMMA challenge: glaucoma grAding from Multi-Modality imAges. *Med Image Anal* (2023) **90**:102938. doi:10.1016/j.media.2023.102938

75. Zhou Y, Yang G, Zhou Y, Ding D, Zhao J. Representation, alignment, fusion: a generic transformer-based framework for multi-modal glaucoma recognition. In: *International conference on medical image computing and computer-assisted intervention*. Springer (2023).

EBM Experimental Biology and Medicine

TYPE Review
PUBLISHED 27 May 2025
DOI 10.3389/ebm.2025.10555

OPEN ACCESS

*CORRESPONDENCE
Huixiao Hong,
huixiao.hong@fda.hhs.gov

RECEIVED 28 February 2025
ACCEPTED 09 May 2025
PUBLISHED 27 May 2025

CITATION
Dong F, Guo W, Liu J, Patterson TA and Hong H (2025) Pharmacovigilance in the digital age: gaining insight from social media data.
Exp. Biol. Med. 250:10555.
doi: 10.3389/ebm.2025.10555

Pharmacovigilance in the digital age: gaining insight from social media data

Fan Dong, Wenjing Guo, Jie Liu, Tucker A. Patterson and Huixiao Hong*

National Center for Toxicological Research, U.S. Food and Drug Administration, Jefferson, AR, United States

Abstract

Pharmacovigilance is essential for protecting patient health by monitoring and managing medication-related risks. Traditional methods like spontaneous reporting systems and clinical trials are valuable for identifying adverse drug events, but face delays in data access. Social media platforms, with their real-time data, offer a novel avenue for pharmacovigilance by providing a wealth of user-generated content on medication usage, adverse drug events, and public sentiment. However, the unstructured nature of social media content presents challenges in data analysis, including variability and potential biases. Advanced techniques like natural language processing and machine learning are increasingly being employed to extract meaningful information from social media data, aiding in early adverse drug event detection and real-time medication safety monitoring. Ensuring data reliability and addressing ethical considerations are crucial in this context. This review examines the existing literature on the use of social media data for drug safety analysis, highlighting the platforms involved, methodologies applied, and research questions explored. It also discusses the challenges, limitations, and future directions of this emerging field, emphasizing the need for ethical principles, transparency, and interdisciplinary collaboration to maximize the potential of social media in enhancing pharmacovigilance efforts.

KEYWORDS

drug safety, artificial intelligence, machine learning, natural language processing, social media, post-market surveillance

Impact statement

Pharmacovigilance explores the transformative potential of social media in enhancing drug safety monitoring. Traditional methods, while foundational, are limited by delayed data collection and analysis, creating gaps in timely adverse drug event detection. This review advances the field by examining the latest methodologies, including natural language processing and machine learning that enable the extraction of meaningful information from unstructured social media data. These advanced techniques provide

tools to overcome challenges such as data variability and bias, making social media a viable complement to established pharmacovigilance practices. The insight from this review impacts the field by demonstrating how social media can fill critical gaps in real-time adverse drug event detection and provide a broader understanding of public sentiment and patient experiences. By emphasizing the need for interdisciplinary collaboration, ethical principles, and transparency, this review lays the foundation for a more agile, inclusive, and effective pharmacovigilance system, ultimately enhancing public health outcomes.

Introduction

Pharmacovigilance is an essential component of healthcare, focused on safeguarding patients by vigilantly monitoring and managing the risks associated with medications. Traditional pharmacovigilance methods, such as spontaneous reporting systems and clinical trial data analysis, have played pivotal roles in detecting and preventing adverse drug events. However, these methods have limitations, including delayed access to critical information due to the lag between data collection and availability. This lag impedes the timely monitoring of medication safety, thereby posing challenges to real-time surveillance.

The advent of social media has introduced a new paradigm in pharmacovigilance, providing a platform for individuals to share their experiences and opinions about medications. Platforms like X (former name Twitter) and Facebook serve as repositories of user-generated content, which offer discernment into medication usage patterns, adverse drug events, and public sentiment surrounding pharmaceuticals. Such a reservoir of data can complement traditional data sources by providing near real-time information on medication safety concerns.

Despite its potential, relying solely on social media data for pharmacovigilance has challenges. A significant issue arises from the unstructured nature of social media content, which can introduce variability and noise into the data, thereby complicating the identification of drug safety signals. Furthermore, social media users may not represent the entire population, leading to potential biases in demographic representation and geographic coverage.

To overcome these challenges, advanced analytical techniques such as natural language processing and machine learning are being employed to analyze social media data more effectively. These methods enable the identification of patterns and trends, thereby assisting in the early detection of potential safety concerns and facilitating real-time monitoring of medication safety. It is crucial to ensure the reliability of social media data by validating findings with conventional data sources and maintaining strict privacy and ethical standards in data usage.

The use of social media data in pharmacovigilance represents a promising strategy for enhancing medication safety monitoring. By addressing the accompanying challenges and employing rigorous methodologies, social media data can serve as a valuable complement to conventional surveillance data. In the future, prioritizing ethical principles, promoting transparency, and fostering interdisciplinary collaboration will prove indispensable in fully harnessing the potential of social media data in safeguarding public health.

Social media platforms have emerged as significant sources of real-time data, where users freely share their experiences and opinions on various topics, including healthcare and medication usage. These platforms enable the collection of patient-reported outcomes, capture discussions on medication usage and safety, and identify the dissemination of misinformation related to drugs and vaccines. Leveraging the capabilities of these platforms empowers researchers and healthcare professionals to delve into the experiences, attitudes, and concerns of the public. This wealth of user-generated content provides a unique perspective on drug safety and efficacy, offering insight that complements traditional pharmacovigilance methods and enhancing our understanding of medication impact in real-world settings.

The use of these platforms addresses a multitude of research questions, spanning from understanding the reasons behind medication changes to evaluating public sentiments towards pharmacovigilance endeavors, and even combating the spread of health-related misinformation. This review examines the current literature on the use of social media data for drug safety analysis, with a focus on the platforms utilized, the key information extracted, the research questions addressed, and the methodologies applied. Additionally, the review discusses the challenges, limitations, and future directions of utilizing social media data for drug safety analysis.

Figure 1 provides an overview of the process for analyzing social media data to support pharmacovigilance. The process starts with data collection from various sources, including general social media platforms (e.g., X, Facebook, Instagram, Reddit, and YouTube), health-specific forums (such as WebMD and other medical forums), Q&A sites (such as Quora and Ask a Patient), and other online content (like Amazon reviews, blogs, news sites, and surveys). The information extracted from these sources is categorized primarily into Patient Experience and Perceptions and Adverse Drug Events. The extracted data undergoes further analysis in four areas:

1. Machine Learning methods for Adverse Drug Event Detection: This involves identifying and categorizing adverse drug events through methods such as supervised, semi-supervised, and unsupervised learning.
2. Public Sentiment and Patient Feedback Analysis: Techniques like quantitative analysis and sentiment analysis are applied to understand public opinion and patient feedback on drug safety.
3. Drug Abuse Monitoring: Quantitative analysis and advanced language models (large language model-based methods) are employed to monitor drug abuse trends based on user discussions.

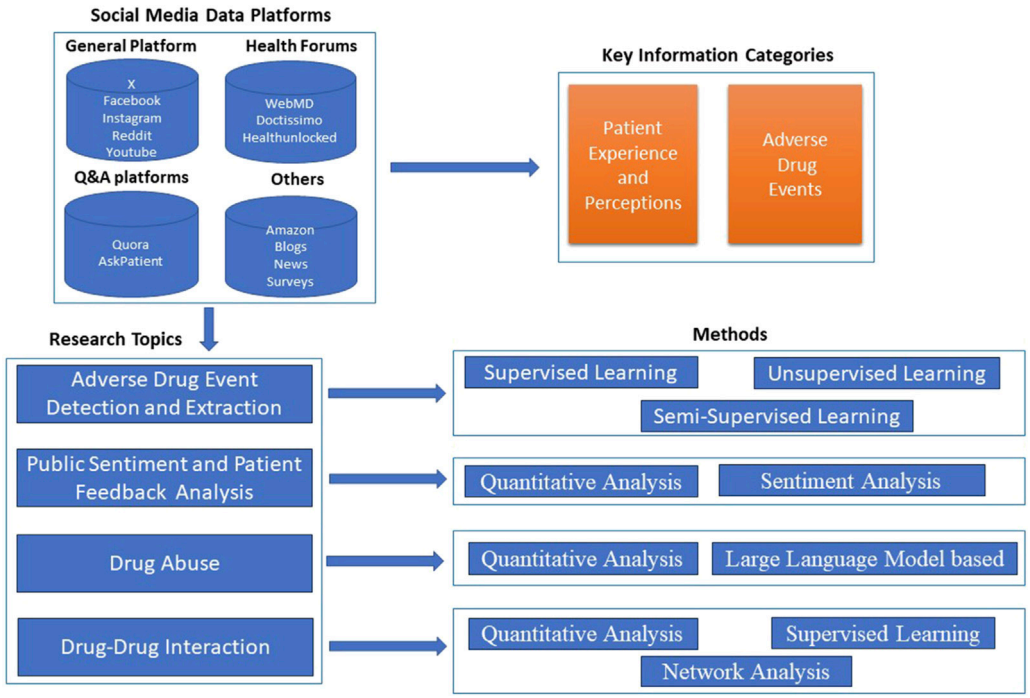

FIGURE 1
Overview of drug safety analysis with social media data.

4. Drug-Drug Interaction Monitoring: Network analysis and supervised learning are used to identify and assess potential interactions between different drugs.

Through these stages the process integrates various machine learning and analysis techniques to draw meaningful information that can enhance pharmacovigilance practices by capturing real-world patient experiences, monitoring safety signals, and improving our understanding of drug-related issues.

Social media platforms utilized for pharmacovigilance

Social media platforms provide diverse online environments for sharing user-generated content which contains data useful for drug safety research. General platforms like X,[1] Facebook,[2] Instagram,[3] Reddit,[4] and YouTube[5] offer broad audience engagement, while health-specific forums such as WebMD[6] as well as Q&A platforms such as Quora[7] and Ask a Patient[8] focus on medical discussions. Additionally, other platforms such as the e-commerce site Amazon[9] and various blogs have user reviews and discussions on drug products, enriching the data pool for drug safety analysis. Collectively, these social media platforms offer data that can facilitate a comprehensive understanding of patient experiences, medication effects, and healthcare trends.

Social media platforms differ in data scale, user demographics, content modality, and real-time accessibility—factors that shape their utilization in pharmacovigilance. X features high-frequency, short-text updates in real time, making it well-suited for detecting emerging safety signals, particularly among its predominantly young U.S. users. Facebook provides large-scale, globally diverse user demographics and facilitates lifestyle sharing, intergenerational interaction, and marketplace activity. Instagram contains visually rich content—photos and videos—primarily around themes like fashion, beauty, and

1 https://x.com/
2 https://www.facebook.com/
3 https://www.instagram.com/
4 https://www.reddit.com/
5 https://www.youtube.com/
6 https://www.webmd.com/
7 https://www.quora.com/
8 https://askapatient.com
9 https://www.amazon.com/

TABLE 1 Data platform Review.

Category	Platform	Start year	Publication
General social media Platform	X	2006	[1–38]
	Facebook	2004	[1, 4, 19, 24–26, 28, 29, 38–47]
	Instagram	2010	[1, 4, 41, 48]
	Reddit	2005	[4, 16, 17, 41, 49–55]
	YouTube	2005	[1, 4, 41, 47, 56]
Online Health Forums	WebMD online health forum	1998	[40, 57, 58]
	Health forum in French (https://www.doctissimo.fr/)	N/A	[59]
	Health forum (Healthunlocked.com)	2010	[60]
Q&A platforms	Quora	2009	[61]
	Ask a Patient	2000	[62, 63]
Others	Amazon	1995	[64, 65]
	Blogs and News	N/A	[1, 24, 29, 43, 66–68]
	Online Surveys	N/A	[69–76]

travel, attracting a younger audience but offering limited textual data. Reddit hosts in-depth, community-driven discussions on topics such as technology and health through anonymous forums, though it lacks real-time immediacy. YouTube delivers both long- and short-form video content across educational and entertainment topics to a global, multi-generational audience, but pharmacovigilance efforts on the platform require resource-intensive video analysis. Health forums focus on structured, medically-oriented discussions within smaller, specialized communities. E-commerce platforms like Amazon provide valuable insight into over-the-counter medication safety through consumer reviews. Meanwhile, blogs and online surveys, though useful for exploring historical public opinion, are declining in relevance compared to more dynamic and interactive social media channels. These variations highlight the importance of tailoring pharmacovigilance strategies to each platform—leveraging the strengths of real-time surveillance on X or visual content on Instagram, while accounting for constraints in scalability, content richness, or demographic coverage.

Social media has evolved significantly since its early days in the 1970s, when online communication was limited to basic chat rooms and forums. In the 2000s, platforms such as Facebook, X (formerly Twitter), and Instagram emerged, enabling users to share experiences in real time. Over time, social media content has expanded from text-based posts to multimedia formats, including images, videos, and live interactions. Access for researchers has also changed—while many platforms initially offered open APIs for data analysis, recent restrictions have limited the availability of user-generated content, posing new challenges for social media-based research. Researchers are employing adaptive strategies such as web scraping, synthetic data generation, and collaborative research agreements with platforms to obtain unrestricted access to social media data for pharmacovigilance research, thereby mitigating the challenges posed by recent API limitations. Table 1 summarizes popular social media platforms and drug safety studies based on data extracted from these platforms.

X has emerged as a pivotal resource in pharmacovigilance, providing insight into public perceptions and experiences regarding medications. Researchers have effectively leveraged this platform to extract valuable information, including adverse drug events, user sentiments, and discussions on drug safety and efficacy. Through the application of analytical methods such as natural language processing, machine learning, and sentiment analysis, they have managed the challenges posed by extensive data volumes and noise in the user-generated content, thereby enhancing drug safety monitoring and public health strategies. For instance, Sule et al. [1] utilized X to combat the dissemination of COVID-19 misinformation from physicians, thereby contributing to the improvement of public health communications. Pathak and Catalan-Matamoros [2] explored X's potential as an early warning system for drug safety signals, with the aim of strengthening pharmacovigilance practices. Hua et al. [8] investigated public perceptions of COVID-19-related medications using X, offering valuable insight for pharmacovigilance and policy-making decisions. Sharma et al. [11] conducted a scoping review utilizing sentiment analysis to comprehend patient experiences with pharmacotherapy. Rezaei et al. [12] applied deep learning techniques to detect adverse drug

events on X, thereby enhancing the efficiency of safety concern identification. Lardon et al. [23] evaluated X as a supplementary data source for pharmacovigilance and compared it with traditional monitoring systems. Khademi et al. [32] developed a model by coupling topic modeling and transformer-based learning for the early detection of vaccine safety signals in X posts, and the detected adverse events were generally aligned with those reported in a spontaneous vaccine safety surveillance system, showcasing the potential of social media data for early detection of emerging vaccine safety issues. These examples underscore the versatility and value of X posts in complementing traditional pharmacovigilance methods, particularly during public health crises like the COVID-19 pandemic, and in understanding off-label medication use.

Facebook offers important user-generated data for pharmacovigilance, covering discussions, comments, and posts on medications, adverse drug reactions, and drug safety feelings. This data helps improve post-marketing drug safety surveillance. For example, Pierce et al. [26] explored the possibility of detecting drug adverse events in Facebook and X earlier than their reports in the FDA Adverse Event Reporting System (FAERS), demonstrating that social media platforms such as Facebook and X can be used for early detection of certain adverse events. Powell et al. [28] investigated the usefulness of Facebook in post-marketing drug safety surveillance by examining its effectiveness in capturing patient experiences and concerns on medications, indicating that Facebook provides data for the detection of early warning signs of potential drug safety. Coloma et al. [29] used Facebook in their evaluation of social media networks' contributions to drug safety surveillance, demonstrating the usefulness of the patient-reported information in pharmacovigilance. These studies collectively highlight the significant role of Facebook in pharmacovigilance, supporting better regulatory decisions and patient care.

Instagram, a popular social media platform owned by Facebook, Meta, allows users to share photos, videos, and engage with others through likes, comments, and direct messaging. For instance, Li et al. [48] focused on developing a machine learning approach for identifying and profiling illicit drug dealers on Instagram by analyzing posts and comments for hashtags and language patterns associated with illegal drug dealings. Through an examination of posts and comments, this study identified key information like hashtags and language patterns indicative of illegal drug activities. This research addresses concerns about drug sales on social media and suggests a mechanism that may help counteract such occurrences.

Reddit's diverse communities offer a wealth of user-generated health data, making it a valuable platform for pharmacovigilance and public health research. For instance, Godinez et al. [51] analyzed Reddit discussions to gain an understanding of the experiences and concerns of individuals transitioning between HIV pre-exposure prophylaxis medications, thereby informing healthcare policies. Guo et al. [50] utilized the Reddit platform for real-time tracking and analysis of COVID-19 symptoms, facilitating early detection and response to the pandemic. Furthermore, Szczypka et al. [55] explored Reddit discussions on Delta-8-tetrahydrocannabinol, shedding light on public perceptions and potential health risks associated with its use. Lastly, Sharp et al. [53] conducted a comprehensive analysis of 11 years of Reddit posts related to dietary supplements among military personnel, providing valuable data on safety, efficacy, and usage patterns within this specific population. These examples collectively underscore the significant role of Reddit in enhancing our understanding of drug safety and informing public health strategies.

YouTube, being a widely utilized video-sharing platform, provides a rich source of information on medication usage and health-related topics. For example, Hansen et al. [56] assessed the accuracy of safety information conveyed in YouTube videos about medication usage during pregnancy. Their aim was to ensure that pregnant women have access to reliable and evidence-based guidance to facilitate informed decision-making for their well-being.

Research on drug safety is increasingly leveraging patient-generated data from health-specific forums and online consultation platforms, such as WebMD. These studies utilize quantitative analysis and natural language processing techniques to extract information directly from patient reviews and discussions, providing a unique perspective on medication adherence, adverse drug reactions, and patient satisfaction. By comparing patient-reported reasons for medication changes against formal adverse event reporting systems and assessing the cognitive levels and intervention preferences of patients with hypertriglyceridemia, these research efforts enhance our understanding of real-world medication experiences and safety concerns, ultimately contributing to the improvement of pharmacovigilance practices.

In addition to WebMD, numerous health forums cater to different languages and focus on various topics. For instance, Abdellaoui et al. [77] used a topic modeling approach to identify instances of noncompliance to drug treatment in patient forum posts. Similarly, Karapetiantz et al. [78] found a discrepancy between personal experiences and negative opinions with the human papillomavirus vaccine in web forums. They also found that descriptions of adverse drug reactions are less detailed in forums compared to the French Pharmacovigilance Database,[10] however, forums provide more unexpected reactions [79]. These examples illustrate the potential of health-specific forums and online consultation platforms in enhancing our understanding of drug safety and improving pharmacovigilance practices. They emphasize the importance of considering patient experiences and

10 https://ansm.sante.fr/page/enhanced-surveillance-of-medicines

perspectives in different languages and contexts. Such an approach not only enriches available data for analysis but also ensures a more comprehensive and inclusive understanding of drug safety.

Q&A platforms like Quora and patient feedback websites such as[8] play a crucial role in drug safety research by providing a space for patients to share their experiences, ask questions about medications, and discuss their treatment preferences. For instance, Xu et al. [61] analyzed the discussions about COVID-19 vaccine clinical trials on Quora, providing insight into public sentiment and common questions about the trials, which can inform future communication strategies and patient education efforts. Similarly, Song et al. [62] conducted a social media listening infosurveillance study to evaluate the needs and experiences of patients with hypertriglyceridemia. They identified common concerns and preferences that can be utilized to guide the development of patient-centered care strategies for this population. Moreover, Duh et al. [63] explored whether social media data could aid in the early detection of drug-related adverse events. They found that patient discussions on platforms like[8] can provide early warning signs of potential adverse events, thereby enhancing the timeliness and effectiveness of pharmacovigilance efforts. These examples underscore the potential of Q&A platforms and patient feedback websites in drug safety research, emphasizing the importance of incorporating patient voices in the study to improve drug safety practices.

E-commerce platforms like Amazon serve as valuable repositories of consumer-generated data for drug safety research. By examining user reviews, ratings, and Q&A sections, researchers can gain insight into the real-world performance and safety of over-the-counter medications and health products. For instance, Adams et al. [64] used an automated method to uncover safety and efficacy issues related to joint and muscle pain treatments from Amazon reviews. Similarly, Gartland et al. [65] focused on creating crowdsourced training datasets for pharmacovigilance intelligent automation, illustrating the potential of platforms like Amazon Turk to provide valuable data for training machine learning models in pharmacovigilance studies. These examples highlight the significance of e-commerce platforms in drug safety research, enhancing our understanding of medication safety and efficacy in real-world contexts.

In the past, news articles and blog posts were frequently used as primary data sources for drug safety research. However, their utilization has witnessed a decline in recent years. Despite the shift from blogs to real time social media platforms, traditional news and blog data can still yield valuable insights for drug safety research. For example, de Vries et al. [66] analyzed a series of healthcare provider communications in newspaper articles spanning from 2001 to 2015 in the Netherlands, demonstrating the value of such media in drug safety research. Similarly, Matsuda et al. [68] analyzed patient narratives sourced from disease-specific blogs, a component of the TOBYO database,[11] revealing valuable real-world medication experiences and emphasizing the potential of such platforms in bolstering drug safety research and pharmacovigilance efforts. These examples emphasize the significant role of news and blog data in understanding public perceptions and experiences related to drug safety.

Online surveys are valuable tools in drug safety research, providing a platform for collecting large-scale patient-generated data. For instance, Grundmann et al. [70] used an online survey to investigate patterns of Kratom use and its health impact in the US. Similarly, Wysota et al. [75] and Nguyen et al. [76] utilized online surveys to understand consumers' knowledge, perceptions, and usage of cannabidiol products. The widespread adoption of online surveys signifies their pivotal role in advancing drug safety research by providing a robust platform for data collection and analysis.

Information extracted from social media platforms

In the realm of pharmacovigilance, social media has emerged as a pivotal source of information, offering unprecedented access to a wealth of data regarding patient experiences, perceptions, and discussions related to medication use and safety. This section delves into the various ways social media data can be harnessed to enhance our understanding of patient experiences, detect and analyze adverse drug events, assess vaccine efficacy and safety, and combat the spread of misinformation. It highlights the importance of leveraging social media platforms to inform healthcare practices, improve pharmacovigilance efforts, and address the challenges posed by misinformation, ultimately aiming to enhance public health and safety. Table 2 shows the categories of key information extracted from social media.

Patient experiences and perceptions

Social media platforms have become invaluable for capturing patient experiences and perceptions regarding medication use, benefits, and safety. Golder et al. [40] and Micale et al. [57] examined online discussions and personal narratives, uncovering reasons behind medication changes, such as adverse events experienced by patients on statin therapies and other treatments, along with factors influencing their satisfaction and concerns. Yamaguchi et al. [42] explored the impact of social media information on self-medication choices, focusing on fenbendazole, and highlighting how such information can lead to

11 https://www.tobyo.jp/

TABLE 2 Extracted key information categories from social media data.

Key information Category	Key information	Reference
Patient Experience and Perceptions	patient experience of adverse events for Discontinuing Statin Therapy	[40]
	Patient experience of adverse events for medication change	[57]
	Patient experience of fenbendazole safety and efficacy	[42]
	Negative opinions and personal experience with HPV vaccine	[78]
	Patient reported Symptoms	[50]
	Patient Experiences with Dabigatran	[80]
	consumer perceptions and attitudes on cannabis products	[76]
Adverse Drug Events	Adverse Drug Events in X posts	[2, 3, 5, 10, 14, 22, 34, 81–83]
	Adverse Drug Events in Forums	[59, 72, 84, 85]

adverse events, emphasizing the need for effective communication strategies and vigilant monitoring. In a similar vein, Karapetiantz et al. [78] analyzed HPV vaccine discussions in online forums, identifying a gap between personal experiences and negative public opinions, which contributes to vaccine hesitancy and signals the need for targeted interventions. Guo et al. [50] further illustrated how social media enhances traditional pharmacovigilance by offering a deeper understanding of real-world drug safety through patient-reported symptoms. Vaughan et al. [80] documented patient experiences with dabigatran, offering insight into patient satisfaction, concerns, and adverse effects that stress the importance of understanding patient perspectives. Additionally, Nguyen et al. [76] highlighted consumer perceptions and attitudes toward cannabis products, demonstrating the influence of social media in shaping public opinion and highlighting concerns related to the use and safety of such products. Collectively, these studies showcase social media's role in strengthening pharmacovigilance by amplifying patient voices and informing healthcare practices that align with patient needs and real-world experiences.

Adverse drug events:

Social media platforms, especially X, are increasingly being used to detect adverse drug events. Pathak et al. [2] and Litvinova et al. [3] demonstrated the potential of X posts as early indicators of safety signals, with Pathak focusing on initial detection and Litvinova refining methods for accurate adverse drug event identification. Yu et al. [5] developed a natural language processing model to analyze X posts for adverse drug events, while Magge et al. [10] used deep learning to extract adverse drug events from the platform. The Web-RADR project, as reported by Gattepaille et al. [14], applied machine learning to identify adverse drug events on X, establishing a benchmark dataset for adverse event recognition. Masino et al. [22] enhanced automated adverse drug event detection using convolutional neural networks, and Fisher et al. [34] introduced a scalable machine learning framework for identifying drug-related harms on social media. Further advancements in ADE detection on social platforms were achieved by Botsis et al. [81], Dong et al. [82], and Zhang et al. [83] through the application of text mining and BERT-based language models, enhancing post-marketing surveillance and pharmacovigilance practices.

Web forums also serve as valuable source for monitoring adverse drug events. Roche et al. [59] extracted adverse drug events from Doctissimo, a medical forum where users report side effects and allergic reactions. Bulcock et al. [72] highlighted HealthUnlocked, a health discussion forum, as a platform for detecting emerging side effects. Audeh et al. [84] explored French web forums where users share serious adverse drug events, and Karapetiantz et al. [85] analyzed 23 health forums using the V4M Scraper tool to identify adverse drug events, drug interactions, and safety concerns. Together, these studies showcased the potential of social media and web forums as real-world sources of adverse drug event data, enriching drug safety research and enabling faster responses to public safety concerns.

Methods for utilizing social media data

The integration of social media data into drug safety monitoring has significantly advanced the detection of adverse drug events, analysis of public sentiment, monitoring of drug abuse, and identification of drug-drug interactions. Social media platforms, with their vast and diverse user-generated content, offer a unique perspective on real-world patient experiences and public perceptions of medications.

In adverse drug events detection, both supervised and unsupervised learning methods, including models like BERT

TABLE 3 Methods for analyzing adverse drug events, public sentiment, drug abuse, and drug-drug interactions using social media data.

Topic Category	Method Category	Details	Advantage	Limitation	Reference
Machine Learning methods for Adverse Drug Event Detection	Supervised Learning	BERT-based model to extract adverse drug events from X posts	High accuracy on X posts	Requires labeled data for effective training	[82]
		natural language processing methods to detect adverse drug events from clinical text	High accuracy in structured clinical environments	Limited generalizability to non-clinical text and informal language	[86]
		Pipeline to extract and normalize adverse drug events	Detect adverse drug events in X posts	Limited to X posts data	[10]
		adverse drug event detection across platforms	High detection accuracy	Limited generalizability to diverse social media platforms	[12]
	Unsupervised Learning	Co-clustering for adverse drug event detection	Detects adverse drug event signals by clustering related data without predefined labels	Validation limited to COVID-19 related data	[87]
		Transformer-based adverse drug event detection	High sensitivity in capturing emerging adverse drug events	Limited to specific drugs and topics in the training set	[49]
		CNN model for adverse drug event detection	Detects adverse drug events without predefined labels	Limited in capturing complex adverse drug events	[22]
	Semi-supervised Learning	Word embeddings-based lexical network for adverse drug events detection	Severity scoring to assess different adverse drug events	Data quality, noise, and bias exist in social media data	[54]
Public Sentiment and Patient Feedback Analysis	Quantitative Analysis	Direct patient feedback analysis through quantitative methods	Provides insight into patient perspectives	Limited by the accuracy of self-reported data	[57]
	Sentiment Analysis	WC-CNN model for sentiment analysis	Detects safety signals by examining user behavior over time	Limited to the Levothyrox case in France	[59]
		Sentiment analysis of public perception of specific drugs for COVID-19 treatment	Captures public perceptions on certain drugs	Limited to specific drugs and COVID-19 context	[39]
		VADER model for sentiment analysis on cannabidiol use for various conditions	Provides insight into public perception of cannabidiol use	Manual labeling needed for classifier training	[9]
Drug Abuse	Large Language Model based	GPT-3 for generating a lexicon for drug abuse detection in social media	Captures slang and misspellings for drug abuse detection	Limited to 98 drugs with limited evaluation	[88]
	Quantitative Analysis	Frequency analysis of opioid misuse, abuse, addiction, overdose, and death	Real-time tracking and insight into opioid abuse trends	Limited to opioid-related data	[36]
		Statistical analysis with data quality metrics and topic modeling for drug abuse content	Structured framework for analyzing drug abuse-related content	Limited social media platforms and limited generalizability	[89]
		NER for adverse drug event identification; PRR for potential adverse drug event detection; topic modeling to identify themes	Comprehensive analysis and real-time monitoring using social media data	Limited to methylphenidate-related posts between 2007 and 2016 only	[90]
		Quantitative analysis of annotated posts for drug abuse	Supervised classification model to detect drug abuse signals in X posts	Requires manually annotated 6,400 X posts containing drug abuse signals	[91]
Drug-Drug Interactions	Quantitative Analysis	Frequency and rates for posts related to Drug-Drug Interactions are analyzed	Manually reviewed and evaluated by two blinded investigators	Limited data and limited manual validation	[92]
	Supervised Learning	Drug-Drug Interactions detection in social media data	Extracts related Drug-Drug Interactions information from social media platforms	Requires an annotated Drug-Drug Interactions corpus	[93]

(Continued on following page)

TABLE 3 (*Continued*) Methods for analyzing adverse drug events, public sentiment, drug abuse, and drug-drug interactions using social media data.

Topic Category	Method Category	Details	Advantage	Limitation	Reference
	Network Analysis	Co-occurrence network for users based on potential Drug-Drug Interactions	Detects relationships and patterns for emerging Drug-Drug Interactions through network analysis	Limited to Instagram platform with privacy and ethical concerns	[94]

and co-clustering algorithms, are applied to extract and analyze adverse events from social media posts. For public sentiment analysis, cutting-edge sentiment analysis models are being used to assess patient feedback and identify potential safety signals. Meanwhile, drug abuse monitoring employs large language models and quantitative analysis to detect trends in misuse, addiction, and overdose incidents. The identification of drug-drug interactions is enhanced through network analysis and supervised learning techniques.

These methods are reshaping pharmacovigilance, enabling faster identification of safety concerns, a deeper understanding of patient experiences, and more effective monitoring of public health issues. Table 3 summarizes the various methods and their applications in utilizing social media data to advance drug safety studies.

Machine learning methods for adverse drug event detection

One of the most active areas of drug safety research is the detection and extraction of adverse drug events from social media posts. Various machine learning approaches—supervised, unsupervised, and semi-supervised—are employed, each with unique strengths and limitations.

Supervised learning approaches, such as those utilizing BERT-based models, achieve high accuracy in extracting adverse drug events but are heavily reliant on large, labeled datasets. This requirement makes them resource-intensive and less adaptable to diverse social media platforms. For example, BERT-based models have demonstrated exceptional performance in extracting adverse drug events from X posts, but their effectiveness hinges on the availability of labeled data [82]. Natural language processing techniques have also been used to detect adverse drug events in clinical documents, achieving good results within structured data but facing challenges when applied to informal or unstructured social media text [86]. Magge et al. [10] used deep learning methods in their DeepADEMiner pipeline to extract and normalize adverse drug event mentions on X posts. Despite its success on specific platforms like X, such models often struggle to generalize across the diverse and evolving landscape of social media environments [12].

Unsupervised learning methods, such as co-clustering, allow adverse drug event detection by grouping related data without requiring predefined labels. These methods have been particularly useful in monitoring adverse drug events associated with COVID-19, though their validation remains largely confined to this context [87]. Transformer-based [49] and CNN-based [22] models enhance adverse drug event detection sensitivity and capture emerging adverse drug events without relying on labeled data. However, these approaches are often constrained by the drugs and topics present in the training set, making them less adaptable to new or evolving drug discussions.

Semi-supervised learning techniques combine the strengths of supervised and unsupervised techniques, using a smaller labeled dataset alongside a larger pool of unlabeled data. This approach strikes a balance between accuracy and flexibility, although it continues to face challenges with scalability and data quality. For instance, word embeddings-based lexical networks have been used to introduce severity scoring for assessing adverse drug events, addressing the inherent issues with data quality, noise, and bias in social media data [54].

In summary, while advancements in supervised, unsupervised, and semi-supervised learning techniques have significantly improved ADE detection from social media, each method has inherent trade-offs. Future research must focus on enhancing generalizability, scalability, and robustness to fully leverage social media data for pharmacovigilance.

Public sentiment and patient feedback analysis

Social media platforms provide unique patient perspectives and public sentiment regarding medications, complementing traditional pharmacovigilance methods. Quantitative analysis methods and sentiment analysis techniques contribute to understanding patient experiences and detecting drug safety signals, though challenges with data quality and generalization persist.

Quantitative analysis methods, often involving manual review of patient posts, offer valuable information on patient attitudes and experiences. However, the accuracy and reliability of self-reported data remain significant limitations [57]. Despite these constraints, such methods are instrumental in capturing nuanced patient feedback and identifying trends in medication use and side effects.

Sentiment analysis techniques are frequently used to track public perceptions of medications and detect emerging drug

safety signals. Advanced models like WC-CNN have been employed to monitor sentiment trends linked to specific drugs, such as Levothyrox in France. While effective in capturing localized sentiment, these models often struggle to generalize across different drugs or regions [59].

Studies have also employed sentiment analysis to understand public perceptions of drugs for specific conditions. For instance, sentiment analysis models like VADER have been applied to assess public attitudes toward COVID-19 treatments [39] and the use of cannabidiol for various health issues [9]. While VADER provides valuable public sentiment, its reliance on manual labeling for classifier training presents scalability challenges, particularly when dealing with large, diverse datasets.

Together, quantitative and sentiment analysis methods enrich drug safety assessments, offering a more comprehensive understanding of medication safety and public attitudes. However, ongoing efforts to address issues with data quality, scalability, and model generalization are essential for maximizing their potential in pharmacovigilance.

Drug abuse

The rise of drug abuse, particularly opioid misuse, has driven significant efforts to monitor drug abuse trends using social media data. By analyzing user-generated content, researchers aim to enable early detection of abuse, addiction, overdose, and other drug-related issues.

Large language models like GPT-3 have been used to generate lexicons for drug abuse detection, capturing slang, misspellings, and colloquialisms frequently used in drug-related discussions. While these lexicons offer a valuable starting point, they typically focus on a narrow range of drugs and often lack comprehensive evaluation, limiting their broader applicability [88].

Quantitative analysis methods, such as frequency analysis, provide real-time tracking of opioid misuse, abuse, addiction, overdose, and related deaths. These methods help identify emerging trends and patterns in drug abuse [36]. More structured approaches, incorporating data quality matrices and topic modeling, provide frameworks for analyzing drug abuse content across social media platforms. However, the diversity and variability of these platforms pose challenges to generalizability and cross-platform applicability [89].

Techniques such as named entity recognition combined with proportional reporting ratios enables more targeted analysis by identifying specific drugs and associated adverse events. For instance, studies have focused on methylphenidate-related social media posts from 2007 to 2016, highlighting the potential of such methods for longitudinal drug abuse research [90].

Supervised learning models further enhance drug abuse monitoring. Sarker et al. [91] developed a supervised classification model trained on 6,400 manually annotated X posts to identify drug abuse-related content. This approach highlights the importance of labeled data in improving the precision and reliability of drug abuse trend analysis on social media.

By combining advanced natural language processing techniques with structured analytical methods, researchers are gaining a deeper understanding of drug abuse trends. However, challenges related to data quality, platform diversity, and scalability remain areas for future improvement.

Drug-drug interaction

Monitoring drug-drug interactions using social media data is an emerging trend in drug safety evaluation. Social media provides the advantage of real-time, user-generated data, allowing for quick identification of potential drug-drug interactions across diverse populations. However, this approach faces challenges, including the need for context-rich analysis, issues with data quality, and privacy concerns on certain platforms. Traditionally, drug-drug interactions detection relied on structured data, but social media offers a dynamic and expansive source of information.

Quantitative approaches analyze the frequency and prevalence of drug-drug interactions related posts, which are then manually reviewed by blinded investigators. While informative, these methods are often limited by data availability and require labor-intensive validation processes [92]. Supervised learning models address these limitations by leveraging annotated drug-drug interactions corpora to extract relevant interaction information from user posts, enhancing detection efficiency [93].

Network analysis has also been applied to study potential drug-drug interactions by constructing co-occurrence networks based on user mentions of interacting drugs. This method facilitates the identification of emerging drug-drug interaction patterns and relationships. However, its application is sometimes limited by platform-specific privacy and ethical concerns, especially on platforms like on Instagram [94].

In conclusion, leveraging social media for monitoring drug-drug interactions presents a promising complement to traditional methods, offering real-time information and access to diverse patient populations. While challenges such as data quality, contextual interpretation, and privacy concerns remain, advancements in quantitative analysis, supervised learning models, and network analysis demonstrate the potential of this approach. With continued refinement and ethical considerations, social media could become a vital tool in enhancing drug safety and public health.

Discussion

Integrating social media data into drug safety research offers valuable insight, but presents several challenges that must be addressed to ensure reliable and actionable findings.

Data reliability and quality

Social media data is often unstructured and informal, complicating the identification of credible adverse drug event reports amidst speculative or inaccurate posts. The variability and frequent lack of contextual information in social media content further hinder interpretation, reducing the reliability of findings. Addressing these issues requires rigorous screening, validation, and contextual analysis. Moreover, the lack of demographic and medical context from social media users makes it challenging to generalize findings across populations. Comparing and pooling data across social media platforms is challenging due to differences in user demographics, content formats, and engagement patterns. Privacy regulations further restrict access to user profiles, making it difficult to analyze demographic information comprehensively. Additionally, a key limitation of current studies is the inability to fully verify whether social media users are real individuals or automated accounts. While many platforms have implemented stricter user verification measures, restricted access to demographic and account data remains a significant challenge for researchers seeking to ensure the authenticity and representativeness of social media-derived insights.

Social media platforms often restrict access to demographic and account information, posing challenges in verifying user identities. AI tools can help mitigate this by detecting bot-like behavior, such as rapid posting patterns and generic language. However, the rise of advanced language models introduces new concerns, as they can generate large volumes of content that may be difficult to distinguish from genuine user experiences. To enhance data reliability, preprocessing need to include methods for filtering posts from suspicious or abnormal accounts, ensuring that subsequent analysis focuses on real-world health experiences shared by actual users.

Data reliability is a key concern in social media-based pharmacovigilance. For data preprocessing, inclusion criteria focus on posts that explicitly mention drugs, adverse drug events, or health experiences. To ensure quality, irrelevant content, spam, and non-English posts are removed. Additionally, posts from suspicious or abnormal user accounts are filtered out to enhance reliability and prioritize real user experiences. While confirming individual accounts as real people remains a challenge, these preprocessing steps help improve data integrity and the robustness of findings.

Ethical and privacy concerns

The use of personal social media data in drug safety research introduces significant ethical and privacy challenges. Researchers must comply with privacy laws and adhere to ethical standards to mitigate risks such as discrimination or stigmatization. Implementing robust privacy protections, anonymization techniques, and transparent data usage practices is essential to maintain public trust and protecting users.

Misinformation and bias

Social media is prone to misinformation and biases that can hinder accurate adverse drug event detection. Distinguishing genuine patient experiences from misleading or biased content requires careful fact-checking and verification to ensure data reliability. Misinformation on social media can distort perceptions of drug safety, emphasizing the need for robust methods to counteract its influence. A key research gap is the need for a deeper exploration of strategies to mitigate the impact of misinformation and bias, as these factors influence all reported findings and approaches discussed in this review. Future research could focus on developing and evaluating advanced AI-driven algorithms for detecting and filtering misinformation. Additionally, platform regulations, combined with multi-source verification mechanisms, could play a crucial role in limiting the spread of biased or inaccurate content while still addressing user privacy concerns. A more systematic investigation into these mitigation strategies would strengthen the reliability of social media-based research findings.

Text mining and modeling challenges

Text mining models face limitations when processing the informal language common on social media, such as slang, abbreviations, and non-standard terms. This issue can reduce the accuracy of automated adverse drug event detection. To address these issues, researchers need to improve text mining models and standardize data validation methods. Combining social media data with traditional pharmacovigilance methods provides a more comprehensive understanding of drug safety.

Regulatory frameworks

The regulatory landscape for incorporating social media data into pharmacovigilance is still evolving. Clear and standardized guidelines are needed to govern ethical data use and alignment with established pharmacovigilance practices. Such frameworks are crucial for maintaining public trust and facilitating the effective use of social media in drug safety research.

Conclusion

The integration of social media data into drug safety research offers promising opportunities to enhance pharmacovigilance. Social media's vast, real-time data can complement traditional

methods, enabling early detection of adverse drug events, monitoring public sentiment, and capturing patient experiences on medication risks and benefits. However, unlocking the full potential of social media in drug safety research requires addressing significant methodological, ethical, and regulatory challenges.

This review highlights the need for rigorous methodologies, including advanced data validation, standardized data processing protocols, and specialized text mining models tailored to the unique characteristics of social media content. Ethical considerations, such as privacy protection and transparent practices, are essential to maintaining public trust. Additionally, as social media evolves, developing a strong regulatory framework to govern the use of social media data in pharmacovigilance is important.

Future research should focus on developing real-time monitoring systems that can utilize social media for the early detection of drug safety concerns. Hybrid models that integrate social media data with traditional pharmacovigilance data hold promise for the potential to improve the accuracy, speed, and scope of safety signal detection. Standardizing data collection and analytical methodologies across studies will enhance consistency and reliability, enabling more actionable findings. Addressing cultural and linguistic diversity in social media content will also be essential to adapt these approaches to global pharmacovigilance efforts.

Collaboration among academia, industry, regulatory agencies, and social media platforms will play a key role in advancing these goals. Such partnerships can foster resource sharing, methodological alignment, and innovation in drug safety monitoring. Regulatory agencies can provide guidance on ethical and privacy standards, while social media platforms can facilitate data access and support anonymization efforts. These collaborative efforts will help establish a robust and responsive pharmacovigilance ecosystem, enhancing post-market surveillance and protecting public health worldwide. By integrating social media data with established pharmacovigilance practices, researchers and healthcare providers can improve post-marketing drug safety monitoring, enhance public health outcomes, and build a collaborative ecosystem that benefits patients and society.

Author contributions

All authors listed have made a substantial, direct, and intellectual contribution to the work and approved it for publication.

Author disclaimer

This article reflects the views of the authors and does not necessarily reflect those of the U.S. Food and Drug Administration. Any mention of commercial products is for clarification only and is not intended as approval, endorsement, or recommendation.

Funding

The author(s) declare that financial support was received for the research and/or publication of this article. This study was funded by the US Food and Drug Administration (FDA).

Conflict of interest

The author(s) declared no potential conflicts of interest with respect to the research, authorship, and/or publication of this article.

Generative AI statement

The author(s) declare that Generative AI was used in the creation of this manuscript. We would like to acknowledge that ChatGPT was used to assist in correcting English grammar errors during the preparation of this manuscript.

References

1. Sule S, DaCosta MC, DeCou E, Gilson C, Wallace K, Goff SL. Communication of COVID-19 misinformation on social media by physicians in the US. *JAMA Netw Open* (2023) **6**(8):e2328928. doi:10.1001/jamanetworkopen.2023.28928

2. Pathak R, Catalan-Matamoros D. Can Twitter posts serve as early indicators for potential safety signals? A retrospective analysis. *Int J Risk & Saf Med* (2023) **34**(1): 41–61. doi:10.3233/jrs-210024

3. Litvinova O, Matin FB, Matin M, Zima-Kulisiewicz B, Tomasik C, Siddiquea BN, et al. Patient safety discourse in a pandemic: a Twitter hashtag analysis study on #PatientSafety. *Front Public Health* (2023) **11**:1268730. doi:10.3389/fpubh.2023.1268730

4. Arillotta D, Floresta G, Guirguis A, Corkery JM, Catalani V, Martinotti G, et al. GLP-1 receptor agonists and related mental health issues; insights from a range of social media platforms using a mixed-methods approach. *Brain Sciences* (2023) **13**(11):1503. doi:10.3390/brainsci13111503

5. Yu D, Vydiswaran VGV. An assessment of mentions of adverse drug events on social media with natural language processing: model development and analysis. *JMIR Med Inform* (2022) **10**(9):e38140. doi:10.2196/38140

6. Xiong S, Batra V, Liu L, Xi L, Sun C. Detecting personal medication intake in twitter via domain attention-based RNN with multi-level features. *Comput Intelligence Neurosci* (2022) **2022**:1–7. doi:10.1155/2022/5467262

7. Klein AZ, O'Connor K, Levine LD, Gonzalez-Hernandez G. Using twitter data for cohort studies of drug safety in pregnancy: proof-of-concept with β-blockers. *JMIR Form Res* (2022) **6**(6):e36771. doi:10.2196/36771

8. Hua Y, Jiang H, Lin S, Yang J, Plasek JM, Bates DW, et al. Using Twitter data to understand public perceptions of approved versus off-label use for COVID-19-related medications. *J Am Med Inform Assoc* (2022) **29**(10):1668–78. doi:10.1093/jamia/ocac114

9. Turner J, Kantardzic M, Vickers-Smith R. Infodemiological examination of personal and commercial tweets about cannabidiol: term and sentiment analysis. *J Med Internet Res* (2021) **23**(12):e27307. doi:10.2196/27307

10. Magge A, Tutubalina E, Miftahutdinov Z, Alimova I, Dirkson A, Verberne S, et al. DeepADEMiner: a deep learning pharmacovigilance pipeline for extraction and normalization of adverse drug event mentions on Twitter. *J Am Med Inform Assoc* (2021) **28**(10):2184–92. doi:10.1093/jamia/ocab114

11. Sharma C, Whittle S, Haghighi PD, Burstein F, Keen H. Sentiment analysis of social media posts on pharmacotherapy: a scoping review. *Pharmacol Res & Perspect* (2020) **8**(5):e00640. doi:10.1002/prp2.640

12. Rezaei Z, Ebrahimpour-Komleh H, Eslami B, Chavoshinejad R, Totonchi M. Adverse drug reaction detection in social media by deepm learning methods. *Cell J* (2020) **22**(3):319–24. doi:10.22074/cellj.2020.6615

13. Li Y, Jimeno Yepes A, Xiao C. Combining social media and FDA adverse event reporting system to detect adverse drug reactions. *Drug Saf* (2020) **43**(9):893–903. doi:10.1007/s40264-020-00943-2

14. Gattepaille LM, Hedfors Vidlin S, Bergvall T, Pierce CE, Ellenius J. Prospective evaluation of adverse event recognition systems in twitter: results from the web-RADR project. *Drug Saf* (2020) **43**(8):797–808. doi:10.1007/s40264-020-00942-3

15. Dietrich J, Gattepaille LM, Grum BA, Jiri L, Lerch M, Sartori D, et al. Adverse events in twitter-development of a benchmark reference dataset: results from IMI WEB-RADR. *Drug Saf* (2020) **43**(5):467–78. doi:10.1007/s40264-020-00912-9

16. van Stekelenborg J, Ellenius J, Maskell S, Bergvall T, Caster O, Dasgupta N, et al. Recommendations for the use of social media in pharmacovigilance: lessons from IMI WEB-RADR. *Drug Saf* (2019) **42**(12):1393–407. doi:10.1007/s40264-019-00858-7

17. Golder S, Scantlebury A, Christmas H. Understanding public attitudes toward researchers using social media for detecting and monitoring adverse events data: multi methods study. *J Med Internet Res* (2019) **21**(8):e7081. doi:10.2196/jmir.7081

18. Golder S, Chiuve S, Weissenbacher D, Klein A, O'Connor K, Bland M, et al. Pharmacoepidemiologic evaluation of birth defects from health-related postings in social media during pregnancy. *Drug Saf* (2019) **42**(3):389–400. doi:10.1007/s40264-018-0731-6

19. Suragh TA, Lamprianou S, MacDonald NE, Loharikar AR, Balakrishnan MR, Benes O, et al. Cluster anxiety-related adverse events following immunization (AEFI): an assessment of reports detected in social media and those identified using an online search engine. *Vaccine* (2018) **36**(40):5949–54. doi:10.1016/j.vaccine.2018.08.064

20. Smith K, Golder S, Sarker A, Loke Y, O'Connor K, Gonzalez-Hernandez G. Methods to compare adverse events in twitter to FAERS, drug information databases, and systematic reviews: proof of concept with adalimumab. *Drug Saf* (2018) **41**(12):1397–410. doi:10.1007/s40264-018-0707-6

21. Patel R, Belousov M, Jani M, Dasgupta N, Winokur C, Nenadic G, et al. Frequent discussion of insomnia and weight gain with glucocorticoid therapy: an analysis of Twitter posts. *npj Digital Med* (2018) **1**:20177. doi:10.1038/s41746-017-0007-z

22. Masino AJ, Forsyth D, Fiks AG. Detecting adverse drug reactions on twitter with convolutional neural networks and word embedding features. *J Healthc Inform Res* (2018) **2**(1-2):25–43. doi:10.1007/s41666-018-0018-9

23. Lardon J, Bellet F, Aboukhamis R, Asfari H, Souvignet J, Jaulent MC, et al. Evaluating Twitter as a complementary data source for pharmacovigilance. *Expert Opin Drug Saf* (2018) **17**(8):763–74. doi:10.1080/14740338.2018.1499724

24. Comfort S, Perera S, Hudson Z, Dorrell D, Meireis S, Nagarajan M, et al. Sorting through the safety data haystack: using machine learning to identify individual case safety reports in social-digital media. *Drug Saf* (2018) **41**(6):579–90. doi:10.1007/s40264-018-0641-7

25. Caster O, Dietrich J, Kürzinger ML, Lerch M, Maskell S, Norén GN, et al. Assessment of the utility of social media for broad-ranging statistical signal detection in pharmacovigilance: results from the WEB-RADR project. *Drug Saf* (2018) **41**(12):1355–69. doi:10.1007/s40264-018-0699-2

26. Pierce CE, Bouri K, Pamer C, Proestel S, Rodriguez HW, Van Le H, et al. Evaluation of Facebook and twitter monitoring to detect safety signals for medical products: an analysis of recent FDA safety alerts. *Drug Saf* (2017) **40**(4):317–31. doi:10.1007/s40264-016-0491-0

27. Price J. What can big data offer the pharmacovigilance of orphan drugs? *Clin Ther* (2016) **38**(12):2533–45. doi:10.1016/j.clinthera.2016.11.009

28. Powell GE, Seifert HA, Reblin T, Burstein PJ, Blowers J, Menius JA, et al. Social media listening for routine post-marketing safety surveillance. *Drug Saf* (2016) **39**(5):443–54. doi:10.1007/s40264-015-0385-6

29. Coloma PM, Becker B, Sturkenboom MC, van Mulligen EM, Kors JA. Evaluating social media networks in medicines safety surveillance: two case studies. *Drug Saf* (2015) **38**(10):921–30. doi:10.1007/s40264-015-0333-5

30. Freifeld CC, Brownstein JS, Menone CM, Bao W, Filice R, Kass-Hout T, et al. Digital drug safety surveillance: monitoring pharmaceutical products in twitter. *Drug Saf* (2014) **37**(5):343–50. doi:10.1007/s40264-014-0155-x

31. Bian J, Topaloglu U, Yu F. Towards large-scale twitter mining for drug-related adverse events. *SHB12 (2012)* (2012) **2012**:25–32. doi:10.1145/2389707.2389713

32. Khademi Habibabadi S, Palmer C, Dimaguila GL, Javed M, Clothier HJ, Buttery J. Australasian institute of digital health summit 2022-automated social media surveillance for detection of vaccine safety signals: a validation study. *Appl Clin Inform* (2023) **14**(1):1–10. doi:10.1055/a-1975-4061

33. Golder S, O'Connor K, Wang Y, Gonzalez Hernandez G. The role of social media for identifying adverse drug events data in pharmacovigilance: protocol for a scoping review. *JMIR Res Protoc* (2023) **12**:e47068. doi:10.2196/47068

34. Fisher A, Young MM, Payer D, Pacheco K, Dubeau C, Mago V. Automating detection of drug-related harms on social media: machine learning framework. *J Med Internet Res* (2023) **25**:e43630. doi:10.2196/43630

35. Zhang T, Lin H, Xu B, Yang L, Wang J, Duan X. Adversarial neural network with sentiment-aware attention for detecting adverse drug reactions. *J Biomed Inform* (2021) **123**:103896. doi:10.1016/j.jbi.2021.103896

36. Black JC, Margolin ZR, Olson RA, Dart RC. Online conversation monitoring to understand the opioid epidemic: epidemiological surveillance study. *JMIR Public Health Surveill* (2020) **6**(2):e17073. doi:10.2196/17073

37. Calac AJ, Haupt MR, Li Z, Mackey T. Spread of COVID-19 vaccine misinformation in the ninth inning: retrospective observational infodemic study. *JMIR Infodemiology* (2022) **2**(1):e33587. doi:10.2196/33587

38. Curtis JR, Chen L, Higginbotham P, Nowell WB, Gal-Levy R, Willig J, et al. Social media for arthritis-related comparative effectiveness and safety research and the impact of direct-to-consumer advertising. *Arthritis Res Ther* (2017) **19**(1):48. doi:10.1186/s13075-017-1251-y

39. Schellack N, Strydom M, Pepper MS, Herd CL, Hendricks CL, Bronkhorst E, et al. Social media and COVID-19-perceptions and public deceptions of ivermectin, colchicine and hydroxychloroquine: lessons for future pandemics. *Antibiotics (Basel)* (2022) **11**(4):445. doi:10.3390/antibiotics11040445

40. Golder S, Weissenbacher D, O'Connor K, Hennessy S, Gross R, Hernandez GG. Patient-reported reasons for switching or discontinuing statin therapy: a mixed methods study using social media. *Drug Saf* (2022) **45**(9):971–81. doi:10.1007/s40264-022-01212-0

41. Yeung AWK, Tosevska A, Klager E, Eibensteiner F, Tsagkaris C, Parvanov ED, et al. Medical and health-related misinformation on social media: bibliometric study of the scientific literature. *J Med Internet Res* (2022) **24**(1):e28152. doi:10.2196/28152

42. Yamaguchi T, Shimizu J, Oya Y, Horio Y, Hida T. Drug-Induced liver injury in a patient with nonsmall cell lung cancer after the self-administration of fenbendazole based on social media information. *Case Rep Oncol* (2021) **14**(2):886–91. doi:10.1159/000516276

43. Härmark L, Weits G, Meijer R, Santoro F, Norén GN, van Hunsel F. Communicating adverse drug reaction insights through patient organizations: experiences from a pilot study in The Netherlands. *Drug Saf* (2020) **43**(8):745–9. doi:10.1007/s40264-020-00932-5

44. Sinha MS, Freifeld CC, Brownstein JS, Donneyong MM, Rausch P, Lappin BM, et al. Social media impact of the Food and drug administration's drug safety communication messaging about zolpidem: mixed-methods analysis. *JMIR Public Health Surveill* (2018) **4**(1):e1. doi:10.2196/publichealth.7823

45. Mackey TK, Liang BA, Strathdee SA. Digital social media, youth, and nonmedical use of prescription drugs: the need for reform. *J Med Internet Res* (2013) **15**(7):e143. doi:10.2196/jmir.2464

46. Mackey TK, Liang BA. Global reach of direct-to-consumer advertising using social media for illicit online drug sales. *J Med Internet Res* (2013) **15**(5):e105. doi:10.2196/jmir.2610

47. Liang BA, Mackey TK. Prevalence and Global Health implications of social media in direct-to-consumer drug advertising. *J Med Internet Res* (2011) **13**(3):e64. doi:10.2196/jmir.1775

48. Li J, Xu Q, Shah N, Mackey TK. A machine learning approach for the detection and characterization of illicit drug dealers on Instagram: model evaluation study. *J Med Internet Res* (2019) **21**(6):e13803. doi:10.2196/13803

49. Smith BP, Hoots B, DePadilla L, Roehler DR, Holland KM, Bowen DA, et al. Using transformer-based topic modeling to examine discussions of delta-8 tetrahydrocannabinol: content analysis. *J Med Internet Res* (2023) **25**:e49469. doi:10.2196/49469

50. Guo M, Ma Y, Eworuke E, Khashei M, Song J, Zhao Y, et al. Identifying COVID-19 cases and extracting patient reported symptoms from Reddit using natural language processing. *Sci Rep* (2023) **13**(1):13721. doi:10.1038/s41598-023-39986-7

51. Godinez H, Xu Q, McMann TJ, Li J, Mackey TK. Analysis of online user discussions on Reddit associated with the transition of use between HIV PrEP therapy. *Front Public Health* (2023) **11**:1073813. doi:10.3389/fpubh.2023.1073813

52. Pepper JK, Zitney LV, Preiss A, Bukowski T, Szczypka G, Kim AE. Can social media monitoring help identify the next EVALI? An examination of Reddit posts about vitamin E acetate and Dank Vapes. *Drug and Alcohol Dependence* (2022) **230**: 109193. doi:10.1016/j.drugalcdep.2021.109193

53. Sharp KJ, Vitagliano JA, Weitzman ER, Fitzgerald S, Dahlberg SE, Austin SB. Peer-to-Peer social media communication about dietary supplements used for weight loss and sports performance among military personnel: pilot content analysis of 11 Years of posts on Reddit. *JMIR Form Res* (2021) **5**(10):e28957. doi:10.2196/28957

54. Lavertu A, Hamamsy T, Altman RB. Quantifying the severity of adverse drug reactions using social media: network analysis. *J Med Internet Res* (2021) **23**(10): e27714. doi:10.2196/27714

55. Szczypka G, Pepper JK, Kim A. Weed light: an exploratory study of delta-8 THC conversations on Reddit. In: *RTI press research brief*. Research Triangle Park (NC): RTI Press (2014).

56. Hansen C, Interrante JD, Ailes EC, Frey MT, Broussard CS, Godoshian VJ, et al. Assessment of YouTube videos as a source of information on medication use in pregnancy. *Pharmacoepidemiol Drug Saf* (2016) **25**(1):35–44. doi:10.1002/pds.3911

57. Micale C, Golder S, O'Connor K, Weissenbacher D, Gross R, Hennessy S, et al. Patient-reported reasons for antihypertensive medication change: a quantitative study using social media. *Drug Saf* (2024) **47**(1):81–91. doi:10.1007/s40264-023-01366-5

58. Park S, Choi SH, Song YK, Kwon JW. Comparison of online patient reviews and national pharmacovigilance data for tramadol-related adverse events: comparative observational study. *JMIR Public Health Surveill* (2022) **8**(1): e33311. doi:10.2196/33311

59. Roche V, Robert JP, Salam H. A holistic AI-based approach for pharmacovigilance optimization from patients behavior on social media. *Artif Intelligence Med* (2023) **144**:102638. doi:10.1016/j.artmed.2023.102638

60. Powell G, Kara V, Painter JL, Schifano L, Merico E, Bate A. Engaging patients via online healthcare fora: three pharmacovigilance use cases. *Front Pharmacol* (2022) **13**:901355. doi:10.3389/fphar.2022.901355

61. Xu Q, McMann TJ, Li J, Wenzel C, Mackey TK. Characterization of COVID-19 vaccine clinical trial discussions on the social question-and-answer site Quora. *Trials* (2023) **24**(1):790. doi:10.1186/s13063-023-07837-5

62. Song J, Cui Y, Song J, Lee C, Wu M, Chen H. Evaluation of the needs and experiences of patients with hypertriglyceridemia: social media listening infosurveillance study. *J Med Internet Res* (2023) **25**:e44610. doi:10.2196/44610

63. Duh MS, Cremieux P, Audenrode MV, Vekeman F, Karner P, Zhang H, et al. Can social media data lead to earlier detection of drug-related adverse events? *Pharmacoepidemiol Drug Saf* (2016) **25**(12):1425–33. doi:10.1002/pds.4090

64. Adams DZ, Gruss R, Abrahams AS. Automated discovery of safety and efficacy concerns for joint & muscle pain relief treatments from online reviews. *Int J Med Inform* (2017) **100**:108–20. doi:10.1016/j.ijmedinf.2017.01.005

65. Gartland A, Bate A, Painter JL, Casperson TA, Powell GE. Developing crowdsourced training data sets for pharmacovigilance intelligent automation. *Drug Saf* (2021) **44**(3):373–82. doi:10.1007/s40264-020-01028-w

66. de Vries E, Denig P, de Vries ST, Monster TBM, Hugtenburg JG, Mol PGM. Drug safety issues covered by lay media: a cohort study of direct healthcare provider communications sent between 2001 and 2015 in The Netherlands. *Drug Saf* (2020) **43**(7):677–90. doi:10.1007/s40264-020-00922-7

67. Larson HJ, Wilson R, Hanley S, Parys A, Paterson P. Tracking the global spread of vaccine sentiments: the global response to Japan's suspension of its HPV vaccine recommendation. *Hum Vaccin & Immunother* (2014) **10**(9):2543–50. doi:10.4161/21645515.2014.969618

68. Matsuda S, Aoki K, Tomizawa S, Sone M, Tanaka R, Kuriki H, et al. Analysis of patient narratives in disease blogs on the internet: an exploratory study of social pharmacovigilance. *JMIR Public Health Surveill* (2017) **3**(1):e10. doi:10.2196/publichealth.6872

69. Zhu XM, Yan W, Sun J, Liu L, Zhao YM, Zheng YB, et al. Patterns and influencing factors of COVID-19 vaccination willingness among college students in China. *Vaccine* (2022) **40**(22):3046–54. doi:10.1016/j.vaccine.2022.04.013

70. Grundmann O. Patterns of Kratom use and health impact in the US-Results from an online survey. *Drug and Alcohol Dependence* (2017) **176**:63–70. doi:10.1016/j.drugalcdep.2017.03.007

71. Brosch S, de Ferran AM, Newbould V, Farkas D, Lengsavath M, Tregunno P. Establishing a framework for the use of social media in pharmacovigilance in europe. *Drug Saf* (2019) **42**(8):921–30. doi:10.1007/s40264-019-00811-8

72. Bulcock A, Hassan L, Giles S, Sanders C, Nenadic G, Campbell S, et al. Public perspectives of using social media data to improve adverse drug reaction reporting: a mixed-methods study. *Drug Saf* (2021) **44**(5):553–64. doi:10.1007/s40264-021-01042-6

73. Ghosh R, Lewis D. Aims and approaches of Web-RADR: a consortium ensuring reliable ADR reporting via mobile devices and new insights from social media. *Expert Opin Drug Saf* (2015) **14**(12):1845–53. doi:10.1517/14740338.2015.1096342

74. Lengsavath M, Dal Pra A, de Ferran AM, Brosch S, Härmark L, Newbould V, et al. Social media monitoring and adverse drug reaction reporting in pharmacovigilance: an overview of the regulatory landscape. *Ther Innov Regul Sci* (2017) **51**(1):125–31. doi:10.1177/2168479016663264

75. Wysota CN, Le D, Clausen ME, Ciceron AC, Fuss C, Bennett B, et al. Young adults' knowledge, perceptions and use of cannabidiol products: a mixed-methods study. *Health Education Res* (2022) **37**(6):379–92. doi:10.1093/her/cyac030

76. Nguyen C, Moeller KE, McGuire M, Melton BL. Consumer perception, knowledge, and uses of cannabidiol. *Ment Health Clinician* (2023) **13**(5):217–24. doi:10.9740/mhc.2023.10.217

77. Abdellaoui R, Foulquié P, Texier N, Faviez C, Burgun A, Schück S. Detection of cases of noncompliance to drug treatment in patient forum posts: topic model approach. *J Med Internet Res* (2018) **20**(3):e85. doi:10.2196/jmir.9222

78. Karapetiantz P, Audeh B, Lillo-Le Louët A, Bousquet C. Discrepancy between personal experience and negative opinion with human papillomavirus vaccine in web forums. *Stud Health Technol Inform* (2020) **272**:417–20. doi:10.3233/SHTI200584

79. Karapetiantz P, Bellet F, Audeh B, Lardon J, Leprovost D, Aboukhamis R, et al. Descriptions of adverse drug reactions are less informative in forums than in the French pharmacovigilance database but provide more unexpected reactions. *Front Pharmacol* (2018) **9**:439. doi:10.3389/fphar.2018.00439

80. Vaughan Sarrazin MS, Cram P, Mazur A, Ward M, Reisinger HS. Patient perspectives of dabigatran: analysis of online discussion forums. *Patient* (2014) **7**(1): 47–54. doi:10.1007/s40271-013-0027-y

81. Botsis T, Kreimeyer K. Improving drug safety with adverse event detection using natural language processing. *Expert Opin Drug Saf* (2023) **22**(8):659–68. doi:10.1080/14740338.2023.2228197

82. Dong F, Guo W, Liu J, Patterson TA, Hong H. BERT-based language model for accurate drug adverse event extraction from social media: implementation, evaluation, and contributions to pharmacovigilance practices. *Front Public Health* (2024) **12**:1392180. doi:10.3389/fpubh.2024.1392180

83. Zhang J, Wang X, Zhou Y. Comparative analysis of semaglutide induced adverse reactions: insights from FAERS database and social media reviews with a focus on oral vs subcutaneous administration. *Front Pharmacol* (2024) **15**:1471615. doi:10.3389/fphar.2024.1471615

84. Audeh B, Bellet F, Beyens MN, Lillo-Le Louët A, Bousquet C. Use of social media for pharmacovigilance activities: key findings and recommendations from the Vigi4Med project. *Drug Saf* (2020) **43**(9):835–51. doi:10.1007/s40264-020-00951-2

85. Karapetiantz P, Audeh B, Redjdal A, Tiffet T, Bousquet C, Jaulent MC. Monitoring adverse drug events in web forums: evaluation of a pipeline and use case study. *J Med Internet Res* (2024) **26**:e46176. doi:10.2196/46176

86. Li Y, Tao W, Li Z, Sun Z, Li F, Fenton S, et al. Artificial intelligence-powered pharmacovigilance: a review of machine and deep learning in clinical text-based adverse drug event detection for benchmark datasets. *J Biomed Inform* (2024) **152**: 104621. doi:10.1016/j.jbi.2024.104621

87. Destere A, Marchello G, Merino D, Othman NB, Gérard AO, Lavrut T, et al. An artificial intelligence algorithm for co-clustering to help in pharmacovigilance before and during the COVID-19 pandemic. *Br J Clin Pharmacol* (2024) **90**(5): 1258–67. doi:10.1111/bcp.16012

88. Carpenter KA, Altman RB. Using GPT-3 to build a lexicon of drugs of abuse synonyms for social media pharmacovigilance. *Biomolecules* (2023) **13**(2):387. doi:10.3390/biom13020387

89. Nasralah T, El-Gayar O, Wang Y. Social media text mining framework for drug abuse: development and validation study with an opioid crisis case analysis. *J Med Internet Res* (2020) **22**(8):e18350. doi:10.2196/18350

90. Chen X, Faviez C, Schuck S, Lillo-Le-Louët A, Texier N, Dahamna B, et al. Mining patients' narratives in social media for pharmacovigilance: adverse effects and misuse of methylphenidate. *Front Pharmacol* (2018) **9**:541. doi:10.3389/fphar.2018.00541

91. Sarker A, O'Connor K, Ginn R, Scotch M, Smith K, Malone D, et al. Social media mining for toxicovigilance: automatic monitoring of prescription medication abuse from twitter. *Drug Saf* (2016) **39**(3):231–40. doi:10.1007/s40264-015-0379-4

92. Allen MR, Wightman GP, Zhu Z, Poliak A, Smith DM, Dredze M, et al. Pharmacovigilance in the age of legalized cannabis: using social media to monitor drug-drug interactions between immunosuppressants and cannabis-derived products. *Drug Saf* (2024) **48**:99–105. doi:10.1007/s40264-024-01481-x

93. Vilar S, Friedman C, Hripcsak G. Detection of drug-drug interactions through data mining studies using clinical sources, scientific literature and social media. *Brief Bioinform* (2018) **19**(5):863–77. doi:10.1093/bib/bbx010

94. Correia RB, Li L, Rocha LM. Monitoring potential drug interactions and reactions via network analysis of Instagram user timelines. *Pac Symp Biocomput* (2016) **21**:492–503. doi:10.48550/arXiv.1510.01006

EBM Experimental Biology and Medicine

TYPE Review
PUBLISHED 23 September 2025
DOI 10.3389/ebm.2025.10746

OPEN ACCESS

*CORRESPONDENCE
Kai Shang,
kkai806@163.com

RECEIVED 11 July 2025
ACCEPTED 08 September 2025
PUBLISHED 23 September 2025

CITATION
Shang K, Liu Y and Qadeer A (2025) Platelet-rich plasma in peripheral nerve injury repair: a comprehensive review of mechanisms, clinical applications, and therapeutic potential.
Exp. Biol. Med. 250:10746.
doi: 10.3389/ebm.2025.10746

Platelet-rich plasma in peripheral nerve injury repair: a comprehensive review of mechanisms, clinical applications, and therapeutic potential

Kai Shang[1]*, Yang Liu[1] and Abdul Qadeer[2]

[1]Department of Orthopedic, The Affiliated Taian City Centeral Hospital of Qingdao University, Taian, Shandong, China, [2]Department of Cell Biology, School of Life Sciences, Central South University, Changsha, China

Abstract

Peripheral nerve injuries (PNIs) pose a significant clinical challenge, often leading to incomplete functional recovery despite current treatments. Platelet-rich plasma (PRP), which contains high levels of growth factors and bioactive molecules, has emerged as a promising regenerative therapy for nerve repair and restoring function. This review consolidates current evidence on PRP applications in treating peripheral nerve injuries, examining molecular mechanisms, clinical outcomes, and therapeutic potential. PRP markedly enhances nerve regeneration, improves recovery of sensory and motor functions, and alleviates neuropathic pain across various nerve injuries. It promotes axonal growth, reduces scar formation, stimulates Schwann cell proliferation, and modulates inflammation through the release of neurotrophic factors, including PDGF, VEGF, TGF-β, and IGF-1. Combining PRP with surgical techniques and biomaterial scaffolds yields better therapeutic results. Key factors influencing efficacy include platelet concentration, leukocyte content, activation methods, and patient-specific variables. PRP is a safe and effective option for peripheral nerve injury repair. However, challenges persist in standardizing preparation protocols, optimizing treatment timing, and fully understanding molecular mechanisms. Future research should focus on personalized PRP formulations, combination therapies, and large-scale randomized controlled trials to develop definitive clinical guidelines.

KEYWORDS

peripheral nerve injury, platelet-rich plasma, nerve regeneration, growth factors, neurotrophic factors, schwann cells, therapeutic target, regenerative medicine

Impact statement

Peripheral nerve injuries often lead to long-term disability, and current treatment options offer limited functional recovery. This review is important because it consolidates and critically evaluates the growing body of research on the use of platelet-rich plasma (PRP) as a novel, biologically based therapy for peripheral nerve repair. While PRP has gained attention in various fields of regenerative medicine, its role in nerve healing is still emerging and not yet standardized. By bringing together recent findings from both preclinical and clinical studies, this work provides new insight into how PRP promotes nerve regeneration through anti-inflammatory effects, stimulation of nerve-supporting cells, and delivery of growth factors that accelerate healing. It also explores how PRP can be combined with existing surgical and biomaterial approaches for improved outcomes. This review contributes to the field by highlighting both the therapeutic promise and the current limitations of PRP, and by outlining future research directions needed to optimize its clinical application. As such, it helps define a clearer path forward for integrating PRP into routine nerve injury management.

Introduction

The central nervous system (CNS), comprising the brain and spinal cord, acts as the central control hub that communicates with various body organs via an extensive network of nerve fibres extending throughout the peripheral nervous system. This communication occurs through electrical and chemical signals that facilitate coordinated physiological functions and responses to environmental stimuli. These peripheral nerves can be systematically classified based on their anatomical locations and functional characteristics into three primary categories: mixed nerves (containing both sensory and motor fibres), motor nerves (responsible for muscle contraction and movement), and sensory nerves (transmitting sensory information from receptors to the CNS) [1, 2].

Peripheral nerve injury (PNI) represents a significant global health concern and a leading cause of long-term disability, affecting millions of individuals worldwide with substantial socioeconomic implications. The consequences of PNI are often devastating, resulting in severe sensory-motor dysfunction that impairs daily activities, chronic neurogenic pain that significantly reduces quality of life, and potential permanent disability requiring long-term rehabilitation [3–5]. The etiology of PNI is diverse and multifactorial, encompassing neurodegenerative diseases that progressively damage nerve structure and function, acute open trauma from accidents or surgical procedures, and chronic nerve compression syndromes such as carpal tunnel syndrome or cubital tunnel syndrome [6, 7].

In the anatomically complex head and neck region, peripheral nerve injuries pose challenges due to the critical functional roles of affected nerves. Damage commonly affects several key cranial and peripheral nerves, including the inferior alveolar nerve (resulting in altered sensation in the lower lip and chin), the lingual nerve (causing taste disturbances and tongue numbness), the facial nerve (leading to facial paralysis and expression difficulties), and the hypoglossal nerve (affecting tongue movement and speech articulation). These injuries can severely impact essential functions such as mastication, speech, facial expression, and overall oral function [8].

While peripheral nerve fibres demonstrate a remarkable regenerative capacity and can achieve spontaneous healing within weeks to months under optimal conditions, this natural recovery process is often incomplete or insufficient, especially in cases involving significant nerve damage, large gaps, or unfavourable local conditions [9]. The clinical reality presents considerable therapeutic challenges, as fewer than half of patients with documented PNI undergo surgical nerve repair, often due to factors such as delayed diagnosis, patient comorbidities, or lack of specialized surgical expertise. Among those who do receive surgical intervention, only 40–50% attain complete functional recovery, highlighting the limitations of current treatment approaches and the urgent need for improved options [10]. Current management strategies include both surgical techniques (such as direct repair, nerve grafting, and nerve transfers) and conservative methods, with non-surgical treatments encompassing targeted physiotherapy programmes, emerging cell-based therapies using stem cells or Schwann cells (SC), and pharmaceutical interventions aimed at managing pain and encouraging nerve regeneration [3–5, 11].

Platelet-rich plasma (PRP) represents an innovative autologous biological therapeutic derived through centrifugal separation of the patient's own blood, specifically isolating the plasma fraction enriched with platelet concentrations that typically exceed normal physiological levels by 3-5-fold [12, 13]. This preparation process involves collecting whole blood, followed by specific centrifugation protocols that concentrate platelets while preserving their functional integrity and bioactive properties. The resulting PRP product serves as a potent reservoir of endogenous bioactive molecules, being particularly rich in multiple growth factors and cytokines essential for tissue repair and regeneration. These include granulocyte-macrophage colony-stimulating factor (GM-CSF) for cellular proliferation, vascular endothelial growth factor A (VEGF-A) for angiogenesis, epithelial growth factor (EGF) for cellular differentiation, transforming growth factor β (TGF-β) for tissue remodeling, platelet-derived growth factor (PDGF) for cellular migration and proliferation, hepatocyte growth factor (HGF) for neuroprotection, and insulin-like growth factor 1 (IGF-1) for nerve regeneration [14].

PRP has established a substantial clinical track record demonstrating therapeutic efficacy across diverse medical applications, including accelerated healing in sports-related injuries, enhanced recovery in spinal cord trauma, improved wound healing in chronic conditions, and successful outcomes in

plastic and reconstructive surgery procedures [15]. Specifically in the context of peripheral nerve injuries, PRP exhibits multifaceted therapeutic mechanisms, demonstrating significant neurogenic properties that promote nerve fibre regeneration, neuroprotective effects that prevent secondary nerve degeneration, and anti-inflammatory activities that modulate detrimental neuroinflammation while creating a favourable microenvironment for healing [8, 16–18]. These comprehensive therapeutic effects are mediated through PRP's complex role in orchestrating nerve regeneration processes, including SC proliferation, axonal sprouting, remyelination, and its documented capacity to alleviate debilitating neuropathic pain through modulation of inflammatory pathways and pain signaling mechanisms [19]. Compelling clinical evidence continues to emerge supporting PRP's therapeutic potential, as exemplified by the case study conducted by García de Cortázar et al. [20], who documented satisfactory neurological recovery and functional improvement in a patient with significant nerve injury following a structured PRP treatment protocol administered over 11 months [20].

Given the demonstrated therapeutic potential of PRP in managing peripheral nerve injuries, along with the urgent clinical need for more effective treatment methods to improve functional recovery, this comprehensive review aims to systematically summarize, critically analyze, and discuss current research progress on PRP applications for PNI. The review will evaluate both preclinical and clinical evidence, treatment protocols, outcomes, and future research directions to enhance PRP-based therapies for peripheral nerve injury management.

Application of PRP in the treatment of peripheral nerve injury

Accumulating evidence from both preclinical and clinical studies shows that PRP has multiple therapeutic properties vital for peripheral nerve repair. The main reason for PRP's effectiveness is its ability to regulate neuroinflammation through a dual mechanism involving direct platelet-derived anti-inflammatory mediators and the recruitment of reparative cell populations that release additional anti-inflammatory factors [21–23]. When activated, platelets in PRP release stored anti-inflammatory cytokines such as interleukin-10 (IL-10) and TGF-β, while also attracting macrophages, mesenchymal stem cells, and other regenerative cells to the injury site. These recruited cells further enhance the anti-inflammatory environment by secreting more anti-inflammatory mediators, resulting in a sustained therapeutic effect that lasts beyond the initial platelet activation phase.

Beyond these anti-inflammatory properties, PRP exhibits significant neuroprotective capabilities by preventing secondary neuronal death and promoting axonal survival following peripheral nerve injury. Furthermore, the neurogenic properties of PRP are mediated through the release of neurotrophic factors, including nerve growth factor (NGF), brain-derived neurotrophic factor (BDNF), and neurotrophin-3 (NT-3), which stimulate axonal sprouting, guide nerve fiber growth, and support the maintenance of neuronal phenotype during the regeneration process [1, 24]. Consequently, these growth factors work synergistically to create an optimal microenvironment that facilitates both proximal nerve stump survival and distal target reinnervation.

Building upon these fundamental mechanisms, the therapeutic potential of PRP has been extensively investigated across various peripheral nerve injuries, with consistent positive outcomes reported for multiple anatomical locations. Comprehensive studies have documented PRP's efficacy in treating injuries to major peripheral nerves, including the sciatic nerve, facial nerve, median nerve, and even applications extending to central nervous system pathologies [1, 21–24]. Moreover, the versatility of PRP treatment is further evidenced by its successful application in diverse clinical scenarios, ranging from complete nerve transection repairs to functional restoration across peripheral nerve gaps [25].

In addition to its regenerative capabilities, PRP therapy has demonstrated significant analgesic properties in treating neuropathic pain associated with peripheral nerve injuries. The pain-relieving mechanisms involve the downregulation of pro-inflammatory cytokines and the modulation of pain signaling pathways at both peripheral and central levels [18, 25–27]. Notably, recent studies have shown that PRP application effectively reduces neuropathic pain in osteoarthritis patients by specifically downregulating microglial activation in the spinal cord, thereby interrupting the central sensitization processes that contribute to chronic pain states [28]. This dual peripheral and central mechanism of pain relief represents a significant advantage over conventional analgesic approaches.

The mechanisms underlying these regenerative effects are significantly mediated through PRP's impact on Schwann cell biology. SC play a crucial role in peripheral nerve regeneration by providing structural support, producing neurotrophic factors, and facilitating remyelination of regenerating axons. Supporting this understanding, Salarinia et al. [29] demonstrated that PRP treatment significantly enhances SC proliferation in experimental spinal cord injury models in rats, leading to improved functional outcomes. Subsequently, investigations have confirmed PRP's ability to promote both SC migration to injury sites and their subsequent proliferation, creating a cellular environment conducive to nerve repair [25, 30]. These cellular effects are attributed to the growth factors present in PRP, particularly PDGF and HGF, which specifically target SC receptors and activate proliferation pathways.

Collectively, the diverse applications and mechanisms of PRP in peripheral nerve regeneration have been systematically documented across multiple research studies, with findings consistently supporting its therapeutic value in nerve repair, functional restoration, pain management, and treatment of degenerative neurological conditions [8, 31–36]. The

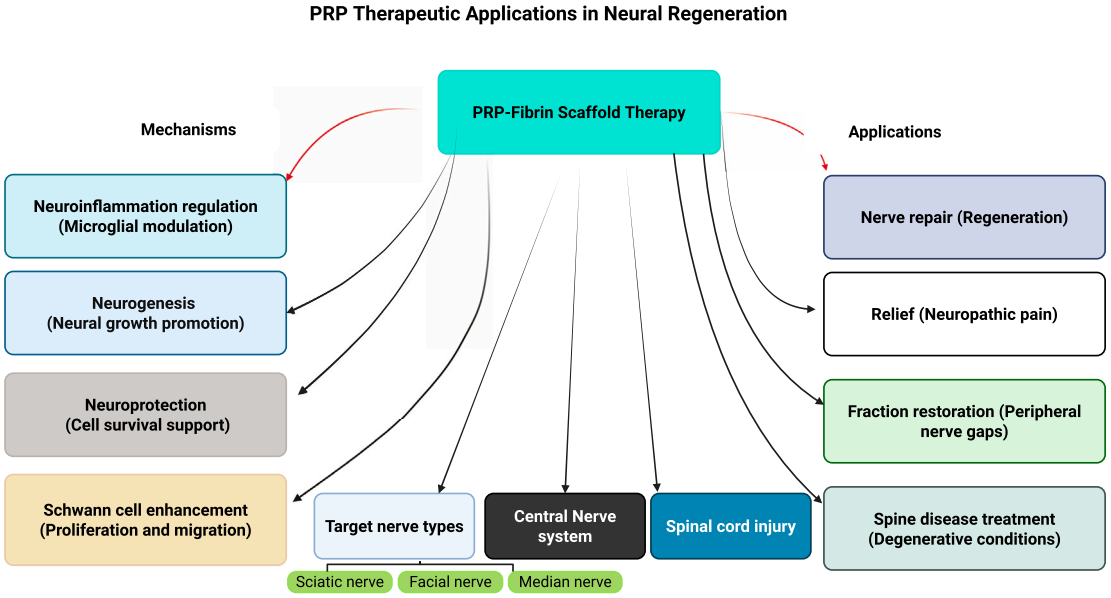

FIGURE 1
Comprehensive framework of platelet-rich plasma therapeutic applications in neural regeneration.

comprehensive body of evidence regarding PRP applications in various peripheral nerve regeneration scenarios is summarized in Figure 1, providing a systematic overview of treatment protocols, outcomes, and clinical effectiveness across different nerve injury types and anatomical locations.

Cellular and molecular mechanisms driving PRP therapy effects

The process of concentrating and separating platelets from the patient's own blood is known as PRP therapy. Upon activation, these platelets release a potent array of bioactive molecules stored within their granules, including cytokines, growth factors, and signaling molecules. These components are fundamental orchestrators of tissue repair and wound healing processes [37]. A primary mechanism involves the direct stimulation of cellular proliferation and differentiation essential for regeneration. Growth factors within PRP, such as PDGF, TGF-β, and VEGF, activate key cell types: mesenchymal stem cells (MSCs), promoting their proliferation and differentiation into various tissue-specific lineages; endothelial cells, stimulating angiogenesis to improve local vascularization; and fibroblasts, enhancing their synthesis of crucial extracellular matrix (ECM) components like collagen and fibronectin [38, 39].

Furthermore, PRP actively promotes the production of essential structural molecules, including fibronectin, collagen, and hyaluronic acid. Collectively, these molecules form a provisional ECM scaffold. This scaffold provides critical mechanical support to the healing site, facilitates cell migration, and creates a conducive environment for tissue regeneration [40]. Critically, PRP also activates and recruits local endogenous stem cells within the injury site, amplifying their potential to differentiate into the specific cell types needed for functional tissue repair [41]. Crucially, the efficacy of these regenerative processes, cellular activation, differentiation, and ECM synthesis, is profoundly enhanced by PRP's ability to modulate the inflammatory environment, shifting it towards a state optimal for repair [42, 43]. PRP exerts significant immunomodulatory actions, suppressing detrimental chronic inflammation and actively promoting resolution and regeneration. This anti-inflammatory activity is intrinsically linked to creating the permissive conditions necessary for the cellular and matrix-building activities described previously.

PRP achieves this essential immunomodulation through several interconnected pathways. Firstly, it serves as a rich source of potent anti-inflammatory molecules, including interleukin-1 receptor antagonist (IL-1ra), Interleukin-4 (IL-4), and Interleukin-10 (IL-10). IL-1ra directly inhibits the potent pro-inflammatory cytokine IL-1β, while IL-4 and IL-10 suppress the production of other key pro-inflammatory mediators like IL-6 and TNF-α, simultaneously promoting anti-inflammatory signaling cascades [42, 44]. Secondly, PRP stimulates the polarization of macrophages away from the pro-inflammatory M1 phenotype towards the anti-inflammatory, pro-repair M2 phenotype. These M2 macrophages secrete high levels of TGF-β and IL-10, further dampening inflammation, exhibit enhanced phagocytic activity to clear cellular debris, and directly contribute to tissue remodeling

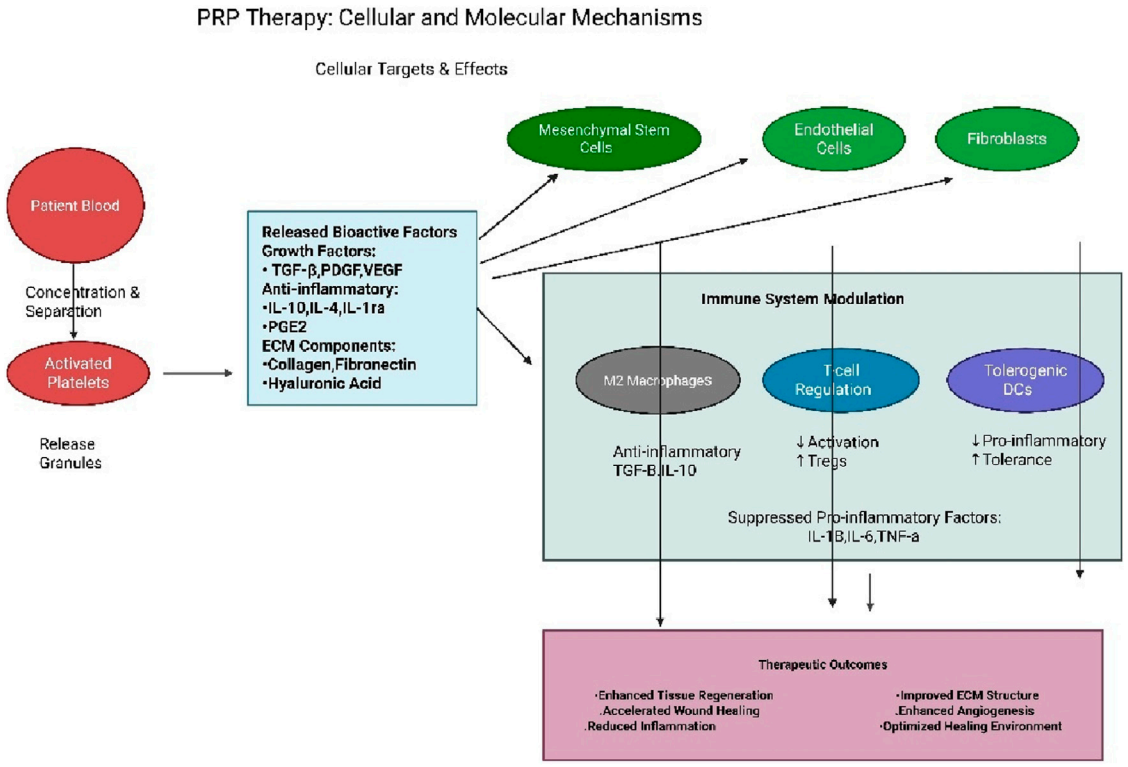

FIGURE 2
The schematic presentation of PRP cellular and molecular therapy.

[44]. Thirdly, components within PRP, notably TGF-β and Prostaglandin E2 (PGE2), act to regulate T-cell responses. TGF-β induces cell cycle arrest and apoptosis in T-cells, while PGE2 downregulates essential co-stimulatory molecules and cytokine receptors on their surface, thereby inhibiting T-cell activation and proliferation [45]. Fourthly, PRP influences dendritic cell (DC) function, promoting the development of tolerogenic DCs. These specialized DCs exhibit reduced expression of pro-inflammatory cytokines and co-stimulatory molecules, instead fostering immune tolerance and the generation of regulatory T-cells (Tregs) [46]. Finally, PRP directly enhances the development, proliferation, and function of Tregs themselves. Tregs are essential for maintaining immune tolerance; they suppress effector T-cells and other immune cells through mechanisms involving the release of anti-inflammatory cytokines (IL-10, TGF-β) and direct cell contact [47].

By orchestrating this complex immunomodulation alongside its direct regenerative effects on cells and matrix synthesis, PRP comprehensively supports the sequential phases of wound healing. During the initial inflammatory phase, PRP helps resolve inflammation efficiently and promotes the formation of granulation tissue. Subsequently, it actively drives the proliferation and migration of key cells like fibroblasts, endothelial cells, and keratinocytes. Finally, it supports the remodeling phase by providing the necessary matrix components and signals. This integrated action accelerates the overall healing process and enhances the functional quality and structural integrity of the regenerated tissue [48]. A schematic overview of PRP's cellular and molecular mechanisms is presented in Figure 2.

The combination of surgical and rehabilitative techniques with PRP therapy

The combination of surgical and rehabilitative techniques with PRP therapy encompasses multiple temporal approaches, each serving distinct therapeutic purposes. A recent exploratory study in rabbits demonstrated that preoperative PRP treatment of the implantation site significantly enhanced fat graft survival, with decreased inflammation and fibrosis and markedly improved angiogenesis compared to control groups [49].

Building upon this preoperative foundation, the therapeutic potential of PRP can be further maximized through its strategic application during the surgical procedure itself. Intraoperative PRP application refers to the planned incorporation of PRP as an integral component of the surgical procedure. This approach is

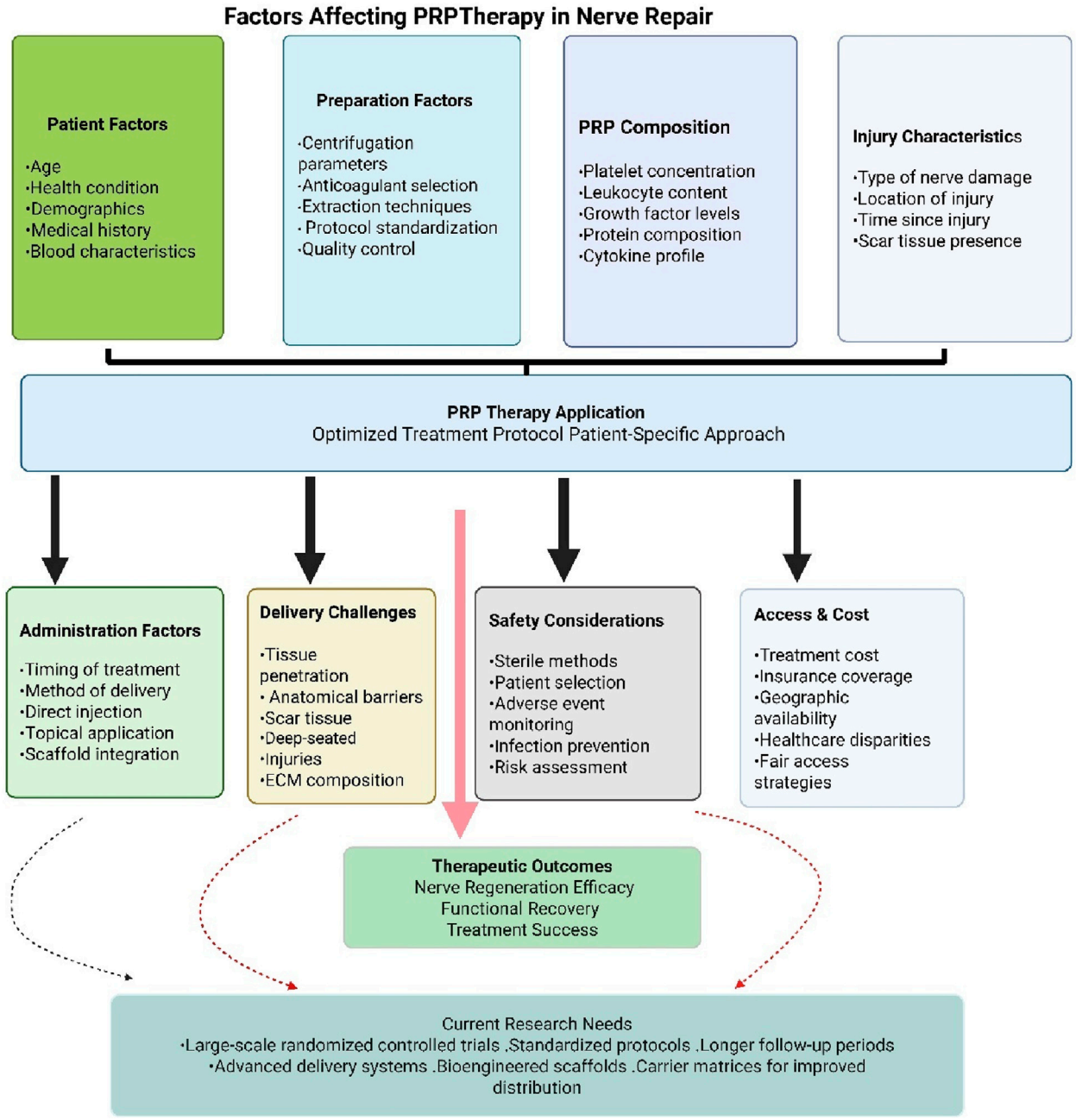

FIGURE 3
Summary of factors affecting PRP therapeutic potential.

typically applied during the final stages of surgery rather than throughout the entire operation, representing a primary therapeutic goal rather than an ancillary treatment. Surgeons strategically apply platelet-rich plasma directly to the surgical site or incorporate it into biological scaffolds immediately before wound closure. This optimizes tissue integration and regeneration through growth factors and bioactive substances that stimulate neovascularization and extracellular matrix production, ensuring maximum therapeutic benefit while the surgical site remains accessible [50].

Postoperative PRP therapy involves administering PRP injections into the surgical site during the recovery period to accelerate tissue regeneration and enhance functional recovery. This approach differs from intraoperative application as it occurs days to weeks after the initial surgical procedure. Postoperative PRP significantly accelerates tissue regeneration, reduces post-

TABLE 1 Therapeutic potential of PRP in peripheral nerve injury treatment.

PRP treatment	Outcomes in PNI	Species	References
PRP	PRP enhances locomotor recovery, spares white matter, promotes angiogenesis and neuronal regeneration, and modulates blood vessel size, leading to the recovery of spinal cord injuries	Rat	[15]
PRP	Promoted the radial nerve in musculoskeletal disorders	Human	[20]
PRP-derived exosomes	Promoted SC proliferation and dorsal root ganglion axon growth Increased the ability of MSCs to promote neural repair and regeneration in patients with PNI.	Mouse	[23, 24]
PRP gel +Collagen film	Promoted facial nerve regeneration	Rats	[53]
PRP	Recovered facial nerve injury followed by promoting vibrissae movement, eyelid closure, and electrophysiological function	Rat	[54]
PRP gel +Collagen/Chitosan composite film	Promoted the proliferation of SC, nerve regeneration and functional recovery in rats with sciatic nerve injury	Rat	[55]
PRP+ Low-dose ultrashort wave therapy	Improve sciatic nerve crush injury regeneration and recovery	Rabbit	[30]
PRP	Promoted nerve regeneration through improvement of angiogenesis and intracellular ubiquitin levels by regulating ITGB8, ribosomal protein S27a (RSP27a) and ubiquilin 1 (UBQLN1)	Rabbit	[56]
PRP + gelatin methacrylate and sodium alginate hydrogel	Enhances growth factors VEGF-A and PDGF-followed by promotion of the migration of SC and the neovascularization of endothelial cells to prevent sciatic nerve defects and facilitate the repairing of peripheral nerve	Rat	[57]
Platelet-rich fibrin	The axon regeneration of the sciatic nerve and sensory function was improved with nerve conduit filled with platelet-rich fibrin Repair peripheral nerve defects	Mouse	[58]
PRP-derived exosomes	Promoted the nerve regeneration by enhancing the proliferation, migration, and secretion of trophic factors by SC	Rat	[59]
PRP	Enhanced the proliferation, secretion and migration of SCs and the regeneration of axons in the early stage as well as VEGF expression and improved repairing of tibial nerve defects	Rabbit	[60]
Freeze-dried PRP	Increased the expression of nerve growth factor and S100B Induced neuro-regeneration and relieved chronic orofacial pain	Rats	[61]
PRP	Treatment of recurrent laryngeal nerve injury Regeneration Promoted the proliferation and migration of SC	Rabbit	[62]
Human umbilical cord blood+ PRP	Improved the spinal cord injury regeneration	Rat	[63, 64]
PRP + chitin	Facilitate the repairing of sciatic nerve defects	Rat	[65]
Platelet-rich fibrin	Enhanced the sciatic nerve regeneration	Rat	[66]
PRP	Enhanced the mature SC proliferation, and microenvironment in the small gap and promote peripheral nerve regeneration	Rabbit	[67]
PRP+ adipose tissue–derived stem cells	Improve recovering of sciatic nerve repairing and prevent its defects	Rat	[68]
PRP+ adipose tissue–derived stem cells	Enhanced the spinal cord injury recovery and improved of repairing central nervous system	Rat	[69]
PRP + Citicoline	Improved sciatic nerve injury following recovery of peripheral nerve injury	Rat	[70]

(Continued on following page)

TABLE 1 (*Continued*) Therapeutic potential of PRP in peripheral nerve injury treatment.

PRP treatment	Outcomes in PNI	Species	References
Leukocyte-platelet rich fibrin	Suppressed proinflammatory cytokines followed by prevention of peripheral nerve inflammation and injuries Facilitated peripheral nerve regeneration	Rat	[71]
PRP	Induces nerve regeneration by promoting neurotrophic factors and anti-inflammatory cytokines by calcium chloride activation Facilitated the recovery of spinal cord dorsal root repair	Rat	[71]
PRP	Improved regeneration and proliferation of SC	Rabbit	[72]
Platelet-rich fibrin	Facilitated the regeneration of sciatic nerves and peripheral nerve injury	Rat	[73]
Platelet-rich fibrin	Improved the regeneration of sciatic nerve Showed positive effect on maxillofacial tissues regeneration	Rabbit	[74]
PRP	Promoted the healing of digital nerve crush injury Decreased the neuropathic pain	Human	[75]

surgical inflammation, and promotes optimal wound healing during the critical recovery phase. The therapy directly delivers growth factors and cytokines to the surgical site through targeted injections that promote angiogenesis, collagen deposition, and cellular proliferation [51].

Integration with rehabilitation protocols represents an advanced approach where PRP therapy is strategically combined with physical therapy and rehabilitation programs following surgical procedures. Physical therapists can incorporate PRP injections as a complementary tool within comprehensive rehabilitation programs to enhance neuromuscular re-education, improve joint stability, and accelerate tissue repair processes. This integrated approach leverages PRP's ability to enhance the healing of injured tissues, reduce pain levels, and improve muscle strength. The synergistic effect of combining biological enhancement with mechanical stimulation ultimately enables a more complete and expedited return to pre-injury functional capacity [52].

Impact of PRP in peripheral nerve injury recovery

The role of PRP in peripheral nerve injury recovery has been summarized in Table 1. PRP represents a concentrated autologous preparation derived from patient blood that contains elevated concentrations of platelets and bioactive growth factors essential for tissue regeneration. The therapeutic mechanism underlying PRP's efficacy centers on its ability to secrete critical growth factors, including PDGF, which promotes cellular proliferation; TGF-β, which modulates inflammatory responses and stimulates tissue repair; and VEGF, which promotes neovascularization to support regenerating neural tissue. Given that PRP is autologous in nature, it exhibits minimal risk of immunogenic reactions, establishing it as a promising therapeutic modality for peripheral nerve injury management [76].

Numerous preclinical and clinical studies across various nerve types, including facial, sciatic, and median nerves, have widely supported the positive effect of PRP on peripheral nerve healing [30, 53, 55–57, 77–85]. In models of facial nerve injury, experimental research showed that PRP can greatly enhance therapeutic outcomes when combined with biocompatible materials like chitosan, which serves as a structured scaffold for controlled and sustained release of growth factors at the injury site [53, 78]. Li et al. showed that PRP has neuroprotective effects on traumatic facial nerve injuries, with notable recovery of SC and significant axonal regeneration [54]. Likewise, studies on sciatic nerve injury consistently indicate that autologous PRP supports nerve regeneration by decreasing M1 macrophages and altering the inflammatory environment [32, 79, 80, 86–89].

PRP has been shown to stimulate SC proliferation and secretion while promoting angiogenesis and affecting intracellular signaling pathways. Notably, PRP significantly upregulated the expression of integrin subunit β-8 (ITGB8), which plays a critical role in angiogenesis after nerve injury [56]. When combined with biomaterial scaffolds such as collagen/chitosan composite membranes or gelatin methacrylate hydrogels, PRP has demonstrated enhanced efficacy in promoting both functional and structural nerve recovery [55, 81, 82].

In median nerve applications, particularly for carpal tunnel syndrome treatment, PRP has shown superior outcomes compared to corticosteroids in clinical trials, providing significant pain relief and functional improvement [77, 83–85, 90–93]. Studies have demonstrated that ultrasound guided PRP injections can provide effective treatment for up to 1 year post-

injection, with predictive factors including patient body weight, distal motor latency, and median nerve cross-sectional area [77, 85].

In recent years, progress in platelet research has highlighted the significance of platelet-derived extracellular vesicles (EVs), including exosomes, and their role in facilitating intercellular communication [94]. A study conducted by Yi et al. [59] isolated platelet-rich plasma–derived exosomes (PRP-Exos) and found that they markedly promoted SC proliferation, migration, and secretion of trophic factors. Additionally, PRP-Exos induced notable changes in both transcriptional and protein expression within SCs, especially increasing the expression of genes crucial for nerve repair. In a rat sciatic nerve crush model, the application of ultrasound-targeted microbubble destruction (UTMD) significantly improved the delivery of PRP-Exos to the injury site, resulting in greater exosome accumulation locally and enhanced regenerative and functional outcomes compared to untreated controls [59].

Other studies have shown that PRP-Exos improve MSC survival by reducing apoptosis, preserving stemness, and delaying senescence. Pretreated MSCs (pExo-MSCs) demonstrated better retention *in vivo*, resulting in enhanced axonal regeneration, remyelination, and neurological recovery. *In vitro*, they further encouraged SC proliferation and dorsal root ganglion axonal extension, mainly through glial cell–derived neurotrophic factor (GDNF) secretion and activation of the PI3K/Akt pathway [24].

Similarly, Zhang et al. (2024) reported that PRP-Exo–treated MSCs (MSCPExo) enhanced SC proliferation and reduced apoptosis after peripheral nerve injury (PNI). Conditioned medium from MSC^{PExo} ($MSC^{PExo\text{-}CM}$) further stimulated SC proliferation, migration, and angiogenesis. Proteomic analysis of the MSC^{PExo} secretome identified 440 proteins, many of which showed strong pro-regenerative and angiogenic functions. ELISA confirmed the enrichment of key trophic factors, and Western blotting validated PI3K/Akt pathway activation. Collectively, these findings highlight PRP-Exos as potent enhancers of MSC paracrine activity and valuable modulators of neural repair [23].

Factors affecting PRP therapy in nerve repair

The factors affecting PRP effectiveness are detailed in Table 2 and depicted graphically in Figure 3 for enhanced clarity. The technique used for preparation, the parameters of centrifugation, and patient-specific characteristics such as age and health condition can significantly influence the composition of PRP. Research demonstrates that PRP efficacy decreases with increasing age, with PRP derived from young donors (18–35 years) showing significantly better therapeutic outcomes compared to PRP from older donors (≥65 years) [124]. Studies show that growth factor levels, including PDGF-BB, TGF-β1, IGF-1, and EGF, are statistically higher in subjects younger than 25 years compared to those aged 26 years or older [125]. Additionally, PRP derived from women older than 45 years does not contain significantly higher concentrations of bioactive components compared to younger groups, suggesting that aging significantly affects the active components of PRP [126]. At the cellular level, elderly patients show decreased numbers of α-granules in platelets, which are the main component releasing active substances, leading to decreased platelet function [127]. Clinical evidence supports these laboratory findings, with PRP therapy showing poor efficacy in elderly patients (≥60 years) for conditions such as facial rejuvenation and Achilles tendinitis treatment [124].

The therapeutic efficacy of PRP in peripheral nerve repair demonstrates significant variability due to differences in leukocyte content, growth factor concentrations, and platelet density across various PRP formulations [128–130]. This heterogeneity underscores the critical need for standardized preparation protocols encompassing appropriate anticoagulant selection, optimal centrifugation parameters, and consistent extraction methodologies to ensure reproducible outcomes in both research and clinical applications [131, 132]. Despite encouraging results from preclinical investigations and early-phase clinical trials, the current body of clinical evidence remains insufficient to definitively establish PRP's effectiveness in nerve repair and regeneration. Existing studies frequently exhibit methodological limitations, including inadequate sample sizes, absence of appropriate control groups, heterogeneous patient populations, and insufficient follow-up durations. Large-scale randomized controlled trials employing standardized protocols and extended observation periods are essential to establish the safety profile, therapeutic efficacy, and optimal clinical applications of PRP therapy in nerve regeneration [133]. Achieving adequate PRP distribution and tissue penetration presents additional complexities, particularly in cases involving scar tissue formation or deep-seated injuries. Anatomical barriers, tissue density variations, and extracellular matrix composition may impede PRP penetration into the neuronal microenvironment, potentially limiting regenerative efficacy. Advanced delivery systems incorporating carrier matrices or bioengineered scaffolds may enhance PRP distribution and retention at nerve injury sites [88]. While PRP therapy generally demonstrates a favorable safety profile, specific risks associated with nerve regeneration applications include hypersensitivity reactions, iatrogenic nerve injury, hematoma formation, and infection. Rigorous adherence to sterile protocols, careful patient selection criteria, and comprehensive adverse event monitoring are essential to minimize these risks and ensure treatment safety [134]. Additionally, therapeutic accessibility remains constrained by economic factors, particularly in regions where insurance coverage or healthcare systems do not support the costs of

TABLE 2 Factors affecting the efficacy of PRP.

Parameters affecting PRP efficacy	Biological outcomes of PRP	References
Concentration of platelet	The platelets concentration in PRP can vary depending on how it is prepared, and the equipment used. Higher platelet concentrations are generally associated with better outcomes, but there is an optimal range, and too high concentrations may not be beneficial	[95, 96]
Contents of leukocyte	PRP can be categorized as either leukocyte-rich or leukocyte-poor, depending on whether leukocytes are present or absent. The amount of leukocytes present can impact the inflammatory response and the healing of tissues	[97–100]
Method of activation for PRP	PRP can be activated through different methods, including thrombin, calcium chloride, or exposure to collagen. This activation subsequently triggers the release of growth factors from platelets, thereby influencing the regenerative properties of PRP.	[101–104]
Buffy coat removal	The method used to separate the buffy coat from whole blood during PRP preparation determines the purity and composition of PRP.	[105, 106]
Time and speed utilized for centrifugation	The separation of blood components and the final composition of PRP are determined by the speed and duration of centrifugation. It is crucial to use optimal centrifugation parameters to obtain PRP with the desired properties	[107–109]
Types of anticoagulants	Anticoagulants like citrate or heparin are utilized to prevent clotting while collecting blood. The selection of anticoagulant can impact the activation of platelets and the stability of PRP.	[43, 106, 110]
Injectable formulation	PRP can be administered in either liquid or gel form, depending on the specific clinical application. The injectable form chosen has a significant impact on the ease of administration and how PRP is distributed within the tissues	[111–114]
Composition of growth factor	The concentration and composition of growth factors, such as TGF-β, PDGF, and VEGF, can vary among different PRP preparations. The specific growth factors released by the platelets and their concentrations play a critical role in the regenerative and healing processes	[115–117]
Injected PRP volume	The distribution, diffusion, and therapeutic effects of PRP in the target tissue can be influenced by the volume injected	[70, 107]
Factors specific to the patient	The response to PRP treatment can be affected by various factors, including age, sex, underlying health conditions, and medications	[118–120]
Clinical hallmarks	The choice of PRP preparation and administration protocol is influenced by the specific condition being treated, such as tendonitis, osteoarthritis, or wound healing, as well as the targeted tissue PRP therapy may be more effective for certain types of tissues, such as tendons, ligaments, and cartilage, compared to others. Additionally, mild to moderate injuries tend to respond better to PRP than severe or chronic conditions. Furthermore, areas with a good blood supply may exhibit enhanced healing with the use of PRP therapy	[18, 34, 121]
Content of fibrin	Fibrin, present in PRP, plays a crucial role in both clot formation and tissue healing. Certain classification systems differentiate PRP preparations based on their fibrin content, categorizing them as either fibrin-rich or fibrin-poor, according to their clotting characteristics and regenerative capabilities	[43, 122]
Contamination of red blood cells	Contamination of red blood cells (RBCs) in PRP can significantly impact the quality and efficacy of PRP in various therapeutic applications	[41, 123]

PRP therapy. Geographic and institutional limitations further compound healthcare disparities. Addressing these challenges requires comprehensive strategies to reduce treatment costs, expand reimbursement coverage, and improve therapeutic accessibility to ensure equitable patient access to this potentially beneficial regenerative approach [110].

Conclusion

The exploration of PRP as a treatment target for PNIs has shown significant promise, especially when PRP is obtained through plasmapheresis. This review emphasizes the positive outcomes seen in both clinical and preclinical studies, where PRP treatment has been linked to better nerve regeneration, improved sensory and motor functions, and less pain. Preclinical studies have provided valuable insights into how PRP promotes nerve repair, including encouraging axonal growth and reducing scar formation. Despite these promising results, several obstacles remain when turning preclinical findings into clinical practice. These include species-specific differences and the need for thorough clinical evaluations to confirm safety and effectiveness in humans. Standardizing PRP preparation methods and optimizing treatment timing are essential steps to improve the consistency and reliability of PRP therapy outcomes. Future research should aim to better understand the molecular

mechanisms behind PRP's therapeutic effects, refine treatment protocols, and expand its clinical use. By tackling these challenges and integrating insights from both human and animal studies, the full potential of PRP as a strong option for nerve regeneration and functional recovery in patients with PNI can be achieved.

Author contributions

Conceptualization, methodology, writing – original draft, data curation, validation, writing – review and editing, KS, YL, and AQ; supervision, resources, and funding: KS. All authors contributed to the article and approved the submitted version.

Funding

The author(s) declare that financial support was received for the research and/or publication of this article. This work was supported by the Tai'an Science and Technology Development Plan Project (2019NS236).

Conflict of interest

The author(s) declared no potential conflicts of interest with respect to the research, authorship, and/or publication of this article.

Generative AI statement

The author(s) declare that no Generative AI was used in the creation of this manuscript.

Any alternative text (alt text) provided alongside figures in this article has been generated by Frontiers with the support of artificial intelligence and reasonable efforts have been made to ensure accuracy, including review by the authors wherever possible. If you identify any issues, please contact us.

References

1. Wang S, Liu Z, Wang J, Cheng L, Hu J, Tang J. Platelet-rich plasma (PRP) in nerve repair. *Regenerative Ther* (2024) **27**:244–50. doi:10.1016/j.reth.2024.03.017

2. Wei C, Guo Y, Ci Z, Li M, Zhang Y, Zhou Y. Advances of schwann cells in peripheral nerve regeneration: from mechanism to cell therapy. *Biomed and Pharmacother* (2024) **175**:116645. doi:10.1016/j.biopha.2024.116645

3. Zhang PX, Li C, Liu SY, Pi W. Cortical plasticity and nerve regeneration after peripheral nerve injury. *Neural Regen Res* (2021) **16**:1518–23. doi:10.4103/1673-5374.303008

4. Xu JG, Xing XX, Zheng MX, Hua XY, Ma SJ, Ma ZZ. Brain plasticity after peripheral nerve injury treatment with massage therapy based on resting-state functional magnetic resonance imaging. *Neural Regen Res* (2021) **16**:388–93. doi:10.4103/1673-5374.290912

5. Martínez-Marcos A, Sañudo JR. Cranial nerves: morphology and clinical relevance. *The Anatomical Rec* (2019) **302**:555–7. doi:10.1002/ar.24106

6. Gu D, Xia Y, Ding Z, Qian J, Gu X, Bai H, et al. Inflammation in the peripheral nervous system after injury. *Biomedicines* (2024) **12**:1256. doi:10.3390/biomedicines12061256

7. Tian H, Chen BP, Li R, Qu WR, Zhu Z, Liu J, et al. Interaction between schwann cells and other cells during repair of peripheral nerve injury. *Neural Regen Res* (2021) **16**:93–8. doi:10.4103/1673-5374.286956

8. Wang S, Liu X, Wang Y. Evaluation of platelet-rich plasma therapy for peripheral nerve regeneration: a critical review of literature. *Front Bioeng Biotechnol* (2022) **10**:808248. doi:10.3389/fbioe.2022.808248

9. Sammartino G, Tia M, Marenzi G, Espedito di Lauro A, D'Agostino E, Claudio PP. Use of autologous platelet-rich plasma (PRP) in periodontal defect treatment after extraction of impacted mandibular third molars. *J Oral Maxillofacial Surg* (2005) **63**:766–70. doi:10.1016/j.joms.2005.02.010

10. Kouyoumdjian JA, Graça C, Ferreira VM. Peripheral nerve injuries: a retrospective survey of 1124 cases. *Neurol India* (2017) **65**:551–5. doi:10.4103/neuroindia.ni_987_16

11. He F, Gu XS, Chu XL, Song XZ, Li Q, Li YR, et al. Basic mechanisms of peripheral nerve injury and treatment *via* electrical stimulation. *Neural Regen Res* (2022) **17**:2185–93. doi:10.4103/1673-5374.335823

12. Machado ES, Leite R, Dos Santos CC, Artuso GL, Gluszczak F, de Jesus LG, et al. Turn Down - turn up: a simple and low-cost protocol for preparing platelet-rich plasma. *Clinics (Sao Paulo)* (2019) **74**:e1132. doi:10.6061/clinics/2019/e1132

13. Mercader-Ruiz J, Beitia M, Delgado D, Sánchez P, Porras B, Gimeno I, et al. Current challenges in the development of platelet-rich plasma-based therapies. *Biomed Res Int* (2024) **2024**:6444120. doi:10.1155/2024/6444120

14. Malange KF, de Souza DM, Lemes JBP, Fagundes CC, Oliveira ALL, Pagliusi MO, et al. The implications of brain-derived neurotrophic factor in the biological activities of platelet-rich plasma. *Inflammation* (2024) **48**:426–46. doi:10.1007/s10753-024-02072-9

15. Chen NF, Sung CS, Wen ZH, Chen CH, Feng CW, Hung HC, et al. Therapeutic effect of platelet-rich plasma in rat spinal cord injuries. *Front Neurosci* (2018) **12**:252. doi:10.3389/fnins.2018.00252

16. Pandunugrahadi M, Irianto KA, Sindrawati O. The optimal timing of platelet-rich plasma (PRP) injection for nerve lesion recovery: a preliminary study. *Int J Biomater* (2022) **2022**:1–7. doi:10.1155/2022/9601547

17. Cao Y, Zhu X, Zhou R, He Y, Wu Z, Chen Y. A narrative review of the research progress and clinical application of platelet-rich plasma. *Ann Palliat Med* (2021) **10**:4823–9. doi:10.21037/apm-20-2223

18. Huang S, Li Q, Li X, Ye H, Zhang L, Zhu X. Recent research progress of wound healing biomaterials containing platelet-rich plasma. *Int J Nanomedicine* (2025) **20**:3961–76. doi:10.2147/ijn.s506677

19. Bohren Y, Timbolschi DI, Muller A, Barrot M, Yalcin I, Salvat E. Platelet-rich plasma and cytokines in neuropathic pain: a narrative review and a clinical perspective. *Eur J Pain* (2022) **26**:43–60. doi:10.1002/ejp.1846

20. García de Cortázar U, Padilla S, Lobato E, Delgado D, Sánchez M. Intraneural platelet-rich plasma injections for the treatment of radial nerve section: a case report. *J Clin Med* (2018) **7**:13. doi:10.3390/jcm7020013

21. Jin X, Fu J, Lv R, Hao X, Wang S, Sun M, et al. Efficacy and safety of platelet-rich plasma for acute nonarteritic anterior ischemic optic neuropathy: a prospective cohort study. *Front Med (Lausanne)* (2024) **11**:1344107. doi:10.3389/fmed.2024.1344107

22. Smail SW, Abdulqadir SZ, Alalem LSS, Rasheed TK, Khudhur ZO, Mzury AFA, et al. Enhancing sciatic nerve regeneration with osteopontin-loaded acellular nerve allografts in rats: effects on macrophage polarization. *Tissue and Cell* (2024) **88**:102379. doi:10.1016/j.tice.2024.102379

23. Zhang Y, Yi D, Hong Q, Liu C, Chi K, Liu J, et al. Platelet-rich plasma-derived exosomes enhance mesenchymal stem cell paracrine function and nerve regeneration potential. *Biochem Biophysical Res Commun* (2024) **699**:149496. doi:10.1016/j.bbrc.2024.149496

24. Zhang Y, Yi D, Hong Q, Cao J, Geng X, Liu J, et al. Platelet-rich plasma-derived exosomes boost mesenchymal stem cells to promote peripheral nerve

regeneration. *J Controlled Release* (2024) **367**:265–82. doi:10.1016/j.jconrel.2024.01.043

25. Kuffler DP. PRP and other techniques for restoring function across peripheral nerve gaps. *J Neurorestoratology* (2024) **12**:100131. doi:10.1016/j.jnrt.2024.100131

26. Kataria S, Wijaya JH, Patel U, Yabut K, Turjman T, Ayub MA, et al. The role of platelet rich plasma in vertebrogenic and discogenic pain: a systematic review and meta-analysis. *Curr Pain Headache Rep* (2024) **28**:825–33. doi:10.1007/s11916-024-01274-y

27. Schol J, Tamagawa S, Volleman TNE, Ishijima M, Sakai D. A comprehensive review of cell transplantation and platelet-rich plasma therapy for the treatment of disc degeneration-related back and neck pain: a systematic evidence-based analysis. *JOR Spine* (2024) **7**:e1348. doi:10.1002/jsp2.1348

28. Yan X, Ye Y, Wang L, Xue J, Shen N, Li T. Platelet-rich plasma alleviates neuropathic pain in osteoarthritis by downregulating microglial activation. *BMC Musculoskelet Disord* (2024) **25**:331. doi:10.1186/s12891-024-07437-7

29. Salarinia R, Sadeghnia HR, Alamdari DH, Hoseini SJ, Mafinezhad A, Hosseini M. Platelet rich plasma: effective treatment for repairing of spinal cord injury in rat. *Acta Orthopaedica et Traumatologica Turcica* (2017) **51**:254–7. doi:10.1016/j.aott.2017.02.009

30. Zhu Y, Jin Z, Wang J, Chen S, Hu Y, Ren L, et al. Ultrasound-guided platelet-rich plasma injection and multimodality ultrasound examination of peripheral nerve crush injury. *NPJ Regen Med* (2020) **5**:21. doi:10.1038/s41536-020-00101-3

31. Apostolakis S, Kapetanakis S. Platelet-rich plasma for degenerative spine disease: a brief overview. *Spine Surg Relat Res* (2024) **8**:10–21. doi:10.22603/ssrr.2023-0079

32. Bastami F, Vares P, Khojasteh A. Healing effects of platelet-rich plasma on peripheral nerve injuries. *J Craniofac Surg* (2017) **28**:e49–e57. doi:10.1097/scs.0000000000003198

33. Fernandes M, Valente S, Santos J, Furukawa R, Fernandes C, Leite V, et al. Platelet-rich fibrin conduits as an alternative to nerve autografts for peripheral nerve repair. *J Reconstr Microsurg* (2017) **33**:549–56. doi:10.1055/s-0037-1603355

34. Delgado D, Padilla S, Sánchez M, Garate A. Platelet-rich plasma, an adjuvant biological therapy to assist peripheral nerve repair. *Neural Regen Res* (2017) **12**:47–52. doi:10.4103/1673-5374.198973

35. Spartalis E, Athanasiou A, Spartalis M, Moris D, Papalampros A, Nikiteas N. Platelet-rich plasma and peripheral nerve regeneration: a potential contraindication to its use after tumor excision. *Expert Opin Biol Ther* (2017) **17**:1045–6. doi:10.1080/14712598.2017.1349480

36. Dou X-Y, An M. Advances in the application of platelet-rich plasma in peripheral nerve injuries. *Anesthesiology Perioper Sci* (2025) **3**:19. doi:10.1007/s44254-025-00100-x

37. Anitua E, Pino A, Azkargorta M, Elortza F, Prado R. High-throughput proteomic analysis of human dermal fibroblast response to different blood derivatives: autologous topical serum derived from plasma rich in growth factors (PRGF) *versus* Leukocyte- and platelet-rich plasma (L-PRP). *Biomolecules* (2022) **12**:1002. doi:10.3390/biom12071002

38. Tatsis D, Vasalou V, Kotidis E, Anestiadou E, Grivas I, Cheva A, et al. The combined use of platelet-rich plasma and adipose-derived mesenchymal stem cells promotes healing. A review of experimental models and future perspectives. *Biomolecules* (2021) **11**:1403. doi:10.3390/biom11101403

39. Foster TE, Puskas BL, Mandelbaum BR, Gerhardt MB, Rodeo SA. Platelet-rich plasma: from basic science to clinical applications. *Am J Sports Med* (2009) **37**:2259–72. doi:10.1177/0363546509349921

40. Stoffels JM, Zhao C, Baron W. Fibronectin in tissue regeneration: timely disassembly of the scaffold is necessary to complete the build. *Cell Mol Life Sci* (2013) **70**:4243–53. doi:10.1007/s00018-013-1350-0

41. Everts P, Onishi K, Jayaram P, Lana JF, Mautner K. Platelet-rich plasma: new performance understandings and therapeutic considerations in 2020. *Int J Mol Sci* (2020) **21**:7794. doi:10.3390/ijms21207794

42. Cheng PG, Yang KD, Huang LG, Wang CH, Ko WS. Comparisons of cytokines, growth factors and clinical efficacy between platelet-rich plasma and autologous conditioned serum for knee osteoarthritis management. *Biomolecules* (2023) **13**:555. doi:10.3390/biom13030555

43. Zhang Z, Liu P, Xue X, Zhang Z, Wang L, Jiang Y, et al. The role of platelet-rich plasma in biomedicine: a comprehensive overview. *iScience* (2025) **28**:111705. doi:10.1016/j.isci.2024.111705

44. Mochizuki T, Ushiki T, Suzuki K, Sato M, Ishiguro H, Suwabe T, et al. Elevated IL-1β and comparable IL-1 receptor antagonist levels are characteristic features of L-PRP in female college athletes compared to Male professional soccer players. *Int J Mol Sci* (2023) **24**:17487. doi:10.3390/ijms242417487

45. Kulesza A, Paczek L, Burdzinska A. The role of COX-2 and PGE2 in the regulation of immunomodulation and other functions of mesenchymal stromal cells. *Biomedicines* (2023) **11**:445. doi:10.3390/biomedicines11020445

46. Iberg CA, Hawiger D. Natural and induced tolerogenic dendritic cells. *The J Immunol* (2020) **204**:733–44. doi:10.4049/jimmunol.1901121

47. Xie M, Xiong W, She Z, Wen Z, Abdirahman AS, Wan W, et al. Immunoregulatory effects of stem cell-derived extracellular vesicles on immune cells. *Front Immunol* (2020) 11–2020. doi:10.3389/fimmu.2020.00013

48. Manole CG, Soare C, Ceafalan LC, Voiculescu VM. Platelet-rich plasma in dermatology: new insights on the cellular mechanism of skin repair and regeneration. *Life (Basel)* (2023) **14**:40. doi:10.3390/life14010040

49. Pak I, Askarov M, Klyuyev D, Tak MS, Batenova U, Yeskermessov D, et al. PRP pre-treatment of the implantation zone improves the survival rate of fat autograft. *Front Bioeng Biotechnol* (2025) 13–2025. doi:10.3389/fbioe.2025.1545419

50. Milano G, Sánchez M, Jo CH, Saccomanno MF, Thampatty BP, Wang JHC. Platelet-rich plasma in orthopaedic sports medicine: state of the art. *J ISAKOS* (2019) **4**:188–95. doi:10.1136/jisakos-2019-000274

51. Xu P, Wu Y, Zhou L, Yang Z, Zhang X, Hu X, et al. Platelet-rich plasma accelerates skin wound healing by promoting re-epithelialization. *Burns and Trauma* (2020) **8**:tkaa028. doi:10.1093/burnst/tkaa028

52. Thu AC. The use of platelet-rich plasma in management of musculoskeletal pain: a narrative review. *J Yeungnam Med Sci* (2022) **39**:206–15. doi:10.12701/jyms.2022.00290

53. Şahin MM, Cayonu M, Dinc SK, Ozkocer E, Ilhan M, Uzunoğlu E, et al. Effects of chitosan and platelet-rich plasma on facial nerve regeneration in an animal model. *Eur Arch Otorhinolaryngol* (2022) **279**:987–94. doi:10.1007/s00405-021-06859-6

54. Li L, Cai J, Yuan Y, Mao Y, Xu L, Han Y, et al. Platelet-rich plasma can release nutrient factors to promote facial nerve crush injury recovery in rats. *Saudi Med J* (2019) **40**:1209–17. doi:10.15537/smj.2019.12.24747

55. Yuan B, Zheng X, Wu ML, Yang Y, Chen JW, Gao HC, et al. Platelet-rich plasma gel-loaded collagen/chitosan composite film accelerated rat sciatic nerve injury repair. *ACS Omega* (2023) **8**:2931–41. doi:10.1021/acsomega.2c05351

56. Wang YS, Wang SL, Liu XL, Kang ZC. Platelet-rich plasma promotes peripheral nerve regeneration after sciatic nerve injury. *Neural Regen Res* (2023) **18**:375–81. doi:10.4103/1673-5374.346461

57. Khaled MM, Ibrahium AM, Abdelgalil AI, El-Saied MA, Yassin AM, Abouquerin N, et al. Efficacy of using adipose-derived stem cells and PRP on regeneration of 40 -mm long sciatic nerve defect bridged by polyglycolic-polypropylene mesh in canine model. *Stem Cell Res Ther* (2024) **15**:212. doi:10.1186/s13287-024-03796-z

58. Hama S, Yokoi T, Orita K, Uemura T, Takamatsu K, Okada M, et al. Peripheral nerve regeneration by bioabsorbable nerve conduits filled with platelet-rich fibrin. *Clin Neurol Neurosurg* (2024) **236**:108051. doi:10.1016/j.clineuro.2023.108051

59. Yi D, Zhang Y, Li M, Chen J, Chen X, Wang L, et al. Ultrasound-targeted microbubble destruction assisted delivery of platelet-rich plasma-derived exosomes promoting peripheral nerve regeneration. *Tissue Eng A* (2023) **29**:645–62. doi:10.1089/ten.tea.2023.0133

60. Zhu Y, Peng N, Wang J, Jin Z, Zhu L, Wang Y, et al. Peripheral nerve defects repaired with autogenous vein grafts filled with platelet-rich plasma and active nerve microtissues and evaluated by novel multimodal ultrasound techniques. *Biomater Res* (2022) **26**:24. doi:10.1186/s40824-022-00264-8

61. Rahmi RD, Radithia D, Soebadi B, Parmadiati AE, Winias S. Nerve growth factor and S100B: molecular marker of neuroregeneration after injection of freeze-dried platelet rich plasma. *J Oral Biol Craniofac Res* (2022) **12**:570–4. doi:10.1016/j.jobcr.2022.07.006

62. Kim JW, Kim JM, Choi ME, Jeon EJ, Park JM, Kim YM, et al. Platelet-rich plasma loaded nerve guidance conduit as implantable biocompatible materials for recurrent laryngeal nerve regeneration. *NPJ Regen Med* (2022) **7**:49. doi:10.1038/s41536-022-00239-2

63. Behroozi Z, Ramezani F, Nasirinezhad F. Human umbilical cord blood-derived platelet -rich plasma: a new window for motor function recovery and axonal regeneration after spinal cord injury. *Physiol and Behav* (2022) **252**:113840. doi:10.1016/j.physbeh.2022.113840

64. Behroozi Z, Ramezani F, Janzadeh A, Rahimi B, Nasirinezhad F. Platelet-rich plasma in umbilical cord blood reduces neuropathic pain in spinal cord injury by altering the expression of ATP receptors. *Physiol and Behav* (2021) **228**:113186. doi:10.1016/j.physbeh.2020.113186

65. Lu CF, Wang B, Zhang PX, Han S, Pi W, Kou YH, et al. Combining chitin biological conduits with small autogenous nerves and platelet-rich plasma for the

repair of sciatic nerve defects in rats. *CNS Neurosci Ther* (2021) **27**:805–19. doi:10.1111/cns.13640

66. Vares P, Dehghan MM, Bastami F, Biazar E, Shamloo N, Heidari Keshel S, et al. Effects of platelet-rich fibrin/collagen membrane on sciatic nerve regeneration. *J Craniofac Surg* (2021) **32**:794–8. doi:10.1097/scs.0000000000007003

67. Bo Feng YZ, Wu L, Zhang L, Shan Y. Efficacy of autologous epineurium small gap coaptation combined with platelet-rich plasma, nerve growth factor, and nerve fragments in the repair of damaged peripheral nerves. *Int J Clin Exp Med* (2020) **13**:2902–13.

68. Chuang MH, Ho LH, Kuo TF, Sheu SY, Liu YH, Lin PC, et al. Regenerative potential of platelet-rich fibrin releasate combined with adipose tissue-derived stem cells in a rat sciatic nerve injury model. *Cell Transpl* (2020) **29**:096368972091943. doi:10.1177/0963689720919438

69. Salarinia R, Hosseini M, Mohamadi Y, Ghorbani A, Alamdari DH, Mafinezhad A, et al. Combined use of platelet-rich plasma and adipose tissue-derived mesenchymal stem cells shows a synergistic effect in experimental spinal cord injury. *J Chem Neuroanat* (2020) **110**:101870. doi:10.1016/j.jchemneu.2020.101870

70. Samadian H, Ehterami A, Sarrafzadeh A, Khastar H, Nikbakht M, Rezaei A, et al. Sophisticated polycaprolactone/gelatin nanofibrous nerve guided conduit containing platelet-rich plasma and citicoline for peripheral nerve regeneration: *in vitro* and *in vivo* study. *Int J Biol Macromolecules* (2020) **150**:380–8. doi:10.1016/j.ijbiomac.2020.02.102

71. Wang Z, Mudalal M, Sun Y, Liu Y, Wang J, Wang Y, et al. The effects of leukocyte-platelet rich fibrin (L-PRF) on suppression of the expressions of the pro-inflammatory cytokines, and proliferation of schwann cell, and neurotrophic factors. *Sci Rep* (2020) **10**:2421. doi:10.1038/s41598-020-59319-2

72. Ikumi A, Hara Y, Yoshioka T, Kanamori A, Yamazaki M. Effect of local administration of platelet-rich plasma (PRP) on peripheral nerve regeneration: an experimental study in the rabbit model. *Microsurgery* (2018) **38**:300–9. doi:10.1002/micr.30263

73. Ikumi A, Hara Y, Okano E, Kohyama S, Arai N, Taniguchi Y, et al. Intraoperative local administration of platelet-rich plasma (PRP) during neurolysis surgery for the treatment of digital nerve crush injury. *Case Rep Orthopedics* (2018) **2018**:1–6. doi:10.1155/2018/1275713

74. Torul D, Bereket MC, Onger ME, Altun G. Comparison of the regenerative effects of platelet-rich fibrin and plasma rich in growth factors on injured peripheral nerve: an experimental study. *J Oral Maxillofacial Surg* (2018) **76**:1823.e1–1823.e12. doi:10.1016/j.joms.2018.04.012

75. Bayram B, Akdeniz SS, Diker N, Helvacioğlu F, Erdem SR. Effects of platelet-rich fibrin membrane on sciatic nerve regeneration. *J Craniofac Surg* (2018) **29**:e239–e243. doi:10.1097/scs.0000000000004256

76. Imam SS, Al-Abbasi FA, Hosawi S, Afzal M, Nadeem MS, Ghoneim MM, et al. Role of platelet rich plasma mediated repair and regeneration of cell in early stage of cardiac injury. *Regenerative Ther* (2022) **19**:144–53. doi:10.1016/j.reth.2022.01.006

77. Shen YP, Li TY, Chou YC, Chen LC, Wu YT. Outcome predictors of platelet-rich plasma injection for moderate carpal tunnel syndrome. *Int J Clin Pract* (2021) **75**:e14482. doi:10.1111/ijcp.14482

78. Mourad SI, Al-Dubai SA, Elsayed SA, El-Zehary RR. Efficacy of platelet-rich fibrin and tacrolimus on facial nerve regeneration: an animal study. *Int J Oral Maxillofacial Surg* (2022) **51**:279–87. doi:10.1016/j.ijom.2021.05.016

79. Ali S, Sun M, Khan MN, Qiang F. Advances in sciatic nerve regeneration: a review of contemporary techniques. *Regenerative Ther* (2025) **29**:563–74. doi:10.1016/j.reth.2025.04.016

80. Yadav A, Ramasamy TS, Lin SC, Chen SH, Lu J, Liu YH, et al. Autologous platelet-rich growth factor reduces M1 macrophages and modulates inflammatory microenvironments to promote sciatic nerve regeneration. *Biomedicines* (2022) **10**:1991. doi:10.3390/biomedicines10081991

81. Kokkalas N, Kokotis P, Diamantopoulou K, Galanos A, Lelovas P, Papachristou DJ, et al. Platelet-rich plasma and mesenchymal stem cells local infiltration promote functional recovery and histological repair of experimentally transected sciatic nerves in rats. *Cureus* (2020) **12**:e8262. doi:10.7759/cureus.8262

82. Dong Q, Yang X, Liang X, Liu J, Wang B, Zhao Y, et al. Composite hydrogel conduit incorporated with platelet-rich plasma improved the regenerative microenvironment for peripheral nerve repair. *ACS Appl Mater Inter* (2023) **15**:24120–33. doi:10.1021/acsami.3c02548

83. Gao N, Yan L, Ai F, Kang J, Wang L, Weng Y. Comparison of the short-term clinical effectiveness of 5% dextrose water, platelet-rich plasma and corticosteroid injections for carpal tunnel syndrome: a systematic review and network meta-analysis of randomized controlled trials. *Arch Phys Med Rehabil* (2023) **104**:799–811. doi:10.1016/j.apmr.2022.11.009

84. Senna MK, Shaat RM, Ali AAA. Platelet-rich plasma in treatment of patients with idiopathic carpal tunnel syndrome. *Clin Rheumatol* (2019) **38**:3643–54. doi:10.1007/s10067-019-04719-7

85. Chen SR, Shen YP, Ho TY, Li TY, Su YC, Chou YC, et al. One-year efficacy of platelet-rich plasma for moderate-to-severe carpal tunnel syndrome: a prospective, randomized, double-blind, controlled trial. *Arch Phys Med Rehabil* (2021) **102**:951–8. doi:10.1016/j.apmr.2020.12.025

86. Park J, Kim J, Jeon W, Kim D, Rhyu I, Kim Y, et al. An inside-out vein graft filled with platelet-rich plasma for repair of a short sciatic nerve defect in rats. *Neural Regen Res* (2014) **9**:1351–7. doi:10.4103/1673-5374.137587

87. Lichtenfels M, Colomé L, Sebben AD, Braga-Silva J. Effect of platelet rich plasma and platelet rich fibrin on sciatic nerve regeneration in a rat model. *Microsurgery* (2013) **33**:383–90. doi:10.1002/micr.22105

88. Ye F, Li H, Qiao G, Chen F, Tao H, Ji A, et al. Platelet-rich plasma gel in combination with schwann cells for repair of sciatic nerve injury. *Neural Regen Res* (2012) **7**:2286–92. doi:10.3969/j.issn.1673-5374.2012.29.007

89. Emel E, Ergün SS, Kotan D, Gürsoy EB, Parman Y, Zengin A, et al. Effects of insulin-like growth factor-I and platelet-rich plasma on sciatic nerve crush injury in a rat model. *J Neurosurg* (2011) **114**:522–8. doi:10.3171/2010.9.JNS091928

90. Kuo YC, Lee CC, Hsieh LF. Ultrasound-guided perineural injection with platelet-rich plasma improved the neurophysiological parameters of carpal tunnel syndrome: a case report. *J Clin Neurosci* (2017) **44**:234–6. doi:10.1016/j.jocn.2017.06.053

91. Nikolaou V, Malahias M, Johnson E, Babis G. Single injection of platelet-rich plasma as a novel treatment of carpal tunnel syndrome. *Neural Regen Res* (2015) **10**:1856–9. doi:10.4103/1673-5374.165322

92. Park GY, Kwon DR. Platelet-rich plasma limits the nerve injury caused by 10% dextrose in the rabbit median nerve. *Muscle Nerve* (2014) **49**:56–60. doi:10.1002/mus.23863

93. Güven SC, Özçakar L, Kaymak B, Kara M, Akıncı A. Short-term effectiveness of platelet-rich plasma in carpal tunnel syndrome: a controlled study. *J Tissue Eng Regen Med* (2019) **13**:709–14. doi:10.1002/term.2815

94. Anitua E, Troya M, Falcon-Pérez JM, López-Sarrio S, González E, Alkhraisat MH. Advances in platelet rich plasma-derived extracellular vesicles for regenerative medicine: a systematic-narrative review. *Int J Mol Sci* (2023) **24**:13043. doi:10.3390/ijms241713043

95. Berrigan WA, Bailowitz Z, Park A, Reddy A, Liu R, Lansdown D. A greater platelet dose May yield better clinical outcomes for platelet-rich plasma in the treatment of knee osteoarthritis: a systematic review. *Arthrosc The J Arthroscopic and Relat Surg* (2025) **41**:809–17. e2. doi:10.1016/j.arthro.2024.03.018

96. Boffa A, De Marziani L, Andriolo L, Di Martino A, Romandini I, Zaffagnini S, et al. Influence of platelet concentration on the clinical outcome of platelet-rich plasma injections in knee osteoarthritis. *The Am J Sports Med* (2024) **52**:3223–31. doi:10.1177/03635465241283463

97. Zhang K, Zhang C, Ren Q, Wang D, Sun L, Wang X, et al. Effects of Leukocyte-rich platelet-rich plasma and Leukocyte-poor platelet-rich plasma on cartilage in a rabbit osteoarthritis model. *Cell Mol Biol* (2024) **70**:217–26. doi:10.14715/cmb/2024.70.2.31

98. Di Martino A, Boffa A, Andriolo L, Romandini I, Altamura SA, Cenacchi A, et al. Leukocyte-rich *versus* leukocyte-poor platelet-rich plasma for the treatment of knee osteoarthritis: a double-blind randomized trial. *The Am J Sports Med* (2022) **50**:609–17. doi:10.1177/03635465211064303

99. Yuan Z, Wang Y, Li Y, Lin C, Wang S, Wang J, et al. Comparison of leukocyte-rich and leukocyte-poor platelet-rich plasma on pressure ulcer in a rat model. *J Burn Care and Res* (2023) **44**:860–8. doi:10.1093/jbcr/irac191

100. Lana JF, Huber SC, Purita J, Tambeli CH, Santos GS, Paulus C, et al. Leukocyte-rich PRP *versus* leukocyte-poor PRP-the role of monocyte/macrophage function in the healing Cascade. *J Clin Orthopaedics Trauma* (2019) **10**:S7–S12. doi:10.1016/j.jcot.2019.05.008

101. Simental-Mendía M, Ortega-Mata D, Tamez-Mata Y, Olivo CAA, Vilchez-Cavazos F. Comparison of the clinical effectiveness of activated and non-activated platelet-rich plasma in the treatment of knee osteoarthritis: a systematic review and meta-analysis. *Clin Rheumatol* (2023) **42**:1397–408. doi:10.1007/s10067-022-06463-x

102. Smith OJ, Talaat S, Tomouk T, Jell G, Mosahebi A. An evaluation of the effect of activation methods on the release of growth factors from platelet-rich plasma. *Plast and Reconstr Surg* (2022) **149**:404–11. doi:10.1097/prs.0000000000008772

103. Gentile P, Calabrese C, De Angelis B, Dionisi L, Pizzicannella J, Kothari A, et al. Impact of the different preparation methods to obtain autologous non-activated platelet-rich plasma (A-PRP) and activated platelet-rich plasma (AA-PRP) in plastic surgery: wound healing and hair regrowth evaluation. *Int J Mol Sci* (2020) **21**:431. doi:10.3390/ijms21020431

104. Cavallo C, Roffi A, Grigolo B, Mariani E, Pratelli L, Merli G, et al. Platelet-rich plasma: the choice of activation method affects the release of bioactive molecules. *Biomed Research International* (2016) **2016**:1–7. doi:10.1155/2016/6591717

105. Li M, Zhao Y, Chen X, Du X, Luo Y, Li Y, et al. Comparative analysis of the quality of platelet concentrates produced by apheresis procedures, platelet rich plasma, and buffy coat. *Transfusion* (2024) **64**:367–79. doi:10.1111/trf.17704

106. Carvalho A, Ferreira AF, Soares M, Santos S, Tomé P, Machado-Simões J, et al. Optimization of platelet-rich plasma preparation for regenerative medicine: comparison of different anticoagulants and resuspension media. *Bioengineering* (2024) **11**:209. doi:10.3390/bioengineering11030209

107. Zhang EJX, Lie VE, Wong KLF, Zhang E. Impact of centrifugation parameters on platelet-rich plasma injection for patella tendinopathy: a systematic review and meta-analysis. *Cureus* (2024) **16**:e63341. doi:10.7759/cureus.63341

108. Castillo-Macías A, Zavala J, Ortega-Lara W, García-Herrera S, Valdez-García J. Optimizing platelet and leucocyte-rich plasma as biomaterials for ophthalmic applications: impact of centrifugation speed. *Clin Ophthalmol* (2023) **Vol. 17**:3787–97. doi:10.2147/opth.s444840

109. Harrison TE, Bowler J, Cheng C-I, Reeves KD. Optimizing platelet-rich plasma: spin time and sample source. *Bioengineering* (2023) **10**:1270. doi:10.3390/bioengineering10111270

110. Gill TJ. CORR insights®: there is wide variation in platelet-rich plasma injection pricing: a United States nationwide study of top orthopaedic hospitals. *Clin Orthop Relat Res* (2024) **482**:685–7. doi:10.1097/corr.0000000000002940

111. Garcia RP, Brodt FP, Marchi CMD, Barja PR, Doria ACOC, Furtado GRD, et al. Comparative study on the efficacy of injectable platelet rich fibrin (i-PRF) and albumin gel (ALB-Gel) in facial rejuvenation: a clinical ultrasonographic evaluation. *J Adv Med Med Res* (2024) **36**:50–64. doi:10.9734/jammr/2024/v36i45398

112. Chen L, Jin S, Yao Y, He S, He J. Comparison of clinical efficiency between intra-articular injection of platelet-rich plasma and hyaluronic acid for osteoarthritis: a meta-analysis of randomized controlled trials. *Ther Adv Musculoskelet Dis* (2023) **15**:1759720X231157043. doi:10.1177/1759720x231157043

113. Xiong Y, Gong C, Peng X, Liu X, Su X, Tao X, et al. Efficacy and safety of platelet-rich plasma injections for the treatment of osteoarthritis: a systematic review and meta-analysis of randomized controlled trials. *Front Med* (2023) **10**:1204144. doi:10.3389/fmed.2023.1204144

114. Zhou Y, Li H, Cao S, Han Y, Shao J, Fu Q, et al. Clinical efficacy of intra-articular injection with P-PRP *versus* that of L-PRP in treating knee cartilage lesion: a randomized controlled trial. *Orthopaedic Surg* (2023) **15**:740–9. doi:10.1111/os.13643

115. Mariani E, Pulsatelli L, Cattini L, Dolzani P, Assirelli E, Cenacchi A, et al. Pure platelet and Leukocyte–platelet-rich plasma for regenerative medicine in Orthopedics—Time-and preparation-dependent release of growth factors and effects on synovial fibroblasts: a comparative analysis. *Int J Mol Sci* (2023) **24**:1512. doi:10.3390/ijms24021512

116. Barbieri M, Colombini A, Stogicza A, de Girolamo L. Effectiveness of plasma rich in growth factors in the management of chronic spinal pain: a case series of 32 patients. *Regenerative Med* (2022) **17**:175–84. doi:10.2217/rme-2021-0128

117. Park Y-B, Kim J-H, Ha C-W, Lee D-H. Clinical efficacy of platelet-rich plasma injection and its association with growth factors in the treatment of mild to moderate knee osteoarthritis: a randomized double-blind controlled clinical trial as compared with hyaluronic acid. *The Am J Sports Med* (2021) **49**:487–96. doi:10.1177/0363546520986867

118. Sánchez M, Jorquera C, López de Dicastillo L, Martínez N, Espregueira-Mendes J, Vergés J, et al. Women show a positive response to platelet-rich plasma despite presenting more painful knee osteoarthritis than men. *Knee Surg Sports Traumatol Arthrosc* (2024) **32**:2516–25. doi:10.1002/ksa.12080

119. Argut SK, Celik D, Ergin ON, Kilicoglu OI. Factors affecting the features of platelet-rich plasma in patients with knee osteoarthritis. *Acta Orthopaedica et Traumatologica Turcica* (2023) **57**:148–53. doi:10.5152/j.aott.2023.22077

120. Rossi L, Ranalletta M, Pasqualini I, Zicaro JP, Paz MC, Camino P, et al. Substantial variability in platelet-rich plasma composition is based on patient age and baseline platelet count. *Arthrosc Sports Med Rehabil* (2023) **5**:e853–e858. doi:10.1016/j.asmr.2023.03.017

121. Zahir H, Dehghani B, Yuan X, Chinenov Y, Kim C, Burge A, et al. *In vitro* responses to platelet-rich-plasma are associated with variable clinical outcomes in patients with knee osteoarthritis. *Scientific Rep* (2021) **11**:11493. doi:10.1038/s41598-021-90174-x

122. Egierska D, Perszke M, Mazur M, Duś-Ilnicka I. Platelet-rich plasma and platelet-rich fibrin in oral surgery: a narrative review. *Dental Med Probl* (2023) **60**:177–86. doi:10.17219/dmp/147298

123. Gupta A, Maffulli N, Jain VK. Red blood cells in platelet-rich plasma: avoid if at all possible. *Biomedicines* (2023) **11**:2425. doi:10.3390/biomedicines11092425

124. Chowdhary K, Sahu A, Iijima H, Shinde S, Borg-Stein J, Ambrosio F. Aging affects the efficacy of platelet-rich plasma treatment for osteoarthritis. *Am J Phys Med Rehabil* (2023) **102**:597–604. doi:10.1097/phm.0000000000002161

125. Taniguchi Y, Yoshioka T, Sugaya H, Gosho M, Aoto K, Kanamori A, et al. Growth factor levels in leukocyte-poor platelet-rich plasma and correlations with donor age, gender, and platelets in the Japanese population. *J Exp Orthopaedics* (2019) **6**:4. doi:10.1186/s40634-019-0175-7

126. Tian J, Li XJ, Ma Y, Mai Z, Yang Y, Luo M, et al. Correlation of bioactive components of platelet rich plasma derived from human female adult peripheral blood and umbilical cord blood with age. *Sci Rep* (2023) **13**:18428. doi:10.1038/s41598-023-45747-3

127. Verma R, Kandwal A, Negi G, Chandra H. Factors affecting the quantity and quality of platelet-rich plasma and platelet-derived growth factor-BB: an observational study. *J Bio-X Res* (2021) **04**:67–70. doi:10.1097/jbr.0000000000000091

128. Rizki RR, Benni BR, Riki RM. Growth factor identification based on speed and duration of centrifugation in platelet rich plasma. *Front Healthc Res* (2024) **1**:69–75. doi:10.63918/fhr.v1.n1.p69-75.2024

129. Goodale MB, Phelps HA, Barnhard JA, Shoben AB, Brunke MW. Lower centrifugation speed and time are positively associated with platelet concentration in a canine autologous conditioned plasma system. *J Am Vet Med Assoc* (2023) **261**:1–6. doi:10.2460/javma.23.04.0218

130. Li H, Xia T, Zeng H, Qiu Y, Wei Y, Cheng Y, et al. Liquid platelet-rich fibrin produced *via* horizontal centrifugation decreases the inflammatory response and promotes chondrocyte regeneration *in vitro*. *Front Bioeng Biotechnol* (2023) **11**:1301430. doi:10.3389/fbioe.2023.1301430

131. Legiawati L, Yusharyahya SN, Bernadette I, Novianto E, Priyanto MH, Gliselda KC, et al. Comparing single-spin *versus* double-spin platelet-rich plasma (PRP) centrifugation methods on thrombocyte count and clinical improvement of androgenetic alopecia: a preliminary, randomized, double-blind clinical trial. *J Clin Aesthet Dermatol* (2023) **16**:39–44.

132. Muthu S, Krishnan A, Ramanathan KR. Standardization and validation of a conventional high yield platelet-rich plasma preparation protocol. *Ann Med Surg (2012)* (2022) **82**:104593. doi:10.1016/j.amsu.2022.104593

133. Pretorius J, Habash M, Ghobrial B, Alnajjar R, Ellanti P. Current status and advancements in platelet-rich plasma therapy. *Cureus* (2023) **15**:e47176. doi:10.7759/cureus.47176

134. Arita A, Tobita M. Adverse events related to platelet-rich plasma therapy and future issues to be resolved. *Regenerative Ther* (2024) **26**:496–501. doi:10.1016/j.reth.2024.07.004

EBM Experimental Biology and Medicine

TYPE Review
PUBLISHED 01 May 2025
DOI 10.3389/ebm.2025.10537

OPEN ACCESS

*CORRESPONDENCE
Muriel W. Lambert,
mlambert@njms.rutgers.edu

RECEIVED 21 February 2025
ACCEPTED 17 April 2025
PUBLISHED 01 May 2025

CITATION
Lambert MW (2025) Critical role of alpha spectrin in DNA repair: the importance of μ-calpain and Fanconi anemia proteins.
Exp. Biol. Med. 250:10537.
doi: 10.3389/ebm.2025.10537

Critical role of alpha spectrin in DNA repair: the importance of μ-calpain and Fanconi anemia proteins

Muriel W. Lambert *

Department of Pathology, Immunology and Laboratory Medicine, Rutgers New Jersey Medical School, Newark, NJ, United States

Abstract

Nonerythroid spectrins are proteins important in maintaining the structural integrity and flexibility of the cell and nuclear membranes and are essential for a number of functionally important cellular processes. One of these proteins, nonerythroid α spectrin (αSpII), plays a critical role in DNA repair, specifically repair of DNA interstrand crosslinks (ICLs), where it acts as a scaffold, recruiting repair proteins to sites of damage. Loss or breakdown of αSpII is an important factor in a number of disorders. One of these is Fanconi anemia (FA), a genetic disorder characterized by bone marrow failure, chromosome instability, cancer predisposition, congenital abnormalities and a defect in DNA ICL repair. Significantly, breakdown of αSpII occurs in cells from a number of FA complementation groups, due to excessive cleavage by the protease, μ-calpain, leading to defective repair of DNA ICLs in telomeric and non-telomeric DNA. Knockdown of μ-calpain in FA cells by μ-calpain siRNA results in restoration of αSpII levels to normal and repair of DNA ICLs in telomeric and non-telomeric DNA, demonstrating the importance of αSpII stability in the repair process. It is hypothesized that there is a mechanistic link between excessive cleavage of αSpII by μ-calpain and defective DNA ICL repair in FA and that FA proteins, which are deficient in FA, play a key role in maintaining the stability of αSpII and preventing its cleavage by μ-calpain. All of these events are proposed to be important key factors involved in the pathophysiology of FA and suggest new avenues for potential therapeutic intervention.

KEYWORDS

alpha spectrin, DNA repair, DNA interstrand crosslinks, μ-calpain, Fanconi anemia proteins

Impact statement

In the nucleus, the structural protein nonerythroid α spectrin (αSpII) plays a central role in repair of DNA interstrand crosslinks (ICLs). Significantly, there is a deficiency in αSpII in the genetic, bone marrow failure disorder, Fanconi anemia (FA), which is characterized by a defect in DNA ICL repair. This is due to excessive cleavage of αSpII by the protease, μ-calpain. Importantly, knockdown of μ-calpain, by siRNA, reverses cleavage of αSpII, restores its levels to normal and enables repair of DNA ICLs in FA cells. FA thus represents another disorder in which excessive cleavage of αSpII by μ-calpain correlates with a major characteristic, in this case defective DNA ICL repair. It demonstrates the importance of αSpII for the DNA ICL repair process. FA proteins are proposed to play a major role in regulating cleavage of αSpII by μ-calpain thus giving them another critical role in DNA repair.

Introduction

Cytoskeletal and nucleoskeletal proteins are critical for maintaining the structure, function and mechanical properties of eukaryotic cells [1–11]. Of particular importance is spectrin, found in both erythroid and nonerythroid cells [12–19]. Spectrin was first identified in erythrocytes and shown to be essential for cell membrane structure, integrity, and flexibility [14, 15, 18, 20–24]. Spectrin also plays a critical role in non-erythroid cells in both the cytoplasm and nucleus and is involved in maintaining the shape, flexibility and elasticity of both the cell and nuclear membranes and is essential for a number of functionally important cytoplasmic and nuclear processes, as well as for mechanical coupling between the nucleus and the cytoplasm [7, 10, 13–17, 25–39]. Total loss of spectrin can lead to cell death [33, 36, 38, 40]. Nonerythroid spectrin has two subunits, αSpII and βSpII [14–17, 34, 35]. Of considerable interest, nuclear αSpII has been shown to directly interact with DNA and play a critical role in DNA repair and in the maintenance of the stability of chromosomes and telomeres after DNA damage [12, 13, 38, 41–46]. It acts as a scaffold and aids in recruitment of repair proteins to sites of damage in both telomeric and non-telomeric DNA [42–49].

Loss or breakdown of spectrin in cells leads to a deficiency in these processes and is clinically manifested in a number of disorders, one of which is the genetic disorder, Fanconi anemia (FA) [13, 38, 44, 48, 50]. FA is characterized by bone marrow failure, a marked propensity to develop cancer, multisystemic congenital abnormalities, chromosomal instability and a defect in ability to repair DNA interstrand cross-links (ICLs) [51–69]. Lambert et. al. have shown a deficiency in αSpII in cells from FA patients from a number of FA complementation groups [12, 13, 44, 48]. This deficiency is due to the excessive activity of the protease, μ-calpain, which cleaves αSpII leading to its breakdown [69, 70]. The breakdown of αSpII correlates with a defect in DNA ICL repair in FA cells in both nontelomeric and telomeric DNA and to chromosome instability [46, 69]. These studies have demonstrated that maintaining the stability of αSpII in the cell is critical for a number of important nuclear and cellular processes and for circumventing telomere dysfunction after DNA ICL damage [46, 69]. Lambert et al. have proposed that excessive cleavage of αSpII by μ-calpain is an important factor in the pathogenesis of FA and a number of the clinical characteristics of this disorder [13, 50, 69].

This review will concentrate on the function of αSpII in the nucleus with emphasis on its interaction with non-telomeric and telomeric DNA, especially after DNA ICL damage, the importance of maintaining the stability of αSpII and preventing its breakdown by μ-calpain, and the role of FA proteins in this process. The consequences of a loss or deficiency in αSpII on DNA repair, telomere integrity/function and chromosome stability after DNA damage, particularly in FA, will be discussed.

Overview of spectrin structure

αSpII is a long flexible protein which contains a modular structure composed of an extended array of triple α-helical repeats connected by short a-helical linker [14–17, 21, 27, 71–73]. This structure aids in its flexibility and ability to expand and contract [14, 25, 71–73]. Nonerythroid spectrin has two subunits, αSpII and βSpII. There is one alpha spectrin gene and four beta spectrin genes [14–17]. There are a number of different spectrin isoforms which originate by extensive mRNA splicing from these genes [14, 27]. In all of these, αSpII and βSpII associate in an antiparallel fashion to form a heterodimer [14–17]. αSpII consists of 21 triple helical repeats and βSpII contains 17 repeats [14–17]. Two heterodimers can link head to head to form a tetramer [14–17]. Nonerythroid spectrin (αSpII/βSpII) is comprised of numerous domains. αSpII contains an EF hand's domain on repeat 21, which is a site of Ca^{2+} binding and signaling (Figure 1) [14–17]. It contains a Src-homology 3 (SH3) domain in repeat 10, which plays an important role in proteinprotein interactions and is involved in signal transduction and intracellular signaling (Figure 1) [14–17, 74, 78–81]. The SH3 domain has a binding site for a kinase, c-Src, lowmolecular weight phosphotyrosine phosphatase (LMW-PTP) and FANCG, a Fanconi anemia (FA) protein. αSpII has a site of cleavage by the protease, calpain, in repeat 11 between residues Y_{1176} and G_{1177}. [75, 76] There is a caspase cleavage site at residue Asp1185, which is activated during apoptosis [82]. αSpII also has a calmodulin binding domain in repeat 11, which can modulate spectrin cleavage by μ-calpain and caspase [83, 84]. Proteolytic cleavage of αSpII by μ-calpain leads to its decreased stability and loss of function, which makes regulation of μ-calpain cleavage of

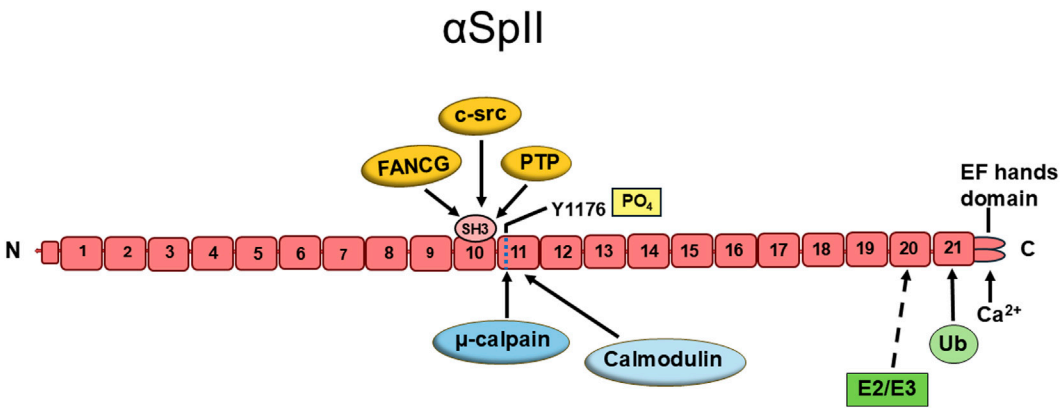

FIGURE 1
The structure and domains of human non-erythroid alpha spectrin (αSpII). αSpII is composed of 21 triple helical repeats. Repeat 10 contains a Src-homology 3 (SH3) domain which is a site of protein-protein interactions. Three proteins targeting this site are: c-src, a kinase; low molecular weight phosphotyrosine phosphatase (PTP); and FANCG. Repeat 11 has a site of cleavage by the protease, μ-calpain, and also contains a binding domain for calmodulin. There is a suggested E2/E3 ubiquitin protein conjugating/ligating site (E2/E3) in repeat 20 and a ubiquitination site (Ub) in repeat 21. At the C-terminus of αSpII are two ER-hand domains which bind calcium. Domains 20 and 21 mediate the dimerization of αSpII at its C-terminus with the N-terminus of βSpII. This structure of αSpII is based on studies and models of a number of investigators. [14–17, 25, 74–77].

αSpII critical for maintaining normal cell and nuclear functioning [74, 76, 78]. There is also a ubiquitination site in repeat 21 and a suggested E2/E3-ubiquitin-conjugating/ligating site in repeat 20 [14, 26]. βSpII has an actin-binding domain on repeat 1, and a pleckstrin homology domain on repeat 7, which is involved in cell signaling, organization of the cytoskeleton, and aiding in the localization of βSpII to the plasma membrane [14–17]. αSpII and βSpII assemble laterally to form heterodimers that assemble into tetramers [14–17]. The tertiary structure of the spectrin repeat imparts elasticity to the protein [14–17, 21, 27, 71–73]. The structural characteristics of αSpII/βSpII enable it to interact with a number of different cellular proteins and participate in a number of important physiological pathways in the cell in both the nucleus and the cytoplasm. Numerous reviews are available with a moredetailed description of spectrin structure [14–17, 20, 24–27, 71–73].

Spectrin and its role in the cytoplasm

Spectrin is a multifunctional protein, as is evidenced by the numerous proteins which interact with both αSpII and βSpII. Goodman and colleagues have created the Spectrinome using Human Proteome, Human Reactome and Human Atlas data which clearly demonstrates the multitude of cellular pathways and functions in which spectrin is involved in the cytoplasm, the nucleus and the cell surface [14]. Since spectrin's numerous interacting protein partners demonstrate the multitude of roles spectrin plays in the cell, it is important to more fully understand these interactions and their impact on cellular function.

One of the best known and critical roles of αSpII/βSpII is providing structural integrity for cell membranes [14, 19, 85, 86]. It acts as a scaffold interacting with ankyrin, actin and other cytoskeletal proteins to form a network crucial for maintaining mechanical support, shape, flexibility and elasticity to the cell membrane [17, 24, 85–89]. αSpII is involved in cell movement and adhesion via interactions with proteins involved in actin dynamics (Figure 2) [31–33, 89]. αSpII plays a role in actin filament reorganization which is critical for a number of processes such as lamellipodia extension and immunological synapse formation between T-cells and antigen-presenting cells [27, 32, 33, 89]. The SH3 domain of αSpII has been shown to bind to proteins involved in actin polymerization and reorganization and plays a crucial role in this process during cell-cell contact, cell adhesion, cell spreading and migration [29, 33, 89–91]. Spectrin interacts with proteins involved in intracellular traffic. It is involved in vesicle and organelle mediated transport [14, 92]. In neurons, αSpII/βSpII and αSpII/βSpIII have an essential role in synaptic vesicle trafficking and synaptic transmission [14, 16, 93]. βSpIII associates with the microtubule motor proteins, kinesin and dynein, and is involved in anterograde and retrograde transport of cargo in axons [14, 94–96]. αSpII and βSpII associate with synaptic vesicles via synapsin I and are critical for this process [14, 28, 29, 97]. αSpII and βSpII have been identified associated with melanosomes in human melanocytes and are thought to be involved in melanosome transport in these cells [98]. Goodman et al have also shown that erythroid spectrin has E2/E3 chimeric ubiquitin conjugating and ligating activity and is capable of ubiquitinating not only alpha spectrin but also ankyrin, band 3, and protein 4.1 [14, 26, 99, 100]. Goodman et al.

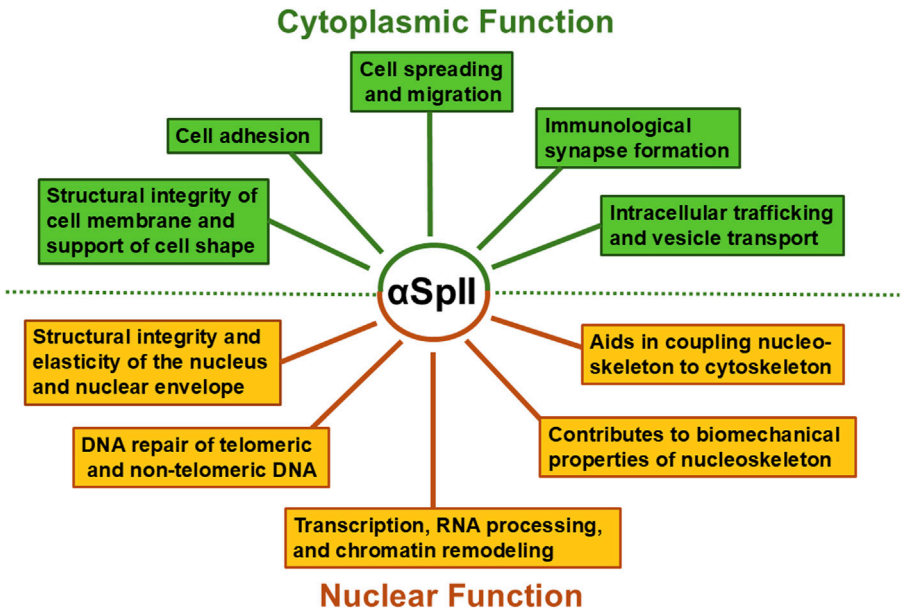

FIGURE 2
Roles for αSpII in the nucleus and cytoplasm. αSpII is involved in multiple functions in both the nucleus and cytoplasm of human non-erythroid cells and thus has an important impact on a number of different cellular pathways.

have proposed that αSpII has similar E2/E3 ubiquitinating activity in the cytoplasm and the nucleus in non-erythroid cells [14, 26, 99, 100]. This activity is very important for protein-protein interactions and the role they play in normal physiological processes in the cell. Thus, αSpII along with βSpII are components of a spectrin scaffold which is critical for a large number of physiological processes in the cytoplasm.

Spectrin and its structural role in the nucleus

Just as interactions of spectrin with specific proteins in the cytoplasm are critical for cellular function, its interactions with both proteins and DNA in the nucleus is critical for nuclear function. Within the nucleus, nonerythroid spectrin is a component of a nucleoskeletal network which plays an essential role in maintaining the structural integrity and elasticity of the nucleus as well as in repair of damage to both nontelomeric and telomeric DNA (Figure 2) [7, 10, 15–17, 27, 37, 46, 50, 101]. Both αSpII and two isoforms of β-spectrin (βSpII and βSpIV∑5) have been identified in the nucleus [12, 13, 38, 39]. Studies have shown that αSpII is present in the peripheral nucleoskeleton, where it interacts with lamins A and B, actin, and nuclear myosin and is anchored to the nuclear envelope by emerin and protein 4.1 [7, 8, 10, 13, 37, 41, 50, 102]. It makes an important contribution to the biomechanical properties of these nucleoskeleton proteins and to nuclear envelope support [7, 10, 37, 102]. It forms a complex with lamins A and B, actin, nuclear myosin, and the LINC complex protein, SUN2, and plays an important role in coupling the nucleoskeleton to the cytoskeleton [7, 10, 13, 37, 41]. αSpII is also associated with the inner nucleoskeleton where it interacts with DNA repair proteins, chromatin remodeling proteins and proteins involved in transcription and RNA processing [6–8, 13, 41, 42].

The cortical network αSpII forms with lamin and actin at the nuclear envelop plays a role in maintaining the elasticity and structural integrity of the nucleus (Figure 2) [7, 10, 15, 17, 27, 37]. Knock-down of αSpII in HeLa cells to levels that are approximately 50% of those found in control cells leads to a decrease in ability of the nucleus to recover from compression [37]. This has been attributed to loss of membrane elasticity due to decreased αSpII [37]. αSpII's modular structure of triple alpha-helical repeats makes an important contribution to the structural stability, elasticity and mechanical resilience of the nucleus and to its ability to recover from compression [37].

Thus, αSpII is an important scaffolding protein which represents 2–3% of the total protein in eukaryotic cells [14]. It has a myriad of functions and any defects or deficiencies in this protein would be central to pathological changes occurring in the cell structure and function (Figure 2). Therefore, maintaining αSpII stability is critical for normal cell functioning. Excessive cleavage of αSpII can upset normal cellular homeostasis and result in various human disease states and disorders. These points will be discussed below.

αII spectrin plays a critical role in DNA repair in the nucleus

In addition to its structural role in the nucleus, αSpII has been shown to have an essential function in the nucleus in repair of DNA damage. Lambert and colleagues have demonstrated that in human cells αSpII plays a critical role in repair of DNA interstrand cross-links (ICLs) in both non-telomeric and telomeric DNA and is needed for chromosomal stability after DNA damage [13, 42–49, 69]. There are numerous lines of evidence which demonstrate the important role of αSpII in DNA repair: (1) αSpII binds directly to DNA at sites of ICLs; (2) αSpII recruits repair proteins to these sites; (3) αSpII is needed for production of incisions produced by the endonuclease XPF-ERCC1 at sites of ICLs; and (4) αSpII is critical for repair of telomeric DNA and telomere integrity after DNA ICL damage [42–46, 69]. Thus, αSpII is important in DNA repair processes in the nucleus and maintenance of telomere integrity after DNA damage. These points will be discussed below.

αSpII localizes to sites of DNA ICLs and binds directly to DNA at these sites

Lambert *et al.* have demonstrated that αSpII from HeLa cell nuclei, as well as purified bovine brain αSpII, bind directly to a DNA substrate containing a 4,5′8-trimethylpsoralen (TMP) plus UVA light induced ICL [42]. Based on the crystal structure of αSpII, it has been proposed that it binds to the minor groove of DNA which opens up after ICL formation [42]. αSpII's binding to the damaged DNA is specific for the ICL; it does not bind to DNA containing a TMP monoadduct [42]. In HeLa and human lymphoblastoid cells damaged with a DNA ICL agent, 8-methoxysporalen (8-MOP) plus UVA light or mitomycin C (MMC), αSpII localizes in damage induced nuclear foci which are sites of DNA ICLs [42–46, 49, 69]. These studies provide strong evidence that αSpII plays a role in the damage recognition steps of the DNA ICL repair process.

αSpII is needed for recruitment of XPF-ERCC1 and repair proteins to sites of ICLs and production of incisions at these sites

αSpII colocalizes in damaged-induced nuclear foci with proteins involved in DNA ICL repair. These include FANCA, FANCF, FANCG, and XPF-ERCC1 [42–46, 69]. XPF-ERCC1 is involved in the unhooking of the ICL and production of endonucleolytic incisions at the site of the ICL [48, 103–106]. Lambert and colleagues demonstrated that, after normal human lymphoblastoid cells or HeLa cells are damaged with a DNA ICL agent, αSpII colocalizes with XPF at damage-induced nuclear foci [43, 46, 69]. Time course studies have shown that αSpII co-localizes with XPF at the same nuclear foci, with foci first appearing 10 h after ICL damage with 8-MOP plus UVA light or MMC (Figure 3) [13, 43]. Foci peak at 16h and disappear by 24h when ICLs are no longer present [13, 43]. The same time course and co-localization observed with αSpII and XPF was also observed with the repair proteins FANCA and FANCF [13, 43]. This indicates that both αSpII and XPF are involved in the same events in DNA ICL repair and suggests that FANCA and FANCF may also play a role.

Additional evidence that αSpII is critical for recruitment of XPF and these repair proteins to sites of ICLs has been demonstrated by immunofluorescence studies in which αSpII has been knocked down by siRNA [45, 46]. Since αSpII is an essential protein for cell survival, total loss of this protein results in cell death [14, 107, 108]. Cells survive, however, when levels are reduced to 35–40% of normal [45, 46]. Reduction of αSpII to these levels followed by damaging DNA with an ICL agent has been shown to result in decreased formation of damage-specific αSpII foci in these cells and loss of localization of XPF to the sites of damage [45]. FA proteins are present in these cells and FANCA and FANCF also localize to the sites of damage with XPF [45]. Thus, αSpII is needed for the recruitment and localization of XPF as well as FANCA and FANCF to sites of DNA ICLs indicating their involvement in ICL repair. Corroborating these findings are studies which have shown that inhibition of expression of the αSpII gene, *SPTAN1*, by miR-125-3p, leads to disruption of localization of XPF and FANCA to mitomycin C induced foci after treatment of lung cancer cells with this DNA interstrand cross-linking agent [109]. This has been suggested as a novel pathway for interrupting repair of DNA ICLs and enhancing the anticancer function of DNA ICL agents [109].

Further support for the importance of αSpII for incisions produced by XPF-ERCC1 is provided by studies which have demonstrated that, on a DNA substrate containing a site-specific tri-methylpsoralen (TMP) ICL, XPF-ERCC1 produces incisions at the site of a DNA ICL [42]. Purified bovine αSpII enhances these incisions but does not itself produce incisions at the site of the ICL [42]. A purified monoclonal antibody against αSpII from normal human lymphoblastoid cells inhibited these incisions [42, 48]. Thus the presence of αSpII is critical for the incisions produced by XPF-ERCC1 at sites of ICLs. The studies described above have led Lambert and colleagues to develop a model in which αSpII acts as a scaffold to aid in recruitment of repair proteins such as XPF-ERCC1 to sites of DNA ICLs; loss of αSpII results in a deficiency in recruitment of XPF and decreased incisions at sites of ICLs leading to a deficiency in DNA repair [42].

The SH3 domain of αSpII is an important site of recruitment for XPF-ERCC1 and repair proteins to sites of DNA ICLs

An important question is by what mechanism does αSpII recruit repair proteins to sites of ICLs? As mentioned above, αSpII consists of 21 triple-helical repeats [14–17]. There is a Src-

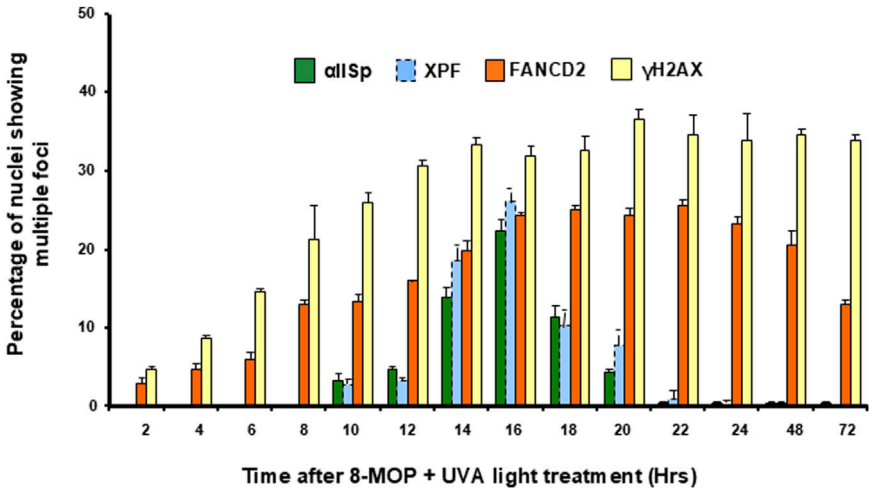

FIGURE 3
Time course for appearance of αSpII, XPF, FANCD2, and γ-H2AX nuclear foci after damage of normal human cells with a DNA ICL agent. The percentage of nuclei showing multiple αSpII, XPF, FANCD2, and γ-H2AX foci was determined at time points from 0 to 72 h after treatment with 8-MOP plus UVA light. Nuclei containing four or more foci were counted as positive. αSpII foci co-localized with XPF foci and had a similar time course after damage of cells with 8-MOP plus UVA light. These foci appeared after FANCD2 foci and had a different time course than the FANCD2 foci. Error bars represent SEM. (Reproduced from Zhang et al., [49] with permission from John Wiley and Sons).

homology 3 (SH3) domain in the 10th repeat (Figure 1) [14–17, 78]. SH3 domains are modular domains which are important in protein-protein interactions and protein network assembly [79, 110]. There are three major classes of protein ligands which bind to SH3 domains, class I, class II and class I@ [74, 79–81]. The SH3 domain of αSpII has a consensus sequence which preferentially binds to class 1@ ligands [74]. A number of FA proteins have consensus sequences that bind to SH3 domains and have the potential to bind to cellular proteins containing these domains [101]. Of particular interest, FANCG has a class1@ consensus sequence [101]. Lambert et al have carried out studies using sitedirected mutagenesis and yeast two hybrid analysis and have shown that FANCG binds directly to the SH3 domain of αSpII via this consensus sequence [101]. FANCG also binds directly to XPF-ERCC1 [101]. FANCG contains seven tetratricopeptide repeat (TPR) motifs, which are motifs that are involved in protein-protein interactions [111–114]. TPR motifs 1, 2, 3, and 6 in FANCG bind directly to the central domain of ERCC1 (residues 120–220) [115]. ERCC1 binds to XPF by its C-terminal domain (residues 220–297) [116–118]. XPF in turn binds to ERCC1 through its C-terminal domain, which differs from its nuclease domain, and produces incisions at the sites of DNA ICLs [118, 119]. Thus the SH3 domain of αSpII plays an important role in the ability of αSpII to recruit XPF-ERCC1, via FANCG, to sites of ICLs, enabling it to create incisions at the site of damage. Knocking down αSpII eliminates its binding to sites of DNA ICLs and recruitment of XPF-ERCC1 to these sites [45, 46]. This, in turn, results in reduction in production of incisions on damaged DNA [45, 46]. Whether αSpII is involved in additional steps in the repair process has not yet been determined.

A model for the role of αSpII in the DNA ICL repair pathway

Repair of DNA ICLs can occur in both replicating and non-replicating DNA [106, 120–125]. This repair process is particularly important in S phase of the cell cycle when DNA replication is stalled at the site of an ICL. Stalled DNA replication forks can trigger DNA ICL repair, thus making replication-coupled ICL repair extremely critical for cell survival [106, 120–125]. Several models have been proposed for repair of ICLs at stalled replication forks. Three of the major pathways for replication-coupled ICL repair are: (1) The Fanconi anemia pathway, which is triggered when two replication forks converge on an ICL. This pathway involves a large number of proteins and a complex series of steps resulting in production of incisions in DNA and unhooking of the ICL; (2) The Neil3 pathway, in which ICLs are resolved by a DNA glycosylase and cleavage of one of the two N-glycosyl bonds forming the ICL; and (3) The acetaldehyde pathway, which denotes a mechanism for repair of acetaldehyde-induced ICLs [106, 125]. In some instances unhooking involves incision of the ICL via the FA pathway and in others the ICL may undergo enzymatic reversal [106, 125].

Replication-coupled ICL repair has been extensively studied in cells from patients with Fanconi anemia (FA) who are deficient in ability to repair DNA interstrand crosslinks [57–61, 106, 123, 124]. FA is a genetic disorder, which, in addition to defective

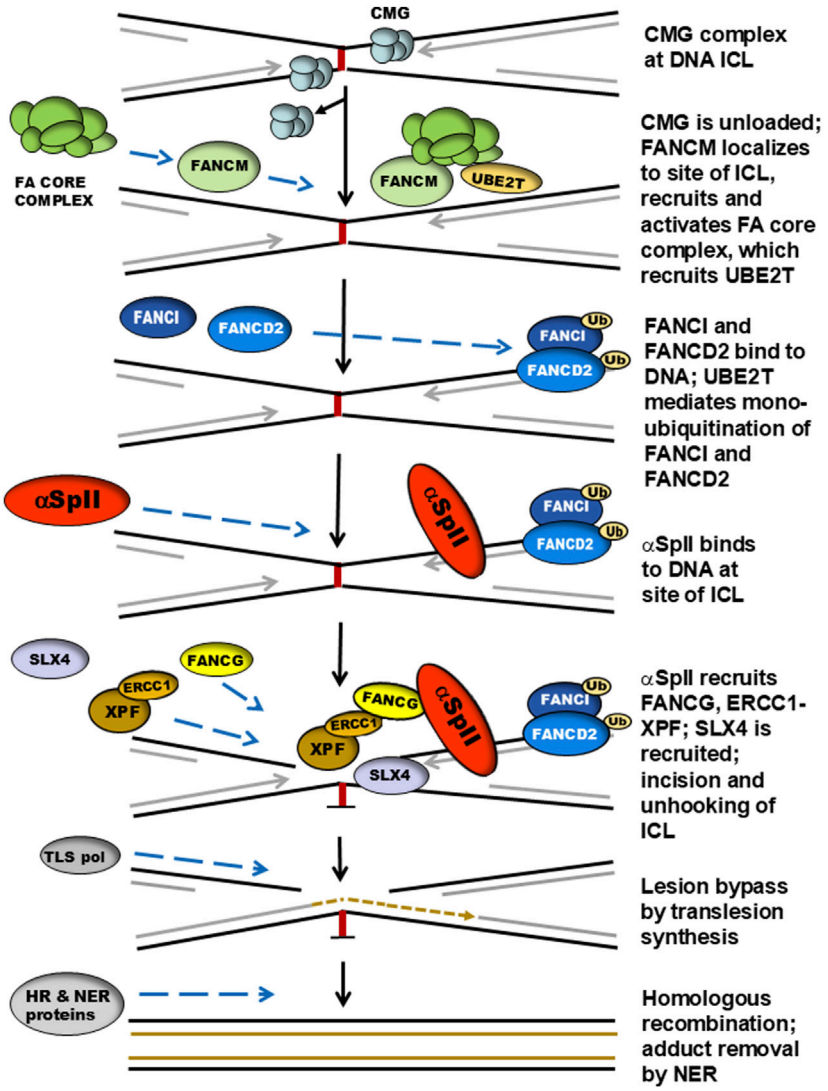

FIGURE 4
A model for the role of αIISp in replication-coupled DNA ICL repair. When DNA replication is stalled at the site of an ICL and replication forks converge, the CMG helicase complex on the leading strand stalls and is unloaded. FANCM recognizes the stalled replication fork and localizes to the damaged DNA. The FANCM complex recruits the FA core complex. FANCD2 and FANCI localize to the site of damage at the stalled replication fork. The core complex recruits UBE2T (FANCT), which monoubiquitinates FANCD2 and FANCI. αSpII subsequently binds to DNA at the site of the ICL downstream of FANCD2-Ub and acts as a scaffold aiding in the recruitment of repair proteins to the site of damage. FANCG binds to the SH3 domain of αSpII and XPF-ERCC1 is recruited and binds to FANCG-αSpII. XPF then produces incisions at the site of damage and is involved in the unhooking of the ICL. SLX4/FANCP plays a role in this step. Translesion DNA synthesis then occurs by a translesion polymerase leading to bypassing the ICL. This is followed by additional steps which include homologous recombination (HR) and adduct removal by nucleotide excision repair (NER). This model emphasizes the role of αSpII in the initial damage-recognition and incision steps of the DNA ICL repair process. It is based on studies on the interaction of αSpII with DNA containing ICLs, on the involvement of numerous proteins involved in the repair process and on other models for ICL repair [42–44, 50, 57, 66, 104, 109, 127, 132–135]. (Modified from Lambert [50], with permission of Sage Publications Ltd.).

DNA ICL repair, is characterized by bone marrow failure, congenital abnormalities, chromosome instability and a predisposition to develop a variety of cancers [51, 52, 57, 61–68]. There are 22 different FA genes (*FANCA* to *FANCW*). Germline mutations in any one of these genes can cause the disorder. The FANC proteins expressed by these genes are all involved in replication-coupled DNA repair and the pathway in which they are involved is known as the Fanconi anemia (FA) pathway [57–61, 104, 126–131]. Since αSpII has been shown to play a critical role in ICL repair during S phase of the cell cycle, to directly interact with proteins in the FA pathway, and to be important in the initial damage recognition and incision steps of the ICL repair process, the involvement of αSpII in this pathway will be described [13, 42–46].

The initial damage recognition step of the ICL repair process is critical. In replication-coupled DNA ICL repair, the site of damage is located at a stalled replication fork [57–59, 66, 106, 121]. Lambert and colleagues have proposed a model for the mechanism of action of αSpII in ICL repair in the FA repair pathway (Figure 4) [13, 50]. It is based on studies on the interaction of αSpII with DNA containing ICLs and with proteins involved in the ICL repair process and on previous models for ICL repair [13, 50, 57, 66, 106, 121, 124, 136]. Although αSpII is not a FANC protein, it plays a critical role in this pathway [13, 50]. In this pathway, replication forks converge at the site of an ICL and the CDC45/MCM2-7/GINS (CMG) helicase complex on the leading strand is unloaded [66, 106, 126, 130]. FANCM and a group of interacting proteins recognize the stalled replication fork and localize to the DNA [57, 66, 106, 125, 127, 131]. The FANCM complex helps recruit the FA core complex (FANCA, FANCB, FANCC, FANCE, FANCF, FANCG, FANCL, FAAP20 and FAAP100), which has E3 ubiquitin ligase activity [57, 66, 106, 125, 131]. FANCD2/FANCI localize at the replication fork stalled at the site of the ICL [106, 136–139]. The core complex recruits a ubiquitinconjugating enzyme, UBE2T (FANCT), which monoubiquitinates FANCI and FANCD2 (the ID complex) (Figure 4). [106, 125, 136–139] αSpII subsequently binds to the site of an ICL on DNA downstream of FANCD2 [18, 50].

After αSpII binds to the DNA, it aids in the recruitment of XPF-ERCC1 to the site of the ICL via recruitment of FANCG [18, 50]. As described above, FANCG directly binds to the SH3 domain of αSpII via its class 1@ consequence sequence and recruits XPFERCC1 [101]. The central domain of ERCC1 binds to TPR motifs 1, 2, 3, and 6 in FANCG; the C-terminal domain of XPF binds to ERCC1 [115–118]. XPF then creates an incision at the site of the ICL leading to unhooking of the ICL [57, 66, 103]. Another endonuclease, SLX4/FANCP is also involved in the incision process and aids in protein coordination [57, 66, 104, 128, 129]. Thus, αSpII recognizes and binds to DNA at sites of ICLs and acts as a scaffold in recruitment of XPF-ERCC1 via FANCG. It then incises the DNA and is involved in the unhooking of the ICL. SLX4/FANCP is recruited and also participates in this step [104–106]. Other FA proteins could be involved in this repair process as well.

After these events, DNA translesion synthesis takes place and the lesion is bypassed by a translesion DNA polymerase [58, 66, 106, 124, 125]. This is followed by homologous recombination and adduct removal by NER [58, 66, 106, 124, 125]. A large number of FA proteins take part in these steps. These stages in the repair process, which involve DNA translesion synthesis, homologous recombination and NER are discussed in detail in numerous reviews and will not be elaborated upon here [57–61, 66, 106, 124–126]. The reader is directed to these reviews. Since the role of αSpII in ICL repair is mainly in the initial damage recognition and incision steps of the repair pathway, these are the components of the FA pathway that have been emphasized here.

The exact relationship between αSpII and FANCD2 in this repair process is not clear. Time course experiments show that αSpII binds to the damaged DNA after FANCD2 (Figure 4) [49]. It does not colocalize with monoubiquitinated FANCD2 (FANCD2Ub) in nuclear foci nor is it required for monoubiquitination of FANCD2 after ICL damage or for its localization to sites of damage [49]. Monoubiquitination of FANCD2 is not required for binding of αSpII to damaged DNA [49]. The time course for localization of FANCD2 to nuclear foci after ICL damage is different than that of αSpII (Figure 3) [49]. FANCD2 foci first appear 2 h after ICL damage, increase up until 16 h, remain fairly stable until 24 h and are still present at 72 h (Figure 3) [49]. In contrast, αSpII foci first appear 10 h after DNA ICL formation, peak at 16 h and disappear by 24 h [49]. Thus, FANCD2-Ub associates in foci with damaged DNA before αSpII foci appear and is still present when αSpII foci are gone [49]. The time course of FANCD2 foci corresponds to that of formation of γH2AX (phosphorylated histone H2A) foci which localize to sites of DNA double strand breaks (Figure 3) [49]. Both FANCD2 and γH2AX foci are present 72 h after damage, which could indicate additional involvement of FANCD2 in later stages in the ICL repair process as has been proposed [49, 50, 136]. The relationship between αSpII and ubiquitinated FANCD2 needs to be further explored.

In human cells, αSpII is also needed for the localization of FANCA and FANCF to sites of ICL damage [43]. FANCA and FANCF do not localize to nuclear foci after ICL damage if αSpII has been knocked down by siRNA [45]. Whether this colocalization of FANCA and FANCF with αSpII and XPF at damage sites is a component of the recruitment of the FA core complex to sites of DNA damage or is a component of the steps involved in the unhooking of the DNA ICL is not clear and needs to be further investigated.

Importance of μ-calpain and FA proteins in the regulation of cleavage of αSpII in FA cells

The importance of αSpII stability in DNA repair is seen in cells from patients with Fanconi anemia (FA) which, as mentioned above, are defective in ability to repair DNA ICLs [43–48, 51–61]. Of significance, Lambert et. al. have shown that there is a deficiency in αSpII in cells from patients from a number of FA complementation groups [12, 13, 45, 69]. Levels of αSpII are 35–40% of those found in normal human cells [12, 13, 45]. This deficiency correlates with reduced levels of repair of DNA ICLs in FA cells which are 35–45% of normal [45, 47, 48]. Levels of DNA repair after DNA ICL damage were determined in FA-A, FA-C, FA-D2, FA-F and FA-G cells by measurement of unscheduled DNA

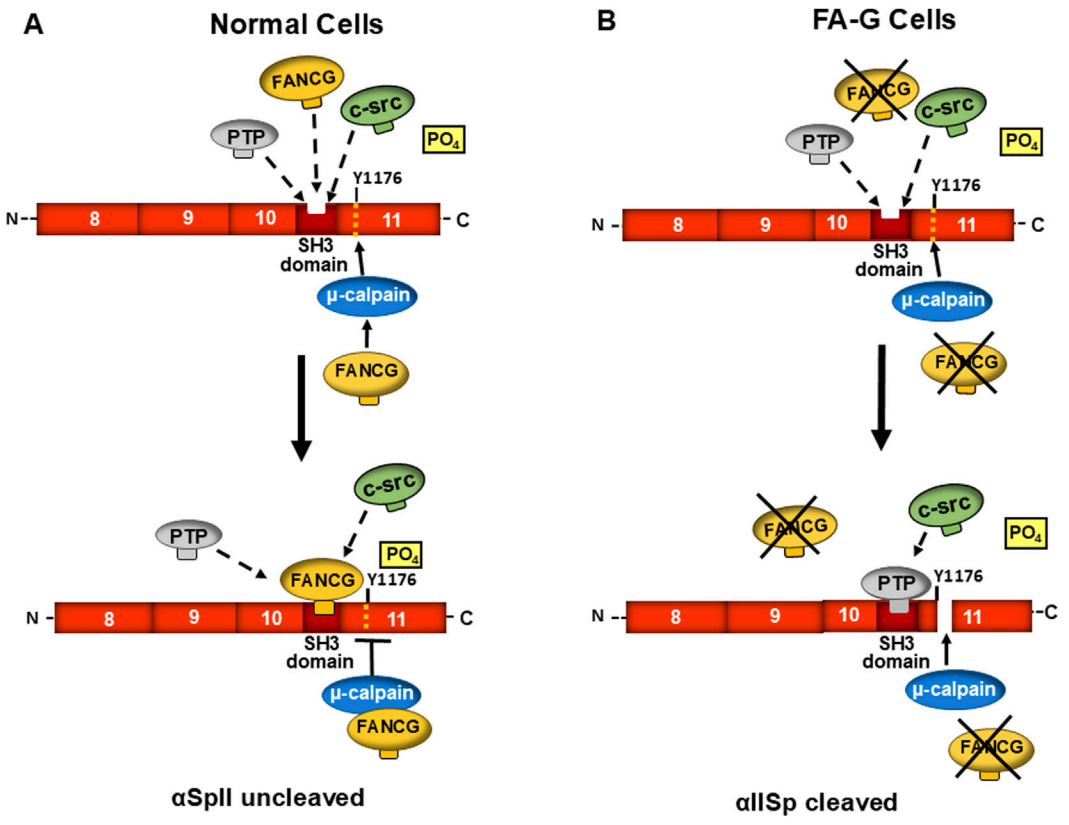

FIGURE 5
A proposed model for the role of FA proteins in maintenance of stability of αSpII in cells and regulation of its cleavage by μ-calpain. FANCG is used as an example of a FA protein in this process. A segment of αSpII containing repeats 8–11 is represented. **(A)** In normal human cells, an equilibrium exists between low molecular weight phosphotyrosine phosphatase (PTP), FANCG, and c-Src for binding to the SH3 domain of αSpII in repeat 10. When c-Src binds to the SH3 domain of αSpII, it phosphorylates Tyr^{1176} (Y1176) at the adjacent μ-calpain cleavage site. This prevents the ability of μ-calpain to cleave αSpII at its cleavage site. When FANCG binds to the SH3 domain, it prevents PTP binding at this site and μ-calpain cleavage of αSpII. FANCG could also bind to μ-calpain and inhibit its ability to cleave αSpII at this site. In both instances, the inability of μ-calpain to cleave αSpII would enhance the stability of αSpII in the cell. **(B)** In FA cells (FA-G cells for example), a functional FANCG protein is absent and not available for binding to the SH3 domain of αIISp or to μ-calpain. There would be a greater probability that PTP would bind to the SH3 domain. This would lead to the dephosphorylation of Y1176 and allow μ-calpain to cleave αSpII at its cleavage site. FANCG would also not be present to bind to μ-calpain and inhibit its activity. Thus, as is found in FA-G cells, there would be greater cleavage of αIISp. Similar events could occur in different FA complementation groups (e.g., FA-A). (Modified from Zhang et al., [69] with permission from the American Chemical Society).

synthesis (UDS), which measures uptake of nucleotides into DNA repair patches [47].

An important question is, what is the cause of the reduced levels of αSpII in FA cells? Lambert et al have shown that this is not due to reduced expression of αSpII, since FA cells express normal levels of αSpII mRNA [70]. They have demonstrated that it is due to increased cleavage of αSpII as a result of excessive activity of the protease, μcalpain, which cleaves αSpII [69]. They have proposed that FA proteins play a critical role in regulation of μ-calpain cleavage of αSpII and that reduced levels of FA proteins in FA cells leads to increased μ-calpain activity and increased cleavage of αSpII [50, 69]. Thus, both increased μ-calpain activity and reduced levels of FA proteins are proposed to play a critical role in the breakdown of αSpII that occurs in FA cells and the reduction in DNA repair. These points and their significance will be discussed below.

Excessive μ-calpain activity in FA cells leads to increased cleavage of αSpII and decreased DNA ICL repair

Within the cell, αSpII is susceptible to cleavage by the protease, μ-calpain [75, 132–134]. αSpII is cleaved by μ-calpain at a single site, Y_{1176}-G_{1177}, which is adjacent to the SH3 domain of αSpII (Figure 5) [75, 76]. Proteolysis of αSpII by μ-calpain leads to destabilization of the spectrin scaffold and the physiological processes and pathways it regulates [24, 27, 33, 75,

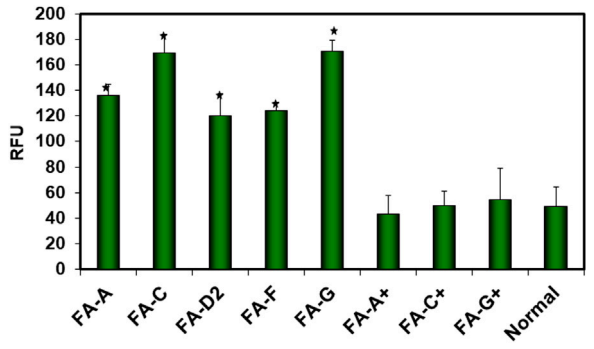

FIGURE 6
μ-Calpain activity in FA cells. μ-Calpain activity was measured in FA-A, FA-C, FA-D2, FA-F and FA-G cells, in corrected FA-A (FA-A+), FA-C (FA-C+), and FA-G (FA-G+) cells which had been stably transfected with a retroviral vector expressing the appropriate FANC cDNA, and in normal cells. Comparison of μ-calpain activity between the groups of cells showed that μ-calpain activity was 3-4 fold greater in FA cells compared to normal cells or corrected FA cells. Activity was determined by measuring cleavage of a fluorogenic calpain substrate and expressed as relative fluorescence units (RFU). Vertical lines represent ± the standard error of the mean for 5–8 separate experiments (*) ($p < 0.0001$). (Reproduced from Zhang et al., [69] with permission from the American Chemical Society).

76, 89]. Susceptibility of αSpII to proteolytic cleavage is controlled by phosphorylation/dephosphorylation of residue Y1176 in μ-calpain's cleavage site [75, 76]. When residue Y1176 is phosphorylated by c-Src, a kinase that binds to the SH3 domain of αSpII, μ-calpain cannot cleave αSpII at its cleavage site [75, 76]. Binding of low-molecular weight phosphotyrosine phosphatase (LMW-PTP) to the SH3 domain of αSpII leads to dephosphorylation of Y1176 and allows μ-calpain to cleave αSpII at this site (Figure 5) [33, 75]. Thus, inhibiting the binding of LMW-PTP to the SH3 domain of αSpII and the subsequent dephosphorylation of Y1176 is important in preventing cleavage of αSpII by μ-calpain. In normal physiological processes, a balance is reached between activation of μ-calpain and substrate-level regulation of αSpII cleavage [75, 76, 135]. This balance depends on maintaining an equilibrium between binding of c-Src and LMW- PTP to the SH3 domain of αSpII, phosphorylation/dephosphorylation of the Y1176 residue and the accessibility of the μ-calpain cleavage site to cleavage by μ-calpain [75, 76].

In FA cells, Lambert et al have shown that in a number of complementation groups (FA-A, FA-C, FA-D2, FA-F, and FA-G) μ-calpain activity is 3-4 fold greater than it is in normal cells (Figure 6) [69]. This is not due to an increase in protein levels of μ-calpain, which are similar to those in normal cells, but to the significantly increased activity of μ-calpain [69]. The excessive activation of μ-calpain activity in FA cells is demonstrated by the presence of the characteristic 150 kDa break-down product of αSpII which is produced by μ-calpain proteolytic cleavage of αSpII [69, 132, 140, 141]. This break-down product is relatively stable and widely used as a measure of μ-calpain cleavage of αSpII [141]. The increase in μ-calpain activity in FA cells correlates with decreased levels of αSpII, which are approximately 35–40% of those found in normal cells [13, 38, 44]. That FA proteins play an important role in modulating the levels of μ-calpain activity found in normal cells is demonstrated by the finding that restoring levels of FA proteins in FA cells to those found in normal cells by transfection of FA cells with a retroviral vector expressing the appropriate FANC cDNA leads to reduction of μ-calpain activity to normal levels (Figure 6) [69].

Evidence that αSpII cleavage in FA cells is due to increased μ-calpain activity is demonstrated by studies which show that in FA-A cells after knockdown of μ-calpain by siRNA and damage with MMC or 8-MOP plus UVA light, αSpII levels are restored to normal and damage-induced αSpII nuclear foci are observed (Figure 7) [13, 38, 44, 69]. XPF co-localizes with SpII in these foci just as it does in normal cells [69]. This is indicative of DNA ICL repair. In addition, there is a decrease in the chromosomal abnormalities (chromatid beaks, inter chromatid exchanges, chromatid fusions and radial formations) observed in FA cells after DNA ICL damage [69]. Thus, there is strong evidence that increased cleavage of αSpII in FA cells is due to excessive activation of μ-calpain in these cells.

Of particular interest, excessive activation of calpain activity also occurs in a number of neurodegenerative diseases and has been proposed to contribute to the neuropathology of many of these disorders [135]. This excessive activation correlates with a loss of SpII and has been proposed to be associated with the clinical manifestations of these disorders [132, 135, 140, 141]. Excessive activation of calpain and is also found in cancer development [132, 135, 140, 141]. FA may be another example of a disorder in which αSpII breakdown by excessive calpain activity plays an important role in the pathological manifestations of the disorder. This will be discussed in a later section.

FA proteins play a critical role in reducing cleavage and maintaining the stability of αSpII in cells

FA proteins are proposed to play a critical role in maintenance of αSpII stability and regulation of its cleavage in the cell [13, 50, 69]. In support of this, in corrected FA cells (FA-A, FA-C, and FA-G) which have been stably transduced with a retroviral vector expressing the appropriate FANC cDNA (FANCA, FANCC, or FANCG), FA protein levels return to those found in normal cells, as do the levels of αSpII [13, 50, 69]. In these corrected FA cells, μ-calpain activity is also at normal levels (Figure 6) [69]. Lambert et al have proposed several mechanisms by which FA proteins could aid in maintenance of αSpII stability in the cell and regulation of its cleavage by

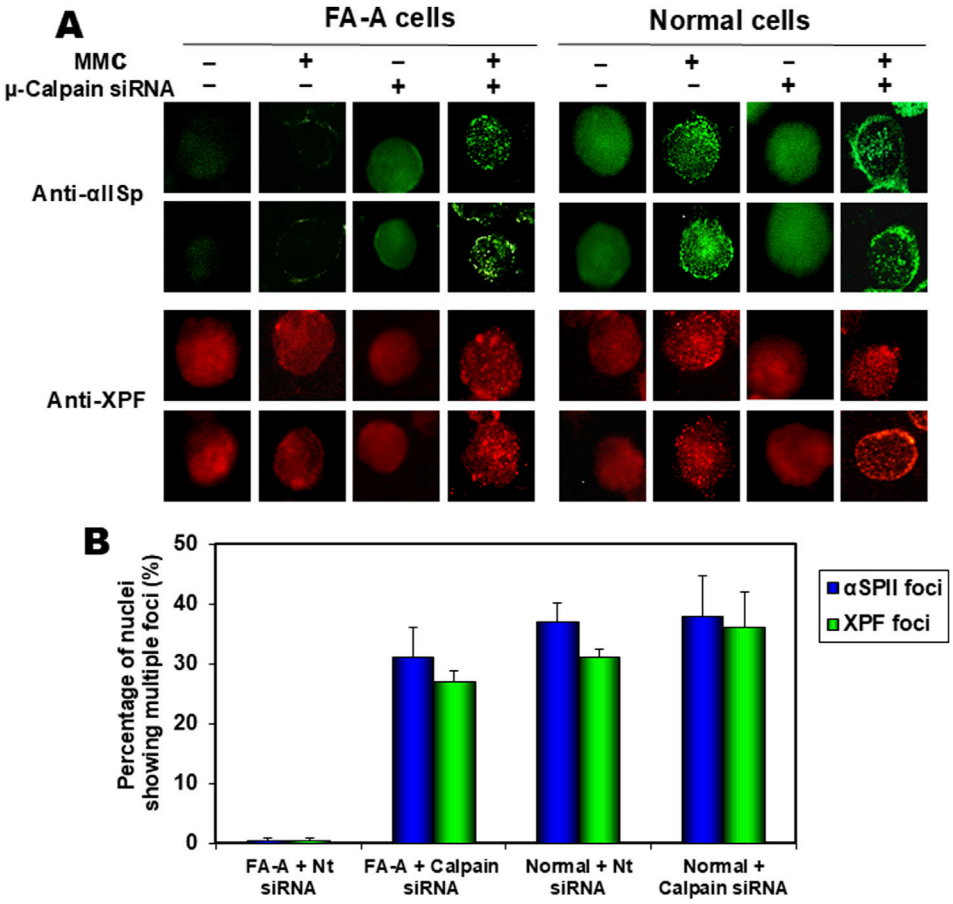

FIGURE 7
Effect of siRNA knock down of μ-calpain in FA cells on formation of αSpII and XPF nuclear foci after damage with an ICL agent, MMC. **(A)** FA-A and normal cells were transfected with non-target siRNA (–) or μ-calpain siRNA (+) and 24 h after transfection, cells were either undamaged or treated with MMC. αSpII and XPF nuclear foci were examined 16 h after MMC treatment using indirect immunofluorescence and staining with anti-αSpII or anti-XPF. After μ-calpain knock down, αSpII levels in FA-A cells were returned to normal levels and αSpII and XPF localized to damage-induced nuclear foci. **(B)** There was no significant difference in the percentage of nuclei showing multiple foci in FA-A cells in which μ-calpain had been knocked down compared to normal cells transfected with either Nt siRNA or μ-calpain siRNA (Reproduced from Zhang et al., [69] with permission from the American Chemical Society).

μ-calpain [13, 50, 69]. One of these is that a FA protein binds to the SH3 domain of αSpII and inhibits the ability of LMW-PTP to bind to the site and dephosphorylate it at Y1176. This, in turn, would prevent the ability of μcalpain to cleave αSpII at its cleavage site and would enhance the stability of αSpII (Figure 5A). In support of this, FANCG has been shown to have a 1@ consensus sequence that directly binds to the SH3 domain of αSpII [101]. This binding could be constitutive. FANCG could exist in equilibrium with c-Src and LMW-PTP for binding to this site. Since affinity of ligands that bind to SH3 domains, in particular the SH3 domain of αSpII, is quite low, the on and off binding rates can be fast, allowing a rapid exchange in binding of these proteins [79, 81]. Importantly, there are a number of patient derived mutations in the *FANCG* gene that result in FANCG having a defect or loss in the consensus sequence that binds to the SH3 domain of αSpII [101]. This could lead to loss of ability of FANCG to bind to αSpII [101]. This would provide LMW-PTP greater accessibility to the SH3 domain and lead to greater cleavage of αSpII by μ-calpain (Figure 5B). FA-G patients have a poorer hematological outcome than patients from other FA complementation groups due to a more severe cytopenia and a higher incidence of AML and leukemia [67, 142]. It would be of interest to determine if this is related to the inability of a defective FANCG to bind to αSpII and aid in preventing excessive cleavage of αSpII by μ-calpain, and in maintaining the stability of αSpII in FA-G cells.

Another possible mechanism by which FA proteins could regulate μ-calpain activity and cleavage of αSpII is that a FA protein binds to μ-calpain and prevents its ability to cleave αSpII. Supporting this is yeast two-hybrid analysis which has shown that FANCA and FANCG bind directly to μ-calpain [69]. This

binding could potentially inhibit μcalpain's activity. Alternatively, a FA protein could bind to αSpII, protecting the μ-calpain cleavage site from attack by μ-calpain. A fourth potential mechanism is that a FA protein could have an effect on the binding of calmodulin to αSpII. Calmodulin binds to αSpII at a site adjacent to μ-calpain's cleavage site and enhances the susceptibility of αSpII to cleavage by μ-calpain [82–84]. A FA protein, in some manner, could interfere with this binding of calmodulin to αSpII and inhibit its ability to stimulate μ-calpain's cleavage of αSpII. In FA cells, a defect in a specific FA protein could lead to enhanced binding of calmodulin to αSpII and enhanced cleavage by μ-calpain. FA proteins also bind to each other, particularly those in the FA core group (FANCA, FANCB, FANCC, FANCE, FANCF, FANCG, and FANCL) [143]. For example, FANCG binds directly to FANCF [143]. It is possible that such interactions could aid in association of FA proteins with αSpII.

There are thus a number of potential mechanisms by which FA proteins could play an important role in regulating the activity of μ-calpain and its ability to cleave αSpII. Different FA proteins could affect a different aspect of the αSpII cleavage process, either directly or indirectly. The stability of αSpII is a critical component in the DNA ICL repair process and excessive cleavage of αSpII in FA cells by μ-calpain is proposed to be an important factor in the DNA repair deficiency in these cells [69]. Lambert et al. have proposed that FA proteins play a significant role in the regulation of αSpII cleavage and its stability in the cell [50, 69]. The exact mechanisms by which this occurs needs to be investigated further.

These studies demonstrate another important role for FA proteins in the cell and in the DNA repair process. In addition to the role FA proteins play in DNA ICL repair, it is proposed that they also act as regulators of the cleavage of αSpII by μ-calpain. This could be important for a large number of cellular processes in which αSpII is required, loss of which could lead to chromosome instability, DNA repair defects, congenital and developmental abnormalities, progression of cancer, neuronal degeneration and neurological disorders, which are characteristics of FA.

αSpII is critical for maintenance of telomere function and chromosome stability after DNA ICL damage

αSpII recruits repair proteins to telomeres after DNA ICL damage

Telomeres are critical for maintenance of chromosome stability and after DNA damage αSpII plays a major role in this process [50, 144–150]. Lambert et al have demonstrated that αSpII is recruited to telomeres in S phase after DNA ICL damage and is critical for the repair of telomeric DNA at the time when telomeres are undergoing DNA replication [46]. αSpII co-localizes with a telomere-specific Cy [3]-labeled nucleic acid (PNA) oligonucleotide probe and with two proteins in the shelterin complex, TRF1 and TRF2, which help protect the telomere and prevent telomere dysfunction (Figure 8) [46, 50]. These studies were carried out in normal human lymphoblastoid cells which have telomerase, a ribonucleoprotein complex important in maintaining the ends of chromosomes [148, 151–153]. Telomerase positive cells were used since telomerase is present in a number of the cell types involved in the clinical manifestations of FA (e.g., highly proliferating cells, bone marrow cells, peripheral blood cells, stem cells which include hematopoietic stem cells, and numerous types of cancer cells) [154, 155]. These studies have demonstrated that αSpII acts as a scaffold and recruits XPF to sites of ICL damage on telomeric DNA in normal human cells, indicating that it aids in repair of the ICL damage in telomeres [46]. Knock down of αSpII in normal cells leads to loss of localization of XPF to sites of damage on telomeric DNA, demonstrating that αSpII is critical in this recruitment process (Figure 9A) [46]. In FA-A cells, in which there is a deficiency in αSpII, XPF, though present, does not form foci at sites of ICLs on telomeric DNA (Figure 9A). After αSpII levels are restored to normal by knocking down μ-calpain, XPF localizes to sites of damage on telomeres (Figure 9B) [46]. This emphasizes the importance of αSpII in localization of XPF to damage sites on telomeres.

There are differences, however, in the repair events in telomeric DNA compared to non-telomeric DNA. Studies have shown that, in normal human lymphoblastoid cells and HeLa cells, both of which express telomerase, FANCD2, unlike αSpII, does not localize in foci in telomeric DNA after ICL damage [46]. FANCD2 was found, however, to localize to telomeres in immortalized telomerase-negative cells after DNA ICL damage [156]. These studies thus indicate that in telomerase-positive cells FANCD2 is not involved in repair of DNA ICLs at telomeres, however, it is involved in ICL repair in telomeres in telomerase-negative cells. It is possible that, in telomerase-positive cells, the repair response to DNA ICLs is similar to, but not identical to, that which occurs in genomic, non-telomeric, DNA. This needs to be explored further.

Dramatic reduction of αSpII levels in cells leads to catastrophic loss of telomeres and chromosomal aberrations after DNA ICL damage

The importance of αSpII in repair of DNA ICLs in telomeric DNA is supported by studies which have demonstrated that, in normal human cells in which αSpII has been knocked-down to levels that are 35% of normal and which have been damaged with

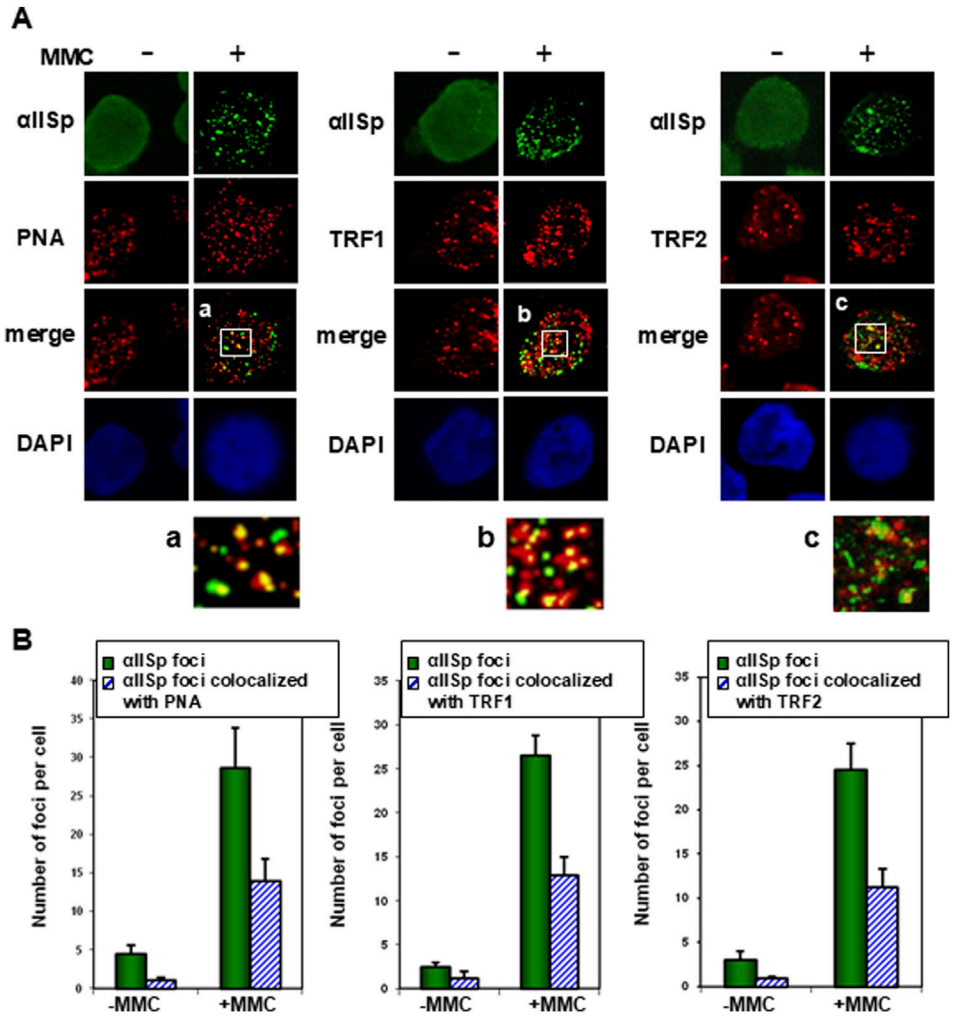

FIGURE 8
αSpII associates with telomeres after DNA ICL damage. **(A)** αSpII associates with a Cy3-labeled telomere specific probe (PNA) as well as two telomeric proteins in the shelterin complex, TRF1 and TRF2, after 16 h treatment with MMC. Cells were examined using a PNS probe as well as immunoFISH and staining with antispectrin, anti-TRF1 or anti-TRF2 antibodies. Nuclear DNA was counterstained with DAPI. Pictures were taken with Z-stack and one slice is displayed. Magnified images are shown of co-localization of αSpII with (a) PNA probe; (b) TRF1 and (c) TRF2. **(B)** The number of αSpII nuclear foci per cell and the number of αSpII foci that co-localized with PNA, TRF1 and TRF2 foci per cell in normal cells before and after MMC treatment was quantitated. Three hundred cells were counted in each group. Error bars represent SEM. (Modified from Zhang et al., [46] with permission of Oxford University Press).

a DNA ICL agent, there is telomere dysfunction, as evidenced by the increased formation of telomere dysfunction-induced foci (TIF) [46]. These foci represent sites of DNA doublestrand breaks (DSBs), which arise when the DNA replication forks are stalled at the site of a DNA ICL, and are an indicator of dysfunctional telomeres [46, 157, 158]. It has been proposed that decreased levels of αSpII can lead to stalling of replication of telomeric DNA at sites of DNA ICLs in S phase [46]. This results in collapse of the replication fork and in the formation of DNA DSBs which are measured by determining the accumulation at telomeres of γH2AX foci, which are markers for DSBs. In addition to increased TIF formation, knock-down of αSpII also leads to catastrophic loss of telomeres after DNA ICL damage (Figure 10) [46]. This loss can be determined by examination of chromosomes for loss of telomeres or production of signal free ends (SFEs) (Figure10) [46]. Since DNA replication in telomeres occurs in S phase, and αSpII localizes to telomeres in S phase after ICL damage, this suggests that αSpII is important in telomere function during replication of ICL-damaged DNA. A loss of αSpII could thus have significant effects on DNA replication after ICL damage and could lead to production of stalled replication forks. If αSpII is not recruited to these stalled replication forks to aid in repair of the DNA damage, it can be hypothesized that this could lead to

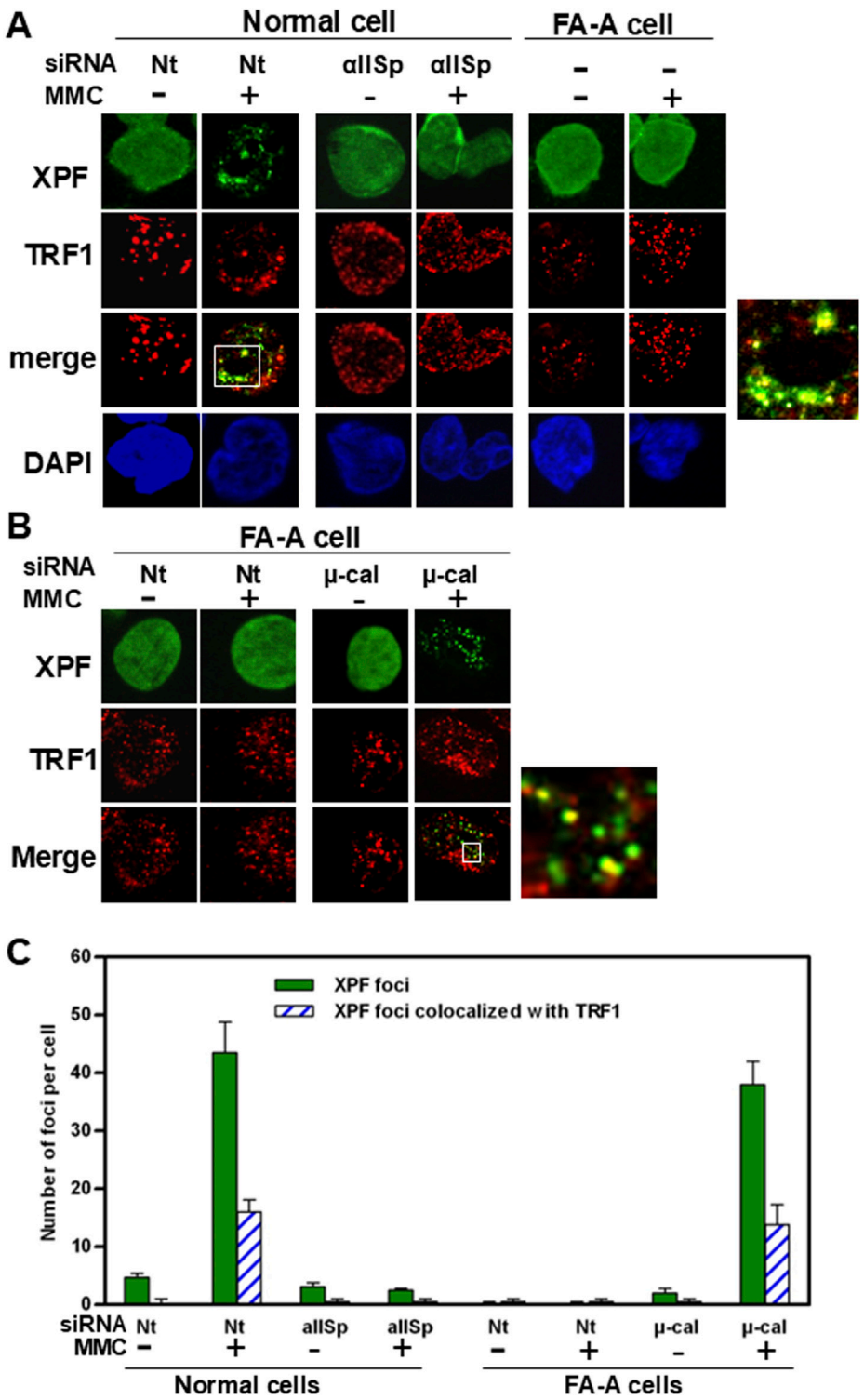

FIGURE 9
αSpII is needed for recruitment of XPF to sites of ICL damage on telomeric DNA. **(A)** In normal cells transfected with Nt siRNA and treated with MMC for 16 h, XPF co-localized with TRF1. A magnified image of co-localization of XPF with TRF1 in MMC-treated Nt-siRNA-transfected cells is shown to the right. Knock-down of αSpII in normal cells leads to loss of localization of XPF with TRF1 at telomeres after cells are treated with MMC. These studies were carried out using immunoFISH and staining with antiXPF and anti-TRF1 antibodies. Nuclear DNA is counterstained with DAPI. **(B)** In FA-A cells, XPF does not form foci in the nucleus after ICL damage. However, in FA-A cells in which μ-calpain (μ-cal) had been knocked down with μ-calpain siRNA and cells were subsequently treated with MMC, XPF co-localized with TRF1 at telomeres. A magnified image of co-
(*Continued*)

FIGURE 9 (Continued)
localization of XPF with TRF1 in FA-A cells in which μ-calpain had been knocked down and then treated with MMC is shown on the right. **(C)** The number of XPF nuclear foci and XPF nuclear foci which colocalized with TRF1 was quantitated in normal and FA-A cells. These numbers were the same between normal cells transfected with Nt-siRNA and FA-A cells transfected with μ-calpain siRNA, both of which had been treated with MMC. (Reproduced from Zhang et al., [46] with permission of Oxford University Press).

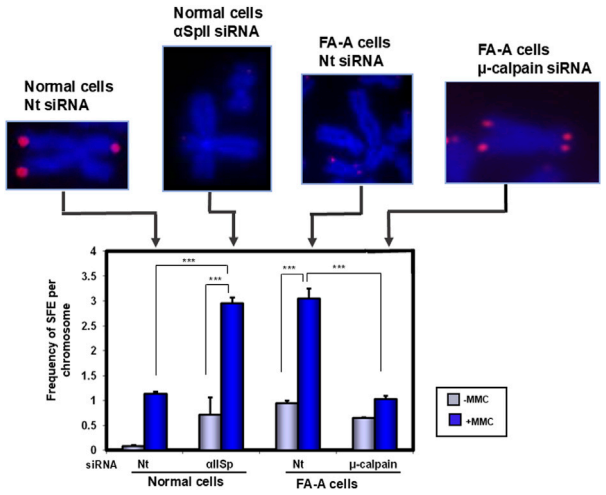

FIGURE 10
A deficiency in αSpII in cells leads to a catastrophic loss of telomeres after DNA ICL damage. In normal human cells in which αSpII has been knocked down by siRNA, there is a loss of telomeres after treatment with a DNA ICL agent, MMC, compared to normal cells transfected with a Nt siRNA [46]. This is noted by the presence of signal free ends (SFEs) on the chromosomes. In FA-A cells, after damage with MMC, there is a catastrophic loss of telomeres, as noted by the presence of (SFEs), compared to the presence of telomeres on undamaged Nt siRNA transfected FA-A cells [46]. However, in FA-A cells after μ-calpain has been knocked down by siRNA so as to increase αSpII levels, and subsequent treatment with MMC, quantitation of the frequency of SFE in chromosomes showed that it was reduced to levels similar to those in normal cells transfected with Nt siRNA. These studies demonstrate that αSpII has a critical role in maintaining telomere function after damage with a DNA ICL agent [46]. Metaphase chromosomes were stained with DAPI (blue) [46]. Telomeric DNA was identified using FISH with a Cy3-labeled telomere specific PNA probe (red) [46]. Error bars are S.E.M. ***$P < 0.0001$ (Modified from Zhang et al. [46] with permission from Oxford University Press).

failure to efficiently restart replication and to telomere dysfunction and loss of telomeres. These studies demonstrate the importance of αSpII in telomere maintenance and function after DNA ICL damage.

Since chromosome stability depends on functioning telomeres, it is critical that after DNA damage the damage is repaired so that chromosome integrity can be preserved. In normal cells in which αSpII has been knocked down, there is a significant increase in chromosomal aberrations, after DNA ICL damage, which accompanies the decrease in DNA repair that occurs in both non-telomeric and telomeric DNA [45, 46, 69]. These aberrations include: chromatid breaks, sister chromatid end-to-end fusions, radials, and chromosome exchanges [45, 46, 69]. This thus demonstrates that, after DNA ICL damage, αSpII in both non-telomeric and telomeric DNA is critical for maintenance of not only telomere function but also chromosomal stability.

Telomere dysfunction in FA cells after DNA ICL

FA serves as an excellent model for the effects that a deficiency in αSpII has on telomere function after DNA damage. As mentioned above, levels of αSpII in FA-A cells are approximately 35–40% of normal [12, 45, 48]. Telomere dysfunction has been observed in FA complementation group A (FA-A) cells after DNA ICL (i.e., MMC or psoralen plus UVA light) damage [46]. This includes a significant increase in TIF formation and a catastrophic loss of telomeres (Figure 10) [46]. This increase correlates with loss of αSpII in these cells, which results in a significant decrease in recruitment of XPF to sites of damage at telomeres as mentioned above (Figure 9A) [46]. These studies indicate that there is a defect in repair of ICLs at telomeres in FA-A cells similar to that seen in normal cells after αSpII has been knocked down.

Knock-down of μ-calpain in FA-A cells corrects the αSpII deficiency, telomere dysfunction, defective DNA repair and chromosome instability after DNA ICL damage

Evidence that loss of αSpII in FA-A cells is a significant factor in the increase in telomere dysfunction and in the catastrophic loss of telomeres that occurs after DNA ICL damage is demonstrated by studies in which μ-calpain has been knocked down by siRNA. Knock down of μ-calpain in FA-A cells leads to restoration of αSpII levels to those found in normal cells and to reduction in the number of TIF positive cells after MMC treatment [46]. In addition, it also results in a significant decrease in the frequency of signal-free ends (SFEs) or telomere loss in FA-A cells after DNA ICL damage (Figure 10) [46]. These studies thus demonstrate that breakdown of αSpII in FA-A cells due to excessive μ-calpain activity results in telomere dysfunction and loss of telomeres, which can be corrected by knocking-down μ-calpain.

In FA-A cells, unlike in normal cells, XPF does not localize to telomeres after DNA ICL damage (Figure 9B) [46]. However, when μ-calpain is knocked down by siRNA and αSpII levels have been restored to normal, XPF co-localizes with αSpII in damage induced foci at telomeres (Figure 9B) [46]. These studies again demonstrate that αSpII plays a critical role in telomere function after DNA ICL damage, and that restoration of αSpII to normal levels in FA cells by knocking down μ-calpain can have a significant effect on increasing the DNA repair capability of these cells and correcting the telomere dysfunction observed after DNA ICL damage [46].

Chromosomal aberrations produced after DNA ICL damage are also corrected in FA cells after restoration of αSpII levels to normal by knocking-down μ-calpain [45, 46]. The aberrations which were corrected include sister chromatid end-to-end fusions, chromosome exchanges, and chromatid breaks and radials and are similar to those produced after ICL damage in normal cells in which αSpII levels have been knocked down [45, 46]. Thus decreasing μ-calpain activity in FA cells and restoring αSpII levels to normal leads to restoration of DNA repair capabilities, localization of XPF to sites of DNA damage, increased chromosomal stability, and a decrease in formation of dysfunctional telomeres and in loss of telomeres after DNA ICL damage. These studies indicate that both loss of αSpII and telomere dysfunction in FA-A cells may be important factors in the chromosomal aberrations which develop after DNA ICL damage.

Of particular interest, FA-A cells in which αSpII levels have been restored to normal are still deficient in the FANCA protein. The question that arises is how DNA ICL repair can still proceed in the absence of this protein. Lambert et. al. have proposed that FA proteins, in addition to a role in DNA repair, are also important in maintaining the stability of αSpII and reducing its cleavage by μ-calpain [46, 69]. When αSpII stability has been restored in FA-A cells by knocking-down μ-calpain, DNA repair is able to proceed, possibly involving an alternative means [49, 50]. In FA-A cells, in which there is a deficiency in FANCA, FANCD2 is not monoubiquitinated [49]. FANCD2-Ub has been shown to be important for the ICL repair pathway to proceed [57–59]. Lambert et al have shown, however, that in FA-A cells in which αSpII levels have been restored, non-Ub FANCD2 foci are observed at levels approximately 80% of normal just as they are in FA-A cells in which levels of αSpII have not been restored [49]. FANCD2-Ub is not present [49]. The non-Ub FANCD2 foci localize to sites of DNA ICL damage and the nonUb FANCD2 foci follow the same time course for formation of nuclear foci after ICL damage as the FANCD2-Ub foci do. However, in the FA-A cells non-Ub FANCD2 foci only appear after levels of αSpII have been returned to normal [49]. Thus non-Ub FANCD2 requires the presence of αSpII in order to localize to sites of damage. αSpII does not colocalize with these non-Ub FANCD2 foci, just as it does not co-localize with FANCD2- Ub foci in normal cells after DNA ICL damage [49]. Lambert et al have proposed that in FA-A cells when levels of αSpII have been returned to normal, non-Ub FANCD2 localizes to sites of damage and plays a role in the DNA repair process [49]. This is potentially an alternate method for DNA ICL repair. Whether this is mainly a back-up mechanism or is also involved in normal ICL repair is not clear. Other studies support the proposal that non-Ub FANCD2 plays a role in DNA ICL repair, in particular, in the nonhomologous recombination step in the repair process and in replication fork recovery [159–163]. The relationship between αSpII and FANCD2-Ub and non-Ub FANCD2 after DNA damage needs to be further investigated.

Importance of loss of αSpII in the pathogenesis of Fanconi anemia

As noted above, breakdown and loss of αSpII in FA cells has a significant effect on both DNA repair and chromosome stability after damage with a DNA interstrand crosslinking agent. Lambert et al. have proposed that this loss is an important contributing factor in the pathogenesis of FA [38, 44]. There are a number of defining characteristics associated with FA pathogenesis, the major ones of which include a defect in DNA repair, chromosome instability, cancer predisposition, bone marrow failure and multisystemic congenital abnormalities [47, 51–69]. Experimental evidence has shown that loss of αSpII in FA cells has a significant impact on several of these characteristics. Breakdown of αSpII in FA cells has been shown to be directly involved in the defect in ability of FA cells to repair DNA ICLs [13, 44, 45]. Loss of αSpII results in failure of XPF/ERCC1 to localize to sites of DNA ICLs and create incisions at these sites leading to defective DNA ICL repair in FA cells in both telomeric and non-telomeric DNA [13, 44, 47, 50]. In addition, excessive breakdown of αSpII in FA cells also results in chromosome instability and production of chromosomal aberrations after DNA ICL damage [44, 45]. It has been shown that failure to repair DNA ICLs, particularly in S phase of the cell cycle can directly lead to the production of DNA double-strand breaks and chromosomal aberrations [164]. This is proposed to be a major cause of chromosomal aberrations in FA cells after DNA ICL damage [44, 45, 50]. Restoration of αSpII levels to normal in FA cells, by knocking down μ-calpain, leads to restoration of DNA ICL repair and chromosome stability [45, 47, 50]. These studies thus indicate that αSpII is critical for two important cellular processes, DNA repair and chromosome stability of DNA ICL damage, which are defective in FA cells and which contribute to the pathogenesis of the disorder.

Another phenotypic characteristic of FA is an increased incidence of cancer (e.g., acute myeloid leukemia (AML) and squamous cell carcinoma) and hemolytic anemia [67, 68, 77, 165]. There is evidence that a deficiency in αSpII plays an important role in cancer development [68, 166]. Loss of αSpII has been reported in the bone marrow of patients with acute

myeloid leukemia (AML) and it has been proposed that a deficiency in αSpII is a contributing factor in the development of AML [165, 167]. Since FA patients can develop AML, it is possible that loss of αSpII is an important component in this process and may be involved in the leukemogenesis and bone marrow failure which can occur [165, 167]. In a number of B-cell malignant lymphomas, there is a strong correlation between loss of αSpII and development of lymphomagenesis [167]. This has led to the suggestion that a deficiency in αSpII is an important factor in lymphomagenesis [167]. Thus breakdown and loss of αSpII in FA cells could play a role in the development of AML and leukemogenesis observed in FA patients and contribute to FA pathogenesis. This needs to be further examined.

FA patients can also have a number of congenital abnormalities, which include radial ray deformities, absent radi, ear malformations, urogenital anomalies, renal deformities, cardiac defects, and neurological abnormalities [67, 168, 169]. αSpII has been proposed to play a role in many developmental processes [36, 170–172]. In αSpII knockout mice the embryos display cardiac, craniofacial and neural tube abnormalities [170]. Cultured fibroblasts from these mice have impaired growth and spreading [170]. These studies indicate that αSpII is important in cellular morphology and development. Since αSpII is critical for and expressed throughout development in mammalian cells, it can be hypothesized that a deficiency in αSpII in FA patients could indirectly have a significant influence on a number of the developmental abnormalities associated with FA.

Other disorders associated with defects in αSpII

αSpII is an essential protein in the cell and an important cellular scaffold which is critical for a diverse number of biological processes, therefore, loss or dysfunction of this protein could be of important clinical significance and play a fundamental role in the etiology of a number of diseases [7, 13–17, 25–39]. Two important causes for a loss or deficiency in αSpII are: (1) enhanced cleavage and break-down of αSpII, or (2) mutations in the gene encoding αSpII, *SPTAN1,* resulting in expression of a defective αSpII. Some disorders in which defects or a deficiency in αSpII are of clinical significance are presented below.

Loss or a deficiency in αSpII is an important factor in the pathophysiology of a number of neurological disorders [135, 169, 173–179]. Mutations in the *SPTAN1* gene are associated with a broad range of neurodevelopmental diseases [169, 174, 175]. One of these is early infantile epileptic encephalopathy, or West Syndrome, which is characterized by progressive brain atrophy, severe neurodevelopmental impairment, mental retardation, difficulty walking, and seizures [169, 174–177]. In this disorder, there is a mutation in the *SPTAN1* gene leading to a defect in the binding of αSpII to βSpII and to βSpIV, which are needed for organization and maintenance of the neuronal actin-spectrin cytoskeleton, as well as for axonal and dendritic growth and development and neuronal excitabiliity [174–177].

In a number of other progressive neurodegenerative disorders there is increased breakdown of αSpII [132, 135, 140, 141, 178–181]. It has been shown that this is due to excessive activation of calpain which results in increased cleavage of αSpII. Excessive activation of calpain and αSpII cleavage is a common feature of neurodegenerative diseases and of traumatic encephalopathy and leads to loss of neuronal integrity and the neuropathology of many of these disorders [132, 135, 140, 141, 178, 179]. In Alzheimer's disease, increased breakdown of αSpII has been demonstrated in numerous cells and tissues and is due to excessive calpain activity but not to changes in levels of calpain [141, 171, 177, 182]. It has been proposed that faulty regulation of the neuronal spectrin skeleton and its breakdown by excessive calpain activity can activate a series of events that leads to the ataxia and neuronal degeneration observed in this and other neurodegenerative disorders [135]. Thus, excessive activation of calpain activity in a number of neurodegenerative diseases results in loss of αSpII [132, 135, 140–142].

Central nervous system and various neurological anomalies are also a clinical characteristic of FA patients. These include: brain and spinal cord anomalies, microcephaly, hydrocephalus, cerebellar defects, and development of medulloblastoma [67, 168, 173, 183–186]. Of considerable interest, FA cells have significantly (3-4 fold) increased levels of breakdown of αSpII due to an excessive increase in μ-calpain activity [13, 50, 69]. FA thus represents another disorder in which loss of αSpII is due to its cleavage by μ-calpain. It can be hypothesized that like some neurodegenerative diseases, excessive activation of μ-calpain activity in FA, leading to significant cleavage of αSpII, may be an important contributing factor in the pathological changes observed in the nervous system and in the pathogenesis of FA. It would be of interest to determine whether there is increased μ-calpain activity and αSpII cleavage in neuronal tissue in FA patients with neurological abnormalities and to speculate that, if a relationship between these two factors were found, this would indicate that breakdown of αSpII is an important factor in progression of these abnormalities.

There is evidence that a deficiency in αSpII plays an important role in development of cancers other than AML. In Lynch Syndrome or hereditary nonpolyposis colorectal cancer, where there is a defect in DNA mismatch repair and a deficiency in the mismatch repair protein, MLH1, there is a significant reduction in levels of αSpII in the tumor cells [187–189]. Since MLH1 directly interacts with αSpII, it has been proposed that loss of MLH1 leads to destabilization of αSpII which, in turn, results in a defect in DNA repair and in the tumor development seen in this disorder [187–189]. These studies, along with those noted above, which suggest that αSpII loss is an important factor in

lymphomagenesis, collectively indicate that there is strong evidence that a deficiency in αSpII plays an important role in development of a number of different types of cancer.

In both acquired and neonatal congenital heart failure, there is dysfunction of αSpII that is due to excessive calpain activity which results in increased cleavage of αSpII [190, 191]. This has been demonstrated by the presence of the 150 kDa αSpII breakdown product of μ-calpain in the cardiac cells [190, 191]. αSpII is required for normal cardiac structure, function and development and plays a central role in the formation and regulation of key structural and signaling pathways in the heart [190, 191]. Breakdown of αSpII, which can occur in heart disease, has a significant effect on the cardiomyocyte spectrin network and on regulation of normal cardiac function [36, 190, 191]. Thus, breakdown of αSpII by excessive μ-calpain activity is also an important factor in heart failure.

αSpII dysfunction can therefore lead to a variety of disorders, particularly since it is a multifunctional protein which is critical for a multitude of diverse cellular processes. As mentioned above, there is a relationship between clinical manifestations of all of the disorders described and a loss or deficiency in αSpII, which in turn is due to either enhanced cleavage of αSpII by excessive proteolytic cleavage by μ-calpain or expression of a defective αSpII due to a mutation in the *SPTAN1* gene. As a result of the diversity of αSpII function, a deficiency in αSpII can lead either directly or indirectly to dysregulation of a number of different cellular pathways and to pathological changes which are manifested in a variety of different disorders. The number of disorders in which deficiencies in αSpII play a direct or indirect role may still not yet be fully recognized.

Conclusions and perspective

αSpII is a critically important and functionally diverse protein which represents 2–3% of all proteins in human cells [14–17]. It forms a network under the plasma membrane and within the cytoplasm ensuring the stability of cell membranes and organelles. It acts as a scaffold interacting with different protein binding partners playing an important role in cell development, cell migration, cell cycle, actin filament organization, intracellular trafficking and signal transduction [24–28]. Within the nucleus, αSpII is part of a nucleoskeletal network which is essential for maintaining the structural integrity of the nuclear envelope and elasticity of the nucleus. It is involved in the biomechanical coupling of the nucleoskeleton to the cytoskeleton. Of particular significance, αSpII plays a critical role in DNA repair where it acts as a scaffold recruiting repair proteins to sites of damage, enabling DNA repair to take place [44, 50].

αSpII's stability within the cell is critical for all of its functions. It is sensitive to cleavage by the protease, μ-calpain, and excessive activation of μ-calpain activity leads to increased cleavage of αSpII and loss of its ability to function in essential cellular processes, which is a contributing factor in a number of disorders [44, 50]. Maintaining a balance between activation of μ-calpain and regulation of spectrin cleavage is thus extremely important. This is particularly critical during the repair of DNA interstrand crosslinks (ICLs), where αSpII plays a critical role in repair of damaged sites, on both telomeric and non-telomeric DNA [46]. Excessive activation of μ-calpain activity leads to cleavage and breakdown of αSpII and loss of its ability to function in DNA repair as well as in cellular systems critical for both the structural and non-structural components of cell function [69]. This, in turn, leads to development of the pathological changes observed in numerous disorders.

One disorder in which there is a deficiency in αSpII is the bone marrow failure disorder, Fanconi anemia (FA), a distinctive hallmark of which is a defect in ability to repair DNA ICLs. αSpII levels in FA cells are 35%–40% of normal and levels of repair are 35–45% of normal [43, 48, 54]. Of particular significance, loss of αSpII in FA cells is due to increased μ-calpain activity, which is 3-4 fold greater than in normal cells, as observed in FA-A, FA-C, FA-D2, FA-F and FA-G cells [69]. This leads to increased cleavage of αSpII and decreased DNA ICL repair capabilities in both telomeric and non-telomeric DNA (Figure 11A). However, when levels of μ-calpain are knocked down, there is decreased cleavage of αSpII, whose levels return to those found in normal cells, and restoration of DNA ICL repair in these cells (Figure 11B). Another characteristic hallmark of FA is chromosome instability. After DNA ICL damage, a number of chromosomal aberrations occur in FA cells such as sister chromatid end-to-end fusions, chromatin breaks, chromosome exchanges and radials [45]. In FA cells in which μ-calpain has been knocked down, αSpII stability is restored leading to restoration of chromosomal stability and a decrease in chromosome aberrations after DNA ICL damage. This indicates that αSpII plays an important role in both DNA repair and chromosome stability after DNA ICL damage.

Lambert et al. have hypothesized that excessive cleavage of αSpII in FA cells is an important contributing factor in the pathogenesis of this disorder [44, 50]. The strongest evidence supporting this is from the studies noted above on the critical role of αSpII in DNA repair and in chromosome stability, since defects in these two processes are of major importance in FA pathogenesis. αSpII has been shown to play a direct role in DNA ICL repair and in the repair defect in FA. It binds directly to DNA containing ICLS and its involvement in the repair process has been demonstrated both by measurement of unscheduled DNA synthesis (UDS) after damage, which measures uptake of nucleotides into DNA repair patches, and by localization of the repair protein, XPF, to sites of DNA ICLs in normal and FA cells [42, 43, 47]. These studies indicate that breakdown of αSpII in FA cells is directly related to the defect in DNA ICL repair. An important question is what are the factors that are important in maintaining the stability of αSpII in FA cells. Studies have demonstrated that one of these is regulation of cleavage of αSpII by μ-calpain.

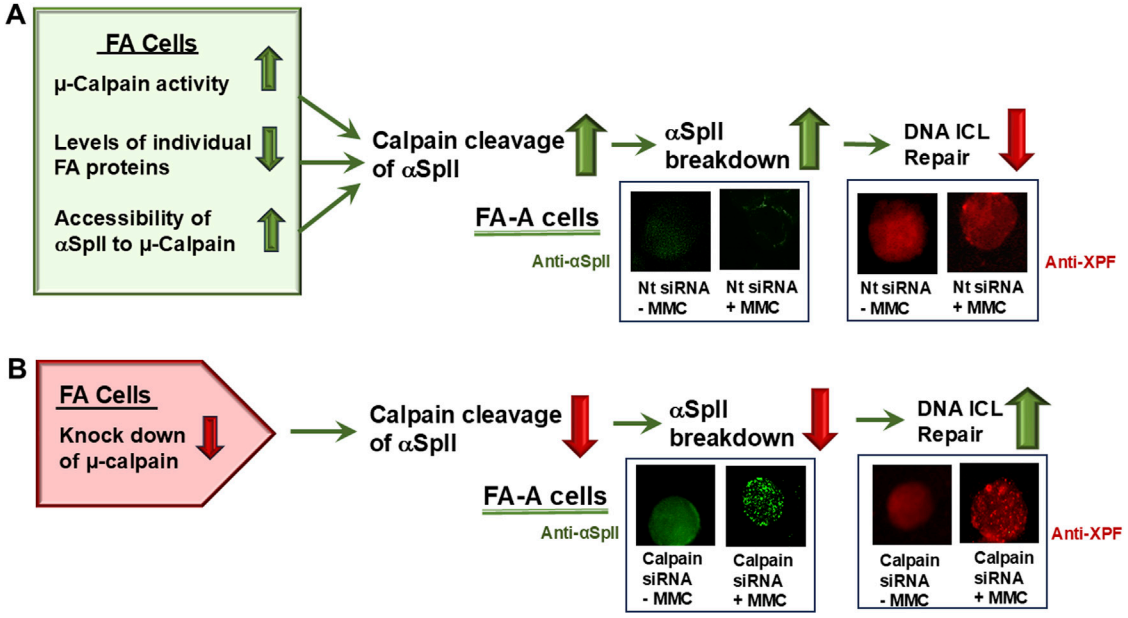

FIGURE 11
Role of μ-calpain in the deficiency of αSpII in FA cells and in defective DNA ICL repair in these cells. FA-A cells are used as a model. **(A)** In FA-A cells, excessive μ-calpain activity, decreased levels of individual FA proteins and increased accessibility of αSpII to μ-calpain lead to increased cleavage of αSpII by μ-calpain. FA-A cells, transfected with a non-target siRNA and examined using indirect immunofluorescence and staining with anti-αSpII, show low levels of αSpII and few nuclear foci after MMC treatment. Staining of the cells with anti-XPF shows that XPF is present in these cells but, after MMC treatment, few XPF foci are seen. **(B)** In FA-A cells, in which μ-calpain has been knocked down by μ-calpain siRNA, there is decreased cleavage of αSpII. Examination of these cells using immunofluorescence shows that αSpII is present in the nucleus and forms foci after treatment with MMC. XPF also forms nuclear foci in these cells after MMC treatment.

Excessive cleavage of αSpII by μ-calpain and its involvement in the DNA repair defect in FA cells has been demonstrated both by the presence of the 150 Kd αSpII breakdown product of μ-calpain in FA cells and by studies which show that knocking down μ-calpain corrects the excessive cleavage of αSpII and the DNA repair defect [69]. This needs to be examined in more FA complementation groups. It will also be important to determine whether there are other proteins involved in αSpII cleavage. Calmodulin, for example, binds to a site on αSpII and can stimulate μ-calpain activity. Studies need to be carried out to determine whether increased binding of calmodulin to αSpII in FA cells plays a role in the increased μ-calpain activity observed and the increased breakdown of αSpII.

FA proteins are known to play a role in the DNA ICL repair pathway. Lambert et al. have hypothesized that they also play an important role, either directly or indirectly, in maintaining αSpII stability. Transfection of FA cells (FA-A, FA-C, and FA-G) with the corresponding FANC-cDNA, which results in expression of either FANCA, FANCC or FANCG, respectively, restores αSpII stability and leads to restoration of chromosomal stability [69]. FANCG has been shown to directly bind to the SH3 domain in αSpII [101]. It has been proposed that FANCG may be involved in aiding in maintenance of αSpII stability by directly preventing binding of low molecular weight phosphotyrosine phosphatase (LMW-PTP) to its SH3 domain, which would lead to dephosphorylation of residue Y1176 at μ-calpain's cleavage site adjacent to the SH3 domain (Figure 1) and allow μcalpain to cleave αSpII at this site [101]. Binding of FANCG to the SH3 domain would aid in preventing cleavage of αSpII by μ-calpain. This needs to be further investigated. Other FA proteins could also interact with αSpII to protect it from cleavage by μ-calpain or bind to μ-calpain or calmodulin and prevent their activity, either directly or indirectly, via other proteins. FANCA and FANCG, for example, have been shown to bind directly to μcalpain [13, 50]. Whether this binding can decrease the activity of μ-calpain and enhance αSpII stability needs to be examined. Similarly, binding of a FA protein to calmodulin could inhibit its ability to bind to μ-calpain and activate it, which would also enhance αSpII stability. Thus, binding of FA proteins to αSpII or to associated proteins such as μcalpain or calmodulin could have an important effect on αSpII stability, protecting it from cleavage by μ-calpain. Studies need to be carried out on all of these possibilities.

Numerous studies have been done on the direct role FA proteins play in repair of DNA ICLs. In one of these, knockdown of the *FANCA* and *FANCD2* genes in human embryonic stem cells was shown to lead to a marked reduction in localization of FANCA and FANCD2 proteins to ICL damage induced foci,

indicating presence of a defect in DNA ICL repair [192]. Chromosomal aberrations such as breaks and radials also formed [192]. It would be interesting to determine, in studies such as these, whether a decrease in FANCA or FANCD2 proteins leads not only to direct effects on DNA ILC repair but also to loss of stability and breakdown of αSpII. If this occurred, it would suggest that loss of the FA protein led to increased breakdown of αSpII and to the increased defect in DNA repair and chromosome stability observed after DNA ICL damage. These studies would also emphasize the importance of FA proteins in aiding in maintenance of the stability of αSpII in cells, as has been suggested.

Another distinctive hallmark of FA is chromosome instability. The importance of αSpII in maintenance of chromosome stability is seen in studies in which knock down of αSpII in normal cells leads to production of chromosomal aberrations [45]. In addition, in FA cells when levels of αSpII are returned to normal by knocking down μ-calpain, chromosome stability is restored indicating that αSpII plays a role in this process [45]. The effect that excessive cleavage of αSpII in FA cells has on chromosome stability could be directly related to the defect in the ICL repair process and the increase in un-repaired DNA which is produced in these cells. It has been shown that un-repaired or misrepaired lesions in DNA can lead to chromosomal aberrations [164]. Cells are particularly sensitive to un-repaired DNA ICLS, which can lead to DNA double-strand break formation in S phase of the cell cycle and to chromosomal aberrations [164]. In FA cells, breakdown of αSpII could thus be important in production of the chromosomal aberrations observed, which particularly occur after DNA ICL damage and which are not effectively repaired in these cells.

Lambert et al. have also hypothesized that excessive cleavage of αSpII in FA cells may be an important contributing factor in some of the other characteristics of FA pathogenesis such as bone marrow failure, development of AML, congenital anomalies and neurological abnormalities [13, 44]. Studies have shown, for example, that there is a loss of αSpII in bone marrow of patients with AML and it has been proposed that this loss may be contributing to AML development and to leukemogenesis [165, 167]. It can be hypothesized that since FA patients can develop AML, a deficiency in αSpII is a contributing factor in its development. Excessive cleavage and loss of αSpII also occurs in a number of neurodegenerative disorders. This is due to excessive activation of calpain and is a common feature of the neuropathology of many of these disorders. Neurological abnormalities are also a characteristic of FA patients [67, 168, 183–186]. It is possible that excessive calpain activity may thus be an important factor contributing to the loss of αSpII and to a number of the neurological anomalies observed in FA. FA could thus represent another disorder in which there is excessive cleavage of αSpII by μ-calpain. Studies needs to be carried out on this in more complementation groups of FA. Since αSpII is a multifunctional protein, it is not surprising that a deficiency in it could lead to deficiencies in multiple cellular pathways and result in a number of the different pathological manifestations observed in FA.

This review has focused on the important role of αSpII in repair of DNA ICLs in telomeric and non-telomeric DNA and on the importance of maintaining the stability of αSpII not only for DNA repair but also for other cellular processes. Two factors which have been shown to be critical for maintaining αSpII stability in the cell are the levels of μ-calpain activity and the presence of FA proteins. Excess μ-calpain activity in FA cells has been demonstrated to lead to breakdown of αSpII. FA proteins are proposed to play a role in regulation of αSpII stability by modulating its cleavage by μ-calpain. Direct binding of FANCG to αSpII has been demonstrated but the effects this binding has on αSpII stability and its cleavage by μ-calpain needs to be further investigated as does the effect of other FA proteins on this process.

Since αSpII has a wide spectrum of functions in a number of different cellular and physiological processes, it is possible that in FA cells excessive cleavage of αSpII by μ-calpain could have an important effect on some of the clinical characteristics of this disorder. Decreasing μ-calpain activity in FA cells could aid in stabilization of αSpII and be of potential therapeutic relevance. Lambert et al. have shown that knocking down μcalpain activity in FA cells to levels found in normal cells does not have any adverse effects on cell survival and it leads to restoration of αSpII to normal levels and enables DNA ICL repair to proceed. Though levels of μ-calpain have been reduced to normal in these cells, the deficiency in the FA protein specific for the FA complementation group being examined has not been corrected. However, DNA repair takes place. FANCD2-Ub is not present but non-Ub FANCD2 is and it localizes in foci at sites of damage. αSpII is needed for this to occur [49]. αSpII localizes in foci at sites of damage along with XPF but not with non-Ub FANCD2. It has been proposed that this could be a backup system in which non-Ub FANCD2 is involved in the repair process [49]. In these FA cells, if a specific FA protein is not available to help stabilize αSpII, restoration of αSpII to normal levels by knocking down μ-calpain could, to some extent, counteract this need for the FA protein in this process. Whether this holds true for all of the FA complementation groups needs to be examined.

It is hypothesized that there is a mechanistic link between excessive μ-calpain activity, cleavage of αSpII, and defective DNA ICL repair, and that these are key factors in the pathogenesis of FA. FA proteins are proposed to play a role in modulating αSpII cleavage by μ-calpain. Correcting the excessive cleavage of αSpII in FA cell is particularly important since αSpII is essential for a number of critical cellular and physiological processes, such as DNA repair. These studies suggest a new direction for correction of a number of the phenotypic deficiencies in FA cells. Thus, stabilization of αSpII in FA by reducing μ-calpain activity, potentially in combination with other modalities, could potentially reduce the DNA repair defect and other systemic deficiencies which lead to the clinical manifestations of this as well as other disorders.

Author contributions

ML wrote the manuscript and prepared the figures.

Funding

The author(s) declare that no financial support was received for the research and/or publication of this article.

Conflict of interest

The author declared no potential conflicts of interest with respect to the research, authorship, and/or publication of this article.

Generative AI statement

The authors declare that no Generative AI was used in the creation of this manuscript.

References

1. Hohmann T, Dehghani F. The cytoskeleton – a complex interacting meshwork. *Cells* (2019) **8**:362. doi:10.3390/cells8040362

2. Svitkina T. The actin cytoskeleton and actin-based motility. *Cold Spring Harbor Perspect Biol* (2018) **10**:a018267. doi:10.1101/cshperspect.a018267

3. Merino F, Pospich S, Raunser S. Towards a structural understanding of the remodeling of the actin cytoskeleton. *Semin Cell & Developmental Biol* (2020) **102**: 51–64. doi:10.1016/j.semcdb.2019.11.018

4. Etienne-Manneville S. Cytoplasmic intermediate filaments in cell biology. *Annu Rev Cell Dev Biol* (2018) **34**:1–28. doi:10.1146/annurev-cellbio-100617-062534

5. Benoit B, Baillet A, Pous C. Cytoskeleton and associated proteins: pleiotropic JNK substrates and regulators. *Int J Mol Sci* (2021) **22**:8375. doi:10.3390/ijms22168375

6. Dechat T, Pfleghaar K, Sengupta K, Shimi T, Shumaker DK, Solimando L, et al. Nuclear lamins: major factors in the structural organization and function of the nucleus and chromatin. *Genes Dev* (2008) **22**:832–53. doi:10.1101/gad.1652708

7. Simon DN, Wilson KL. The nucleoskeleton as a genome-associated dynamic network of networks. *Nat Rev Mol Cell Biol* (2011) **12**:695–708. doi:10.1038/nrm3207

8. Goldman RD, Gruenbaum Y, Moir RD, Shumaker DK, Spann TP. Nuclear lamins: building blocks of nuclear architecture. *Genes & Development* (2002) **16**: 533–47. doi:10.1101/gad.960502

9. Wilson KL, Dawson SC. Functional evolution of nuclear structure. *J Cell Biol* (2011) **195**:171–81. doi:10.1083/jcb.201103171

10. Zhong Z, Wilson KL, Dahl KN. Beyond lamins: other structural components of the nucleoskeleton. *Methods Cell Biol* (2010) **98**:97–119. doi:10.1016/s0091-679x(10)98005-9

11. Lammerding J, Schulze PC, Takahaski T, Kozlov S, Sullivan T, Kamm RD, et al. Lamin A/C deficiency causes defective nuclear mechanics and mechanotransduction. *J Clin Invest* (2004) **113**:370–8. doi:10.1172/jc119670

12. McMahon LW, Walsh CE, Lambert MW. Human α spectrin II and the Fanconi anemia proteins FANCA and FANCC interact to form a nuclear complex. *J Biol Chem* (1999) **274**:32904–8. doi:10.1074/jbc.274.46.32904

13. Lambert MW. Spectrin and its interacting partners in nuclear structure and function. *Exp Biol Med* (2018) **243**:507–24. doi:10.1177/1535370218763563

14. Goodman SR, Johnson D, Youngentob SL, Kakhniashvili D. The spectrinome: the interactome of a scaffold protein creating nuclear and cytoplasmic connectivity and function. *Exp Biol Med* (2019) **244**:1273–302. doi:10.1177/1535370219867269

15. Winkelmann JC, Forget BG. Erythroid and nonerythroid spectrins. *Blood* (1993) **81**:3173–85. doi:10.1182/blood.v81.12.3173.bloodjournal81123173

16. Goodman SR, Zimmer WE, Clark MB, Zagon IS, Barker JE, Bloom ML. Brain spectrin: of mice and men. *Brain Res Bull* (1995) **36**:593–606. doi:10.1016/0361-9230(94)00264-2

17. de Matteis MA, Morrow JS. Spectrin tethers and mesh in the biosynthetic pathway. *J Cell Sci* (2000) **113**:2331–43. doi:10.1242/jcs.113.13.2331

18. Marchesi VT, Steers E. Selective solubilization of a protein component of the red cell membrane. *Science* (1968) **159**:203–4. doi:10.1126/science.159.3811.203

19. Goodman SR, Zagon IS, Kulikowski RR. Identification of a spectrin-like protein in nonerythroid cells. *Proc Natl Acad Sci USA* (1981) **78**:7570–4. doi:10.1073/pnas.78.12.7570

20. Goodman SR, Shiffer KA. The spectrin membrane skeleton of normal and abnormal human erythrocytes: a review. *Am J Physiology-Cell Physiol* (1983) **244**: C121–C141. doi:10.1152/ajpcell.1983.244.3.c121

21. Brown JW, Bullitt E, Sriswasdi S, Harper S, Speicher DW, McKnight CJ. The physiological molecular shape of spectrin: a compact supercoil resembling a Chinese finger trap. *PLOS Comput Biol* (2015) **11**:e1004302. doi:10.1371/journal.pcbi.1004302

22. Goodman SR, Kurdia A, Ammann L, Kakhniashvili D, Daescu O. The human red blood cell proteome and interactome. *Exp Biol Med* (2007) **232**:1391–408. doi:10.3181/0706-mr-156

23. Goodman SR, Daescu O, Kakhniashvili D, Zivanic M. The proteomics and interactomics of human erythrocytes. *Exp Biol Med* (2013) **238**:509–18. doi:10.1177/1535370213488474

24. Machnicka B, Czogalla A, Hryniewicz-Jankowska A, Bogusławska DM, Grochowalska R, Heger E, et al. Spectrins: a structural platform for stabilization and activation of membrane channels, receptors and transporters. *Biochim Biophys Acta (Bba) - Biomembranes* (2014) **1838**:620–34. doi:10.1016/j.bbamem.2013.05.002

25. Bennet V, Baines AJ. Spectrin and ankyrin-based pathways: metazoan inventions for integrating cells into tissues. *Physiol Rev* (2001) **81**:353–92. doi:10.1152/physrev.2001.81.3.1353

26. Goodman SR, Chapa RP, Zimmer WE. Spectrin's chimeric E2/E3 enzymatic activity. *Exptl Biol Med* (2015) **240**:1039–49. doi:10.1177/1535370215596084

27. Machnicka B, Grochowalska R, Bogusławska DM, Sikorski AF, Lecomte MC. Spectrin-based skeleton as an actor in cell signaling. *Cell Mol Life Sci* (2012) **69**: 191–201. doi:10.1007/s00018-011-0804-5

28. Sikorski A, Sangerman J, Goodman SR, Critz S. Spectrin (βSpIIΣ1) is an essential component of synaptic transmission. *Brain Res* (2000) **852**:161–6. doi:10.1016/s0006-8993(99)02253-2

29. Goodman SR. Discovery of nonerythroid spectrin to the demonstration of its key role in synaptic transmission. *Brain Res Bull* (1999) **50**:345–6. doi:10.1016/s0361-9230(99)00098-2

30. Ponceau A, Albiges-Rizo C, Colin-Aronovicz Y, Destaing O, Lecomte MC. αIISpectrin regulates invadosome stability and extracellular matrix degradation. *PLoS ONE* (2015) **10**:e0120781. doi:10.1371/journal.pone.0120781

31. Trinh-Trang-Tan M-M, Bigot S, Picot J, Lecomte M-C, Kordeli E. AlphaII-spectrin participates in the surface expression of cell adhesion molecule L1 and neurite outgrowth. *Exp Cell Res* (2014) **322**:365–80. doi:10.1016/j.yexcr.2014.01.012

32. Meissner JM, Sikorski AF, Nawara T, Grzesiak J, Marycz K, Bogusławska DM, et al. αII-spectrin in T cells is involved in the regulation of cell-cell contact leading to immunological synapse formation? *PLOS ONE* (2017) **12**:e0189545. doi:10.1371/journal.pone.0189545

33. Metral S, Machnicka B, Bigot S, Colin Y, Dhermy D, Lecomte M-C. αII-spectrin is critical for cell adhesion and cell cycle. *J Biol Chem* (2009) **284**:2409–18. doi:10.1074/jbc.m801324200

34. Zagon IS, Higbee R, Riederer BM, Goodman SR. Spectrin subtypes in mammalian brain: an immunoelectron microscopic study. *J Neurosci* (1986) **6**: 2977–86. doi:10.1523/jneurosci.06-10-02977.1986

35. Gascard P, Mohandas N. New insights into functions of erythroid proteins in nonerythroid cells. *Curr Opin Hematol* (2000) **7**:123–9. doi:10.1097/00062752-200003000-00009

36. Stankewich MC, Cianci CD, Stabach PR, Ji L, Nath A, Morrow J. Cell organization, growth, and neural and cardiac development require αII-spectrin. *J Cell Sci* (2011) **124**:3956–66. doi:10.1242/jcs.080374

37. Armiger TJ, Spagnol ST, Dahl KN. Nuclear mechanical resilience but not stiffness is modulated by αII-spectrin. *J Biomech* (2016) **49**:3983–9. doi:10.1016/j.jbiomech.2016.10.034

38. Lambert MW. Functional significance of nuclear α spectrin. *J Cell Biochem* (2015) **116**:1816–30. doi:10.1002/jcb.25123

39. Tse WT, Tang J, Jin O, Korsgren C, John KM, Kung AL, et al. A new spectrin, beta IV, has a major truncated isoform that associates with promyelocytic leukemia protein nuclear bodies and the nuclear matrix. *J Biol Chem* (2001) **276**:23974–85. doi:10.1074/jbc.m009307200

40. Thenappan A, Shukkla V, Abdul Khalek FJ, Li Y, Shetty K, Liu P, et al. Loss of TGFβ adaptor protein β2SP leads to delayed liver regeneration in mice. *Hepatology* (2011) **53**:1641–50. doi:10.1002/hep.24111

41. Sridharan DM, McMahon LW, Lambert MW. αII-Spectrin interacts with five groups of functionally important proteins in the nucleus. *Cell Biol Int* (2006) **30**:866–78. doi:10.1016/j.cellbi.2006.06.005

42. McMahon LW, Sangerman J, Goodman SR, Kumaresan K, Lambert MW. Human alpha spectrin II and the FANCA, FANCC, and FANCG proteins bind to DNA containing psoralen interstrand cross-links. *Biochemistry* (2001) **40**:7025–34. doi:10.1021/bi002917g

43. Sridharan D, Brown M, Lambert WC, McMahon LW, Lambert MW. Nonerythroid alpha II spectrin is required for recruitment of FANCA and XPF to nuclear foci induced by DNA interstrand cross-links. *J Cell Sci* (2003) **116**:823–35. doi:10.1242/jcs.00294

44. Lambert MW. Nuclear alpha spectrin: critical roles in DNA interstrand cross-link repair and genomic stability. *Exp Biol Med* (2016) **241**:1621–38. doi:10.1177/1535370216662714

45. McMahon LW, Zhang P, Sridharan DM, Lefferts JA, Lambert MW. Knockdown of αII spectrin in normal human cells by siRNA leads to chromosomal instability and decreased DNA interstrand cross-link repair. *Biochem Biophysical Res Commun* (2009) **381**:288–93. doi:10.1016/j.bbrc.2009.02.038

46. Zhang P, Herbig U, Coffman F, Lambert MW. Non-erythroid alpha spectrin prevents telomere dysfunction after DNA interstrand cross-link damage. *Nucleic Acids Res* (2013) **41**:5321–40. doi:10.1093/nar/gkt235

47. Kumaresan K, Sridharan D, McMahon L, Lambert MW. Deficiency in incisions produced by XPF at the site of a DNA interstrand cross-link in Fanconi anemia cells. *Biochemistry* (2007) **46**:14359–68. doi:10.1021/bi7015958

48. Brois DW, McMahon LW, Ramos NI, Anglin LM, Walsh CE, Lambert MW. A deficiency in a 230 kDa DNA repair protein in Fanconi anemia complementation group A cells is corrected by the FANCA cDNA. *Carcinogenesis* (1999) **20**:1845–53. doi:10.1093/carcin/20.9.1845

49. Zhang P, Sridharan D, Lambert MW. Nuclear α spectrin differentially affects monoubiquitinated versus non-ubiquitinated FANCD2 function after DNA interstrand cross-link damage. *J Cell Biochem* (2016) **117**:671–83. doi:10.1002/jcb.25352

50. Lambert MW. The functional importance of lamins, actin, myosin, spectrin and the LINC complex in DNA repair. *Exp Biol Med* (2019) **244**:1382–406. doi:10.1177/1535370219876651

51. Mathew CG. Fanconi anaemia genes and susceptibility to cancer. *Oncogene* (2006) **25**:5875–84. doi:10.1038/sj.onc.1209878

52. de Winter JP, Joenje H. The genetic and molecular basis of Fanconi anemia. *Mutat Research/Fundamental Mol Mech Mutagenesis* (2009) **668**:11–9. doi:10.1016/j.mrfmmm.2008.11.004

53. Moldovan G-L, D'Andrea A. How the Fanconi anemia pathway guards the genome. *Annu Rev Genet* (2009) **43**:223–49. doi:10.1146/annurev-genet-102108-134222

54. Kumaresan KR, Lambert MW. Fanconi anemia, complementation group A, cells are defective in ability to produce incisions at sites of psoralen interstrand cross-links. *Carcinogenesis* (2000) **21**:741–51. doi:10.1093/carcin/21.4.741

55. Lambert MW, Tsongalis GJ, Lambert WC, Parrish DD. Correction of the DNA repair defect in Fanconi anemia complementation groups A and D cells. *Biochem Biophysical Res Commun* (1997) **230**:587–91. doi:10.1006/bbrc.1996.6008

56. Brosh RM, Bellani M, Liu Y, Seidman MM. Fanconi anemia: a DNA repair disorder characterized by accelerated decline of the hematopoietic stem cell compartment and other features of aging. *Ageing Res Rev* (2017) **33**:67–75. doi:10.1016/j.arr.2016.05.005

57. Niraj J, Farkkila A, D'Andrea AD. The Fanconi anemia pathway in cancer. *Annu Rev Cancer Biol* (2019) **3**:457–78. doi:10.1146/annurev-cancerbio-030617-050422

58. Kim H, D'Andrea AD. Regulation of DNA cross-link repair by the Fanconi anemia/BRCA pathway. *Genes & Development* (2012) **26**:1393–408. doi:10.1101/gad.195248.112

59. Kottemann MC, Smogorzewska A. Fanconi anaemia and the repair of Watson and Crick DNA crosslinks. *Nature* (2013) **493**:356–63. doi:10.1038/nature11863

60. Mamrak NE, Shimamura A, Howlett NG. Recent discoveries in the molecular pathogenesis of the inherited bone marrow failure syndrome Fanconi anemia. *Blood Rev* (2017) **31**:93–9. doi:10.1016/j.blre.2016.10.002

61. Cheung RS, Taniguchi T. Recent insights into the molecular basis of Fanconi anemia: genes, modifiers, and drivers. *Int J Hematol* (2017) **106**:335–44. doi:10.1007/s12185-017-2283-4

62. Rosenberg PS, Greene MH, Alter BP. Cancer incidence in persons with Fanconi anemia. *Blood* (2003) **101**:822–6. doi:10.1182/blood-2002-05-1498

63. Swuec P, Ranault L, Borg A, Shah F, Murphy VJ, van Twest S, et al. The FA core complex contains a homo-dimeric catalytic module for symmetric mono-ubiquitination of FANCI-FANCD2. *Cell Rep* (2017) **18**:611–23. doi:10.1016/j.celrep.2016.11.013

64. Nalepa G, Clapp DW. Fanconi anaemia and cancer: an intricate relationship. *Nat Rev Cancer* (2018) **18**:168–85. doi:10.1038/nrc.2017.116

65. Garaycoechea JI, Patel KJ. Why does the bone marrow fail in Fanconi anemia? *Blood* (2014) **123**:26–34. doi:10.1182/blood-2013-09-427740

66. Rageul J, Kim H. Fanconi anemia and the underlying causes of genomic instability. *Environ Mol Mutagenesis* (2020) **61**:693–708. doi:10.1002/em.22358

67. Fiesco-Roa MO, Giri N, McReynolds LJ, Best AF, Alter BP. Genotype-phenotype associations in Fanconi anemia: a literature review. *Blood Rev* (2019) **37**:100589–68. doi:10.1016/j.blre.2019.100589

68. Webster ALH, Sanders MA, Pater K, Dietrich R, Noonan RJ, Lach FP, et al. Genomic signature of Fanconi anemia DNA repair pathway deficiency in cancer. *Nature* (2022) **612**:495–502. doi:10.1038/s41586-022-05253-4

69. Zhang P, Sridharan D, Lambert MW. Knockdown of μ-calpain in Fanconi anemia, FA-A, cells by siRNA restores αII spectrin levels and corrects chromosomal instability and defective DNA interstrand cross-link repair. *Biochemistry* (2010) **49**:5570–81. doi:10.1021/bi100656j

70. Lefferts JA, Lambert MW. Fanconi anemia cell lines deficient in αII spectrin express normal levels of αII spectrin mRNA. *Biochem Biophysical Res Commun* (2003) **307**:510–5. doi:10.1016/s0006-291x(03)01213-0

71. Grum VL, Li D, MacDonald RI, Mondragon A. Structures of two repeats of spectrin suggest models of flexibility. *Cell* (1999) **98**:523–35. doi:10.1016/s0092-8674(00)81980-7

72. Zhang R, Zhang C, Zhao Q, Li D. Spectrin: structure, function and disease. *Sci China Life Sci* (2013) **56**:1076–85. doi:10.1007/s11427-013-4575-0

73. Morrow JS, Marchesi VT. Self-assembly of spectrin oligomers *in vitro*: a basis for a dynamic cytoskeleton. *The J Cel Biol* (1981) **88**:463–8. doi:10.1083/jcb.88.2.463

74. Cesareni G, Panni S, Nardelli G, Castagnoli L. Can we infer peptide recognition specificity mediated by SH3 domains? *FEBS Lett* (2002) **513**:38–44. doi:10.1016/s0014-5793(01)03307-5

75. Nicolas G, Fournier CM, Galand C, Malbert-Colas L, Bournier O, Kroviarski Y, et al. Tyrosine phosphorylation regulates alpha II spectrin cleavage by calpain. *Mol Cell Biol* (2002) **22**:3527–36. doi:10.1128/mcb.22.10.3527-3536.2002

76. Nedrelow JH, Cianci CD, Morrow JS. C-Src binds αII spectrin's Src homology 3 (SH3) domain and blocks calpain susceptibility by phosphorylating Tyr1176. *J Biol Chem* (2003) **278**:7735–41. doi:10.1074/jbc.m210988200

77. Ackermann A, Brieger A. The role of nonerythroid spectrin αII in cancer. *J Oncol* (2019) **2019**:7079604. doi:10.1155/2019/7079604

78. Ziemnicka-Kotula D, Xu J, Gu H, Potempska A, Kim KS, Jenkins EC, et al. Identification of a candidate human spectrin Src homology 3 domainbinding protein suggests a general mechanism of association of tyrosine kinases with the spectrin-based membrane skeleton. *J Biol Chem* (1998) **273**:13681–92. doi:10.1074/jbc.273.22.13681

79. Mayer BJ. SH3 domains: complexity in moderation. *J Cell Sci* (2001) **114**:1253–63. doi:10.1242/jcs.114.7.1253

80. Ren R, Mayer BJ, Cicchetti P, Baltimore D. Identification of a ten-amino acid proline-rich SH3 binding site. *Science* (1993) **259**:1157–61. doi:10.1126/science.8438166

81. Kay BK, Williamson MP, Sudol M. The importance of being proline: the interaction of proline-rich motifs in signaling proteins with their cognate domains. *FASEB J* (2000) **14**:231–41. doi:10.1096/fasebj.14.2.231

82. Rotter B, Kroviarski Y, Nicolas G, Dhermy D, Lecomte MC. AlphaII-spectrin is an *in vitro* target for caspase-2, and its cleavage is regulated by calmodulin binding. *Biochem J* (2004) **378**:161–8. doi:10.1042/BJ20030955

83. Harris AS, Croall DE, Morrow JS. Calmodulin regulates fodrin susceptibility to cleavage by calcium-dependent protease I. *J Biol Chem* (1989) **264**:17401–8. doi:10.1016/s0021-9258(18)71508-1

84. Simonovic M, Zhang Z, Cianci CD, Steitz TA, Morrow JS. Structure of the calmodulin αII-spectrin complex provides insight into the regulation of cell plasticity. *J Biol Chem* (2006) **281**:34333–40. doi:10.1074/jbc.m604613200

85. Wu S, Sangerman J, Li M, brough GH, Goodman SR, Stevens T. Essential control of an endothelial cell ISOC by the spectrin membrane skeleton. *The J Cell Biol* (2001) **154**:1225–34. doi:10.1083/jcb.200106156

86. Bennett V, Healy J. Organizing the fluid membrane bilayer: diseases linked to spectrin and ankyrin. *Trends Mol Med* (2008) **14**:28–36. doi:10.1016/j.molmed.2007.11.005

87. Unsain N, Stefani FD, Caceres A. The actin/spectrin membrane-associated periodic skeleton in neurons. *Front Synaptic Neurosci* (2018) **10**:10. doi:10.3389/fnsyn.2018.00010

88. Han B, Zhou R, Xia C, Zhuang X. Structural organization of the actin-spectrinbased membrane skeleton in dendrites and soma of neurons. *Proc Natl Acad Sci USA* (2017) **114**:E6678-E6685–E6685. doi:10.1073/pnas.1705043114

89. Machnicka B, Grochowalska R, Boguslawska DM, Sikorski AF. The role of spectrin in cell adhesion and cell-cell contact. *Exp Biol & Med* (2019) **244**:13011312. doi:10.1177/1535370219859003

90. Bialkowska K, Saido TC, Fox j. SH3 domain of spectrin participates in the activation of Rac in specialized calpain-induced integrin signaling complexes. *J Cell Sci* (2005) **118**:381–95. doi:10.1242/jcs.01625

91. Rotter B, Bournier O, Nicolas G, Dhermy D, Lecomte M-C. αII-Spectrin interacts with Tes and EVL, two actin-binding proteins located at cell contacts. *Biochem J* (2005) **388**:631–8. doi:10.1042/bj20041502

92. Godi A, Santone I, Pertile P, Devarajan P, Stabach PR, Morrow JS, et al. ADP ribosylation factor regulates spectrin binding to the Golgi complex. *Proc Natl Acad Sci USA* (1998) **95**:8607–12. doi:10.1073/pnas.95.15.8607

93. Levine J, Willard M. Fodrin: axonally transported polypeptides associated with the internal periphery of many cells. *The J Cel Biol* (1981) **90**:631–42. doi:10.1083/jcb.90.3.631

94. Holleran EA, Ligon LA, Tokito M, Stankewich MC, Morrow JS, Holzbaur ELF. βIII spectrin binds to the Arp1 subunit of dynactin. *J Biol Chem* (2001) **276**:36598–605. doi:10.1074/jbc.m104838200

95. Hirokawa N, Noda Y, Tanaka Y, Niwa S. Kinesin superfamily motor proteins and intracellular transport. *Nat Rev Mol Cell Biol* (2009) **10**:682–96. doi:10.1038/nrm2774

96. Takeda S, Yamazaki H, Seog DH, Kanai Y, Terada S, Hirokawa N. Kinesin superfamily protein 3 (KIF3) motor transports fodrin-associating vesicles important for neurite building. *J Cell Biol* (2000) **148**:1255–65. doi:10.1083/jcb.148.6.1255

97. Sikorski AF, Terlecki G, Zagon IS, Goodman SR. Synapsin I-mediated interaction of brain spectrin with synaptic vesicles. *The J Cel Biol* (1991) **114**:313–8. doi:10.1083/jcb.114.2.313

98. Watabe H, Valencia JC, Le Pape E, Yamaguchi Y, Nakamura M, Rouzaud F, et al. Involvement of dynein and spectrin with early melanosome transport and melanosomal protein trafficking. *J Invest Dermatol* (2008) **128**:162–74. doi:10.1038/sj.jid.5701019

99. Hsu J, Goodman SR. Spectrin and ubiquitination: a review. *Cell Mol Biol (Noisy-le-Grand, France)* (2005) **Suppl 51**:OL801–OL807.

100. Sangerman J, Kakhniashvili D, Brown A, Shartava A, Goodman SR. Spectrin ubiquitination and oxidative stress: potential roles in blood and neurological disorders. *Cell & Mol Biol Lett* (2001) **6**:607–36.

101. Lefferts JA, Wang C, Sridharan D, Baralt M, Lambert MW. The SH3 domain of αII spectrin is a target for the fanconi anemia protein, FANCG. *Biochemistry* (2009) **48**:254–63. doi:10.1021/bi801483u

102. Holaska JM, Wilson KL. An emerin "Proteome": purification of distinct emerin-containing complexes from HeLa cells suggests molecular basis for diverse roles including gene regulation, mRNA splicing, signaling, mechanosensing, and nuclear architecture. *Biochemistry* (2007) **46**:8897–908. doi:10.1021/bi602636m

103. Faridounnia M, Folkers GE, Boelens R. Function and interactions of ERCC1-XPF in DNA damage response. *Molecules* (2018) **23**:3205. doi:10.3390/molecules23123205

104. Hoogenboom WS, Boonen RACM, Knipscheer P. The role of SLX4 and its associated nucleases in DNA interstrand crosslink repair. *Nucleic Acids Res* (2019) **47**:2377–88. doi:10.1093/nar/gky1276

105. Zhang H, Chen Z, Ye Y, Ye Z, Cao D, Xiong Y, et al. SLX4IP acts with SLX4 and XPF–ERCC1 to promote interstrand crosslink repair. *Nucleic Acids Res* (2019) **47**:10181–201. doi:10.1093/nar/gkz769

106. Semlow DR, Walter JC. Mechanisms of vertebrate DNA interstrand cross-link repair. *Annu Rev Biochem* (2021) **90**:107–35. doi:10.1146/annurev-biochem-080320-112510

107. Lee J, Coyne RS, Dubreuil RR, Goldstein LS, Branton D. Cell shape and interaction defects in alpha-spectrin mutants of *Drosophila melanogaster*. *The J Cel Biol* (1993) **123**:1797–809. doi:10.1083/jcb.123.6.1797

108. Norman KR, Moerman DG. A Spectrin is essential for morphogenesis and body wall muscle formation in *Caenorhabditis elegans*. *The J Cell Biol* (2002) **157**:665–77. doi:10.1083/jcb.200111051

109. Zhang R, Liu C, Niu Y, Jing Y, Zhang H, Wang J, et al. MicroRNA-128-3p regulates mitomycin C-induced DNA damage response in lung cancer cells through repressing*SPTAN1*. *Oncotarget* (2017) **8**:58098–107. doi:10.18632/oncotarget.12300

110. McPherson PS. Regulatory role of SH3 domain-mediated protein-protein interactions in synaptic vesicle endocytosis. *Cell Signal* (1999) **11**:229–38. doi:10.1016/s0898-6568(98)00059-x

111. D'Andrea LD, Regan L. TPR proteins: the versatile helix. *Trends Biochem Sci* (2003) **28**:655–62. doi:10.1016/j.tibs.2003.10.007

112. Blatch GL, Lassle M. The tetratricopeptide repeat: a structural motif mediating protein-protein interactions. *Bioessays* (1999) **21**:932–9. doi:10.1002/(sici)1521-1878(199911)21:11<932::aid-bies5>3.0.co;2-n

113. Blom E, van de Vrugt HJ, Vries Yd, de Winter JP, Arwert F, Joenje H. Multiple TPR motifs characterize the Fanconi anemia FANCG protein. *DNA Repair* (2004) **3**:77–84. doi:10.1016/j.dnarep.2003.09.007

114. Hussain S, Wilson JB, Blom E, Thompson LH, Sung P, Gordon SM, et al. Tetratricopeptide-motif-mediated interaction of FANCG with recombination proteins XRCC3 and BRCA2. *DNA Repair* (2006) **5**:629–40. doi:10.1016/j.dnarep.2006.02.007

115. Wang C, Lambert MW. The Fanconi anemia protein, FANCG, binds to the ERCC1-XPF endonuclease via its tetratricopeptide repeats and the central domain of ERCC1. *Biochemistry* (2010) **49**:5560–9. doi:10.1021/bi100584c

116. de Laat WL, Sijbers AM, Odijk H, Jaspers NG, Hoeijmakers JH. Mapping of interaction domains between human repair proteins ERCC1 and XPF. *Nucleic Acids Res* (1998) **26**:4146–52. doi:10.1093/nar/26.18.4146

117. Tripsianes K, Folkers GE, Ab E, Das D, Odijk H, Jaspers NGJ, et al. The structure of the human ERCC1/XPF interaction domains reveals a complementary role for the two proteins in nucleotide excision repair. *Structure* (2005) **13**:1849–58. doi:10.1016/j.str.2005.08.014

118. Choi YJ, Ryu KS, Ko YM, Chae YK, Pelton JG, Wemmer DE, et al. Biophysical characterization of the interaction domains and mapping of the contact residues in the XPF-ERCC1 complex. *J Biol Chem* (2005) **280**:28644–52. doi:10.1074/jbc.m501083200

119. Das D, Faridounnia M, Kovacic L, Kaptein R, Boelens R, Folkers GE. Singlestranded DNA binding by the helix-hairpin-helix domain of XPF protein contributes to the substrate specificity of the ERCC1-XPF protein complex. *J Biol Chem* (2017) **292**:2842–53. doi:10.1074/jbc.m116.747857

120. Akkari YM, Bateman RL, Reifsteck CA, Olson SB, Grompe M. DNA replication is required to elicit cellular responses to psoralen-induced DNA interstrand cross-links. *Mol Cell Biol* (2000) **20**:8283–9. doi:10.1128/mcb.20.21.8283-8289.2000

121. Raschle M, Knipscheer P, Enoiu M, Angelov T, Sun J, Griffith JD, et al. Mechanism of replication-coupled DNA interstrand crosslink repair. *Cell* (2008) **134**:969–80. doi:10.1016/j.cell.2008.08.030

122. Williams HL, Gottesman ME, Gautier J. The differences between ICL repair during and outside of S phase. *Trends Biochem Sci* (2013) **38**:386–93. doi:10.1016/j.tibs.2013.05.004

123. Taniguchi T, Garcia-Higuera I, Andreassen PR, Gregory RC, Grompe M, D'Andrea AD. S-phase-specific interaction of the Fanconi anemia protein, FANCD2, with BRCA1 and RAD51. *Blood* (2002) **100**:2414–20. doi:10.1182/blood-2002-01-0278

124. Knipscheer P, Räschle M, Smogorzewska A, Enoiu M, Ho TV, Scharer OD, et al. The Fanconi anemia pathway promotes replicationdependent DNA interstrand cross-link repair. *Science* (2009) **326**:1698–701. doi:10.1126/science.1182372

125. Renaudin X, Rosselli F. The FANC/BRCA pathway releases replication blockades by eliminating DNA interstrand cross-links. *Genes* (2020) **11**:585. doi:10.3390/genes11050585

126. Amunugama R, Willcox S, Wu RA, Abdullah UB, El-Sagheer AH, Brown T, et al. Replication fork reversal during DNA interstrand crosslink repair requires CMG unloading. *Cell Rep* (2018) **23**:3419–28. doi:10.1016/j.celrep.2018.05.061

127. Huang J, Liu S, Bellani MA, Thazhathveetil AK, Ling C, de Winter J, et al. The DNA translocase FANCM/MHF promotes replication traverse of DNA interstrand crosslinks. *Mol Cell* (2013) **52**(52):434–46. doi:10.1016/j.molcel.2013.09.021

128. Klein Douwel D, Boonen RA, Long DT, Szypowska AA, Raschle M, Walter JC, et al. XPF-ERCC1 acts in unhooking DNA interstrand crosslinks in cooperation with FANCD2 and FANCP/SLX4. *Mol Cell* (2014) **54**:460–71. doi:10.1016/j.molcel.2014.03.015

129. Guervilly J-H, Gaillard PH. SLX4: multitasking to maintain genome stability. *Crit Rev Biochem Mol Biol* (2018) **53**:475–514. doi:10.1080/10409238.2018.1488803

130. Trakselis MA, Seidman MM, Brosh RM, Jr. Mechanistic insights into how CMG helicase facilitates replication past DNA roadblocks. *DNA Repair* (2017) **55**:76–82. doi:10.1016/j.dnarep.2017.05.005

131. Ling C, Huang J, Yan Z, Li Y, Ohzeki M, Ishiai M, et al. Bloom syndrome complex promotes FANCM recruitment to stalled replication forks and facilitates both repair and traverse of DNA interstrand crosslinks. *Cell Discov* (2016) **2**:16047. doi:10.1038/celldisc.2016.47

132. Huh GY, Glantz SB, Je S, Morrow JS, Kim JH. Calpain proteolysis of αII-spectrin in the normal adult human brain. *Neurosci Lett* (2001) **316**:41–4. doi:10.1016/s0304-3940(01)02371-0

133. Pike BR, Flint J, Dutta S, Johnson E, Wang KKW, Hayes RL. Accumulation of non-erythroid αII-spectrin and calpain-cleaved αII-spectrin breakdown products in cerebrospinal fluid after traumatic brain injury in rats. *J Neurochem* (2001) **78**:1297–306. doi:10.1046/j.1471-4159.2001.00510.x

134. Siman R, Baudry M, Lynch G. Brain fodrin: substrate for calpain I, an endogenous calcium-activated protease. *Proc Natl Acad Sci USA* (1984) **81**:3572–6. doi:10.1073/pnas.81.11.3572

135. Miazek A, Zalas M, Skrzymowska J, Bogin BA, Grzymajło K, Goszczynski TM, et al. Age-dependent ataxia and neurodegeneration caused by an αII spectrin mutation with impaired regulation of its calpain sensitivity. *Scientific Rep* (2021) **11**:7312. doi:10.1038/s41598-021-86470-1

136. Liang CC, Li Z, Lopez-Martinez D, Nicholson WV, Venien-Bryan C, Cohn MA. The FANCD2-FANCI complex is recruited to DNA interstrand crosslinks before monoubiquitination of FANCD2. *Nat Commun* (2016) **7**:12124. doi:10.1038/ncomms12124

137. Li L, Tan W, Deans AJ. Structural insight into FANCI-FANCD2 monoubiquitination. *Essays Biochem* (2020) **64**:807–17. doi:10.1042/ebc20200001

138. Tan W, van Twest S, Leis A, Bythell-Douglas R, Murphy VJ, Sharp M, et al. Monoubiquitination by the human Fanconi anemia core complex clamps FANCI:FANCD2 on DNA in filamentous arrays. *Elife* (2020) **9**:e54128. doi:10.7554/elife.54128

139. Alcon P, Kaczmarczk AP, Ray KK, Liolios T, Guilbaud G, Sijacki Y, et al. FANCD2-FANCI surveys DNA and recognizes double-to single-stranded junctions. *Nature* (2023) **632**:1165–73. doi:10.1038/s41586-024-07770-w

140. Czogalla A, Sikorski AF. Spectrin and calpain: a 'target' and a 'sniper' in the pathology of neuronal cells. *Cell Mol Life Sci* (2005) **62**:1913–24. doi:10.1007/s00018-005-5097-0

141. Vanderklish PW, Bahr BA. The pathogenic activation of calpain: a marker and mediator of cellular toxicity and disease states. *Int J Exp Pathol* (2000) **81**:323–39. doi:10.1111/j.1365-2613.2000.00169.x

142. Faivre L, Guardiola P, Lewis C, Dokal I, Ebell W, Zatterale A, et al. Association of complementation group and mutation type with clinical outcome in fanconi anemia. European Fanconi Anemia Research Group. *Blood* (2000) **96**:4064–70.

143. Siddique MA, Nakanishi K, Taniguchi T, Grompe M, D'Andrea AD. Function of the Fanconi anemia pathway in Fanconi anemia complementation group F and D1 cells. *Exp Hematol* (2001) **29**:1448–55. doi:10.1016/s0301-472x(01)00754-8

144. Palm W, de Lange T. How shelterin protects mammalian telomeres. *Annu Rev Genet* (2008) **42**:301–34. doi:10.1146/annurev.genet.41.110306.130350

145. O'Sullivan RJ, Karlseder J. Telomeres: protecting chromosomes against genome instability. *Nat Rev Mol Cell Biol* (2010) **11**:171–81. doi:10.1038/nrm2848

146. Murnane JP. Telomere dysfunction and chromosome instability. *Mutat Research/Fundamental Mol Mech Mutagenesis* (2012) **730**:28–36. doi:10.1016/j.mrfmmm.2011.04.008

147. de Lange T. Shelterin-mediated telomere protection. *Annu Rev Genet* (2018) **52**:223–47. doi:10.1146/annurev-genet-032918-021921

148. Smith EM, Pendlebury DF, Nandakumar J. Structural biology of telomeres and telomerase. *Cell Mol Life Sci* (2020) **77**:61–79. doi:10.1007/s00018-019-03369-x

149. Roka K, Solomou EE, Kattamis A. Telomere biology: from disorders to hematological diseases. *Front Oncol* (2023) **13**:1167848. doi:10.3389/fonc.2023.1167848

150. Hu H, Yan HL, Nguyen THD. Structural biology of shelterin and telomeric chromatin: the pieces and an unfinished puzzle. *Biochem Soc Trans* (2024) **52**:1551–64. doi:10.1042/bst20230300

151. Smogorzewska A, de Lange T. Regulation of telomerase by telomeric proteins. *Annu Rev Biochem* (2004) **73**:177–208. doi:10.1146/annurev.biochem.73.071403.160049

152. Blackburn EH. Telomeres and telomerase. *The Keio J Med* (2000) **49**:859–65. doi:10.2302/kjm.49.59

153. Stern JL, Bryan TM. Telomerase recruitment to telomeres. *Cytogenet Genome Res* (2008) **122**:243–54. doi:10.1159/000167810

154. Kim NW, Piatyszek MA, Prowse KR, Harley CB, West MD, Ho PL, et al. Specific association of human telomerase activity with immortal cells and cancer. *Science* (1994) **266**:2011–5. doi:10.1126/science.7605428

155. Broccoli DM, Young JW, de Lange T. Telomerase activity in normal and malignant hematopoietic cells. *Proc Natl Acad Sci USA* (1995) **92**:9082–6. doi:10.1073/pnas.92.20.9082

156. Fan Q, Zhang F, Barrett B, Ren K, Andreassen PR. A role for monoubiquitinated FANCD2 at telomeres in ALT cells. *Nucleic Acids Res* (2009) **37**:1740–54. doi:10.1093/nar/gkn995

157. Takai H, Smogorzewska A, de Lange T. DNA damage foci at dysfunctional telomeres. *Curr Biol* (2003) **13**:1549–56. doi:10.1016/s0960-9822(03)00542-6

158. Martinez P, Thanasoula M, Munoz P, Liao C, Tejera A, McNees C, et al. Increased telomere fragility and fusions resulting from TRF1 deficiency lead to degenerative pathologies and increased cancer in mice. *Genes & Development* (2009) **23**:2060–75. doi:10.1101/gad.543509

159. Wilson JB, Blom E, Cunningham RM, Xiao Y, Kupfer GM, Jones NJ. Several tetratricopeptide repeat (TPR) motifs of FANCG are required for assembly of the BRCA2/D1-D2-G-X3 complex, FANCD2 monoubiquitylation and phleomycin resistance. *Mutat Research/Fundamental Mol Mech Mutagenesis* (2010) **689**:12–20. doi:10.1016/j.mrfmmm.2010.04.003

160. Wilson JB, Yamamoto K, Marriott AS, Hussain S, Sung P, Hoatlin ME, et al. FANCG promotes formation of a newly identified protein complex containing BRCA2, FANCD2 and XR CC3. *Oncogene* (2008) **27**:3641–52. doi:10.1038/sj.onc.1211034

161. Raghunandan M, Chaudhury I, Kellich SL, Hanenberg H, Soeback A. FANCD2, FANCJ and BRCA2 cooperate to promote replication fork recovery independently of the Fanconi anemia complex. *Cell Cycle* (2015) **143**:342–53. doi:10.4161/1538410.2014.987614

162. Sobeck A, Stone S, Hoatlin ME. DNA structure-induced recruitment and activation of the Fanconi anemia pathway protein FANCD2. *Mol Cell Biol* (2007) **27**:4283–92. doi:10.1128/mcb.02196-06

163. Yuan F, El Hokayem J, Zhou W, Zhang Y. FANCI protein binds to DNA and interacts with FANCD2 to recognize branched structures. *J Biol Chem* (2009) **284**:24443–52. doi:10.1074/jbc.M109.016006

164. Natarajan AT, Palitti F. DNA repair and chromosomal alterations. *Mutat Research/Genetic Toxicol Environ Mutagenesis* (2008) **657**:3–7. doi:10.1016/j.mrgentox.2008.08.017

165. Wolqust LP, Cannizzarro LA, Rameshjk H, Xue X, Wang D, Bhattacharuya PK, et al. Spectrin isoforms: differential expression in normal hematopoiesis and alterations in neoplastic bone marrow disorders. *Am J Clin Path* (2011) **136**:300–8. doi:10.1309/AJCPSA5RNM9IGFJF

166. Li S, Liu T, Li K, Bai X, Xi K, Chai X, et al. Spectrins and human diseases. *Translational Res* (2022) **243**:78–88. doi:10.1016/j.trsl.2021.12.009

167. Gorman EB, Chen L, Albanese J, Ratech H. Patterns of spectrin expression in B-cell lymphomas: loss of spectrin isoforms is associated with nodule-forming and germinal center-related lymphomas. *Mod Pathol* (2007) **20**:1245–52. doi:10.1038/modpathol.3800962

168. Hoover A, Turcotte LM, Phelan R, Barbus C, Rayannavar A, Miller BS, et al. Longitudinal clinical manifestations of Fanconi anemia: a systematized review. *Blood Rev* (2024) **68**:101225. doi:10.1016/j.blre.2024.101225

169. Tohyama J, Nakashima M, Nabatame S, Gaik-Siew C, Miyata R, Rener-Primec Z, et al. SPTAN1 encephalopathy: distinct phenotypes and genotypes. *J Hum Genet* (2015) **60**:167–73. doi:10.1038/jhg.2015.5

170. Riederer BM, Zagon IS, Goodman SR. Brain spectrin(240/235) and brain spectrin(240/235E): differential expression during mouse brain development. *J Neurosci* (1987) **7**:864–74. doi:10.1523/jneurosci.07-03-00864.1987

171. Zagon IS, Riederer BM, Goodman SR. Spectrin expression during mammalian brain ontogeny. *Brain Res Bull* (1987) **18**:799–807. doi:10.1016/0361-9230(87)90219-x

172. Zimmer WE, Ma Y, Zagon IS, Goodman SR. Developmental expression of brain beta-spectrin isoform messenger RNAs. *Brain Res* (1992) **594**:75–83. doi:10.1016/0006-8993(92)91030-i

173. Bartlett AL, Wagner JE, Jones B, Wells S, Sabulski A, Fuller C, et al. Fanconi anemia neuroinflammatory syndrome: brain lesions and neurologic injury in Fanconi anemia. *Blood Adv* (2024) **8**:3027–37. doi:10.1182/bloodadvances.2024012577

174. Wang Y, Ji T, Nelson AD, Glanowska K, Murphy GG, Jenkins PM, et al. Critical roles of αII spectrin in brain development and epileptic encephalopathy. *J Clin Invest* (2018) **128**:760–73. doi:10.1172/JCI95743

175. Saitsu H, Tohyama J, Kumada T, Egawa K, Hamada K, Okada I, et al. Dominant-negative mutations in α-II spectrin cause West syndrome with severe cerebral hypomyelination, spastic quadriplegia, and developmental delay. *The Am J Hum Genet* (2010) **86**:881–91. doi:10.1016/j.ajhg.2010.04.013

176. Syrbe S, Harms FL, Parrini E, Montomoli M, Mutze U, Helbig KL, et al. Delineating SPTAN1 associated phenotypes: from isolated epilepsy to encephalopathy with progressive brain atrophy. *Brain* (2017) **140**:2322–36. doi:10.1093/brain/awx195

177. Lorenzo DN, Edwards RJ, Slavutsky A. Spectrins: molecular organizers and targets of neurological disorders. *Nat Rev Neurosci* (2023) **24**:195–212. doi:10.1038/s41583-022-00674-6

178. Lynch G, Baudry M. Brain spectrin, calpain and long-term changes in synaptic efficacy. *Brain Res Bull* (1987) **18**:809–15. doi:10.1016/0361-9230(87)90220-6

179. Yan X-X, Jeromin A. Spectrin breakdown products (SBDPs) as potential biomarkers for neurodegenerative diseases. *Curr Translational Geriatr Exp Gerontol Rep* (2012) **1**:85–93. doi:10.1007/s13670-012-0009-2

180. Nilsson E, Alafuzoff I, Blennow K, Blomgren K, Hall CM, Janson I, et al. Calpain and calpastatin in normal and Alzheimer-degenerated human brain tissue. *Neurobiol Aging* (1990) **11**:425–31. doi:10.1016/0197-4580(90)90009-o

181. Peterson C, Vanderklish P, Seubert P, Cotman C, Lynch G. Increased spectrin proteolysis in fibroblasts from aged and Alzheimer donors. *Neurosci Lett* (1991) **121**:239–43. doi:10.1016/0304-3940(91)90694-o

182. Saito K, Elce JS, Hamos JE, Nixon RA. Widespread activation of calcium-activated neutral proteinase (calpain) in the brain in Alzheimer disease: a potential molecular basis for neuronal degeneration. *Proc Natl Acad Sci USA* (1993) **90**:2628–32. doi:10.1073/pnas.90.7.2628

183. Fiesco-Roa MÓ, García-de Teresa B, Leal-Anaya P, van 't Hek R, Wegman-Ostrosky T, Frías S, et al. Fanconi anemia and dyskeratosis congenita/telomere biology disorders: two inherited bone marrow failure syndromes with genomic instability. *Front Oncol* (2022) **12**:949435. doi:10.3389/fonc.2022.949435

184. Stivaros SM, Alston R, Wright NB, Chandler K, Bonney D, Wynn RF, et al. Central nervous system abnormalities in Fanconi anaemia: patterns and frequency on magnetic resonance imaging. *The Br J Radiol* (2015) **88**:20150088. doi:10.1259/bjr.20150088

185. Johnson-Tesch BA, Gawande RS, Zhang L, MacMillan ML, Nascene DR. Fanconi anemia: correlating central nervous system malformations and genetic complementation groups. *Pediatr Radiol* (2017) **47**:868–76. doi:10.1007/s00247-017-3817-x

186. Aksu T, Gumruk F, Bayhan T, Coşkun Ç, Oğuz KK, Unal S. Central nervous system lesions in Fanconi anemia: experience from a research center for Fanconi anemia patients 184. Anemia patients. *Pediatr Blood & Cancer* (2020) **67**:e28722. doi:10.1002/pbc.28722

187. Ackermann A, Schrecker C, Bon D, Friedrichs N, Bankov K, Wild P, et al. Downregulation of SPTAN1 is related to MLH1 deficiency and metastasis in colorectal cancer. *PLoS ONE* (2019) **14**:e0213411. doi:10.1371/journal.pone.0213411

188. Hinrichsen I, Ernst B, Nuber F, Passmann S, Schafer D, Steinke V, et al. Reduced migration of MLH1 deficient colon cancer cells depends on SPTAN1. *Mol Cancer* (2014) **13**:11. doi:10.1186/1476-4598-13-11

189. Brieger A, Adryan B, Wolpert F, Passmann S, Zeuzem S, Trojan J. Cytoskeletal scaffolding proteins interact with Lynch-Syndrome associated mismatch repair protein MLH1. *Proteomics* (2010) **10**:3343–55. doi:10.1002/pmic.200900672

190. Jain P, Spaeder MC, Donofrio MT, Sinha P, Jonas RA, Levy RJ. Detection of alpha II-spectrin breakdown products in the serum of neonates with congenital heart disease. *Pediatr Crit Care Med* (2014) **15**:229–35. doi:10.1097/pcc.0000000000000059

191. Lubbers ER, Murphy NP, Musa H, Huang CY-M, Gupta R, Price MV, et al. Defining new mechanistic roles for αII spectrin in cardiac function. *J Biol Chem* (2019) **294**:9576–91. doi:10.1074/jbc.ra119.007714

192. Tulpule A, Lensch MW, Miller JD, Austin K, D'Andrea A, Schlaeger TM, et al. Knockdown of Fanconi anemia genes in human embryonic stem cells reveals early developmental defects in the hematopoietic lineage. *Blood* (2010) **115**:3453–62. doi:10.1182/blood-2009-10-246694

EBM Experimental Biology and Medicine

TYPE Mini Review
PUBLISHED 18 December 2024
DOI 10.3389/ebm.2024.10334

OPEN ACCESS

*CORRESPONDENCE
Olga S. Chumakova,
chumakovaolga@bk.ru

RECEIVED 02 August 2024
ACCEPTED 28 November 2024
PUBLISHED 18 December 2024

CITATION
Chumakova OS and Mershina EA (2024) Circulating microRNA as promising biomarkers in hypertrophic cardiomyopathy: can advanced cardiac magnetic resonance unlock new insights in research?
Exp. Biol. Med. 249:10334.
doi: 10.3389/ebm.2024.10334

Circulating microRNA as promising biomarkers in hypertrophic cardiomyopathy: can advanced cardiac magnetic resonance unlock new insights in research?

Olga S. Chumakova[1]* and Elena A. Mershina[2]

[1]National Medical Research Center of Cardiology Named After E. I. Chazov, Moscow, Russia, [2]Medical Research and Education Center Lomonosov Moscow State University, Moscow, Russia

Abstract

Hypertrophic cardiomyopathy (HCM) is a genetic cardiac disorder associated with an increased risk of arrhythmias, heart failure, and sudden cardiac death. Current imaging and clinical markers are not fully sufficient in accurate diagnosis and patient risk stratification. Although known cardiac biomarkers in blood are used, they lack specificity for HCM and primarily stratify for death due to heart failure in overt cases. Non-coding RNAs, particularly microRNAs, have emerged as promising biomarkers due to their role in regulating gene expression in both healthy and pathological hearts. Circulating microRNA signatures may dynamically reflect the progression of HCM, offering potential utility in diagnosis and disease monitoring as well as inform biologic pathways for innovative therapeutic strategies. However, studying microRNAs in cardiovascular diseases is still in its early stages and poses many challenges. This review focuses on emerging research perspectives using advanced cardiac magnetic resonance techniques. We presume, that the search for circulating miR signatures associated with specific adverse myocardial features observed on cardiac magnetic resonance imaging - such as fibrosis, disarray, and microvascular disease - represents a promising direction in HCM research.

KEYWORDS

hypertrophic cardiomyopathy, non-coding RNAs, microRNAs, cardiac magnetic resonance, biomarkers, fibrosis, disarray, microvasculature

Impact statement

We are pleased to submit our manuscript, which highlights a perspective direction in hypertrophic cardiomyopathy research. Our study focuses on non-coding RNAs, specifically microRNAs, as promising cardiac biomarkers, and advanced cardiac magnetic resonance (CMR) imaging as a research tool that could facilitate the

discovery of novel circulating miR biomarkers. The current biomarkers are not specific for HCM, and their use is limited by risk stratification for heart failure death. By reviewing recent literature, we discuss the potential to identify specific circulating microRNA signatures linked to adverse microanatomical features of HCM observed using advanced CMR. We aim to engage the HCM scientific community in future interdisciplinary collaborations. The brief review of evolving modalities already applied in some areas of clinical practice may be of interest to a broad audience of practitioners, including cardiologists, radiologists, laboratory specialists, and genetics.

Introduction

Hypertrophic cardiomyopathy (HCM) is the most common genetic cardiac disorder, characterized by left ventricular (LV) hypertrophy in the absence of abnormal loading conditions [1]. In addition to cardiomyocyte hypertrophy, histological hallmarks include myocardial fibrosis (focal and diffuse), extensive disarray, and microvascular disease (MVD), all linked to arrhythmias, sudden cardiac death (SCD), and heart failure [2–6]. HCM exhibits significant heterogeneity in LV morphology [7], clinical course [8], and genetic etiology, involving both monogenic and polygenic components. Over recent decades, genetic studies have focused on protein-coding genes, identifying sarcomeric gene variants as the primary cause in approximately half of HCM patients [9–11]. This has established sarcomere dysfunction as a crucial mechanism in HCM [12], prompting the development of new treatments, such as cardiac myosin inhibitors [13]. Despite notable advancements, challenges remain in altering disease progression [14]. In clinical practice, there is a need for disease-specific plasma biomarkers to differentiate HCM from secondary LV hypertrophy, enhance risk stratification, and monitor phenotype evolution in preclinical mutation carriers. A fundamental question is how to identify the signaling pathways and regulatory networks that mediate the phenotypic expression of HCM's complex genetics.

This paper reviews micro non-coding ribonucleic acids (microRNAs or miRs), known as negative controllers of gene expression, as promising biomarkers for HCM. A special focus is placed on a) myocardial microanatomical features of HCM as a research field for disease-specific biomarkers; b) whether cardiac magnetic resonance (CMR) tissue characterization techniques

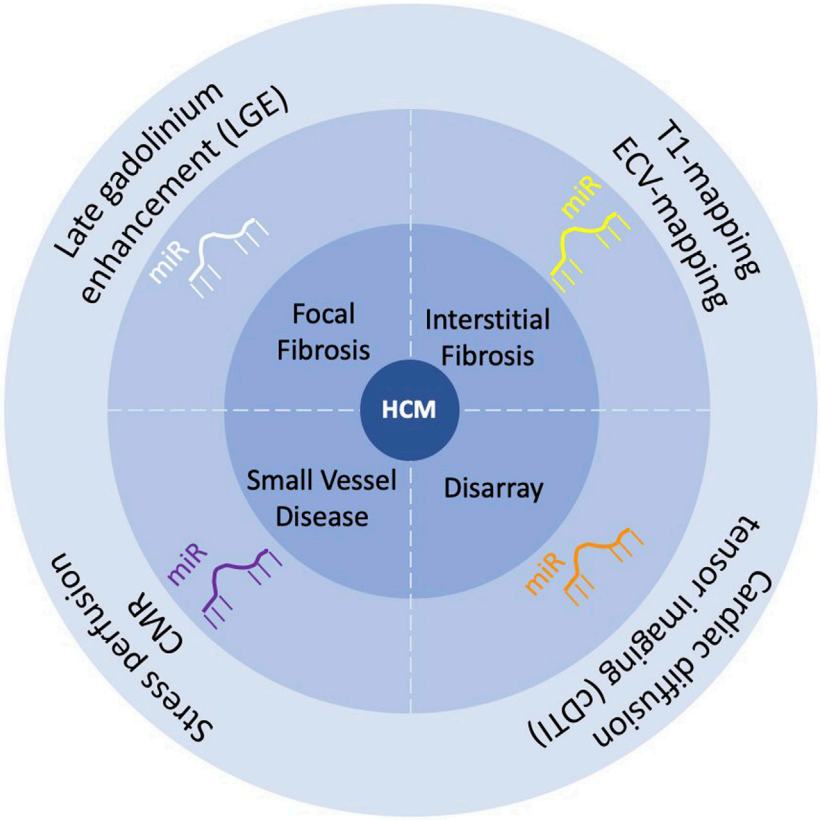

FIGURE 1
Scheme of the review "Circulating microRNA as promising biomarkers in hypertrophic cardiomyopathy: Can advanced cardiac magnetic resonance unlock new insights in research?".

hold potential to advance the discovery of circulating biomarkers, such as miRs, in HCM (Figure 1).

Current biomarkers for HCM

Since myocardial biopsy is not typically used in managing HCM, biomarkers are sought from cardiac imaging, clinical features, and circulating molecules. Similar to other cardiovascular diseases, a multi-parametric approach is employed for the diagnosis and risk stratification in HCM.

The only validated diagnostic marker for HCM is LV myocardial thickness, defined as ≥15 mm in adult probands and routinely assessed using echocardiography or CMR [1]. However, this marker has limitations: it cannot always reliably distinguish HCM from secondary LV hypertrophy or metabolic disorders and is insufficient to detect preclinical and early-stage disease. Furthermore, the quality of echocardiographic image may be compromised by patient-related factors, while CMR, although more precise, is not universally accessible and has procedural restrictions. Supporting diagnostic tools include electrocardiogram, family screening, genetic testing, and clinical assessment to exclude phenocopies. Currently, there are no specific blood biomarkers for HCM. While several molecules reflecting myocardial wall stretch, fibrosis, inflammation, apoptosis, necrosis, and endothelial dysfunction have demonstrated correlations with imaging findings [15], they have not been integrated into clinical practice due to insufficient evidence of specificity, thereby limiting their diagnostic utility. Moreover, none of these biomarkers exhibit adequate sensitivity to detect subclinical HCM [16].

Few imaging markers and clinical features - such as ventricular tachycardia, unexplained syncope, and a family history of SCD - are incorporated into SCD risk stratification algorithms [17, 18]. However, these models do not include blood biomarkers and show modest predictive value. Current European guidelines recommend the use of N-terminal pro-B-type natriuretic peptide (NT-proBNP) and troponin T for assessing mortality risk in overt HCM, particularly for death due to heart failure [1]. Additionally, NT-proBNP can serve as a surrogate marker for evaluating the therapeutic efficacy of cardiac myosin inhibitors [19, 20]. However, no risk models are currently designed to predict heart failure or other non-SCD-related mortality in HCM.

Challenges in identifying blood biomarkers for HCM may be attributed to historically small sample sizes in cardiomyopathy studies, inaccurate phenotype characterization, and truly weak biomarker correlations. Furthermore, simplistic approach based on a limited set of pre-selected biomarkers may not capture the complex underlying pathways.

Recent advancements in omics technologies, enabling the quantification of thousands of low-abundance circulating molecules (e.g., RNA, proteins, metabolites), have led to the discovery of novel biomarkers. Studies have demonstrated the ability of compiled protein and miR panels to differentiate HCM from hypertensive heart disease [21, 22] and subclinical HCM from controls [23, 24].

Circulating ncRNAs as biomarkers: case of miRs

Advances in cardiovascular genetics have shifted scientific interest toward the non-protein-coding genome and its non-coding RNA (ncRNA) transcripts [25]. The foremost function of ncRNAs is to regulate protein-coding gene expression, thereby affecting fundamental processes such as growth, differentiation, metabolism, apoptosis, and autophagy [26–29]. With growing evidence on the involvement of ncRNAs in heart diseases [30] and the advent of advanced computational methods, researchers can now explore the diagnostic, prognostic, and therapeutic potential of ncRNAs as biomarkers and novel targets for intervention [31].

Among various types of ncRNAs [32], miRs are the most abundant [33] and of particular interest in human diseases, including HCM [34]. MiRs are small molecules (~20–22 nucleotides) that form a coordinated regulatory system and control gene expression post-transcriptionally by binding to their messenger RNAs, resulting in cleavage or translational repression [35]. A single miR can have numerous high- and low-affinity gene targets, and a single gene can be regulated by multiple miRs.

MiRs are detected not only in tissues but also in the bloodstream, making them attractive biomarkers for cardiac diseases, where biopsy is uncommon. They enter circulation from living and dead cells via active secretion or passive release. Despite the RNase-rich environment of blood, circulating miRs remain stable [36], protected within extracellular vesicles or bound to RNA-binding proteins [37, 38]. As conserved regulators of gene expression, miRs serve as dynamic biomarkers that reflect disease stages [39]. In heart failure studies, circulating miRs significantly improved the diagnostic power of NT-proBNP, which may be particularly beneficial for identifying heart failure with preserved ejection fraction, where standard clinical assessment, imaging, and NT-proBNP alone may not be definitive [40, 41].

MiRs in HCM

Studies in animal and human tissues indicate that miRs significantly influence HCM [39, 42–48]. Several miRs, such as miR-1, -21, -30b, -132, -133a, -133b, -150, -199a-3p, and -486-3p, consistently show altered expression across at least two independent studies, suggesting a role in HCM development [39, 45, 47]. Plasma miR levels may reflect myocardial pathology, and around 30 circulating miRs have been identified as potential HCM biomarkers. However, the diagnostic accuracy of individual circulating miRs remains moderate [34].

Recent research has expanded miR panels to improve diagnostic accuracy. A six-miR set, including miR-181a-5p, -181c-5p, -328-3p, -301a-3p, -193b-3p, and -142-3p, outperformed individual miRs and differentiated sarcomeric variant carriers with and without the HCM phenotype with high statistical significance [23]. In a larger study involving 555 patients, transcriptomic profiling of 1,141 miRs identified a panel of 20+ circulating miRs that effectively discriminated HCM from hypertensive LV hypertrophy. Subsequent pathway analysis linked these miRs to key signaling pathways, including Ras-MAPK [22].

In our study, patients harbouring disease-causing *MYH7* variants had significantly higher plasma levels of miR-499a-5p compared to those with other sarcomeric variants, genotype-negative patients, and healthy controls [49]. MiR-499 is part of the "myo-miRs," encoded by introns of cardiac myosin genes, including *MYH7*. These genes regulate muscle function by controlling the expression of both contractile proteins and regulatory miRs [50]. This finding supports a gene-oriented approach to studying miRs, as different genetic backgrounds may lead to distinct miR profiles that influence the disease phenotype.

Limitations of circulating miRs for biomarkers

While circulating miRs hold promise as biomarkers, several challenges must be addressed before their clinical application. Unlike miRs measured in tissues, which can be cell-type-specific [51], circulating miRs often do not provide clear tissue- or disease-specific signals. Of the 2,600+ miRs identified, only a few - such as miR-1, -133a, -208a/b, and -499 - are categorized as cardiac-specific [52]. Inconsistencies in miR profiles between studies complicate their reliability as biomarkers. This variability may stem from differences in cohort characteristics, methodological processes, or the complex nature of miR regulation, where miRs typically have modest effects on many targets rather than having a dramatic impact on single genes. However, the combined effects of miRs on targets within a shared pathway can be synergistic [53], suggesting that miR panels, rather than individual miRs, could enhance diagnostic accuracy. Further challenges and solutions are detailed elsewhere [34, 54].

Microanatomical features of HCM as a research field

Microanatomical changes in the myocardium, such as fibrosis, disarray, and MVD, are closely associated with HCM and its major clinical outcomes, as demonstrated in early histological studies [2–6], making them attractive substrates for the discovery of non-invasive biomarkers. Importantly, these changes are not merely secondary to LV hypertrophy but are also present in non-hypertrophied LV segments [55] and at the preclinical stage [56–58]. In mouse models, early administration of mavacamten, a first-in-class cardiac myosin inhibitor, suppressed the development of myocardial disarray and fibrosis by attenuating hypertrophic and profibrotic gene expression [59]. This highlights the role of specific signaling pathways in these adverse microanatomical changes in HCM. The identification of miR signatures associated with these features appears to be a promising avenue for HCM research.

Non-invasive myocardial characterization with CMR imaging

CMR tissue characterization techniques offer a non-invasive, radiation-free assessment of fibrosis, microstructure, and microvascular health in HCM, with ongoing research improving their clinical utility.

Late gadolinium enhancement (LGE) is widely used to demonstrate replacement fibrosis, indicating scar tissue resulting from cardiomyocyte death. In contrast, interstitial fibrosis, which represents increased extracellular matrix and volume (ECV) without the pre-requisite cardiomyocyte death, is best evaluated using native T1-mapping and ECV measurements [60]. Both LGE (2-standard deviation technique) and T1/ECV-mapping have been histologically validated to accurately reflect myocardial fibrosis and collagen volume [6, 61–65]. Cardiac diffusion tensor imaging (cDTI) is an innovative CMR technique that assesses myocardial microstructure by mapping water diffusion along muscle fibers [66]. This method may reveal myocyte disarray, as demonstrated in preclinical models [67], although histological validation in humans is still needed. MVD can be assessed through perfusion CMR imaging, which quantifies myocardial blood flow, myocardial perfusion reserve, and perfusion defects [68]. It is important to adjust perfusion maps for LGE, as LGE contributes to resting perfusion defects in 30% of patients, potentially confounding the assessment of ischemic burden in HCM [69].

Although CMR-derived tissue parameters display specific features, they are not pathognomonic for HCM and can also be seen in other conditions. Caution is needed, as, for instance, markers like T1 relaxation time and ECV may reflect amyloidosis or edema. Tissue findings on CMR should be interpreted in the context of HCM and in conjunction with other markers, such as LV hypertrophy or the presence of sarcomere mutation.

The clinical application of CMR tissue markers in HCM is currently limited to fibrosis detection. The distribution and severity of focal and interstitial fibrosis aid in differentiating HCM from its phenocopies, such as Fabry disease and amyloidosis [70]. Extensive replacement fibrosis is increasingly recognized as a prognostic marker for SCD and all-cause mortality [71], with LGE >15% of LV mass now serving as a

second-line indication for implantable cardioverter-defibrillators [17, 72]. T1 mapping assists in distinguishing HCM from hypertensive LV hypertrophy [73], while ECV has been associated with heart failure outcomes [74]. An ongoing large observational study (NCT01915615), integrating genetic, blood, and CMR markers - including LGE, T1 mapping, and ECV - is likely to offer further insight into their prognostic capabilities in HCM [75]. CMR-based assessment of MVD and myocardial disarray remains research-focused and is not yet part of the etiological diagnosis of HCM. However, to date, cDTI, although in need of technical improvements [66], has demonstrated the ability to discriminate preclinical HCM from healthy controls [67], and its correlation with ventricular arrhythmias highlights its prognostic potential alongside LGE and ECV [65].

CMR tissue characterization techniques as a research tool in HCM

CMR, with its ability to accurately track pathological processes in the myocardium, is increasingly used in clinical trials of new therapeutics for non-ischemic cardiomyopathies [76]. CMR imaging series serve as surrogate markers of treatment efficacy and, as a merit, provide mechanistic insights into the molecular pathways of natural (placebo group) and treatment response over shorter time periods. In HCM, cardiac myosin inhibitors have been evaluated in clinical trials using surrogate clinical and imaging endpoints. The EXPLORER-HCM CMR substudy showed significant reductions in LV mass, wall thickness, and left atrial volume index, suggesting that mavacamten alters HCM pathophysiology [20]. Meanwhile, LGE and ECV were not significantly changed, supporting the irreversible nature of myocardial fibrosis. Recent research by Joy et al. showed associations of CMR-derived disarray and MVD with stages of phenotype evolution [67], suggesting potential future applications of these techniques in HCM research before and after therapeutic interventions. Notably, in overt disease, the presence versus absence of sarcomeric mutation has different effects on microstructure and microvasculature [67]. Stress perfusion CMR has recently been used as a validation tool for another potentially more cost-effective and clinically practical marker of MVD – impaired myocardial work on echocardiogram [77].

CMR techniques for discovery of circulating biomarkers in HCM

Several conventional blood biomarkers have been shown in association with CMR-derived tissue characteristics, particularly LGE [15]. NT-proBNP and troponin T exhibit positive correlations with increasing LGE and ECV levels in a graded manner [78, 79]. Other biomarkers linked to necrosis (troponin I), fibrosis (matrix metalloproteinase-9, endostatin, apelin), inflammation and apoptosis (high sensitivity C-reactive protein, TNF-alpha), and endothelial dysfunction (big endothelin-1) show correlations with LGE and MVD [15], although validation in larger studies is required.

Proteomic and transcriptomic studies aimed at identifying biomarker signatures associated with adverse myocardial changes observed on CMR are a relatively new line of research. However, several studies have already been conducted in various conditions, including HCM.

A large study in healthy individuals identified a circulating protein signature associated with interstitial fibrosis. Prospective follow-up using progression to heart failure as an endpoint may provide validation for the discovered protein panel [80]. In patients with heart failure and preserved LV ejection fraction, unique biomarker patterns correlated with ECV (7 proteins) and myocardial perfusion reserve (6 proteins) [81]. In HCM, quantitative proteomics identified a six-biomarker panel related to myocardial substrate changes and SCD risk, with five of the six biomarkers elevated in subclinical HCM patients [24]. Proteomic profiling of 701 patients with sarcomeric HCM identified circulating biomarkers associated with adverse imaging and clinical phenotypes, including LGE [82].

A complementary CMR and transcriptome profiling approach identified a circulating miR signature as a biomarker for LGE-positive cardiomyopathy in muscular dystrophy [83]. In HCM, the relationship between miRs and tissue CMR parameters has been investigated in six studies, all of which had relatively small sample sizes and primarily focused on fibrosis, employing LGE and T1-mapping techniques [48, 84–88] (Table 1). Several candidate individual miRs with moderate to strong diagnostic value have been identified. Notably, the study by Fang et al. demonstrated the significant superiority of miR panels over single miR markers for diagnostic purposes. In that study, individual miRs showed moderate diagnostic performance for interstitial fibrosis (AUC 0.663–0.742), while combining eight miRs substantially improved the diagnostic accuracy (AUC 0.87) [84].

Discussion

MiRs are promising biomarkers, as their altering profiles can reflect distinct molecular processes in the heart. Given the heterogeneity of HCM, likely due to a cascade of molecular and structural changes, it is essential to investigate biomarkers across all stages of the disease. Before the onset of overt LV hypertrophy, HCM is characterized by abnormalities in myocardial microstructure, which emphasize their relevance in early pathogenesis. We presume that circulating molecules associated with these specific changes could be the strong candidates for further validation in larger studies as both disease-specific and prognostic biomarkers.

Given the limitations and biases of myocardial biopsy, CMR serves as a valuable tool for cardiac research. Advanced CMR technologies, currently being validated in preclinical models and

TABLE 1 Studies aimed at identifying MiR biomarkers associated with adverse myocardial changes observed on CMR in hypertrophic cardiomyopathy.

CMR tools	Studying myocardial characteristics	RNA class	Number of patients	Main conclusion	Ref
Postcontrast T1 mapping	Diffuse fibrosis if T1 time <470 ms	Circulating miRs	63 (+4 controls)	Individual miRs had moderate diagnostic value (AUC: 0.663–0.742), but combination of 8 miRs greatly improved diagnostic value (AUC 0.87) for the presence of diffuse fibrosis; 11 miR levels inversely correlated with T1 time	[84]
LGE	Focal fibrosis	Myocardial miRs	21 (+4 controls)	MiR-642a-3p expression was positively correlated to the quantification of LGE (r = 0.467)	[85]
LGE	Focal fibrosis	Circulating miRs	41 (+41 controls)	MiR-29a is significantly associated with both hypertrophy and fibrosis (r = 0.691)	[86]
LGE	Focal fibrosis	Circulating miRs	24 (+11 controls)	Elevated miR-4454 levels were significantly correlated with cardiac fibrosis (r = 0.560)	[87]
LGE	Focal fibrosis	Myocardial and circulating miRs	42 (+30 controls)	Circulating miR-221 is consistent with that in myocardial tissue, and correlated with myocardial fibrosis and hypertrophy (r = 0.630, AUC:0.764)	[48]
LGE	Focal fibrosis	Circulating miRs and lncRNAs	69	LncRNA-MIAT might be associated with the development of fibrosis in HCM via negatively regulating the expression of miR-29a (AUC:0.810)	[88]

CMR, cardiac magnetic resonance; RNA, Ribonucleic acid; LGE, late gadolinium enhancement; miR, microRNA; lncRNA, long-noncoding RNA.

human histology, enable the non-invasive visualization and quantification of myocardial microanatomical changes at all stages of the disease, including the preclinical phase. Preclinical HCM appears to be of particular interest for biomarker discovery, offering a unique opportunity to explore ncRNA signatures and potentially uncover disease-specific pathways without the confounding influence of secondary changes related to hemodynamic abnormalities. The expanding availability of genetic testing, including cascade family screening, is facilitating the identification of mutation carriers, making such studies feasible. When conducting discovery studies in overt HCM, the genotype of patients should be considered, as both miRs and myocardial microstructure are sensitive to the genotype status.

Novel HCM therapeutics, such as myosin inhibitors and gene editing, hold the potential to reverse the disease phenotype. Incorporating candidate miR panels into such self-controlled trials could enhance biomarker discovery by identifying those that reflect reversible adverse myocardial changes. A complementary imaging and genome-based biomarker approach could deeper insights into the complex underlying processes and identify novel targets for emerging therapeutic technologies.

HCM is a slowly progressive disease with a low event rate, making prospective studies is costly and time-consuming. Nevertheless, longitudinal studies with adequate sample size are essential to evaluate the prognostic power of candidate miR panels. Although conducting such studies in HCM is challenging, growing awareness and diagnostic expertise among professionals, emerging international cardiomyopathy collaborations, and advances in potentially curative therapies foster optimism.

Besides miRs, there are two other types of ncRNAs in the scope of interest in HCM: long non-coding RNAs (lncRNAs), which account for 80%–90% of all ncRNAs, and circular RNAs (circRNAs), a newer class of ncRNAs known for their stability due to a closed ring structure [89, 90]. To the best of our knowledge, only one study has investigated myocardial fibrosis in HCM by integrating CMR with relevant circulating lncRNAs [88]. This field remains largely unexplored, and significant efforts are required to advance our understanding.

Conclusion

Enhanced myocardial characterization and staging of HCM using advanced CMR techniques holds promise for identifying circulating miRs as biomarkers. MiR signatures associated with adverse microanatomical changes detected by CMR could be the strong candidates for longitudinal validation studies. To ensure comprehensive and reliable results, future research should consider patients' genetic status.

Author contributions

OC proposed the concept, wrote the first draft of the manuscript and supervised the project. All authors contributed to the article and approved the submitted version.

Funding

The author(s) declare that financial support was received for the research, authorship, and/or publication of this article. This research was supported by the Russian Science Foundation (grant No. 20-15-00353).

Acknowledgments

The authors would like to express their gratitude to Prof. Olga Favorova for her invaluable assistance in proofreading and editing the manuscript.

Conflict of interest

The author(s) declared no potential conflicts of interest with respect to the research, authorship, and/or publication of this article.

References

1. Elliott PM, Anastasakis A, Borger MA, Borggrefe M, Cecchi F, Charron P, et al. 2014 ESC guidelines on diagnosis and management of hypertrophic cardiomyopathy: the task force for the diagnosis and management of hypertrophic cardiomyopathy of the European society of cardiology (ESC). *Eur Heart J* (2014) **35**:2733–79. doi:10.1093/eurheartj/ehu284

2. Basso C, Thiene G, Corrado D, Buja G, Melacini P, Nava A. Hypertrophic cardiomyopathy and sudden death in the young: pathologic evidence of myocardial ischemia. *Hum Pathol* (2000) **31**(8):988–98. doi:10.1053/hupa.2000.16659

3. Maron BJ, Roberts WC. Hypertrophic cardiomyopathy and cardiac muscle cell disorganization revisited: relation between the two and significance. *Am Heart J* (1981) **102**(1):95–110. doi:10.1016/0002-8703(81)90419-1

4. Maron BJ, Wolfson JK, Epstein SE, Roberts WC. Intramural ("small vessel") coronary artery disease in hypertrophic cardiomyopathy. *J Am Coll Cardiol* (1986) **8**(3):545–57. doi:10.1016/S0735-1097(86)80181-4

5. Varnava AM, Elliott PM, Mahon N, Davies MJ, McKenna WJ. Relation between myocyte disarray and outcome in hypertrophic cardiomyopathy. *Am J Cardiol* (2001) **88**(3):275–9. doi:10.1016/S0002-9149(01)01640-X

6. Galati G, Leone O, Pasquale F, Olivotto I, Biagini E, Grigioni F, et al. Histological and histometric characterization of myocardial fibrosis in end-stage hypertrophic cardiomyopathy: a clinical-pathological study of 30 explanted hearts. *Circ Heart Fail* (2016) **9**(9):e003090. doi:10.1161/CIRCHEARTFAILURE.116.003090

7. Soler R, Méndez C, Rodríguez E, Barriales R, Ochoa JP, Monserrat L. Phenotypes of hypertrophic cardiomyopathy. An illustrative review of MRI findings. *Insights Imaging* (2018) **9**(6):1007–20. doi:10.1007/s13244-018-0656-8

8. Marian AJ, Braunwald E. Hypertrophic cardiomyopathy: genetics, pathogenesis, clinical manifestations, diagnosis, and therapy. *Circ Res* (2017) **121**(7):749–70. doi:10.1161/CIRCRESAHA.117.311059

9. Ho CY, Day SM, Ashley EA, Michels M, Pereira AC, Jacoby D, et al. Genotype and lifetime burden of disease in hypertrophic cardiomyopathy: insights from the sarcomeric human cardiomyopathy registry (SHaRe). *Circulation* (2018) **138**(14):1387–98. doi:10.1161/CIRCULATIONAHA.117.033200

10. Geisterfer-Lowrance AA, Kass S, Tanigawa G, Vosberg HP, McKenna W, Seidman CE, et al. A molecular basis for familial hypertrophic cardiomyopathy: a β cardiac myosin heavy chain gene missense mutation. *Cell* (1990) **62**(5):999–1006. doi:10.1016/0092-8674(90)90274-I

11. Seidman CE, Seidman JG. Identifying sarcomere gene mutations in hypertrophic cardiomyopathy: a personal history. *Circ Res*, **108**(6)(2011). p. 743–50. doi:10.1161/CIRCRESAHA.110.223834

12. Spudich JA. Three perspectives on the molecular basis of hypercontractility caused by hypertrophic cardiomyopathy mutations. *Pflügers Archiv - Eur J Physiol* (2019) **471**(5):701–17. doi:10.1007/s00424-019-02259-2

13. Olivotto I, Oreziak A, Barriales-Villa R, Abraham TP, Masri A, Garcia-Pavia P, et al. Mavacamten for treatment of symptomatic obstructive hypertrophic cardiomyopathy (EXPLORER-HCM): a randomised, double-blind, placebo-controlled, phase 3 trial. *Lancet* (2020) **396**(10253):759–69. doi:10.1016/S0140-6736(20)31792-X

14. McKenna WJ, Crean A, Greenway S, Tadros R, Veselka J, Woo A. Hypertrophic cardiomyopathy: evolution to the present, ongoing challenges, and opportunities. *Can J Cardiol* (2024) **40**(5):738–41. doi:10.1016/j.cjca.2024.03.005

15. Matthia EL, Setteducato ML, Elzeneini M, Vernace N, Salerno M, Kramer CM, et al. Circulating biomarkers in hypertrophic cardiomyopathy. *J Am Heart Assoc* (2022) **11**(23):e027618. doi:10.1161/JAHA.122.027618

16. Ho JE, Shi L, Day SM, Colan SD, Russell MW, Towbin JA, et al. Biomarkers of cardiovascular stress and fibrosis in preclinical hypertrophic cardiomyopathy. *Open Heart* (2017) **4**(2):e000615. doi:10.1136/openhrt-2017-000615

17. Ommen SR, Ho CY, Asif IM, Balaji S, Burke MA, Day SM, et al. 2024 AHA/ACC/AMSSM/HRS/PACES/SCMR guideline for the management of hypertrophic cardiomyopathy. *J Am Coll Cardiol* (2024) **83**(23):2324–405. doi:10.1016/j.jacc.2024.02.014

18. O'Mahony C, Jichi F, Pavlou M, Monserrat L, Anastasakis A, Rapezzi C, et al. A novel clinical risk prediction model for sudden cardiac death in hypertrophic cardiomyopathy (HCM Risk-SCD). *Eur Heart J* (2014) **35**(30):2010–20. doi:10.1093/eurheartj/eht439

19. Maron MS, Masri A, Choudhury L, Olivotto I, Saberi S, Wang A, et al. Phase 2 study of Aficamten in patients with obstructive hypertrophic cardiomyopathy. *J Am Coll Cardiol* (2023) **81**(1):34–45. doi:10.1016/j.jacc.2022.10.020

20. Saberi S, Cardim N, Yamani M, Schulz-Menger J, Li W, Florea V, et al. Mavacamten favorably impacts cardiac structure in obstructive hypertrophic cardiomyopathy: EXPLORER-HCM cardiac magnetic resonance substudy analysis. *Circulation* (2021) **143**(6):606–8. doi:10.1161/CIRCULATIONAHA.120.052359

21. Shimada YJ, Raita Y, Liang LW, Maurer MS, Hasegawa K, Fifer MA, et al. Comprehensive proteomics profiling reveals circulating biomarkers of hypertrophic cardiomyopathy. *Circ Heart Fail* (2021) **14**(7):e007849. doi:10.1161/CIRCHEARTFAILURE.120.007849

22. Liang LW, Hasegawa K, Maurer MS, Reilly MP, Fifer MA, Shimada YJ. Comprehensive transcriptomics profiling of MicroRNA reveals plasma circulating biomarkers of hypertrophic cardiomyopathy and dysregulated signaling pathways. *Circ Heart Fail* (2023) **16**(6):e010010. doi:10.1161/CIRCHEARTFAILURE.122.010010

23. Sucharov CC, Neltner B, Pietra AE, Karimpour-Fard A, Patel J, Ho CY, et al. Circulating MicroRNAs identify early phenotypic changes in sarcomeric hypertrophic cardiomyopathy. *Circ Heart Fail* (2023) **16**(6):e010291. doi:10.1161/CIRCHEARTFAILURE.122.010291

24. Captur G, Heywood WE, Coats C, Rosmini S, Patel V, Lopes LR, et al. Identification of a multiplex biomarker panel for hypertrophic cardiomyopathy using quantitative proteomics and machine learning. *Mol and Cell Proteomics* (2020) **19**(1):114–27. doi:10.1074/mcp.RA119.001586

25. Small EM, Olson EN. Pervasive roles of microRNAs in cardiovascular biology. *Nature* (2011) **469**(7330):336–42. doi:10.1038/nature09783

26. Misir S, Wu N, Yang BB. Specific expression and functions of circular RNAs. *Cell Death Differ* (2022) **29**(3):481–91. doi:10.1038/s41418-022-00948-7

27. Yao RW, Wang Y, Chen LL. Cellular functions of long noncoding RNAs. *Nat Cel Biol* (2019) **21**(5):542–51. doi:10.1038/s41556-019-0311-8

28. Ambros V. The functions of animal microRNAs. *Nature* (2004) **431**(7006):350–5. doi:10.1038/nature02871

29. Zhao Y, Wang Z, Zhang W, Zhang L. MicroRNAs play an essential role in autophagy regulation in various disease phenotypes. *BioFactors* (2019) **45**(6):844–56. doi:10.1002/biof.1555

30. Das A, Samidurai A, Salloum FN. Deciphering non-coding RNAs in cardiovascular health and disease. *Front Cardiovasc Med* (2018) **5**:73. doi:10.3389/fcvm.2018.00073

31. Bauersachs J, Solomon SD, Anker SD, Antorrena-Miranda I, Batkai S, Viereck J, et al. Efficacy and safety of CDR132L in patients with reduced left ventricular ejection fraction after myocardial infarction: rationale and design of the HF-REVERT trial. *Eur J Heart Fail* (2024) **26**(3):674–82. doi:10.1002/ejhf.3139

32. Seal RL, Chen L, Griffiths-Jones S, Lowe TM, Mathews MB, O'Reilly D, et al. A guide to naming human non-coding RNA genes. *EMBO J* (2020) **39**(6):e103777. doi:10.15252/embj.2019103777

33. Kozomara A, Birgaoanu M, Griffiths-Jones S. miRBase: from microRNA sequences to function. *Nucleic Acids Res* (2019) **47**(D1):D155–D162. doi:10.1093/nar/gky1141

34. Ntelios D, Georgiou E, Alexouda S, Malousi A, Efthimiadis G, Tzimagiorgis G. A critical approach for successful use of circulating microRNAs as biomarkers in cardiovascular diseases: the case of hypertrophic cardiomyopathy. *Heart Fail Rev* (2022) **27**(1):281–94. doi:10.1007/s10741-021-10084-y

35. Bartel DP. MicroRNAs. *Cell* (2004) **116**(2):281–97. doi:10.1016/S0092-8674(04)00045-5

36. Mitchell PS, Parkin RK, Kroh EM, Fritz BR, Wyman SK, Pogosova-Agadjanyan EL, et al. Circulating microRNAs as stable blood-based markers for cancer detection. *Proc Natl Acad Sci USA* (2008) **105**(30):10513–8. doi:10.1073/pnas.0804549105

37. Vickers KC, Palmisano BT, Shoucri BM, Shamburek RD, Remaley AT. MicroRNAs are transported in plasma and delivered to recipient cells by high-density lipoproteins. *Nat Cel Biol* (2011) **13**(4):423–33. doi:10.1038/ncb2210

38. Margolis L, Sadovsky Y. The biology of extracellular vesicles: the known unknowns. *Plos Biol* (2019) **17**(7):e3000363. doi:10.1371/journal.pbio.3000363

39. Bagnall RD, Tsoutsman T, Shephard RE, Ritchie W, Semsarian C. Global MicroRNA profiling of the mouse ventricles during development of severe hypertrophic cardiomyopathy and heart failure. *PLoS One* (2012) **7**:9e44744. doi:10.1371/journal.pone.0044744

40. Guo M, Luo J, Zhao J, Shang D, Lv Q, Zang P. Combined use of circulating miR-133a and NT-proBNP improves heart failure diagnostic accuracy in elderly patients. *Med Sci Monit* (2018) **24**:8840–8. doi:10.12659/MSM.911632

41. Wong LL, Zou R, Zhou L, Lim JY, Phua DCY, Liu C, et al. Combining circulating MicroRNA and NT-proBNP to detect and categorize heart failure subtypes. *J Am Coll Cardiol* (2019) **73**(11):1300–13. doi:10.1016/j.jacc.2018.11.060

42. Carè A, Catalucci D, Felicetti F, Bonci D, Addario A, Gallo P, et al. MicroRNA-133 controls cardiac hypertrophy. *Nat Med* (2007) **13**(5):613–8. doi:10.1038/nm1582

43. Leptidis S, El Azzouzi H, Lok SI, de Weger R, Olieslagers S, Kisters N, et al. A deep sequencing approach to uncover the miRNOME in the human heart. *PLoS One* (2013) **8**(2):e57800. doi:10.1371/journal.pone.0057800

44. Kuster DWD, Mulders J, Ten Cate FJ, Michels M, Dos Remedios CG, da Costa Martins PA, et al. MicroRNA transcriptome profiling in cardiac tissue of hypertrophic cardiomyopathy patients with MYBPC3 mutations. *J Mol Cell Cardiol* (2013) **65**:59–66. doi:10.1016/j.yjmcc.2013.09.012

45. Song L, Su M, Wang S, Zou Y, Wang X, Wang Y, et al. MiR-451 is decreased in hypertrophic cardiomyopathy and regulates autophagy by targeting TSC 1. *J Cell Mol Med* (2014) **18**(11):2266–74. doi:10.1111/jcmm.12380

46. Gao J, Collyer J, Wang M, Sun F, Xu F. Genetic dissection of hypertrophic cardiomyopathy with myocardial RNA-seq. *Int J Mol Sci* (2020) **21**(9):3040. doi:10.3390/ijms21093040

47. Palacín M, Reguero JR, Martín M, Díaz Molina B, Morís C, Alvarez V, et al. Profile of MicroRNAs differentially produced in hearts from patients with hypertrophic cardiomyopathy and sarcomeric mutations. *Clin Chem* (2011) **57**(11):1614–6. doi:10.1373/clinchem.2011.168005

48. Huang D, Chen Z, Wang J, Chen Y, Liu D, Lin K. MicroRNA-221 is a potential biomarker of myocardial hypertrophy and fibrosis in hypertrophic obstructive cardiomyopathy. *Biosci Rep* (2020) **40**(1):BSR20191234. doi:10.1042/BSR20191234

49. Baulina N, Pisklova M, Kiselev I, Chumakova O, Zateyshchikov D, Favorova O. Circulating miR-499a-5p is a potential biomarker of MYH7—associated hypertrophic cardiomyopathy. *Int J Mol Sci* (2022) **23**(7):3791. doi:10.3390/ijms23073791

50. Van Rooij E, Quiat D, Johnson BA, Sutherland LB, Qi X, Richardson JA, et al. A family of microRNAs encoded by myosin genes governs myosin expression and muscle performance. *Develop Cel* (2009) **17**(5):662–73. doi:10.1016/j.devcel.2009.10.013

51. Sood P, Krek A, Zavolan M, Macino G, Rajewsky N. Cell-type-specific signatures of microRNAs on target mRNA expression. *Proc Natl Acad Sci* (2006) **103**(8):2746–51. doi:10.1073/pnas.0511045103

52. Chistiakov DA, Orekhov AN, Bobryshev YV. Cardiac-specific miRNA in cardiogenesis, heart function, and cardiac pathology (with focus on myocardial infarction). *J Mol Cell Cardiol* (2016) **94**:107–21. doi:10.1016/j.yjmcc.2016.03.015

53. Liu N, Olson EN. MicroRNA regulatory networks in cardiovascular development. *Develop Cel* (2010) **18**(4):510–25. doi:10.1016/j.devcel.2010.03.010

54. Düsing P, Zietzer A, Jansen F. MicroRNA-based diagnostics in heart diseases. *JACC: Basic Translational Sci* (2021) **6**(11):897–9. doi:10.1016/j.jacbts.2021.08.004

55. De Gaspari M, Basso C, Perazzolo Marra M, Elia S, Bueno Marinas M, Angelini A, et al. Small vessel disease: another component of the hypertrophic cardiomyopathy phenotype not necessarily associated with fibrosis. *J Clin Med* (2021) **10**(4):575. doi:10.3390/jcm10040575

56. Garcia-Canadilla P, Cook AC, Mohun TJ, Oji O, Schlossarek S, Carrier L, et al. Myoarchitectural disarray of hypertrophic cardiomyopathy begins pre-birth. *J Anat* (2019) **235**(5):962–76. doi:10.1111/joa.13058

57. McKenna WJ, Stewart JT, Nihoyannopoulos P, McGinty F, Davies MJ. Hypertrophic cardiomyopathy without hypertrophy: two families with myocardial disarray in the absence of increased myocardial mass. *Heart* (1990) **63**(5):287–90. doi:10.1136/hrt.63.5.287

58. Varnava A, Baboonian C, Davison F, de Cruz L, Elliott PM, Davies MJ, et al. A new mutation of the cardiac troponin T gene causing familial hypertrophic cardiomyopathy without left ventricular hypertrophy. *Heart* (1999) **82**(5):621–4. doi:10.1136/hrt.82.5.621

59. Green EM, Wakimoto H, Anderson RL, Evanchik MJ, Gorham JM, Harrison BC, et al. A small-molecule inhibitor of sarcomere contractility suppresses hypertrophic cardiomyopathy in mice. *Science* (2016) **351**(6273):617–21. doi:10.1126/science.aad3456

60. Messroghli DR, Moon JC, Ferreira VM, Grosse-Wortmann L, He T, Kellman P, et al. Clinical recommendations for cardiovascular magnetic resonance mapping of T1, T2, T2* and extracellular volume: a consensus statement by the Society for Cardiovascular Magnetic Resonance (SCMR) endorsed by the European Association for Cardiovascular Imaging (EACVI). *J Cardiovasc Magn Reson* (2016) **19**(1):75. doi:10.1186/s12968-017-0389-8

61. Miller CA, Naish JH, Bishop P, Coutts G, Clark D, Zhao S, et al. Comprehensive validation of cardiovascular magnetic resonance techniques for the assessment of myocardial extracellular volume. *Circ Cardiovasc Imaging* (2013) **6**(3):373–83. doi:10.1161/CIRCIMAGING.112.000192

62. Schelbert EB, Hsu LY, Anderson SA, Mohanty BD, Karim SM, Kellman P, et al. Late gadolinium-enhancement cardiac magnetic resonance identifies postinfarction myocardial fibrosis and the border zone at the near cellular level in *ex vivo* rat heart. *Circ Cardiovasc Imaging* (2010) **3**(6):743–52. doi:10.1161/CIRCIMAGING.108.835793

63. Iles LM, Ellims AH, Llewellyn H, Hare JL, Kaye DM, McLean CA, et al. Histological validation of cardiac magnetic resonance analysis of regional and diffuse interstitial myocardial fibrosis. *Eur Heart J - Cardiovasc Imaging* (2015) **16**(1):14–22. doi:10.1093/ehjci/jeu182

64. Moon JCC, Reed E, Sheppard MN, Elkington AG, Ho SY, Burke M, et al. The histologic basis of late gadolinium enhancement cardiovascular magnetic resonance in hypertrophic cardiomyopathy. *J Am Coll Cardiol* (2004) **43**(12):2260–4. doi:10.1016/j.jacc.2004.03.035

65. Ariga R, Tunnicliffe EM, Manohar SG, Mahmod M, Raman B, Piechnik SK, et al. Identification of myocardial disarray in patients with hypertrophic cardiomyopathy and ventricular arrhythmias. *J Am Coll Cardiol* (2019) **73**(20):2493–502. doi:10.1016/j.jacc.2019.02.065

66. Dall'Armellina E, Ennis DB, Axel L, Croisille P, Ferreira PF, Gotschy A, et al. Cardiac diffusion-weighted and tensor imaging: a Society for Cardiovascular Magnetic Resonance (SCMR) special interest group consensus statement. *J Cardiovasc Magn Reson* (2024) **21**:101109. doi:10.1016/j.jocmr.2024.101109

67. Joy G, Kelly CI, Webber M, Pierce I, Teh I, McGrath L, et al. Microstructural and microvascular phenotype of sarcomere mutation carriers and overt hypertrophic cardiomyopathy. *Circulation* (2023) **148**(10):808–18. doi:10.1161/CIRCULATIONAHA.123.063835

68. Petersen SE, Jerosch-Herold M, Hudsmith LE, Robson MD, Francis JM, Doll HA, et al. Evidence for microvascular dysfunction in hypertrophic cardiomyopathy: new insights from multiparametric magnetic resonance imaging. *Circulation* (2007) **115**(18):2418–25. doi:10.1161/CIRCULATIONAHA.106.657023

69. Villa AD, Sammut E, Zarinabad N, Carr-White G, Lee J, Bettencourt N, et al. Microvascular ischemia in hypertrophic cardiomyopathy: new insights from high-resolution combined quantification of perfusion and late gadolinium enhancement. *J Cardiovasc Magn Reson* (2016) **18**:4. doi:10.1186/s12968-016-0223-8

70. Arbelo E, Protonotarios A, Gimeno JR, Arbustini E, Barriales-Villa R, Basso C, et al. 2023 ESC Guidelines for the management of cardiomyopathies. *Eur Heart J* (2023) **44**(37):3503–626. doi:10.1093/eurheartj/ehad194

71. Kamp NJ, Chery G, Kosinski AS, Desai MY, Wazni O, Schmidler GS, et al. Risk stratification using late gadolinium enhancement on cardiac magnetic resonance imaging in patients with hypertrophic cardiomyopathy: a systematic review and meta-analysis. *Prog Cardiovasc Dis* (2021) **66**:10–6. doi:10.1016/j.pcad.2020.11.001

72. Zeppenfeld K, Tfelt-Hansen J, de Riva M, Winkel BG, Behr ER, Blom NA, et al. 2022 ESC Guidelines for the management of patients with ventricular arrhythmias and the prevention of sudden cardiac death. *Eur Heart J* (2022) **43**(40):3997–4126. doi:10.1093/eurheartj/ehac262

73. Hinojar R, Varma N, Child N, Goodman B, Jabbour A, Yu CY, et al. T1 mapping in discrimination of hypertrophic phenotypes: hypertensive heart disease and hypertrophic cardiomyopathy: findings from the international T1 multicenter cardiovascular magnetic resonance study. *Circ Cardiovasc Imaging* (2015) **8**(12):e003285. doi:10.1161/CIRCIMAGING.115.003285

74. Yang EY, Ghosn MG, Khan MA, Gramze NL, Brunner G, Nabi F, et al. Myocardial extracellular volume fraction adds prognostic information beyond myocardial replacement fibrosis. *Circ Cardiovasc Imaging* (2019) **12**(12):e009535. doi:10.1161/CIRCIMAGING.119.009535

75. Kramer CM, Appelbaum E, Desai MY, Desvigne-Nickens P, DiMarco JP, Friedrich MG, et al. Hypertrophic Cardiomyopathy Registry: the rationale and

design of an international, observational study of hypertrophic cardiomyopathy. *Am Heart J* (2015) **170**(2):223–30. doi:10.1016/j.ahj.2015.05.013

76. Benz DC, Gräni C, Antiochos P, Heydari B, Gissler MC, Ge Y, et al. Cardiac magnetic resonance biomarkers as surrogate endpoints in cardiovascular trials for myocardial diseases. *Eur Heart J* (2023) **44**(45):4738–47. doi:10.1093/eurheartj/ehad510

77. Garcia Brás P, Rosa SA, Cardoso I, Branco LM, Galrinho A, Gonçalves AV, et al. Microvascular dysfunction is associated with impaired myocardial work in obstructive and nonobstructive hypertrophic cardiomyopathy: a multimodality study. *J Am Heart Assoc* (2023) **12**(8):e028857. doi:10.1161/JAHA.122.028857

78. Neubauer S, Kolm P, Ho CY, Kwong RY, Desai MY, Dolman SF, et al. Distinct subgroups in hypertrophic cardiomyopathy in the NHLBI HCM registry. *J Am Coll Cardiol* (2019) **74**(19):2333–45. doi:10.1016/j.jacc.2019.08.1057

79. Ho CY, Abbasi SA, Neilan TG, Shah RV, Chen Y, Heydari B, et al. T1 measurements identify extracellular volume expansion in hypertrophic cardiomyopathy sarcomere mutation carriers with and without left ventricular hypertrophy. *Circ Cardiovasc Imaging* (2013) **6**(3):415–22. doi:10.1161/CIRCIMAGING.112.000333

80. Bakhshi H, Michelhaugh SA, Bruce SA, Seliger SL, Qian X, Ambale Venkatesh B, et al. Association between proteomic biomarkers and myocardial fibrosis measured by MRI: the multi-ethnic study of atherosclerosis. *EBioMedicine* (2023) **90**:104490. doi:10.1016/j.ebiom.2023.104490

81. Siggins C, Pan JA, Löffler AI, Yang Y, Shaw PW, Balfour PC, et al. Cardiometabolic biomarker patterns associated with cardiac MRI defined fibrosis and microvascular dysfunction in patients with heart failure with preserved ejection fraction. *Front Cardiovasc Med* (2024) **11**:1334226. doi:10.3389/fcvm.2024.1334226

82. Tahir UA, Kolm P, Kwong RY, Desai MY, Dolman SF, Deng S, et al. Protein biomarkers of adverse clinical features and events in sarcomeric hypertrophic cardiomyopathy. *Circ Heart Fail* (2024) **5**:e011707. doi:10.1161/CIRCHEARTFAILURE.124.011707

83. Becker S, Florian A, Patrascu A, Rösch S, Waltenberger J, Sechtem U, et al. Identification of cardiomyopathy associated circulating miRNA biomarkers in patients with muscular dystrophy using a complementary cardiovascular magnetic resonance and plasma profiling approach. *J Cardiovasc Magn Reson* (2016) **18**(1):25. doi:10.1186/s12968-016-0244-3

84. Fang L, Ellims AH, Moore XL, White DA, Taylor AJ, Chin-Dusting J, et al. Circulating microRNAs as biomarkers for diffuse myocardial fibrosis in patients with hypertrophic cardiomyopathy. *J Transl Med* (2015) **13**(1):314. doi:10.1186/s12967-015-0672-0

85. Zhang C, Zhang H, Zhao L, Wei Z, Lai Y, Ma X. Differential expression of microRNAs in hypertrophied myocardium and their relationship to late gadolinium enhancement, left ventricular hypertrophy and remodeling in hypertrophic cardiomyopathy. *Diagnostics* (2022) **12**(8):1978. doi:10.3390/diagnostics12081978

86. Roncarati R, Viviani Anselmi C, Losi MA, Papa L, Cavarretta E, Da Costa Martins P, et al. Circulating miR-29a, among other up-regulated MicroRNAs, is the only biomarker for both hypertrophy and fibrosis in patients with hypertrophic cardiomyopathy. *J Am Coll Cardiol* (2014) **63**(9):920–7. doi:10.1016/j.jacc.2013.09.041

87. Thottakara T, Lund N, Krämer E, Kirchhof P, Carrier L, Patten M. A novel miRNA screen identifies miRNA-4454 as a candidate biomarker for ventricular fibrosis in patients with hypertrophic cardiomyopathy. *Biomolecules* (2021) **11**(11):1718. doi:10.3390/biom11111718

88. Zhou J, Zhou Y, Wang C. LncRNA-MIAT regulates fibrosis in hypertrophic cardiomyopathy (HCM) by mediating the expression of miR-29a-3p. *J Cell Biochem* (2019) **120**(5):7265–75. doi:10.1002/jcb.28001

89. Baulina NM, Kiselev IS, Chumakova OS, Favorova OO. Circular RNAs: biogenesis, functions, and role in myocardial hypertrophy. *Biochemistry (Mosc)* (2024) **89**(S1):S1–S13. doi:10.1134/S0006297924140013

90. Shahzadi SK, Naidoo N, Alsheikh-Ali A, Rizzo M, Rizvi AA, Santos RD, et al. Reconnoitering the role of long-noncoding RNAs in hypertrophic cardiomyopathy: a descriptive review. *Int J Mol Sci* (2021) **22**(17):9378. doi:10.3390/ijms22179378

EBM Experimental Biology and Medicine

TYPE Review
PUBLISHED 18 September 2024
DOI 10.3389/ebm.2024.10167

OPEN ACCESS

*CORRESPONDENCE
Qihe Xu,
qihe.xu@kcl.ac.uk
Jeffrey B. Kopp,
jeffreyk@intra.niddk.nih.gov
An-Long Xu,
xuanlong@bucm.edu.cn

RECEIVED 14 March 2024
ACCEPTED 22 August 2024
PUBLISHED 18 September 2024

CITATION
Liu W-B, Fermin D, Xu A-L, Kopp JB and Xu Q (2024) Single-cell RNA sequencing data locate ALDH1A2-mediated retinoic acid synthetic pathway to glomerular parietal epithelial cells.
Exp. Biol. Med. 249:10167.
doi: 10.3389/ebm.2024.10167

Single-cell RNA sequencing data locate ALDH1A2-mediated retinoic acid synthetic pathway to glomerular parietal epithelial cells

Wen-Bin Liu[1], Damian Fermin[2], An-Long Xu[1]*, Jeffrey B. Kopp[3]* and Qihe Xu[4]*

[1]Beijing Research Institute of Chinese Medicine, Beijing University of Chinese Medicine, Beijing, China, [2]Department of Internal Medicine, Division of Nephrology, University of Michigan, Ann Arbor, MI, United States, [3]Kidney Disease Section, Kidney Diseases Branch, National Institute of Diabetes and Digestive and Kidney Diseases, National Institutes of Health, Bethesda, MD, United States, [4]Renal Sciences and Integrative Chinese Medicine Laboratory, Department of Inflammation Biology, School of Immunology & Microbial Sciences, Faculty of Life Sciences & Medicine, King's College London, London, United Kingdom

Abstract

Aldehyde dehydrogenase 1, family member A2, is a retinoic acid-synthesizing enzyme encoded by *Aldh1a2* in mice and *ALDH1A2* in humans. This enzyme is indispensable for kidney development, but its role in kidney physiology and pathophysiology remains to be fully defined. In this review, we mined single-cell and single-nucleus RNA sequencing databases of mouse and human kidneys and found that glomerular parietal epithelial cells (PECs) express a full set of genes encoding proteins needed for cellular vitamin A uptake, intracellular transport, and metabolism into retinoic acid. In particular, *Aldh1a2/ALDH1A2* mRNAs are selectively enriched in mouse and human PECs. *Aldh1a2* expression in PECs is greatly increased in a mouse model of anti-glomerular basement membrane glomerulonephritis and moderately induced in a mouse model of ischemia-reperfusion acute kidney injury. *Aldh1a2* expression in PECs is substantially repressed in a chronic kidney disease mouse model combining diabetes, hypertension, and partial nephrectomy and is moderately repressed in mouse models of focal segmental glomerulosclerosis and diabetic nephropathy. Single-nucleus RNA sequencing data show that *ALDH1A2* mRNA expression in PECs is diminished in patients with chronic kidney disease associated with diabetes, hypertension and polycystic kidney disease. In addition to data mining, we also performed Spearman's rank correlation coefficient analyses and identified gene transcripts correlated with *Aldh1a2/ALDH1A2* transcripts in mouse PECs and PEC subtypes, and in human PECs of healthy subjects and patients with AKI or CKD. Furthermore, we conducted Gene Ontology pathway analyses and identified the biological pathways enriched among these *Aldh1a2/ALDH1A2*-correlated genes. Our data mining and analyses led us to hypothesize that ALDH1A2-mediated retinoic acid synthesis in PECs plays a yet-undefined role in the kidney and that its dysregulation mediates injury. Conditional, PEC-

selective *Aldh1a2* knockout, RNA silencing and transgenic mouse models will be useful tools to test this hypothesis. Clinical studies on genetics, epigenetics, expression and functions of *ALDH1A2* and other genes needed for retinoic acid biosynthesis and signaling are also warranted.

KEYWORDS

***Aldh1a2*, retinoic acid, scRNA-seq, snRNA-seq, acute kidney injury, chronic kidney disease, rapidly progressive glomerulonephritis, parietal epithelial cells**

Impact statement

In mice, the *Aldh1a2* gene is indispensable for kidney development. In humans, loss-of-function mutations of *ALDH1A2* are not tolerated and partial loss-of-function mutations lead to severe developmental problems in multiple organs, including the kidney. However, the exact kidney cell types that express *Aldh1a2/ALDH1A2* in adult kidneys and the roles of retinoic acid signalling in these cells are poorly understood. By mining the latest scRNA-seq and snRNA-seq databases of mouse and human kidneys in health and disease, we highlight glomerular PECs as the major site of *Aldh1a2/ALDH1A2* expression and this expression is differentially dysregulated in different kidney diseases. We hypothesize that normal *ALDH1A2*-mediated retinoic acid synthesis in PECs plays important roles in maintaining kidney health and defending against disease. Further experimental and clinical studies against this hypothesis may lead to novel strategies for stratified diagnosis, cost-effective prevention, and efficacious treatment of kidney diseases.

Introduction

Aldehyde dehydrogenase 1 family member A2 (Aldh1a2/ALDH1A2) is an enzyme that catalyzes the second-step oxidation of vitamin A (retinol) and the irreversible conversion of retinaldehyde to retinoic acid (RA). In mice, the enzyme is encoded by *Aldh1a2*, which is indispensable for kidney development [1, 2]. In humans, the enzyme is encoded by *ALDH1A2*, an intronic variant of which causes increased enzyme activity and is associated with increased serum RA and newborn kidney size [3]. On the other hand, biallelic partially loss-of-function *ALDH1A2* coding variants result in severe congenital anomaly syndromes, including small kidneys and neonatal lethality [4, 5]. In addition, non-coding *ALDH1A2* variants reduce *ALDH1A2* expression in chondrocytes and contribute to severe hand osteoarthritis in adults [6]. This is in keeping with the notion that RA biosynthesis may continue to be active in post-natal life and may play cell-type specific roles [7]. However, whether *Aldh1a2* and *ALDH1A2* play any roles in kidney health and disease remains to be fully characterized. To address this issue, we mined single-cell RNA sequencing (scRNA-seq) and single-nucleus RNA sequencing (snRNA-seq) databases (Table 1) to evaluate *Aldh1a2/ALDH1A2* expression in different kidney cell types in mice and humans and examine how expression changes in kidney diseases. It is hoped that these data will facilitate generating hypotheses on the role of *Aldh1a2* and *ALDH1A2* in kidney health and disease and will guide in devising strategies for further studies. Our analytical workflow is illustrated in Figure 1.

TABLE 1 Databases explored in the present study.

Database category and name	Website	Date of last access
Mouse databases		
Kidney Cell Explorer [8]	https://cello.shinyapps.io/kidneycellexplorer/	6th Feb. 2024
Mouse PEC Landscape [9]	https://wenbinliu.shinyapps.io/mouse_PECs/	6th Feb. 2024
Kidney Interactive Transcriptomics 1 million cell atlas of mouse DKD and its treatments [10] Mouse IRI Kidney [11]	http://humphreyslab.com/SingleCell	6th Feb. 2024 6th Feb. 2024
Human databases		
KPMP Human Kidney Tissue Atlas [12]	https://atlas.kpmp.org/explorer/dataviz	6th Feb. 2024
Kidney Interactive Transcriptomics Human DKD snRNA + scATAC-seq [13] Human ADPKD snRNA + scATAC-seq [14]	http://humphreyslab.com/SingleCell	6th Feb. 2024 6th Feb. 2024
Susztaklab Kidney Biobank [15]	https://susztaklab.com/hk_genemap/snRNA	6th Feb. 2024
Human Protein Atlas [16]	https://www.proteinatlas.org/ENSG00000128918-ALDH1A2/tissue/kidney#	6th Feb. 2024

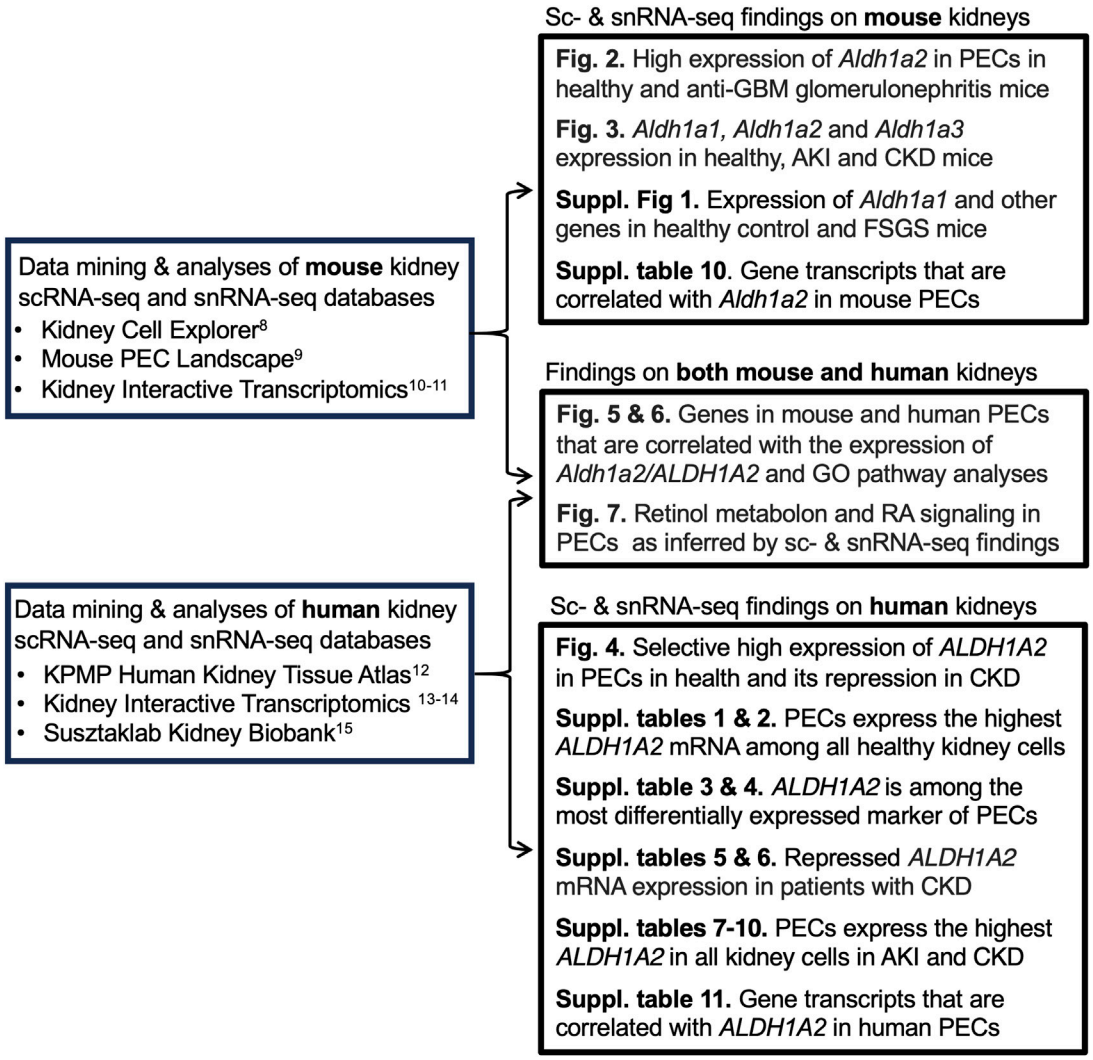

FIGURE 1
Analytical workflow of our data analyses and findings.

Data from mouse models

While mining the scRNA-seq database, Mouse Kidney Cell Explorer (Table 1), we discovered that healthy mouse PECs expressed *Stra6*, *Rbp1* and *Aldh1a2*, in a selective manner compared to other kidney cell types and did so at relatively high levels. These genes respectively encode a retinol uptake receptor, an intracellular retinol-binding protein and an enzyme catalyzing retinaldehyde conversion to retinoic acid (RA) (Figures 2A, B) [8]. Mouse PECs also manifested abundant expression of the ubiquitously expressed *Rdh10*, which encodes the main enzyme converting retinol to retinaldehyde. Hence, mouse PECs are likely active in RA synthesis.

As Aldh1a2/ALDH1A2 is the main enzyme catalyzing the final step of RA biosynthesis, we are particularly interested its expression and function. We hypothesize that Aldh1a2/ALDH1A2 in PECs, through catalyzing RA biosynthesis, play important roles in kidney health, and that their dysregulation contributes to kidney disease. To address this hypothesis, we gathered experimental evidence from published mouse models of acute kidney injury (AKI) and chronic kidney disease (CKD), particularly those manifesting injury to, or activation of, PECs and/or podocytes, *e.g.*, anti-glomerular basement membrane (GBM) glomerulonephritis, which often manifests as rapidly progressive glomerulonephritis (RPGN); primary podocyte diseases minimal change disease (MCD) and focal segmental glomerulosclerosis (FSGS), which often manifest as nephrotic syndrome. We also examined the data for mouse models of diabetic nephropathy, which may manifest podocyte injury and is the most common CKD in the developed world.

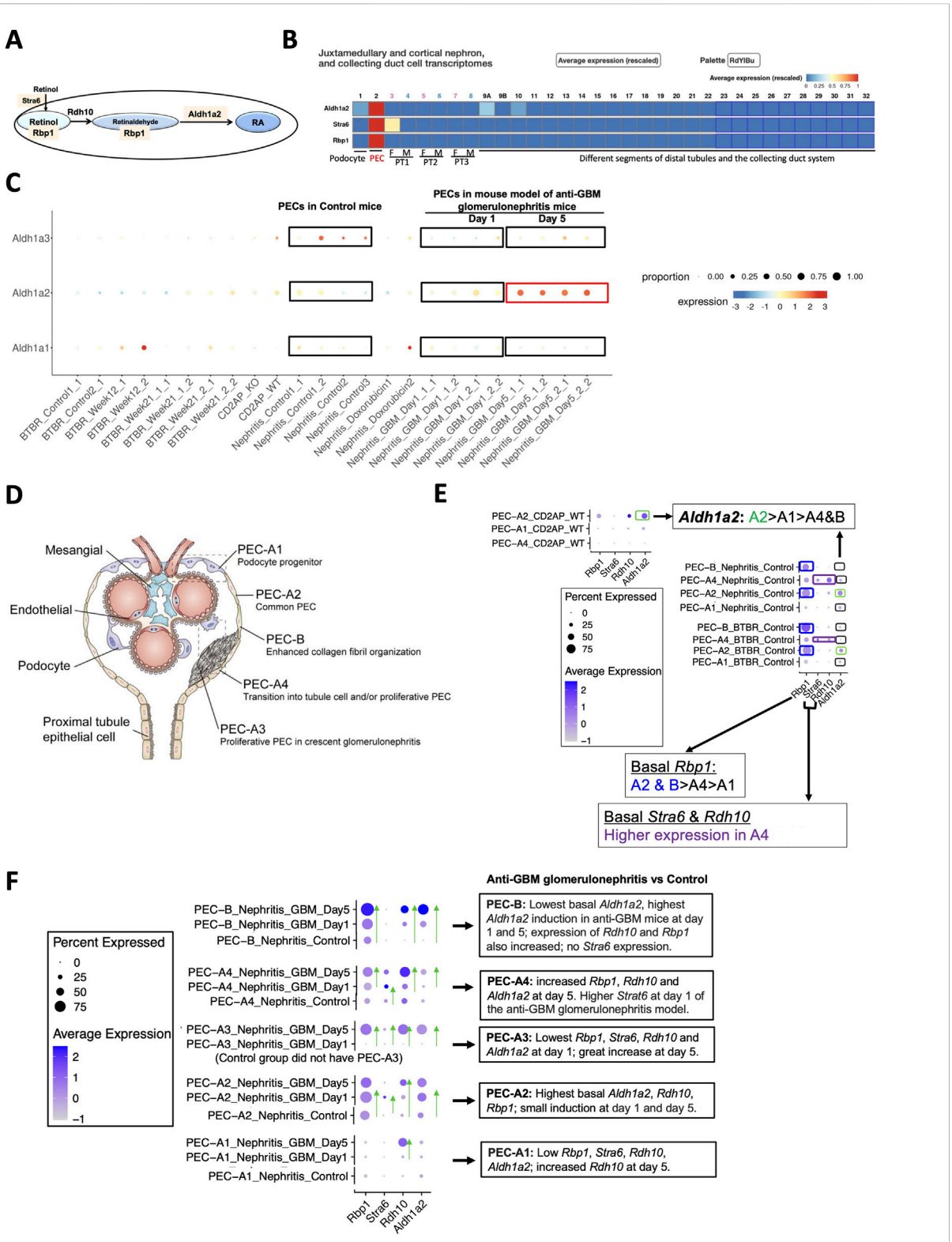

FIGURE 2
Mouse PECs have high *Stra6*, *Rbp1* and *Aldh1a2* mRNA expression, which is further induced in anti-GBM glomerulonephritis mice. **(A)** Diagram illustrates roles of Aldh1a2, Stra6, Rbp1 and Rdh10 proteins in the retinol metabolon. RA: retinoic acid. Pink shades indicate selective *Aldh1a2*, *Stra6* and *Rbp1* mRNA expression in mouse PECs. **(B)** Mouse renal scRNA-seq data were extracted from the Kidney Cell Explorer website. Relative average expression levels are color-coded (red > yellow > blue) with the highest expression normalized as 1. PT1, PT2 and PT3 denote segments 1, 2 and

(*Continued*)

FIGURE 2 (Continued)
3 of proximal tubule; F: female; M: male. **(C)** ScRNA-seq analysis of mouse PECs revealed distinct changes in mRNA expression of *Aldh1a1*, *Aldh1a2* and *Aldh1a3* in anti-GBM glomerulonephritis mice compared to healthy controls. Dot sizes indicate the relative proportion of PECs expressing the specific *Aldh1a* isoform, while the relative expression levels are color-coded, shown on a spectrum of blue (low expression) to red (high expression). To facilitate comparison, control and anti-GBM glomerulonephritis mice from day-1 and day-5 samples, among others, are highlighted by rectangle selection and text description. Nephritis_Control: samples of the control mice; Nephritis_GBM: samples of the anti-GBM glomerulonephritis mice. Other groups are irrelevant to studies of the anti-GBM glomerulonephritis mice but are nonetheless shown to demonstrate the specificity of the changes observed in the anti-GBM glomerulonephritis mice. **(D)** Diagram illustrates different PEC subtypes, among other glomerular cell types, adapted from Liu et al 2023 [9]. **(E)** ScRNA-seq analysis of PEC subtypes in wild-type and healthy control mice revealed differing levels of physiological mRNA expression of *Aldh1a2, Stra6, Rbp1 and Rdh10*. The bubble plot shows expression levels of *Aldh1a2*, *Stra6, Rbp1* and *Rdh10* in different PEC subtypes. Dot sizes indicate the proportion of PECs expressing a specific gene and brighter blue color indicates higher expression levels. The highest expression of *Aldh1a2* in PEC-A2 is highlighted by green rectangle selection; higher expression of *Rbp1* in PEC-A2 and PEC-B is highlighted by blue rectangle selection, while higher expression of *Stra6* and *Rdh10* in PEC-A4 is indicated by purple rectangle selection. **(F)** ScRNA-seq analysis of healthy control versus anti-GBM glomerulonephritis mice (day 1 and 5) revealed different changes in mRNA expression of *Aldh1a2*, *Stra6, Rbp1* and *Rdh10* in PEC subtypes. Dot sizes indicate the proportion of PECs expressing a specific gene; brighter blue color indicates higher expression levels. The trend of increase in expression is indicated by green arrows pointing to the higher expression. Cd2ap_WT are wild-type control mice for comparison with *Cd2ap* knockout mice (Supplementary Figure S1); Nephritis_Control: control mice RNA expression; Nephritis_GBM: anti-GBM glomerulonephritis mouse RNA expression.

Analysis of the Mouse PEC Landscape database containing scRNA-seq gene expression data for PECs from healthy mice and mouse models of kidney disease [9] (Table 1) revealed that *Aldh1a2* expression in PECs increased substantially in murine anti-GBM glomerulonephritis, on day 5 after intravenous injection of sheep anti-rat glomeruli serum (Figure 2C). In contrast, the expression of *Aldh1a3* decreased, while no change in *Aldh1a1* expression was observed in this model. Hence, Aldh1a2 likely plays the main role in PECs in this anti-GBM glomerulonephritis mouse model, although Aldh1a1, -2 and -3 isoenzymes all accomplish the final step of RA biosynthesis. Given that PECs play major roles in anti-GBM glomerulonephritis [17], it is compelling to further examine the expression and role of *Aldh1a2* in PECs in health and in anti-GBM glomerulonephritis.

As shown in Figure 2D, mouse PECs can be subdivided into five sub-types: PEC-A1 (podocyte progenitor), PEC-A2 (common PEC), PEC-A3 (proliferative PEC contributing to crescent formation), PEC-A4 (tubular progenitor) and PEC-B (pro-fibrogenic PECs). PEC-A1, A2, A4 and PEC-B are present in both healthy and diseased kidneys, while PEC-A3 only have been found in murine anti-GBM glomerulonephritis [9]. We compared *Aldh1a2, Stra6*, *Rbp1* and *Rdh10* mRNA expression in these PEC subtypes. As shown in Figure 2E, PEC subtypes differ in basal expression of *Aldh1a2*: the highest *Aldh1a2* expression was observed in PEC-A2 in wild-type healthy control mice. Wild-type healthy control mouse PEC-A2 also have higher expression of *Rbp1* compared with other PEC sub-types. In contrast, wild-type healthy mouse PEC-B had the lowest expression of *Aldh1a2*. As shown in Figure 2F, in anti-GBM glomerulonephritis mice, *Aldh1a2* expression was progressively and greatly induced in PEC-B, mildly increased in PEC-A2, and was substantially higher on day 5 than on day 1 in PEC-A3 cells, but expression did not change in PEC-A1 cells. Consequently, by day 5, PEC-B cells became the PEC subtype with the highest expression of *Aldh1a2*. PEC-B cells are a minor PEC subtype in healthy mice but numbers increase progressively and become the major PEC subtype in anti-GBM glomerulonephritis mice by day 5 [9]. It will be important to determine the role of *Aldh1a2* in PEC-B in anti-GBM glomerulonephritis. Supporting the concept that increased *Aldh1a2* expression in PEC-B plays particular roles by catalyzing retinol activation and RA synthesis, the substantial progressive induction of *Aldh1a2* expression in PEC-B paralleled the similar, progressive induction of *Rbp1* and *Rdh10* expression in PEC-B (Figure 2F).

PEC-A2 not only had the highest basal expression of *Aldh1a2* and *Rbp1* but also manifested relatively high expression in mouse anti-GBM glomerulonephritis on days 1 and 5, suggesting that RA signaling in PEC-A2 may also contribute to pathogenesis. In PEC-B, PEC-A3 and PEC-A4, *Aldh1a2*, *Rbp1* and *Rdh10* expression increased on day 5 versus day 1. This suggests that RA signaling in these PEC subtypes may play particular roles in the later stage of anti-GBM glomerulonephritis. In contrast, PEC-A1 had little *Aldh1a2, Rdh10, Stra6* and *Rbp1* expression in control mice and on day 1 of anti-GBM glomerulonephritis but had higher *Rdh10* mRNA expression on day-5 compared to day-1 in anti-GBM glomerulonephritis (Figure 2F).

PECs have intimate crosstalk with podocytes and may contribute to FSGS pathogenesis [18]. Towards understanding whether RA signaling might play a role in experimental FSGS, we compared *Aldh1a2, Stra6*, *Rbp1* and *Rdh10* mRNA expression in different PEC subtypes in FSGS mouse models, induced either by doxorubicin or by *Cd2ap* gene knockout, compared to healthy control mice. As shown in Supplementary Figure S1, expression of *Aldh1a2, Stra6*, *Rbp1* and *Rdh10* in PEC sub-types was not induced in mouse models of FSGS and, instead, showed a trend toward repression in some PEC subtypes in the disease models.

Next, we searched the Kidney Interactive Transcriptomics database (Table 1), particularly focusing on data from a recent scRNA-seq study of a multifactorial CKD model in female mice in comparison with female wild-type control mice — the CKD model (AAV mice) was characterized by obesity and diabetes caused by a homozygous point mutation in the gene for the leptin

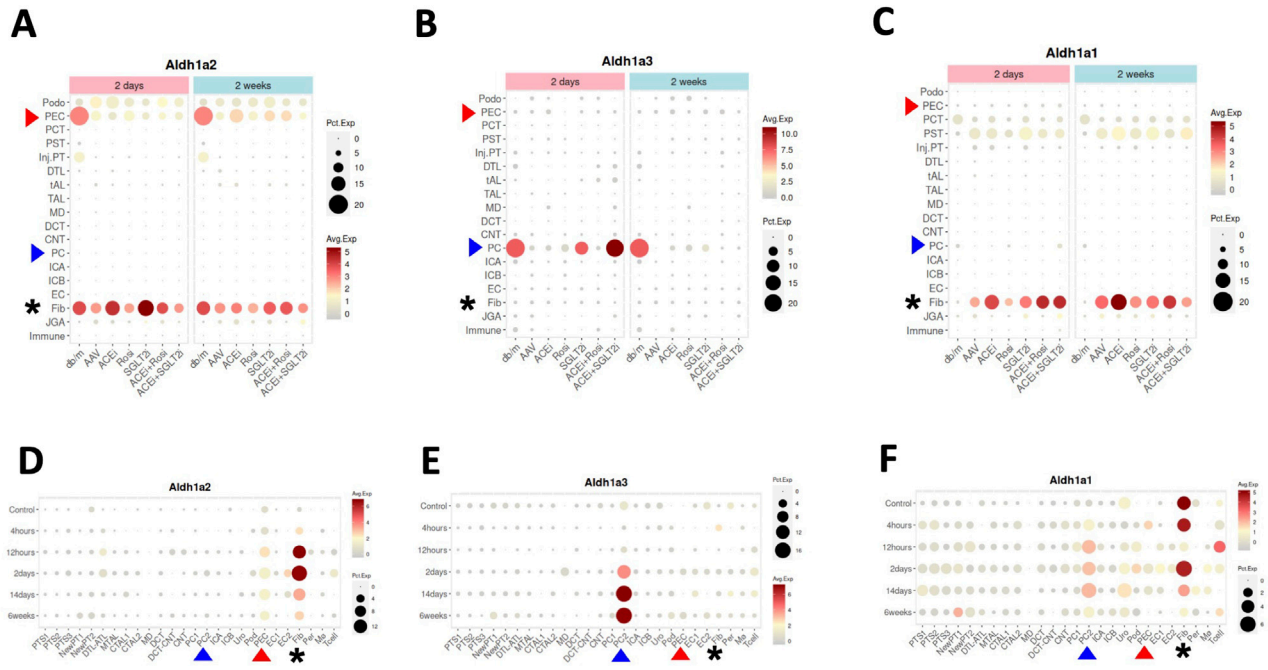

FIGURE 3
Aldh1a1, Aldh1a2 and *Aldh1a3* expression in kidney cells of female healthy and CKD mice, and of male healthy and AKI mice induced by ischemia-reperfusion. **(A–C)** show *Aldh1a2*, *Aldh1a3* and *Aldh1a1* mRNA expression in the CKD study and **(D–F)** show *Aldh1a2*, *Aldh1a3* and *Aldh1a1* mRNA expression in the AKI study. Dot sizes indicate the proportion of cells expressing a particular gene. Expression levels are color-coded. Red and blue arrowheads point to gene expression in PECs and PCs, respectively, while the expression levels of fibroblasts are marked by black asterisks. As shown in **(A–C)**, neither repression of *Aldh1a2* expression in PECs and *Aldh1a3* expression in medullary PCs (PC2), nor induction of *Aldh1a1* expression in fibroblasts in the AAV mice (a CKD model characterized by hypertension induced by unilateral nephrectomy and adeno-associated virus mediated renin transgene in *db/db* mice) versus in that of healthy controls (db/m) was effectively rescued by various treatment regimens, especially at the 2-week time point. ACEi: CKD treated with angiotensinogen converting enzyme (ACE) inhibitor; Rosi: CKD treated with PPARγ pharmacological agonist rosiglitazone; SGLT2i: CKD treated with sodium-glucose cotransporter-2 inhibitor; ACEi + Rosi: CKD treated with ACE inhibitor and the thiazolidinedione rosiglitazone; ACEi + SGLT2i: CKD treated with an ACE inhibitor and an SGLT2 inhibitor. As shown in **(D–F)**, in the setting of AKI, *Aldh1a2* expression in PECs and fibroblasts, *Aldh1a3* expression in PC2, and A*ldh1a1* expression in PC2 were all induced, while *Aldh1a1* expression in fibroblasts was repressed in a biphasic fashion. The Y-axis presents data from control mice and experimental group mice from 4 h to 6 weeks after ischemia-reperfusion injury. Data were downloaded with permission from Kidney Interactive Transcriptomics [10, 11].

receptor (*db/db*), hypertension induced by adeno-associated virus mediated renin transgene combined with unilateral nephrectomy [10]. In healthy control mice (db/m), selective high expression of *Aldh1a2*, and low level expression of *Aldh1a1* and *Aldh1a3*, were found in PECs (Figures 3A–C). *Aldh1a2* expression in PECs and *Aldh1a3* expression in the collecting duct principal cells (PCs) were markedly repressed in the CKD model (AAV mice). Neither was effectively rescued by a peroxisome proliferator-activated receptor (PPAR)-γ agonist, an angiotensinogen converting enzyme inhibitor, a sodium-glucose cotransporter-2 inhibitor, or combined therapies (Figures 3A, B) [10].

Because *Aldh1a2* and *Aldh1a3* are the major RA synthesizing enzymes in PECs and PCs, respectively, repressed expression could cause reduced RA activity in these cells. Exposure of cultured PCs to media containing aldosterone, angiotensin II or high glucose repressed retinoic acid receptor (RAR)-dependent RA signaling [19]. Thus, repression of *Aldh1a3* expression in PCs by these (and other) CKD mediators is a plausible mechanism for the repressed RA/RAR signaling pathway in PCs in this complex, but clinically relevant, CKD murine model.

As our previous work has shown that RA/RAR activities in PCs show opposite responses to acute versus chronic kidney injury stimuli [19], we asked whether *Aldh1a2* expression in PECs might also change differentially in AKI versus CKD. By further exploring the Kidney Interactive Transcriptomics database, we found that *Aldh1a2* in PECs, and *Aldh1a1* and *Aldh1a3* expression in medullary PCs (PC2) were induced in male mice subjected to ischemia-reperfusion AKI. Further, *Aldh1a1* expression in male fibroblasts was repressed at 12 h after ischemia-reperfusion, had recovered at 2 days, and was again repressed at 2–6 weeks (Figures 3D–F) [11]. These were in contrast with findings in female CKD mice, in which *Aldh1a2* expression in PECs and *Aldh1a3* expression in PCs were both repressed (Figures 3A, B). It deserves further exploration whether these differences are due to opposite effects of AKI and CKD, or due to other factors, e.g., sex.

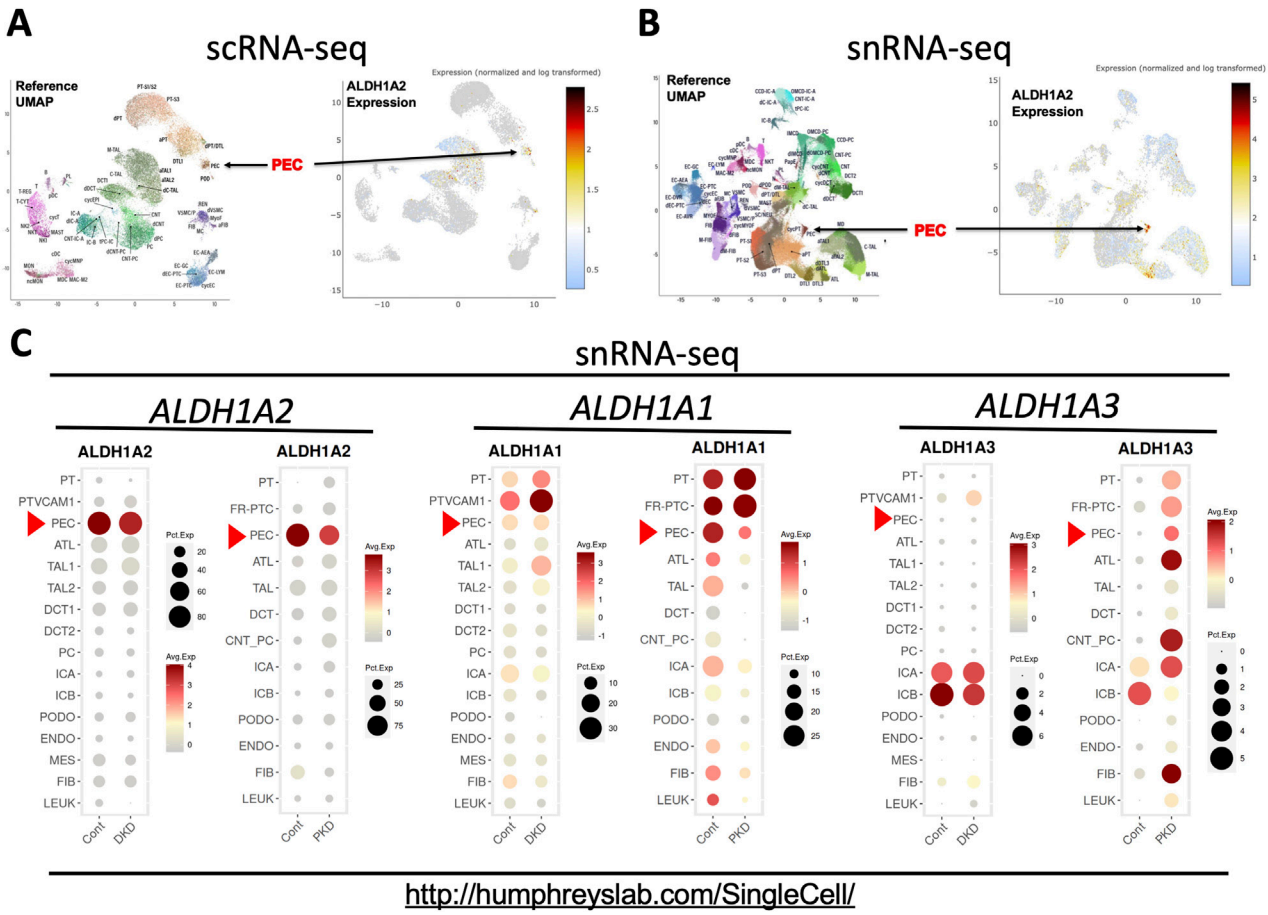

FIGURE 4
scRNA-seq and snRNA-seq analysis shows that selective high expression of *ALDH1A2* expression in PECs in healthy subjects is repressed in patients with CKD. **(A,B)** Shown are the reference uniform manifold approximation and projection (UMAP) data, the UMAP illustration of *ALDH1A2* expression of the scRNA-seq, and the snRNA-seq data, respectively. The names and positions of particular cell types are shown as distinct clusters in the reference UMAPs (left). The normalized and log transformed expression of *ALDH1A2* mRNA in these clusters are color-coded and shown in the right panels. Arrows point to the PEC clusters. The data are downloaded from the Human Kidney Tissue Atlas (https://atlas.kpmp.org/explorer/dataviz) of the Kidney Precision Medicine Project with permission [12]. Accessed on 6th February 2024. Funded by the National Institute of Diabetes and Digestive and Kidney Diseases (Grant numbers are listed in the table key to Supplementary Table S1). **(C)** shows snRNA-seq analysis of *ALDH1A1, ALDH1A2 and ALDH1A3* expression in healthy subjects and patients with diabetic kidney disease (DKD) and late-stage ADPKD (PKD). Dot sizes indicate the proportion of cells expressing a particular gene; relative gene expression levels are color-coded. The web link shows the source of the displayed information. Red arrowheads point to the mRNA expression in PECs. Data were downloaded with permission from Kidney Interactive Transcriptomics [13, 14].

Data from human studies

The Kidney Precision Medicine Project (KPMP), part of the Human BioMolecular Atlas Program [20], has recently published the online Human Kidney Tissue Atlas (Table 1), containing scRNA-seq and snRNA-seq analyses of kidney tissues from healthy subjects and patients with AKI and CKD [12]. Both scRNA-seq and snRNA-seq indicated that PECs had the highest expression of *ALDH1A2* mRNA among all kidney cell types (Figures 4A, B). In the scRNA-seq dataset, only PECs, thick ascending limb (TAL) cells and degenerated proximal tubule epithelial cells and descending thin limb (DTL) cells differentially expressed *ALDH1A2* mRNA, with PECs having the highest cellular expression percentage (35%) and the highest mean expression level (Supplementary Table S1). In the snRNA-seq dataset, *ALDH1A2* was differentially expressed in PECs and a few other cell types, with PECs having the highest percentage (88%) and mean expression level (Supplementary Table S2). In the scRNA-seq and snRNA-seq datasets, *ALDH1A2* was the No. 129 (Supplementary Table S3) and No. 1 (Supplementary Table S4) most differentially expressed gene in PECs, respectively.

Further supporting highly cell-specific and abundant expression of *ALDH1A2* mRNA in healthy human PECs, the Kidney Interactive Transcriptomics snRNA-seq datasets from

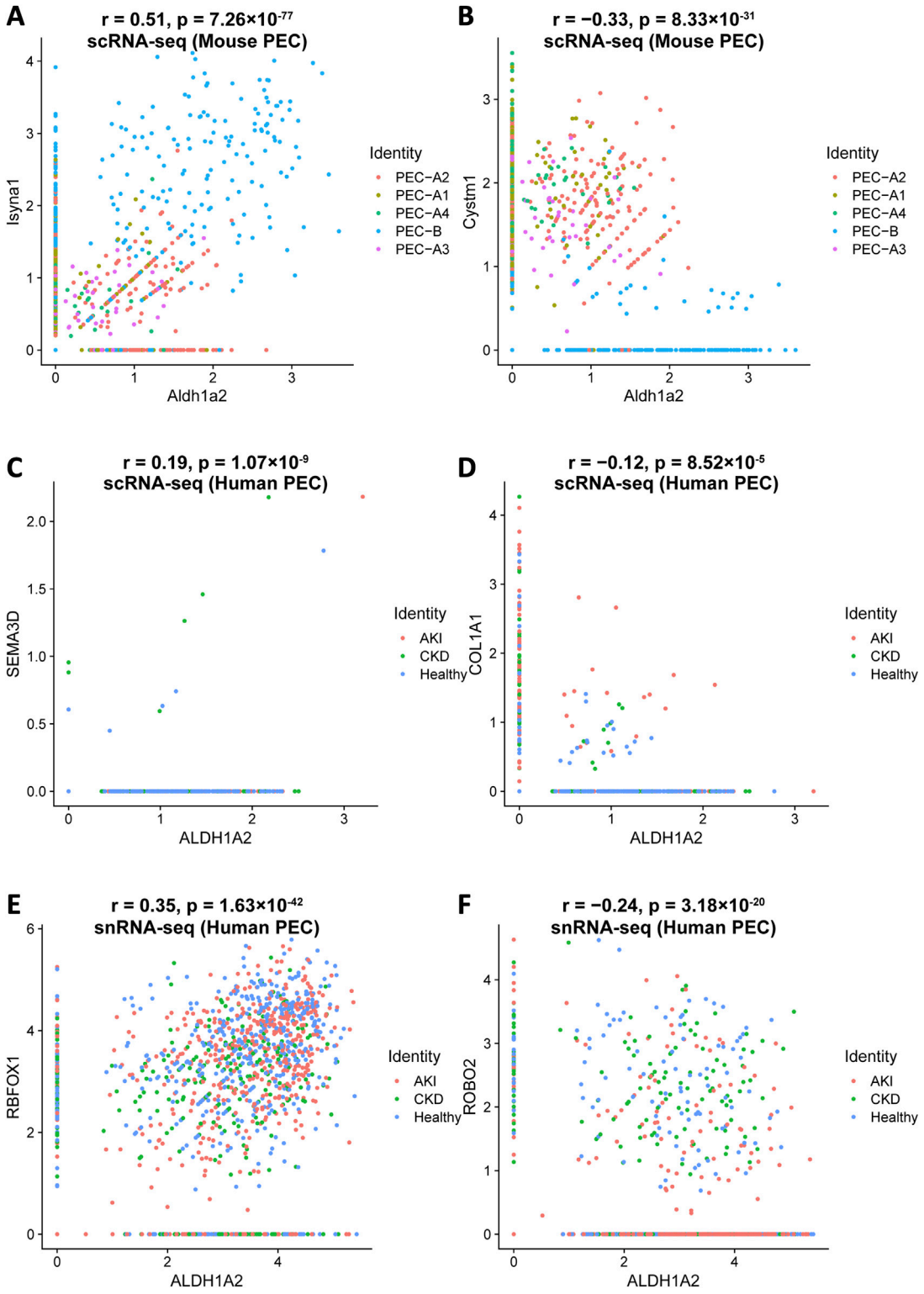

FIGURE 5
Top genes most significantly correlated with *Aldh1a2/ALDH1A2* expression in mouse and human PECs. Illustrations of top gene transcripts most significantly correlated with the *Aldh1a2* transcript in all mouse PEC subtypes in the Mouse PEC Landscape dataset (Supplementary Tables S10.1 and 10.2) and gene transcripts most significantly correlated with the *ALDH1A2* transcript in all human PECs in both scRNA-seq and snRNA-seq datasets of the KPMP Human Kidney Tissue Atlas (Supplementary Tables S11.1–11.4). **(A,B)** ScRNA-seq scatter plots showing the gene transcripts that are

(*Continued*)

FIGURE 5 (Continued)
the most positively **(A)** and negatively **(B)** correlated with the transcript abundance of *Aldh1a2* in mouse PECs, respectively. **(C,D)** ScRNA-seq scatter plots showing the gene transcripts that are the most positively **(C)** and negatively **(D)** correlated with the transcript abundance of *ALDH1A2* in human PECs, respectively. **(E,F)** SnRNA-seq scatter plots showing the gene transcripts that are the most positively **(E)** and negatively **(F)** correlated with the transcript abundance of *ALDH1A2* in human PECs, respectively.

the Humphrey Lab and the snRNA-seq dataset of the Susztak Lab (Table 1) both reported that over 80% PECs had positive expression of *ALDH1A2* mRNA (Figure 4C; Supplementary Table S5) [13–15]. The selective, high physiological *ALDH1A2* mRNA expression in human PECs contrasts with the low physiological *ALDH1A3* expression in all renal cells, including PECs, and the ubiquitous expression *of ALDH1A1* in most renal cells and modest expression in PECs (Figure 4C). Hence, both scRNA-seq and snRNA-seq studies support *ALDH1A2* as selectively expressed at the mRNA level in healthy human PECs.

Next, we queried the KPMP datasets for *ALDH1A2* expression in healthy subjects (Supplementary Tables S1, S2) and CKD patients (Supplementary Tables S6, S7). A moderate reduction in *ALDH1A2*-expressing percentages in PECs was found in CKD patients compared to healthy controls, both in scRNA-seq (27% vs. 35%) and snRNA-seq datasets (77% vs. 88%). In subjects with AKI, however, this trend was observed in the scRNA-seq (25%), but not the snRNA-seq dataset (89%) (Supplementary Tables S8, S9).

To further examine how *ALDH1A2* mRNA expression in PECs changes in CKD patients, we assessed the Kidney Interactive Transcriptomics snRNA-seq analysis of patients with mild to moderate diabetic nephropathy and end-stage autosomal dominant polycystic kidney disease (ADPKD), and the Susztak Lab snRNA-seq analysis of kidney tissues from patients with CKD associated with diabetes or hypertension (Table 1) [13–15]. A reduction in *ALDH1A2* mRNA expression in PECs was observed in all these CKD subject cohorts, compared with healthy controls (Figure 4C; Supplementary Table S5).

Integrated analysis of *Aldh1a2/ALDH1A2* and other genes in mouse and human PECs

Understanding how *Aldh1a2/ALDH1A2* expression correlates with that of other genes in PECs might direct further causal studies to identify up- and downstream genes of *Aldh1a2/ALDH1A2* and other genes that are co-regulated for physiological or pathophysiological reasons. To this end, we analyzed the Mouse PEC Landscape dataset and the KPMP Human Kidney Tissue Atlas dataset (Table 1) [9, 12], and identified gene transcripts that were positively or negatively correlated with *Aldh1a2* mRNA expression levels in scRNA-seq analyses of all mouse PECs and PEC-A1, A2, A3, A4 and PEC-B, separately (Supplementary Table S10) and those correlated with *ALDH1A2* mRNA expression in both scRNA-seq and snRNA-seq analyses of all human PECs, as well as PECs of healthy subjects and patients with AKI or CKD (Supplementary Tables S11). As shown in Figures 5A, B, *Isyna1* (r = 0.51) and *Cystm1* (r = −0.33) are the top genes positively and negatively correlated with *Aldh1a2* in mouse PECs, respectively. Notably, both genes are highly differentially expressed in mouse PEC-A and PEC-B subtypes. An analysis of the human PEC scRNA-seq dataset revealed *SEMA3D* and *COLA1A1* as the most correlated with *ALDH1A2*, but both have low correlation coefficients (r = 0.19 and −0.12, respectively, Figures 5C, D). In snRNA-seq analysis of human PECs, *RBFOX1* (r = 0.35) and *ROBO2* (r = −0.24) are the most significantly positively and negatively correlated with *ALDH1A2*, respectively (Figures 5E, F). Interestingly, both *ALDH1A2* and *RBFOX1* are among the top-3 most specifically expressed genes in human PECs (Supplementary Table S4), while *ROBO2* expression in the AKI dataset appears different from healthy control and CKD dataset, i.e., PECs with high *ALDH1A2* and repressed *ROBO2* expression are enriched in AKI (Figure 5F).

We further explored the Gene Ontology pathways enriched in *Aldh1a2*-correlated genes in the mouse scRNA-seq PEC dataset and *ALDH1A2*-correlated genes in scRNA-seq and snRNA-seq human PEC datasets. In mouse PECs, "protein localization to endoplasmic reticulum" and "cotranslational protein targeting to membrane" are the leading pathways enriched by genes positively correlated with *Aldh1a2* (Figure 6A), while enriched pathways among genes negatively correlated with *Aldh1a2* are "keratan sulfate catabolic process," response to growth factor" and "negative regulation of response to stimuli", etc (Figure 6B). As shown in Figures 6C, D, genes correlated with *ALDH1A2* in human PECs in the scRNA-seq dataset and those in the snRNA-seq dataset poorly overlap—only 5.1% and 2.4% of the genes positively and negatively correlated with *ALDH1A2* are shared in the two datasets, respectively. Hence, unsurprisingly, Gene Ontology pathways enriched among those genes correlated with *ALDH1A2* in human PECs annotated in the scRNA-seq and snRNA-seq datasets also vary. While "establishment or maintenance of cell polarity" and "maintenance of protein location in cell" are the top-2 pathways enriched by genes positively correlated with *ALDH1A2* in the scRNA-seq dataset, those most enriched in the snRNA-seq dataset are "urogenital system development" and "cell morphogenesis" (Figures 6E, G). The top-2 pathways

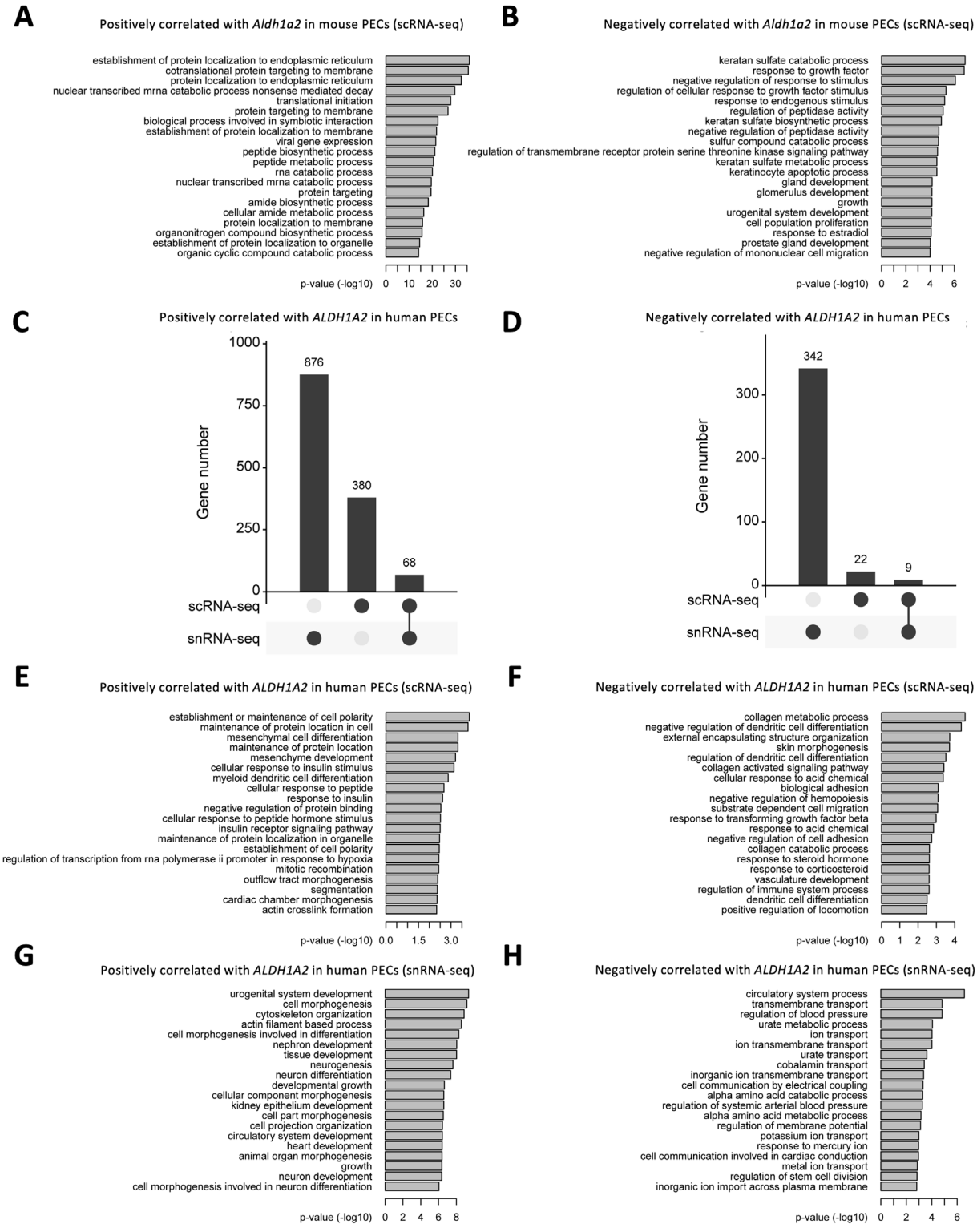

FIGURE 6
Bioinformatic analyses of genes correlated with *Aldh1a2/ALDH1A2* expression in mouse and human PECs. **(A,B)** Bar plots showing the -log10 (P-value) of enrichment analysis of representative Gene Ontology biological pathways among the gene list with positive **(A)** and negative **(B)** correlations with *Aldh1a2* in all mouse PECs of the Mouse PEC Landscape scRNA-seq dataset. **(C,D)** Upset plots showing the distribution of genes with positive **(C)** and negative **(D)** correlations with *ALDH1A2* in the scRNA-seq and snRNA-seq datasets of the KPMP Human Kidney Tissue Atlas. **(E,F)** Bar plots showing the -log10 (P-value) of enrichment analysis of representative Gene Ontology biological pathways among the

(*Continued*)

FIGURE 6 (Continued)
gene list with positive **(E)** and negative **(F)** correlations with *ALDH1A2* in human PECs in the scRNA-seq dataset of the KPMP Human Kidney Tissue Atlas. **(G,H)** Bar plots showing the -log10 (P-value) of enrichment analysis of representative Gene Ontology biological pathways among the gene list with positive **(G)** and negative **(H)** correlations with *ALDH1A2* in human PECs of the snRNA-seq dataset of the KPMP Human Kidney Tissue Atlas.

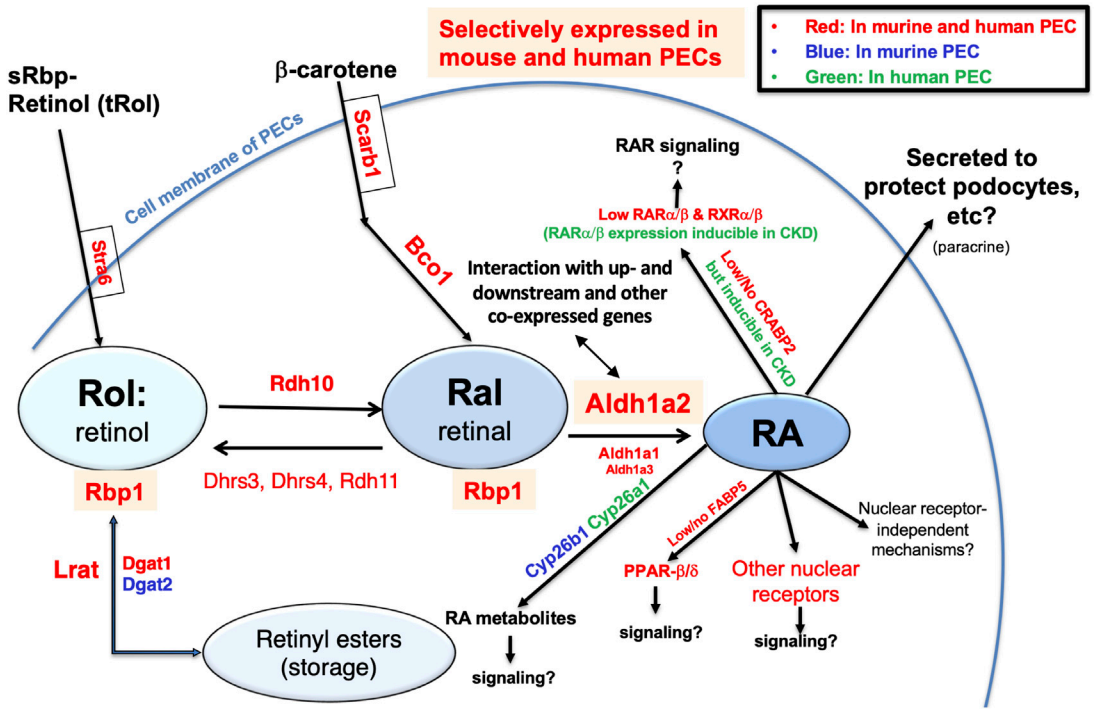

FIGURE 7
Retinol metabolon and RA signaling in human and mouse PECs as inferred by physiological (and pathophysiological) mRNA expression levels in scRNA-seq and snRNA-seq databases. Mouse PEC gene expression data extracted from Kidney Cell Explorer (Table 1) and human PEC gene expression data extracted from the Susztak Lab Kidney Biobank (Table 1) were used to predict the expression of proteins in the retinol metabolon and RA signaling pathways in mouse and human PECs. These included proteins involved in cellular uptake of retinol and β-carotene; enzymes catalyzing conversion among retinol, retinyl esters and retinaldehyde (retinal); RA synthesizing and catabolizing enzymes; intracellular carrier proteins of retinoids; and receptors and signaling molecules mediating the biological effects of RA. Components expressed in PECs of mice, humans, and both species, as predicted by scRNA-seq and snRNA-seq data, are encoded by blue, green and red fonts, respectively. Retinyl esters, retinol, retinal, RA, and proteins selectively expressed in both mouse and human PECs are highlighted by color shades.

enriched by genes negatively correlated with *ALDH1A2* in the scRNA-seq dataset are "collagen metabolic process" and "negative regulation of dendritic cell differentiation," while the top-2 pathways enriched by genes negatively correlated with *ALDH1A2* in the snRNA-seq dataset are "circulatory system process" and "transmembrane transport" (Figures 6F, H). It awaits further investigation to answer why scRNA-seq and snRNA-seq datasets give rise to largely different sets of *ALDH1A2*-correlated genes and their related Gene Ontology pathways and to understand the biological implications of these findings.

Finally, to generate an integrated understanding of the expression and role of the *Aldh1a2*/*ALDH1A2* genes in mouse and human PECs, against the backdrop of the combined retinol metabolon and RA signaling pathway, we used the Kidney Cell Explorer mouse kidney scRNA-seq data and the Susztak Lab human kidney snRNA-seq data (Table 1) to predict the retinol metabolon and RA signaling in PECs of both species. In brief, as summarized in Figure 7, both mouse and human PECs are predicted to express receptors mediating cellular retinol and β-carotene uptake, carrier proteins mediating intracellular retinol and retinaldehyde transport, enzymes catalyzing interconversion between retinol, retinyl esters and retinaldehyde, as well as enzymes involved in RA synthesis and catabolism. These predictions, if confirmed experimentally, suggest that *Aldh1a2*/*ALDH1A2* may exert

their functions in PECs through RA-mediated signaling pathways. In PECs of both species, the findings of low or no expression of *Crabp2/CRABP2* and *Fabp5/FABP5*, low expression of *Ppard/PPARD* and RAR and RXR isotypes, and high expression of other nuclear receptors that heterodimerize with RXRs neither support nor exclude the possibility of RA-RAR or RA-*PPARβ/δ* signaling in PECs. Other nuclear receptor-dependent and independent signaling induced by RA or RA metabolites could also have a role to play. Additionally, RA release could act on other cells, including podocytes, through a paracrine mechanism. In CKD patients, *CRABP2*, *RARA* and *RARB* expression in PECs were induced [15], suggesting that physiological and pathological RA signaling pathways might differ.

Discussion

Recent scRNA-seq studies have shown that *Aldh1a2* mRNA expression in PECs changes differentially in different mouse glomerular disease models, ranging from a substantial increase in anti-GBM glomerulonephritis (Figures 2C, F), marked repression in CKD (Figure 3A), and moderate induction in mice undergoing ischemia-reperfusion-induced AKI (Figure 3D), to a moderate repression in mouse models of FSGS manifesting nephrotic syndrome (Supplementary Figure S1). ScRNA-seq and snRNA-seq clinical studies also show diminished *ALDH1A2* mRNA expression in PECs in patients with CKD, including those with diabetes, hypertension and ADPKD. So far, scRNA-seq or snRNA-seq studies directly comparing kidney tissues from patients with anti-GBM glomerulonephritis, MCD and FSGS have not yet been reported. Given the aforementioned findings, further clinical studies on the genetics, epigenetics and gene expression of *ALDH1A2* and genes encoding other components of the retinol metabolon and RA signaling in healthy subjects and patients with kidney disease are warranted.

Consistent with scRNA-seq and snRNA-seq-based findings, human PECs have been reported to manifest ALDH1A activity that is repressed by an ALDH1A inhibitor [21] and ALDH1A2 shows positive staining in PECs in normal human kidneys, as documented by the Human Protein Atlas (Table 1). PECs have been reported to stain positive with an *Aldh1a1/2* antibody in both healthy and FSGS mice, also supporting the observation that Aldh1a2 protein is expressed in mouse PECs [21]. Using *RARE-LacZ* mice as a reporter of RA-RAR-dependent transcriptional activity, PECs do not show any physiological RA-RAR activity. However, this activity can be triggered upon podocyte injury 4 days after doxorubicin-induced podocyte injury and this activity is subsequently switched off as proteinuria becomes heavier, due to albumin sequestration of RA and hence preventing RA from activating RAR [21].

In young mice and in cultured PECs, activation of RA/RAR signaling induces PEC differentiation into podocytes, while inhibition of this signaling impairs the regeneration of podocytes. In contrast, RA rescues podocyte regeneration repressed by heavy albuminuria and ameliorates FSGS [21]. In view that RA signaling through RARs triggers PEC differentiation into podocytes, it makes sense that RA signaling via RAR is physiologically inhibited to preserve the PEC phenotype. In FSGS mice, most PECs showing RA/RAR activity are outside FSGS lesions while most of those within FSGS lesions do not respond to RA and do not differentiate into podocytes, suggesting that in addition to albuminuria, other local molecular and cellular factors in the FSGS niche may also affect RA/RAR signaling in the PECs [21].

Mechanisms remain elusive for how RAR signaling in PECs is physiologically repressed, how this signaling is activated upon podocyte injury, and whether these pathophysiological processes observed in FSGS mouse models are also at play in humans. These are important questions to answer and the related mechanistic insights could be harnessed for the treatment of FSGS.

The substantial induction of *Aldh1a2* mRNA expression in PECs of anti-GBM glomerulonephritis mice (Figures 2C, F) and the substantial repression of *Aldh1a2* mRNA expression in PECs in a murine model of CKD (Figure 3A) are important findings. Given the well-established hormetic effects of RA [7], these changes in *Aldh1a2* expression and subsequent RA activity could have profound effects on PECs and their crosstalk with other cells. To determine the role of *Aldh1a2* in PECs, conditional, PEC-selective *Aldh1a2* knockout, RNA silencing and/or strategies for rescuing repressed Aldh1a2 activity in PECs, *e.g.,* PEC-selective *Aldh1a2* transgenic mice, could be useful tools. *Aldh1a* antisense oligonucleotides and other types of Aldh1a inhibitors, RA inactivation inhibitors, as well as RAR and RXR agonists and antagonists could also be useful tools in experimental studies.

Dysregulation of retinol metabolism and RA signaling in type-1 and type-2 diabetes and diabetic nephropathy and the efficacy of RA in treating experimental models of diabetic nephropathy are all well documented [22–27]. In particular, proteomic analysis of renal cortices of wild-type control and *db/db* mice has identified RA as a key dysregulated signaling hub in type-2 diabetes, characterized by dysregulated RA-synthesizing enzymes and reduced RA biosynthesis [23]. In *db/db* mice and *ob/ob* mice (loss-of-function mutation of the leptin gene), O-GlcNAcylation, a posttranslational modification that adds O-linked β-N-acetylglucosamine to serine or threonine residues of many proteins including Stra6/STRA6 and Aldh1a1/ALDH1A1, is significantly increased in diabetic kidney tissues [24]. This leads to suppressed retinol metabolism and downstream signaling [24]. RNA-seq analysis of kidney biopsy samples from patients with early

and advanced diabetic nephropathy and of normal kidney tissues identified biphasic changes in expression of genes involved in the RA pathway, characterized by an upregulation in the early stage, but downregulation in the late stage, of diabetic nephropathy [25]. These results, together with the scRNA-seq and snRNA-seq data from diabetic nephropathy murine models and patients (Figures 3A–C, 4C) suggest the need for better understanding of the dynamics of retinol metabolon and RA signaling in different stages of diabetes and diabetic nephropathy, and the importance of further investigations at translational, posttranslational and bioactivity levels.

Few studies referenced in this report have directly examined the effects of sex on the expression and activity of the retinol metabolon and RA signaling in the kidney. The only exception is the Mouse Kidney Cell Explorer database, in which sex-specific differences in gene expression in kidney proximal tubules have been well documented, including the female selective expression of *Stra6* in segment 1 proximal tubule cells (Figure 2B) [8]. Another hint of possible sex differences in *Aldh1a2* mRNA expression is observed in two mouse studies from the same laboratory, one using males only, while the other using females only (Figures 3A, D). However, without direct comparison in well-designed studies one cannot be sure that the different *Aldh1a2* mRNA expressing percentages in these reports are sex-dependent. Future studies should directly compare both sexes.

Mechanistically, many important questions await answers. Although likely, whether effects of Aldh1a2/ALDH1A2 in PECs are mediated by RA synthesis remains unknown. If so, which RA subtypes and signaling pathways are operative in PECs in health and disease? Given that *Aldh1a2* is differentially expressed in PEC subtypes, which may interconvert, it is important to identify the role of *Aldh1a2* in the interconversion among PEC subtypes. For example, as platelet-derived growth factor receptor (PDGFR) signaling plays a role in FSGS [28], and *Pdgfra and Pdgfrb* expression are both strongly expressed in PEC-B but not in PEC-A isotypes [9], it will be intriguing to learn whether changes in *Aldh1a2* expression and RA signaling play any role in the increased PEC-B cell numbers in anti-GBM glomerulonephritis, FSGS, and other kidney diseases [9, 28] and whether and how Aldh1a2, RA and PDGFR signaling pathways crosstalk in PECs. As some PECs are progenitor cells [21, 29], it will be important to determine the roles of *Aldh1a2* expression and RA signaling in the stemness of these progenitor subpopulations and in their trans-differentiation into podocytes and proximal tubular cells [21, 29]. Finally, repression of *Aldh1a2*/ALDH1A2 in PECs in both a murine CKD model (Figure 3A) and in patients with CKD (Figure 4C) is in stark contrast with enhanced *Aldh1a2* expression in PECs and fibroblasts in mice with AKI induced by ischemia-reperfusion, peaking at 12 h and 2 days, and remaining elevated 6 weeks after ischemia-reperfusion, when kidney functions have returned to normal [11]. The authors did not observe these mice beyond 6 weeks. Future research will need to examine AKI models of different etiologies and severity and follow up longer to examine whether different types and severity of AKI have different *Aldh1a2* responses and whether AKI-to-CKD transition is accompanied with repressed *Aldh1a2* expression, and if so, whether such changes in *Aldh1a2* expression play a causal role in AKI-to-CKD transition.

In conclusion, snRNA-seq and scRNA-seq studies have identified PECs as the major site of expression of the *Aldh1a2/ALDH1A2* gene. Current evidence has led us to hypothesize that RA biosynthesis catalyzed by Aldh1a2/ALDH1A2 in PECs may play an important role in kidney health and disease in an autocrine and/or paracrine fashion. We have previously reported that RA/RAR activity is physiologically confined to the collecting duct in mouse kidneys [19, 30] and that in cultured collecting duct cells, several genes implicated in the defense against kidney injury are targets of the endogenous RA/RAR activity [31], and that the RA/RAR activity in collecting duct cells is regulated differentially by AKI and CKD mediators [19]. We have further hypothesized a major defense role for the RA/RAR signaling in the collecting duct, especially PCs, in renal tubulointerstitial injury [32].

Taken together, research addressing the roles of Aldh1a2/ALDH1A2 in PECs and of RA/RAR activity in collecting duct cells promises to shed new light on the mechanisms of glomerular and tubulointerstitial defense, how this defense is overcome in disease, and how properly restoring dysregulated defense could be developed into novel therapies. In particular, harnessing insights from these two lines of research, retinoid and non-retinoid therapies regulating RAR-dependent and RAR-independent RA signaling pathways could be developed to maximize the beneficial effects while minimizing unwanted effects of retinoids [33, 34].

Author contributions

QX and JBK conceptualized and led the drafting and revision of the manuscript. A-LX provided the Mouse PEC Landscape database, especially the key data listed in Figures 2C–F, 5, 6; Supplementary Figure S1; Supplementary Tables S10, S11. QX and W-BL led the data mining, data collection and drafted the figures, tables and texts. JBK, A-LX, W-BL, and DF critically revised the draft and contributed comments to improve the manuscript. All authors contributed to the article and approved the submitted version.

Funding

The author(s) declare financial support was received for the research, authorship, and/or publication of this article. The study

was supported by grants from the PKD Charity UK (Grant number: ARPKD-19-02) and Kidney Research UK (Grant number RP38/2014) and NIH/NIDDK Intramural Research Program (Z01 DK-043308). The funding sources had no role in the design, data collection, analysis, manuscript preparation, interpretation, and the decision to submit this manuscript for publication.

Acknowledgments

We thank the authors of all the databases we mined in this study. Without their open sharing of data, this work would not have been possible. In particular, we gratefully acknowledge the contribution of Dr Andrew McMahon (University of Southern California), Dr. Katalin Susztak (University of Pennsylvania), and Dr. Benjamin Humphreys (Washington University) in making their kidney biobank transcriptional data available to the field and thank Dr Jonathan Levinsohn (University of Pennsylvania) for helpful discussions on the data from the Susztak Laboratory.

Conflict of interest

The authors declare that the research was conducted in the absence of any commercial or financial relationships that could be construed as a potential conflict of interest.

Supplementary material

The Supplementary Material for this article can be found online at: https://www.ebm-journal.org/articles/10.3389/ebm.2024.10167/full#supplementary-material

References

1. Rosselot C, Spraggon L, Chia I, Batourina E, Riccio P, Lu B, et al. Non-cell-autonomous retinoid signaling is crucial for renal development. *Development* (2010) **137**(2):283–92. doi:10.1242/dev.040287

2. Kumar S, Sandell LL, Trainor PA, Koentgen F, Duester G. Alcohol and aldehyde dehydrogenases: retinoid metabolic effects in mouse knockout models. *Biochim Biophys Acta (Bba) - Mol Cell Biol Lipids* (2012) **1821**(1):198–205. doi:10.1016/j.bbalip.2011.04.004

3. El Kares R, Manolescu DC, Lakhal-Chaieb L, Montpetit A, Zhang Z, Bhat PV, et al. A human ALDH1A2 gene variant is associated with increased newborn kidney size and serum retinoic acid. *Kidney Int* (2010) **78**(1):96–102. doi:10.1038/ki.2010.101

4. Beecroft SJ, Ayala M, McGillivray G, Nanda V, Agolini E, Novelli A, et al. Biallelic hypomorphic variants in ALDH1A2 cause a novel lethal human multiple congenital anomaly syndrome encompassing diaphragmatic, pulmonary, and cardiovascular defects. *Hum Mutat* (2021) **42**(5):506–19. doi:10.1002/humu.24179

5. Leon E, Nde C, Ray RS, Preciado D, Zohn IE. ALDH1A2 disorder: a new genetic syndrome due to alteration of the retinoic acid pathway. *Am J Med Genet A* (2023) **191**(1):90–9. doi:10.1002/ajmg.a.62991

6. Zhu L, Kamalathevan P, Koneva LA, Zarebska JM, Chanalaris A, Ismail H, et al. Variants in ALDH1A2 reveal an anti-inflammatory role for retinoic acid and a new class of disease-modifying drugs in osteoarthritis. *Sci Transl Med* (2022) **14**(676):eabm4054. doi:10.1126/scitranslmed.abm4054

7. Napoli JL. Post-natal all-trans-retinoic acid biosynthesis. *Methods Enzymol* (2020) **637**:27–54. doi:10.1016/bs.mie.2020.02.003

8. Ransick A, Lindström NO, Liu J, Zhu Q, Guo JJ, Alvarado GF, et al. Single-cell profiling reveals sex, lineage, and regional diversity in the mouse kidney. *Developmental Cell* (2019) **51**(3):399–413.e7. doi:10.1016/j.devcel.2019.10.005

9. Liu WB, Huang GR, Liu BL, Hu HK, Geng J, Rui HL, et al. Single cell landscape of parietal epithelial cells in healthy and diseased states. *Kidney Int* (2023) **104**(1):108–23. doi:10.1016/j.kint.2023.03.036

10. Wu H, Gonzalez Villalobos R, Yao X, Reilly D, Chen T, Rankin M, et al. Mapping the single-cell transcriptomic response of murine diabetic kidney disease to therapies. *Cell Metab* (2022) **34**(7):1064–78.e6. doi:10.1016/j.cmet.2022.05.010

11. Kirita Y, Wu H, Uchimura K, Wilson PC, Humphreys BD. Cell profiling of mouse acute kidney injury reveals conserved cellular responses to injury. *Proc Natl Acad Sci U S A* (2020) **117**(27):15874–83. doi:10.1073/pnas.2005477117

12. Lake BB, Menon R, Winfree S, Hu Q, Melo Ferreira R, Kalhor K, et al. An atlas of healthy and injured cell states and niches in the human kidney. *Nature* (2023) **619**(7970):585–94. doi:10.1038/s41586-023-05769-3

13. Wilson PC, Muto Y, Wu H, Karihaloo A, Waikar SS, Humphreys BD. Multimodal single cell sequencing implicates chromatin accessibility and genetic background in diabetic kidney disease progression. *Nat Commun* (2022) **13**(1):5253. doi:10.1038/s41467-022-32972-z

14. Muto Y, Dixon EE, Yoshimura Y, Wu H, Omachi K, Ledru N, et al. Defining cellular complexity in human autosomal dominant polycystic kidney disease by multimodal single cell analysis. *Nat Commun* (2022) **13**(1):6497. doi:10.1038/s41467-022-34255-z

15. Abedini A, Ma Z, Frederick J, Dhillon P, Balzer MS, Shrestha R, et al. Spatially resolved human kidney multi-omics single cell atlas highlights the key role of the fibrotic microenvironment in kidney disease progression. BioRxiv (2022). doi:10.1101/2022.10.24.513598

16. Uhlén M, Fagerberg L, Hallström BM, Lindskog C, Oksvold P, Mardinoglu A, et al. Proteomics. Tissue-based map of the human proteome. *Science* (2015) **347**(6220):1260419. doi:10.1126/science.1260419

17. Anguiano L, Kain R, Anders HJ. The glomerular crescent: triggers, evolution, resolution, and implications for therapy. *Curr Opin Nephrol Hypertens* (2020) **29**(3):302–9. doi:10.1097/mnh.0000000000000596

18. Bronstein R, Pace J, Gowthaman Y, Salant DJ, Mallipattu SK. Podocyte-parietal epithelial cell interdependence in glomerular development and disease. *J Am Soc Nephrol* (2023) **34**(5):737–50. doi:10.1681/asn.0000000000000104

19. Papadimitriou A, Romagnani P, Angelotti ML, Noor M, Corcoran J, Raby K, et al. Collecting duct cells show differential retinoic acid responses to acute versus chronic kidney injury stimuli. *Sci Rep* (2020) **10**(1):16683. doi:10.1038/s41598-020-73099-9

20. Jain S, Pei L, Spraggins JM, Angelo M, Carson JP, Gehlenborg N, et al. Advances and prospects for the human BioMolecular atlas Program (HuBMAP). *Nat Cell Biol* (2023) **25**(8):1089–100. doi:10.1038/s41556-023-01194-w

21. Peired A, Angelotti ML, Ronconi E, la Marca G, Mazzinghi B, Sisti A, et al. Proteinuria impairs podocyte regeneration by sequestering retinoic acid. *J Am Soc Nephrol* (2013) **24**(11):1756–68. doi:10.1681/asn.2012090950

22. Zhang Y, Wang T, Hu X, Chen G. Vitamin A and diabetes. *J Med Food* (2021) **24**(8):775–85. doi:10.1089/jmf.2020.0147

23. Starkey JM, Zhao Y, Sadygov RG, Haidacher SJ, Lejeune WS, Dey N, et al. Altered retinoic acid metabolism in diabetic mouse kidney identified by 18O isotopic labeling and 2D mass spectrometry. *PLoS One* (2010) **5**(6):e11095. doi:10.1371/journal.pone.0011095

24. Chen CH, Lin KD, Ke LY, Liang CJ, Kuo WC, Lee MY, et al. O-GlcNAcylation disrupts STRA6-retinol signals in kidneys of diabetes.

Biochim Biophys Acta (Bba) - Gen Subjects (2019) **1863**(6):1059–69. doi:10.1016/j.bbagen.2019.03.014

25. Fan Y, Yi Z, D'Agati VD, Sun Z, Zhong F, Zhang W, et al. Comparison of kidney transcriptomic profiles of early and advanced diabetic nephropathy reveals potential new mechanisms for disease progression. *Diabetes* (2019) **68**(12):2301–14. doi:10.2337/db19-0204

26. Han SY, So GA, Jee YH, Han KH, Kang YS, Kim HK, et al. Effect of retinoic acid in experimental diabetic nephropathy. *Immunol Cell Biol* (2004) **82**(6):568–76. doi:10.1111/j.1440-1711.2004.01287.x

27. Kim CS, Park JS, Ahn CW, Kim KR. All-trans retinoic acid has a potential therapeutic role for diabetic nephropathy. *Yonsei Med J* (2015) **56**(6):1597–603. doi:10.3349/ymj.2015.56.6.1597

28. Jia T, Xu T, Smeets B, Buhl EM, Moeller MJ, Floege J, et al. The role of platelet-derived growth factor in focal segmental glomerulosclerosis. *J Am Soc Nephrol* (2023) **34**(2):241–57. doi:10.1681/asn.2022040491

29. Hong X, Nie H, Deng J, Liang S, Chen L, Li J, et al. $WT1^+$ glomerular parietal epithelial progenitors promote renal proximal tubule regeneration after severe acute kidney injury. *Theranostics* (2023) **13**(4):1311–24. doi:10.7150/thno.79326

30. Wong YF, Kopp JB, Roberts C, Scambler PJ, Abe Y, Rankin AC, et al. Endogenous retinoic acid activity in principal cells and intercalated cells of mouse collecting duct system. *PLoS One* (2011) **6**(2):e16770. doi:10.1371/journal.pone.0016770

31. Wong YF, Wilson PD, Unwin RJ, Norman JT, Arno M, Hendry BM, et al. Retinoic acid receptor-dependent, cell-autonomous, endogenous retinoic acid signaling and its target genes in mouse collecting duct cells. *PLoS One* (2012) **7**(9):e45725. doi:10.1371/journal.pone.0045725

32. Xu Q. The renal collecting duct rises to the defence. *Nephron* (2019) **143**(2):148–52. doi:10.1159/000502452

33. Xu Q, Lucio-Cazana J, Kitamura M, Ruan X, Fine LG, Norman JT. Retinoids in nephrology: promises and pitfalls. *Kidney Int* (2004) **66**(6):2119–31. doi:10.1111/j.1523-1755.2004.66002.x

34. Wei Q, Dong Z. The yin and yang of retinoic acid signaling in kidney diseases. *J Clin Invest* (2020) **130**(10):5124–6. doi:10.1172/jci141712

EBM Experimental Biology and Medicine

TYPE Review
PUBLISHED 24 July 2025
DOI 10.3389/ebm.2025.10647

OPEN ACCESS

*CORRESPONDENCE
Samille Henriques Pereira,
samillehenriques@gmail.com
Flávio Guimarães da Fonseca,
fdafonseca@icb.ufmg.br

RECEIVED 28 April 2025
ACCEPTED 08 July 2025
PUBLISHED 24 July 2025

CITATION
Godinho IP, Dória ÍF, Rocha VdM, Miranda BA, Salomão LFC, Stancioli B, Paim AAO, Coelho dos Reis JGA, Pereira SH and da Fonseca FG (2025) Insights into the expansion of Oropouche virus in Brazil: epidemiological and environmental aspects. *Exp. Biol. Med.* 250:10647. doi: 10.3389/ebm.2025.10647

Insights into the expansion of Oropouche virus in Brazil: epidemiological and environmental aspects

Igor Pereira Godinho[1], Ítalo Faria Dória[1], Victor de Melo Rocha[1], Bárbara Alves Miranda[1], Lucas Fernandes Chamhum Salomão[1], Brunello Stancioli[2], Adriana Alves Oliveira Paim[1], Jordana G. Alves Coelho dos Reis[1], Samille Henriques Pereira[1]* and Flávio Guimarães da Fonseca[1]*

[1]Laboratório de Virologia Básica e Aplicada, Departamento de Microbiologia, Universidade Federal de Minas Gerais, Belo Horizonte, Brazil, [2]Faculdade de Direito, Universidade Federal de Minas Gerais, Belo Horizonte, Brazil

Abstract

The Oropouche virus (OROV), an arbovirus transmitted primarily by the *Culicoides paraensis* midge, has caused significant outbreaks in the Americas, especially in the Amazon region. The virus's spread is closely linked to a combination of environmental, climatic, and ecological factors. These include deforestation, urbanization, and changes in rainfall patterns, which influence the proliferation of vectors, and, consequently, increase the chances of mutations and reassortment events to occur. In 2024 and 2025, the number of OROV cases increased significantly, with outbreaks extending beyond the traditionally endemic Amazon region, highlighting the growing geographic expansion of the disease throughout Brazil. Despite its growing dispersion, diagnostic and therapeutic tools for OROV remain limited. Current diagnostic strategies rely almost exclusively on molecular detection methods, and there are no vaccines for effective prevention. Additionally, immunological responses to OROV infection are not fully understood, and further studies are needed. The ecological dynamics influencing OROV transmission, particularly the role of environmental changes in shaping vector populations, highlight the need for more integrated surveillance and control strategies. The ongoing expansion of OROV outside its traditional hotspots may be indicative of broader environmental shifts that facilitate viral spread. Therefore, continuous monitoring of both environmental and epidemiological data is crucial to understanding and mitigating the impact of OROV in the future. Collaborative efforts among researchers, policymakers, and local communities will be essential to prevent further outbreaks and minimize the health burden

caused by OROV. This review summarizes important and up-to-date data information to the ongoing epidemic of Oropouche fever, focusing on topics that are particularly important to Public Health.

KEYWORDS

Orthobunyavirus oropoucheense, Oropouche fever, *Culicoides paraensis*, epidemiology, climate change, environmental impacts

Impact statement

Climate change, environmental alterations due to anthropogenic activity, and human mobility have significantly altered the occurrence and dispersion of infectious diseases. This is particularly relevant when the disease is transmitted by arthropod vectors and/or has sylvatic hosts. Oropouche fever, caused by the Oropouche virus (OROV - Orthobunyavirus oropoucheense) is an iconic example of this new pattern of disease transmission. Since the virus description, in the 1950s, the OROV has remained restricted to equatorial forests, especially in the Amazon basin, where its main mosquito vector (Culicoides paraensis) is found. However, in the last 3 years, OROV cases have increased, and the virus is now dispersed to Brazil's states outside the Amazon region, posing a significant threat to public health resources. This review focuses on epidemiological characteristics of oropouche fever in Brazil and possible environmental aspects underlying the unprecedented OROV dispersion within the country.

Introduction

The Oropouche virus (OROV - *Orthobunyavirus oropoucheense*) is an arthropod-borne virus (arbovirus) belonging to the *Peribunyaviridae* family, *Orthobunyavirus* genus, and classified within the Simbu serogroup. Viruses in this group are known for their broad host range, vector-mediated transmission, and potential for reassortment events that contribute to genetic diversity. In 2024, OROV gained prominence due to a significant increase in reported cases across the Americas [1, 2].

The OROV was first isolated in 1955 from blood samples of a forestry worker in the Vega de Oropouche community, Trinidad and Tobago, a country in the Caribbean region of Central America [3]. This early identification marked the beginning of research on the virus, which was initially linked to a zoonotic transmission cycle involving both wild mammals and arthropod vectors. In 1960, the virus was detected in Brazil for the first time, isolated from a sloth (*Bradypus tridactylus*) near the construction site of the Belém-Brasília highway, state of Pará. In the same area, *Ochlerotatus serratus* mosquitoes were found to be infected with OROV [4]. Between 1960 and 1980, OROV was responsible for several epidemics in the state of Pará, with approximately 11,000 people infected. These epidemics affected different mesoregions - including metropolitan Belém - except for the southwestern part of the state. It was only from the 1980s onwards that cases of OROV infection began to be reported in the cities of Manaus and Barcelos, in the state of Amazonas. In the past decade, an outbreak of OROV occurred in the capital of Amazonas [5], as well as in the city of Mazagão, Amapá [6, 7]. In the following years, new OROV epidemics occurred, including in 1988, when outbreaks were reported in Tocantinópolis, state of Tocantins, and Porto Franco, state of Maranhão [8]. In the state of Rondônia, OROV was reported in 1991 in the cities of Ariquemes and Ouro Preto D'Oeste [9]. Since then, OROV has been recorded in several urban centers across the northern and northeastern regions of Brazil [8, 10].

OROV is an enveloped, spherical, and pleomorphic virus with a genome composed of three linear segments of single-stranded, negative-sense RNA [2]. Each RNA segment contains complementary nucleotide sequences that promote the circularization of the viral genome, with a helical nucleocapsid protein that comprises a ribonucleoprotein complex [11]. The tri-segmented genome structure facilitates genetic reassortment, a key mechanism driving viral diversity within this virus group [12–14].

OROV is primarily transmitted by biting midges of the species *C. paraensis* [10, 15] (Figure 1A) with reported transmission rates ranging from 25% to 83% [16]. The virus is maintained in nature through two distinct transmission cycles: sylvatic and urban (Figure 1B). In the sylvatic cycle, the virus circulates among wild vertebrate hosts that serve as amplifiers, including non-human primates such *as Callithrix penicillata* [17], *Sapajus apella* [18], and *Alouatta caraya* [19], as well as sloths (*Bradypus tridactylus*) [4] and rodents (*Proechimys spp.*). Antibodies have also been detected in wild birds [20]. Additionally, some studies have identified neutralizing antibodies in domestic animals, including *Canis lupus familiaris* (dogs) and *Bos indicus/taurus* (cattle), in the state of Mato Grosso, Brazil [21]. The duration of viremia in these hosts is critical for the transmission dynamics, as it influences the likelihood of the virus being taken up by biting arthropods during their blood meals. In the urban cycle, *C. paraensis* serves as the primary vector. Humans, acting as accidental hosts, are key in amplifying the virus within urban environments, especially in densely populated regions. The interaction between urban and sylvatic environments creates an ecological bridge, allowing for the virus exchange between the two cycles, thereby contributing to the pathogen's spread in areas with both natural and anthropogenic factors. The distribution of *C. paraensis* is

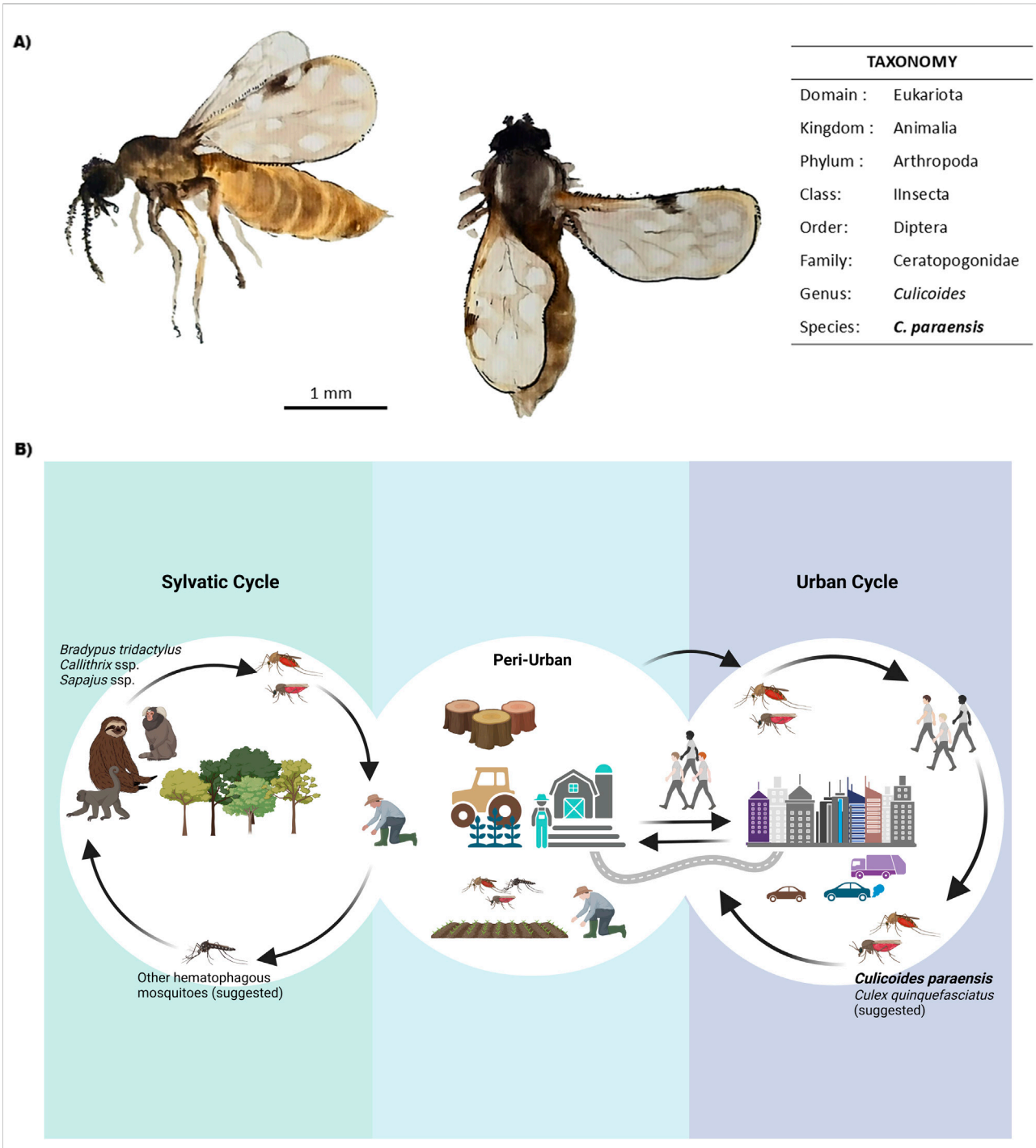

FIGURE 1
OROV transmission dynamics and main vectors. **(A)** *Culicoides paraensis* general aspect and taxonomic classification. Scale bar = 1 mm. Watercolor Illustration by F. da Fonseca. **(B)** Schematic representation of OROV transmission cycles. The sylvatic cycle involves primates, sloths, and other mammals as hosts, as well as some bird species (not shown). All possible arthropod vectors are not yet well known. The interaction between sylvatic and peri-urban environments primarily occurs due to deforestation and agricultural activities, which favor the transmission of diseases to humans. In the urban cycle, the virus is maintained by vectors such as *Culicoides paraensis* and possibly *Culex quinquefasciatus*, allowing dissemination in densely populated areas. *Original figure created with Biorender*.

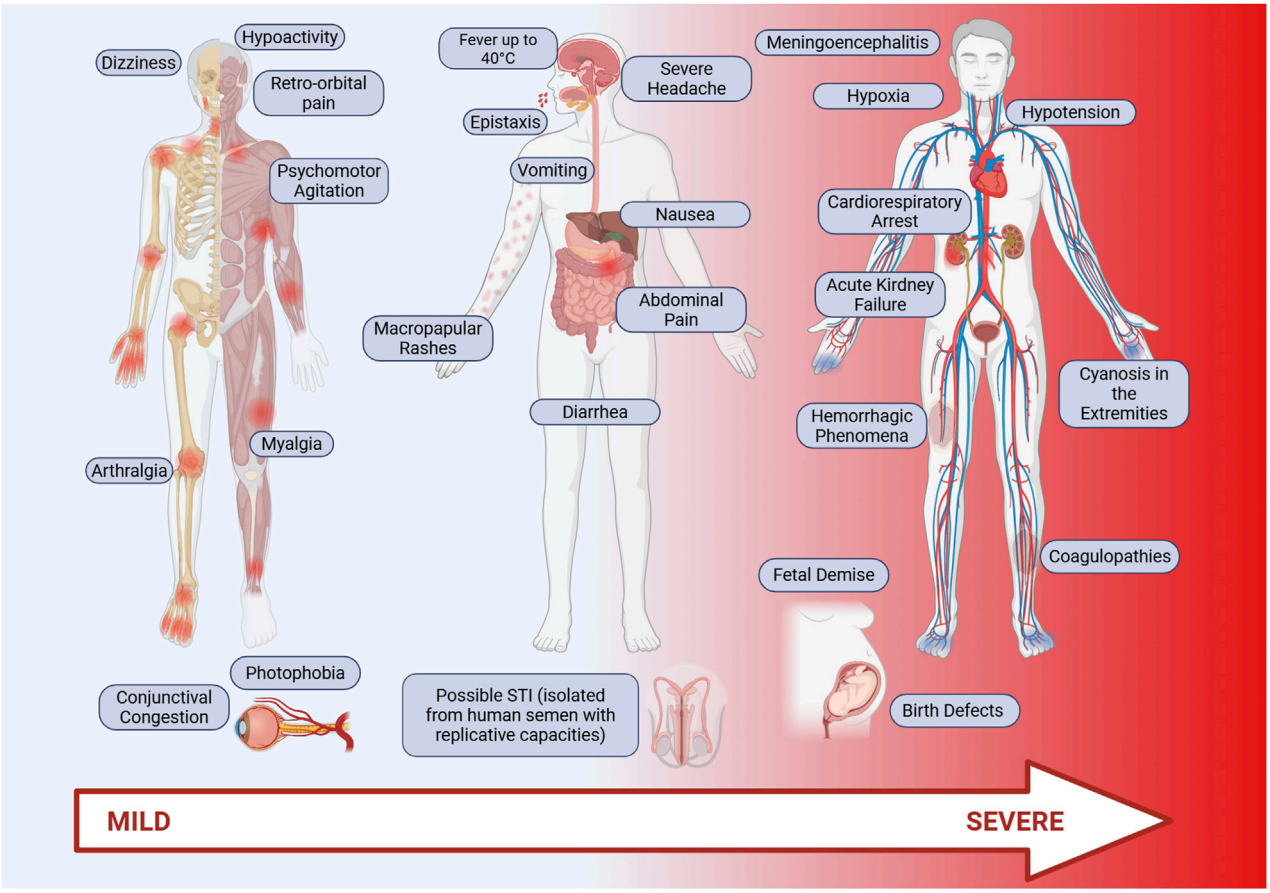

FIGURE 2
Main symptoms of Oropouche fever. Oropouche fever is characterized by acute clinical symptoms, including high fever (above 39°C), intense headache, retro-orbital pain, myalgia, arthralgia, chills, general malaise, nausea, vomiting, diarrhea, and abdominal pain. Additionally, maculopapular rashes are common, typically starting on the trunk and spreading to the limbs. In some cases, hemorrhagic signs such as epistaxis, gum bleeding, and spontaneous bleeding may occur. Additional symptoms such as photophobia, dizziness, drowsiness, and a burning sensation are frequently observed, especially in more severe infections. Patients with severe forms of the disease may develop coagulopathies, hemorrhagic phenomena, acute kidney failure, and, in extreme cases, death. Infection may also affect the central nervous system, leading to meningitis or encephalitis. *Original figure created with Biorender.*

mainly concentrated in the Amazon basin, but it has also been detected in other tropical areas, facilitating the potential for wider geographical spread of the disease [17–19].

Recent studies have demonstrated the vector competence of other mosquito species for OROV infection in immunocompromised mice, including *Aedes aegypti* and *Aedes albopictus*, in addition to *Culex quinquefasciatus*, suggesting that OROV can be transmitted by more common vector species in the Americas [10, 22]. A recent study analyzed the presence of OROV RNA in seven positive insect individuals, belonging to the species *Cx. quinquefasciatus*, *Limatus durhamii*, and *Aedes albopictus*. Although additional studies on vector competence and capacity are necessary for confirmation, these findings suggest that *Cx. quinquefasciatus* may be a potential primary vector in urban areas [23]. In other environments, the virus has also been isolated from other species, such as *Aedes serratus*, *Coquillettidia venezuelensis*, *Ochlerotatus serratus*, *Mansonia venezuelensis*, and *Aedes aegypti*; nonetheless, the *C. paraensis* remains the main vector [7, 16, 22, 24–27]. Environmental factors such as deforestation, climate change, and other anthropological interferences in the environment accelerate the dispersal of vectors and, consequently, the spread of the disease [28].

Human-to-human transmission has not yet been described in the literature, except for vertical transmission during pregnancy [29–31]. There have been two cases in which the genetic material of the virus was identified in organic tissues of the dead fetus, in the placenta, and in umbilical cord blood [30, 32], in addition to a baby with congenital anomalies who died 47 days after birth [33]. Antibodies to OROV were also found in the serum and cerebrospinal fluid samples from four newborns with neurological malformations. In some cases, fetuses that were

infected by OROV during pregnancy presented microcephaly, ventriculomegaly, agenesis of the corpus callosum, and malformation in the joints [25, 32]. Nonetheless, there are still many gaps in the disease transmission cycle and epidemiology that need to be elucidated, such as the probable reservoirs and vectors that promote epizootic events. Indeed, the complex epidemiological features of OROV transmission can be illustrated in a recent report describing the isolation of replication-capable OROV in semen samples from an Italian patient, raising concerns about possible sexual transmission [33].

Oropouche fever is an acute febrile disease with symptoms resembling those of other arboviruses such as Dengue, Zika, Chikungunya, and Mayaro, making clinical diagnosis challenging [5, 34]. The incubation period for OROV is still not well established, but it typically ranges from 3 to 10 days. Following this period, individuals may exhibit a wide range of symptoms, which may vary depending on the virus strain (Figure 2). Common symptoms include high fever (exceeding 39°C, occasionally reaching 40°C), headache, myalgia, arthralgia, chills, malaise, nausea, vomiting, photophobia, retro-orbital pain, diarrhea, abdominal pain, and, in some cases, maculopapular rashes that begin on the torso and spread to the limbs. Hemorrhagic signs, such as spontaneous bleeding, epistaxis, and gum bleeding, have also been reported. With the increase disease spread in 2024, additional symptoms were described, including severe headache, conjunctival congestion, dizziness, drowsiness, severe abdominal pain, anorexia, weakness, and a burning sensation in the body [7, 35]. In some cases, the disease can rapidly progress to more severe manifestations, such as coagulopathies, hemorrhagic phenomena [36, 37], acute kidney failure, and even death [38]. Up to the last quarter of May 2025, 7 deaths were caused by OROV infection in Brazil since the beginning of the current epidemics. Despite the potential for severe complications, the disease is self-limited in most cases, naturally evolving to a complete recovery after 2–7 days of symptoms. However, when the central nervous system is affected, the disease may progress to meningitis or encephalitis, [35, 38, 39]. During the progression of the infection, patients may also present blurred vision, difficulty seeing, hypoactivity, ocular edema, psychomotor agitation, hypotension, hypoxia, cyanosis in the extremities, cold and clammy skin, and, eventually, cardiorespiratory arrest, as observed in a clinical study by Bandeira et al. [36].

Immunity to OROV and advances in vaccine development and diagnosis

Despite the epidemiological relevance of OROV, the mechanisms of interaction between the virus and the human or animal immune systems remain poorly understood. The innate immune response serves as the first line of defense against OROV, as it does for other infectious agents. The viral evasion mechanisms involved in this response are less specific and share characteristics with the immune escape strategies of arboviruses in general. In response to OROV infection, the adaptive immune system mounts a robust cellular and humoral response. Cytotoxic T lymphocytes ($CD8^+$) play a central role in clearing infected cells, while helper T lymphocytes ($CD4^+$) contribute by producing cytokines that stimulate B lymphocyte activation and antibody production. The viral envelope glycoproteins GN and GC are critical for viral attachment and entry into host cells and serve as primary targets for neutralizing antibodies [40]. Hematological alterations are also observed during OROV infection, with neutropenia being a common finding, although some patients may exhibit moderate leukocytosis [9].

The currently recognized viral invasion pathways suggest that the blood-brain barrier (BBB) is likely breached during host infection by OROV through a Trojan Horse-like mechanism since human peripheral blood leukocytes were found to have their genome in monocytes, B and T cells, considering the prevalence of neurological manifestations and pathogenesis [41]. In this process, the virus is transported through the bloodstream, hidden within infected phagocytes, and this capacity, after blocking the Interferon pathway, allows the virus to evade immune recognition and reach target organs and tissues, where it can replicate while bypassing barriers such as the BBB in an immunosuppression scenario. The virus had shown infectivity *in vitro* to astrocytes, as wells dysregulating immune innate pathways, and also was found in peripheral blood leukocytes [42, 43], suggesting a major pathway to surpass the barrier and infect neural cells *in vivo*. Nevertheless, a neural invasion pathway may also contribute to OROV pathogenesis, as viral accumulation has been detected within neurons and in *ex vivo* models that preserve brain cytoarchitecture. Notably, infection is associated with the induction of proinflammatory cytokines and neuronal cell death, which may underlie the development of neurological sequelae, potentially of a chronic nature [44]. Studies in suckling mice models have shown viral tropism for neuroprogenitor cells, with glial cells and astrocytes found alongside apoptotic neurons. Moreover, the animals presented splenomegaly and meningitis, although without viral detection in the liver and spleen [45].

The hepatotropic nature of OROV has been previously described [46]. In experimental studies using golden hamsters, high viral titers were detected in the liver, indicating efficient viral replication [487]. Although clinical cases of hepatitis have not been reported in OROV-infected patients, elevated liver enzyme levels have been observed. Notably, in experimental models using mice deficient in interferon regulatory factors, extensive liver damage was documented, supporting the possibility of hepatic involvement. These findings suggest that OROV may exhibit liver tropism, as evidenced by increased serum transaminase levels in patients with Oropouche fever [48].

The activation of the immune system following OROV tissue invasion was evaluated, identifying the key host defense pathways involved in controlling infection and disease progression. Their study demonstrated that OROV pathogenesis and immune responses in primary murine cells occur through RIG-I-like receptor (RLR) signaling, particularly via MDA5, RIG-I, and MAVS. These pathways lead to the activation of type I interferon (IFN-α/β) responses. In knockout models where key regulatory genes such as MAVS, IRF-3, and IRF-7 were suppressed, as well as IFNAR-deficient mice, uncontrolled OROV replication was observed. These animals developed severe hypercytokinemia, liver damage, and high mortality rates, whereas wild-type mice did not develop any signs of severe disease. This finding highlights the critical role of type I IFN responses in restricting viral dissemination. In summary, the induction of type I IFN through MAVS, IRF-3, and IRF-7 is essential for controlling OROV infection in mice [48].

Evasion of the host immune system by *Orthobunyavirus* can occur through the inhibition of the innate antiviral response, particularly by interfering with type I interferon (IFN-α/β) signaling, which is essential for the initial antiviral defense. Viral proteins, including NSs from other bunyaviruses, function as interferon antagonists by inhibiting the transcription of interferon-stimulated genes (ISGs) [49]. Additionally, modulation of autophagy and apoptosis may play a role, as orthobunyaviruses can manipulate cellular processes to facilitate viral replication while preventing early apoptosis in host cells. Another key immune evasion strategy involves the downmodulation of toll-like receptor (TLR) signaling, as the virus can alter viral proteins or modulate host protein patterns to evade TLR recognition. For instance, circumvention of TLR3 signaling, which detects double-stranded RNA, has been described as an evasion strategy by orthobunyaviruses to avoid early immune detection [50]. Understanding the mechanisms of interaction between OROV and the immune system is essential for developing effective control and treatment strategies. Advances in immunological and virological research will provide new insights into mitigating the impact of this emerging pathogen [51].

The lack of vaccines or specific therapies against OROV represents further challenges associated with controlling outbreaks and reducing the impact on public health. The lack of preventive immunizations makes exposed communities entirely dependent on vector control measures, which are often insufficient to contain the spread of the pathogen [52, 53]. In addition, the lack of antiviral therapies limits clinical management, which is based on palliative care to alleviate the symptoms of Oropouche fever. At the same time, rapid and accurate diagnosis plays a critical role in outbreak response and individual patient management [52]. OROV-infected patients present clinical features that are similar to those of other arboviruses, such as dengue, Zika, and chikungunya viruses, making presumptive clinical diagnosis very difficult [54].

The development of vaccines for arboviruses has been a significant challenge *per se*. Genetic instability, high mutation rates, and cross-reactions between some arboviruses are among existing difficulties. In the case of OROV, the segmented nature of its genome further exacerbates the problem as recombination events may increase virus mutation rates as well as the appearance of unforeseen virus variants. In addition, there are currently no animal models that mimic OROV-based human pathophysiology, hindering pre-clinical evaluations of candidate vaccines. These factors represent important gaps for the development of effective immunogens against OROV [9, 55]. Indeed, there have been very few studies on OROV vaccine development. One such study employed the vesicular stomatitis virus as a vector expressing the OROV GPC complex, and immunizations with this experimental vaccine were able to partially protect mice from the appearance of some disease signals after challenges with wild-type OROV [56].

Advances in studies involving other orthobunyaviruses, such as the *Schmallenberg virus* (SBV), may offer valuable insights to be applied to OROV, considering that these viruses share genetic and antigenic characteristics. Inactivated vaccine candidates using different viruses and viral titers were evaluated in cattle and goats, resulting in neutralizing antibody responses and good seroconversion. At least four vaccine candidates employing inactivated viruses significantly reduced viral loads [57]. Another study from the same research group revealed that the use of the SBV Gc glycoprotein as an antigen could confer protective immunity against SBV infection [58]. Furthermore, bioinformatic studies identified a highly immunogenic region within the N protein, which was then used as a vaccine candidate in knockout mice. After immunization with subunit vaccines containing this specific region, mice challenged with virulent SBV showed attenuated clinical signs and reduced viremia. The study also demonstrated that this region of the N protein is conserved among members of the Simbu group, suggesting potential for testing cross-immunity against OROV [59].

The successful management of viral outbreaks has been inherently linked to the availability of effective vaccines; however, two other basic elements in public health approaches are essential to control the disease: i) identification of infected patients through correct diagnosis, and ii) medical support for affected individuals. Indeed, the correct diagnosis of OROV is essential for both individual health management and epidemiological control. The clinical overlap between OROV infections and other febrile illnesses caused by arboviruses, such as Dengue, Zika, and Chikungunya, poses significant diagnostic challenges. Misdiagnosis can result in inappropriate treatments, delayed interventions, and public health inaction. Rapid identification of OROV cases enables the mapping of outbreak zones, assessing viral spread, and the implementation of targeted control strategies, including vector control campaigns and public awareness initiatives [54, 60].

OROV detection typically involves identifying the viral genome in plasma or serum samples from patients in the acute, febrile phase of the disease. A dual-target RT-qPCR assay has been described for the simultaneous detection of Mayaro virus (MAYV) and OROV, focusing on the NSP1 gene of MAYV and the S segment of OROV. This method incorporates customized internal controls using synthetic plasmids containing viral sequences. The protocol, published in 2017, demonstrated high sensitivity and specificity [61], and has been widely adopted by both private and State laboratories in Brazil.

Up to the writing of this review manuscript, no commercial serological tests, such as ELISA and rapid tests, were widely available. Serological tests for detecting IgM and IgG immunoglobulins are carried out using protocols developed in-house, highlighting the fact that the disease has been generally neglected. In 2001, an ELISA using the recombinant nucleocapsid protein (N) as an antigen was described. The protein was produced in a prokaryotic system and tested on samples from patients in Brazil and Peru. The test showed high sensitivity and specificity for detecting Oropouche fever [62]. The development of mouse monoclonal antibodies for the detection of OROV in indirect immunofluorescence (IFA) and immunohistochemistry (IHQ) assays was recently published [63].

Although the development of vaccines and diagnostic tools for OROV presents substantial challenges, recent advances in both areas offer hope for better control and management of this emerging viral threat. The complexity of OROV, with its high mutation rates and clinical similarities to other arboviruses, underscores the urgent need for continued research and innovation. Collaborative efforts and sustained investment in basic and applied research are crucial for developing effective vaccines and diagnostic tools, ultimately enhancing global public health responses to outbreaks of OROV and similar emerging viruses.

Epidemiology and geographic distribution

In the last 20 years, OROV has been detected throughout South America, including countries such as Peru, Bolivia, Ecuador, Colombia, Venezuela, and French Guiana, besides Brazil [64]. The virus has also been detected again in the Caribbean - Haiti reported an outbreak in 2014 - and sporadic cases were reported in Central America, such as in Panama. Despite all early and late reports, Oropouche fever has been historically underdiagnosed due to its clinical similarity to other arboviral diseases, such as Dengue, Zika, and Chikungunya, making past and present surveillance difficult and current control efforts challenging [65].

In 2011, a novel orthobunyavirus was described in Peru and was retrospectively linked to outbreaks that occurred in 1999. Upon isolation and analysis, it was confirmed that the pathogen, named Iquitos virus, is a recombinant derivative of OROV [14]. Furthermore, in 2017, a study demonstrated the recombination potential between Oropouche and Schmallenberg viruses, both members of the *Peribunyaviridae* family. Although this

TABLE 1 Absolute numbers of OROV cases in Brazil in 2024 (epidemiological week 1–52) and 2025 (epidemiological week 1–22). Epidemiological data on OROV in Brazil were obtained from the Brazilian Ministry of Health and the Pan American Health Organization databases [25, 68].

Region/State	Cases (n)	
	2024 (EW 1-52)	2025 (EW 1-22)
Northern states	**5,804**	**109**
Amazonas	3,231	
Rondônia	1,711	7
Acre	276	
Roraima	277	1
Pará	172	1
Amapá	129	87
Tocantins	8	13
Northeastern states	**1,517**	**1,837**
Bahia	891	7
Ceará	257	633
Pernambuco	146	643
Alagoas	120	3
Sergipe	34	
Maranhão	33	
Piauí	30	1
Paraíba	6	550
Southeastern states	**6,283**	**9,863**
Espírito Santo	5,868	6,271
Minas Gerais	249	1,232
Rio de Janeiro	157	2,302
São Paulo	9	58
Southern states	**178**	**43**
Santa Catarina	178	15
Paraná		28
Center-western states	**19**	**1**
Mato Grosso	18	
Mato Grosso do Sul	1	1
Brazil	**13,801**	**11,853**

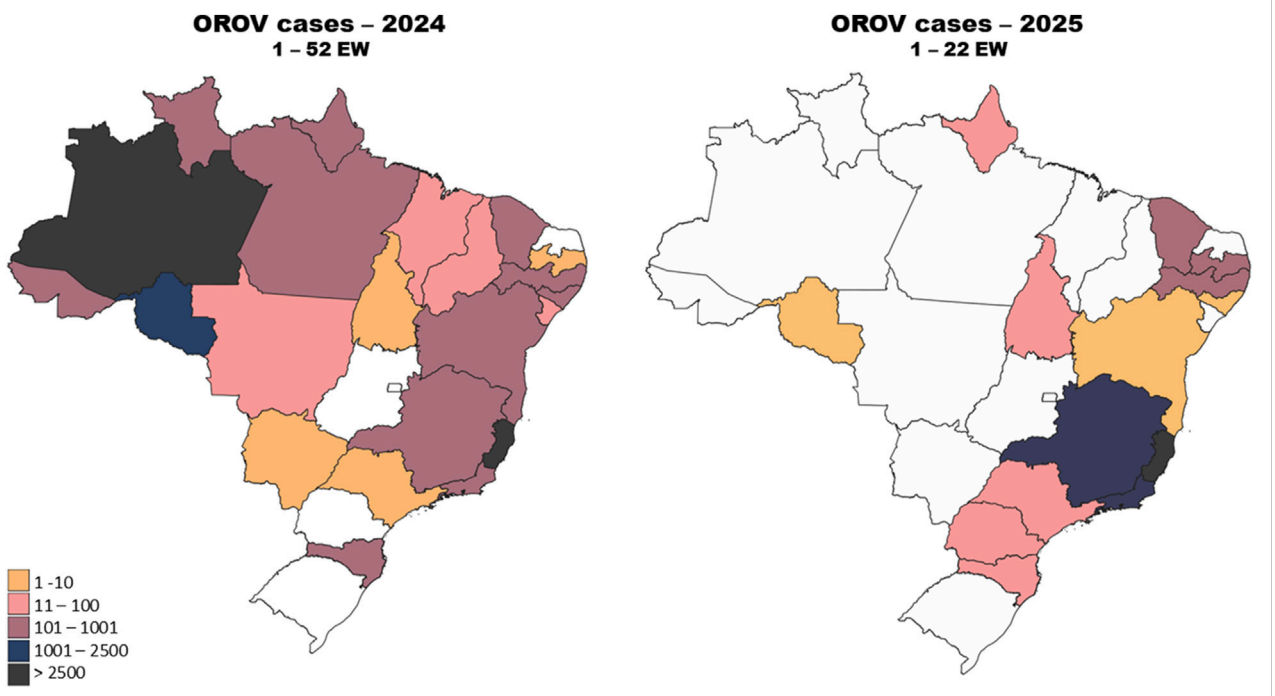

FIGURE 3
Geographical distribution of Oropouche fever cases in Brazil in 2024 and 2025. Confirmed cases of Oropouche fever in epidemiological week 1–52 of 2024 (left panel). Confirmed cases of Oropouche fever in epidemiological week 1–22 of 2025 (right panel). The Amazon region stands out in 2024, accounting for over 50% of the cases. The spread of the disease beyond the Amazon region reflects the geographical expansion of the disease. In 2025, the state of Espírito Santo accounted for the majority of cases, indicating an early epicenter outside the Amazon region. Epidemiological data on OROV in Brazil were obtained from the Brazilian Ministry of Health [67].

experiment was conducted under laboratory conditions, it highlights the recombination capability of viruses within this family [66]. To date, four OROV genotypes have been identified: genotype I, found in Trinidad and Brazil; genotype II, identified in Brazil and Peru; genotype III, circulating in Brazil and Panama; and genotype IV, detected in the Amazon region of Brazil [8].

In 2024, the Pan American Health Organization (PAHO) confirmed cases have been reported in eleven countries and one territory in the American continent: Barbados, Bolivia, Brazil, Canada, Colombia, Cuba, Ecuador, United States of America (imported cases), Guyana, Cayman Islands (imported case), Panama, and Peru. Additionally, imported OROV cases have been reported in a few European countries (30 cases in total) [25].

In 2024, Brazil reported cases in 22 out of the country's 26 states, plus the federal district of Brasilia. This marked a substantial geographic expansion within the Country, implying that outbreaks were no longer limited to the northern region, where the virus is considered endemic. This scenario began in 2023 with three extra-Amazonian cases being reported in the states of Minas Gerais (1 case) and Espírito Santo (2 cases). In the next year, the Amazon basin region accounts for 52.9% of the reported cases, with all of its seven states reporting cases (Table 1). The virus's spread was noted in several non-endemic areas, including the Southeast, South, and Central-West regions of the Country, further highlighting its increasing reach. Autochthonous transmission was reported in 15 non-Amazonian states [25, 67] (Figure 3; Table 1). Whilst the Amazon and other northern states remain as the epicenters of OROV activity, the emergence of cases in regions such as São Paulo, Rio de Janeiro, and Mato Grosso suggests that the virus's distribution is shifting, possibly driven by factors like climate change and human movement [67]. In the first 5 months of 2025, Oropouche fever occurrence remained concerningly high, with 11,853 confirmed cases across Brazil up to the end of May. More cases were reported in the first weeks of 2025 than in the same period of 2024, highlighting the rising trend in infections. Cases were recorded in states throughout Brazil [25] (Table 1; Figure 3).

Environmental impacts and OROV expansion

The spread of the OROV is intricately linked to environmental changes, which alter the dynamics of both vector populations and the virus itself. Climate changes, for instance, has contributed to rising temperatures and irregular rainfall patterns, creating favorable (and sometimes unpredictable) conditions for the proliferation of

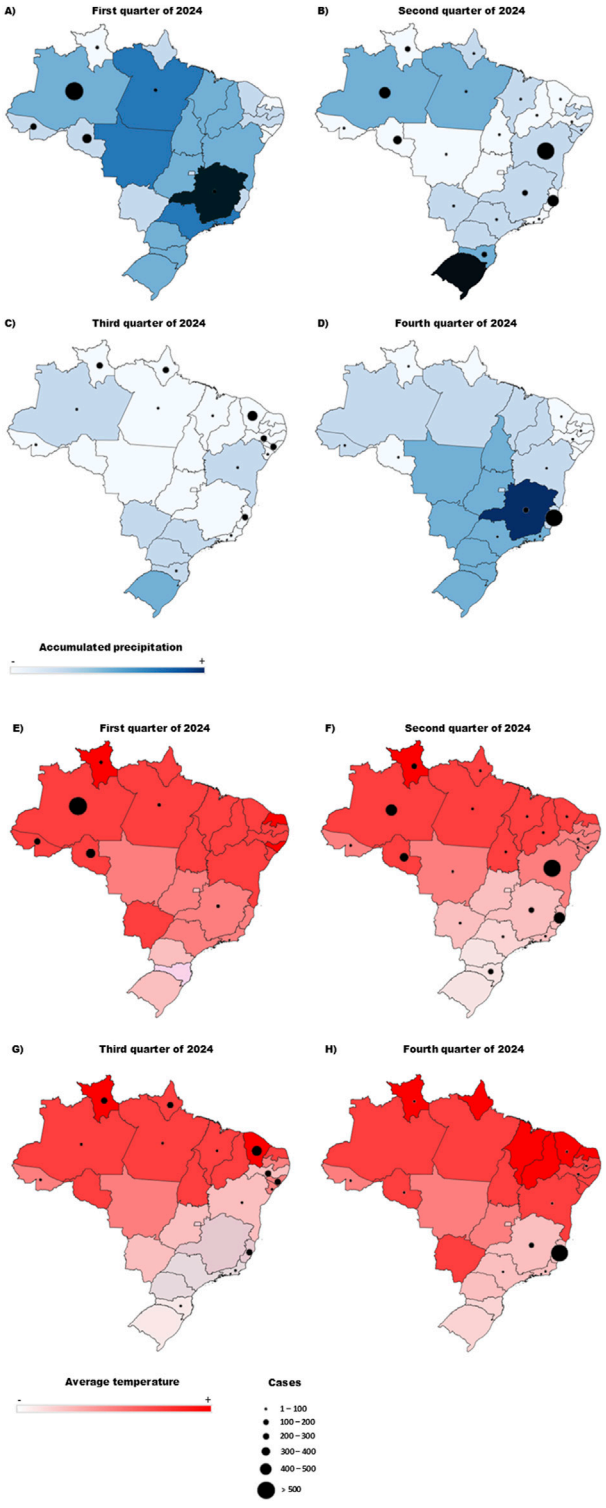

FIGURE 4
Projection of OROV case numbers across the four-quarters of 2024 concerning temperature and accumulated precipitation. **(A,E)** Relationship between temperature and number of cases in the first trimester/relationship between precipitation accumulation and number of cases in the first trimester. **(B,F)** Relationship between temperature and number of cases in the second trimester/relationship between precipitation accumulation and number of cases in the second trimester. **(C,G)** Relationship between temperature and number of cases in the third trimester/relationship between precipitation accumulation and number of cases in the third trimester. **(D,H)** Relationship between temperature and number of cases in the fourth trimester/relationship between precipitation accumulation and number of cases in the fourth trimester. The color scale determines the temperature gradient **(A–E)** and the accumulated precipitation gradient **(F–G)**, and the size of the circles represents the number of cases.

arthropod vectors. The rainy season in the Amazon region, which lasts from January to June, provides ideal conditions for *C. paraensis* populations to thrive, and during periods of increased rainfall, their populations spike, resulting in a higher risk of transmission. Studies have shown that the increase in precipitation during the rainy season directly correlates with the population numbers of *C. paraensis* and subsequent OROV outbreaks in the region [65]. In Figures 4A–D, the correlation between the number of cases and the average quarterly temperature in 2024 is shown. When evaluating the expansion of the virus to other states (Figures 4B,C), a trend in rising may have contributed to this spread. Conversely, when analyzing the relationship between the number of cases and accumulated precipitation (Figures 4E–H), the peak in cases did not coincide with periods of highest rainfall. However, considering the precipitation from the previous quarter, it is possible that accumulated rainfall created favorable environmental conditions, such as increased humidity and the formation of breeding sites for vectors, which may have influenced the rise in cases in the subsequent quarter.

In addition to climate change, human activities such as deforestation and urbanization have significantly altered local and regional ecology parameters, contributing to the spread of OROV. The loss of native forests and the expansion of urban areas disrupt the habitats of arthropod vectors and reservoir hosts, like primates and sloths. As human settlements encroach on previously forested areas, the proximity between humans, vectors, and reservoirs increases, facilitating the transmission of the virus. In regions like Cusco, Peru, where deforestation has been rampant, outbreaks have been recorded, suggesting that changes in the local ecosystem, such as the loss of vegetation and alterations to animal and insect populations, have contributed to the emergence of OROV [28].

Moreover, the construction of large-scale infrastructure projects, such as dams and roads, has been associated with the spread of OROV. These infrastructure projects often result in environmental changes that promote vector breeding and transference to areas where the insects where previously absent. For example, in the Tucuruí region of Pará State, Brazil, the flooding caused by the construction of a dam created favorable breeding grounds for *Culicoides* mosquitoes, leading to increased occurrence of anti-OROV antibodies in local

wildlife, such as in birds and primates [9]. These environmental disruptions, along with changes in local ecosystems, increase the opportunities for the virus to be transmitted between vectors and susceptible hosts [23]. As a result to of regional ecological changes, the virus has now spread from this original confinement in the Amazon basin to neighboring regions and even far states within the Country. The increasing number of outbreaks in the southeastern and southern regions of Brazil, where the virus was previously absent, highlights the combined impact of climate change and human activities on the disease's distribution. The alteration of ecosystems, the proliferation of vectors, and the movement of people to new areas have all contributed to OROV's broader geographical spread, challenging public health systems that are not used to managing the disease in non-endemic areas [23].

In a recent study, the complex interaction between ecological and environmental factors, coupled with human mobility, was discussed as a contributing factor to the increase in cases in 2024. The introduction of the virus into large urban centers and its subsequent spread to small inland cities are closely linked to the dynamics of the *C. paraensis* vector, whose opportunistic characteristics and ability to colonize both urban and rural environments favor transmission. Furthermore, the study reveals that agricultural activities, such as banana, cassava, and cocoa crops, provide ideal habitats for mosquito reproduction, creating conditions to the maintenance and spread of the virus. Environmental changes, such as deforestation and the degradation of biomes like the Atlantic Forest and Caatinga, amplify the risk of new outbreaks, as arthropod populations tend to search for new environments to survive, highlighting the importance of continuous surveillance. In addition to ecological and environmental factors, genomic studies have revealed that the current OROV epidemic may have been driven by the emergence of a novel reassortant lineage, designated OROVBR-2015-2024, which combines genomic segments from distinct geographical origins. This lineage presents synapomorphic non-synonymous mutations in both the L segment, which encodes the RNA-dependent RNA polymerase, and the M segment, which encodes the viral envelope glycoproteins. Notably, mutations such as I957V in the Amazonian AM-I clade and I958T in the non-Amazonian SC-2 clade are located in the M segment and may play a role in modulating viral entry or immune evasion. These genetic alterations are particularly relevant, as the M segment directly influences viral tropism and host cell interactions, potentially affecting replication kinetics and transmission dynamics. Altogether, these findings suggest that viral adaptation may have contributed to increased transmissibility or fitness of OROV outside the Amazon region [60].

Furthermore, climate models suggest that the continued warming of the planet and changes in precipitation patterns will further affect the distribution of OROV vectors. As temperatures rise and rainfall becomes more erratic, new regions may become suitable for *Culicoides* vectors to proliferate, creating new hotspots for OROV outbreaks. This phenomenon is particularly concerning because it may introduce the virus into regions with less experience in managing vector-borne diseases, making them more vulnerable to outbreaks.

Discussion

Oropouche fever remains a significant public health concern in tropical Latin America. Although originally confined to the Amazon basin, OROV has recently expanded into southeastern and southern Brazil, reflecting changes in its epidemiological dynamics. This expansion is driven by increased human population mobility, urban growth, and environmental factors such as rising temperatures and altered rainfall patterns that favor vector proliferation. Addressing OROV transmission requires an integrated approach that considers both ecological pressures and public health interventions.

The pathogenesis of OROV is still not fully elucidated, particularly in terms of viral-host immune interactions. The absence of specific antiviral treatments and licensed vaccines continues to hinder effective disease control. While diagnostic technologies have improved, early detection and surveillance remain limited—especially in endemic and resource-constrained areas. Strengthening diagnostic capacity is a short-term priority to enable rapid response to emerging outbreaks.

Environmental changes, such as deforestation and large-scale infrastructure development, have disrupted vector habitats and facilitated viral spread beyond traditional endemic zones. However, repeated references to these drivers across studies highlight the urgent need for long-term strategies that address root ecological causes. Coordinated public policies that align health surveillance with environmental protection are essential. In the long term, controlling OROV will require not only continued genomic and ecological monitoring but also investment in vaccine research and sustainable land-use practices to mitigate vector expansion. From the legal point of view, it is important to mention that Brazil possesses a robust legal framework for environmental protection, which extends beyond the Amazon - its most internationally recognized biome - to include all other, lesser-known ecosystems within the national territory. Moreover, Brazil is a signatory to all editions of the Conference of the Parties (COP). Notably, COP30 will be held in Belém, the most influential and significant Brazilian capital in the Amazon region. The conference is scheduled to take place in November 2025 and is already being referred to as the 'Amazon COP'.

The current regional OROV outbreak must be addressed within a One Health framework, recognizing the interconnectedness of human, animal, and environmental

health. Key aspects warranting further investigation include the role of environmental and anthropogenic factors in peri-urban areas, the presence of secondary vectors capable of supporting OROV replication, and the occurrence of imported cases in regions where Culicoides species of the same genus are present. Additionally, exploring whether the OROVBR-2015-2024 variant exhibits altered vector tropism, hepatocyte affinity, or neurotropism in extra-Amazonian contexts could reveal important pathophysiological insights. A deeper understanding of virus-host interactions—both *in vivo* and *ex vivo*, including apoptosis pathways—may help uncover critical knowledge gaps. Such efforts are essential for improving diagnostic capabilities and informing the development of effective antivirals, vaccines, and therapeutic strategies to mitigate the public health impact of Oropouche virus infections [68].

Author contributions

IG investigation, writing, images, and review; ID investigation, images, review, and data analysis; VR images and review; BM investigation, writing, and review; LS investigation, writing, and review; BS investigation, writing, and review AP investigation, writing, and review; JC investigation, writing, images, review, and supervised the project SP investigation, writing, images, review, and supervised the project; FF investigation, writing, images, review, and supervised the project.

Funding

The author(s) declare that financial support was received for the research and/or publication of this article. SP is a fellowship recipient from FAPEMIG (APQ-05041-23). The study was also financed by the Coordenação de Aperfeiçoamento de Pessoal de Nível Superior – Brasil (CAPES) – Finance Code 001, through fellowships given to post-graduation students involved in the work. FF and JA is a CNPq fellow.

Acknowledgments

We would like to thank CAPES, CNPq, and FAPEMIG for providing fellowships to graduate and undergraduate students. We also thank the UFMG's Microbiology post-graduation program for the creation of an encouraging scientific environment.

Conflict of interest

The author(s) declared no potential conflicts of interest with respect to the research, authorship, and/or publication of this article.

Generative AI statement

The author(s) declare that no Generative AI was used in the creation of this manuscript.

References

1. Riccò M, Corrado S, Bottazzoli M, Marchesi F, Gili R, Bianchi FP, et al. (Re-)Emergence of oropouche virus (OROV) infections: systematic review and meta-analysis of observational studies. *Viruses* (2024) **16**:1498. doi:10.3390/v16091498

2. de Souza WM, Calisher CH, Carrera JP, Hughes HR, Nunes MRT, Russell B, et al. ICTV virus taxonomy profile: Peribunyaviridae 2024. *The J Gen Virol* (2024) **105**:002034. doi:10.1099/jgv.0.002034

3. Anderson CR, Spence L, Downs WG, Aitken TH. Oropouche virus: a new human disease agent from Trinidad, West Indies. *The Am J Trop Med Hyg* (1961) **10**:574–8. doi:10.4269/ajtmh.1961.10.574

4. Pinheiro F, Pinheiro M, Bensabath G, Causey O, Shope R. Oropouche virus epidemic in Belém. *Revista de Serviço Especial de Saúde Publica* (1962) **12**:15–23. Available online at: https://patuaback.iec.gov.br/server/api/core/bitstreams/04423538-c0d5-47ac-8a54-c9b3f57ead13/content.

5. Mourão MPG, Bastos Md S, Figueiredo RMPd, Gimaque JBd L, Alves Vd CR, Saraiva Md GG, et al. Arboviral diseases in the western brazilian amazon: a perspective and analysis from a tertiary health and research center in manaus, state of Amazonas. *Rev Soc Bras Med Trop* (2015) **48**:20–6. doi:10.1590/0037-8682-0133-2013

6. T Borborema CA, Pinheiro FP, Albuqiierque BC, A Trâ AP, da Bosa vassos S, Travassos da Rosa JF, et al. (2025). Primeiro registro de epidemias cai,jsadas pelo vírus oropouche no estado do amazonas.

7. Pinheiro FP, Travassos da Rosa APA, Travassos da Rosa JFS, Ishak R, Freitas RB, Gomes MLC, et al. Oropouche virus. I. A review of clinical, epidemiological, and ecological findings. *The Am J Trop Med Hyg* (1981) **30**:149–60. doi:10.4269/ajtmh.1981.30.149

8. Vasconcelos HB, Nunes MRT, Casseb LMN, Carvalho VL, Pinto da Silva EV, Silva M, et al. Molecular epidemiology of oropouche virus, Brazil. *Emerging Infect Dis* (2011) **17**:800–6. doi:10.3201/eid1705.101333

9. Files MA, Hansen CA, Herrera VC, Schindewolf C, Barrett ADT, Beasley DWC, et al. Baseline mapping of Oropouche virology, epidemiology, therapeutics, and vaccine research and development. *NPJ Vaccin* (2022) **7**:38. doi:10.1038/s41541-022-00456-2

10. Cardoso BF, Serra OP, Heinen LBd S, Zuchi N, Souza VCd, Naveca FG, et al. Detection of oropouche virus segment s in patients and in culex quinquefasciatus in the state of mato grosso, Brazil. *Mem Inst Oswaldo Cruz* (2015) **110**:745–54. doi:10.1590/0074-02760150123

11. Hopkins FR, Álvarez-Rodríguez B, Heath GR, Panayi K, Hover S, Edwards TA, et al. The native orthobunyavirus ribonucleoprotein possesses a helical architecture. *mBio* **13**. doi:10.1128/mbio.01405-22

12. Navarro JC, Giambalvo D, Hernandez R, Auguste AJ, Tesh RB, Weaver SC, et al. Isolation of madre de dios virus (orthobunyavirus; Bunyaviridae), an oropouche virus Species Reassortant, from a Monkey in Venezuela. *The Am Soc Trop Med Hyg* (2016) **95**:328–38. doi:10.4269/ajtmh.15-0679

13. Ladner JT, Savji N, Lofts L, Travassos da Rosa A, Wiley MR, Gestole MC, et al. Genomic and phylogenetic characterization of viruses included in the Manzanilla and Oropouche species complexes of the genus Orthobunyavirus, family Bunyaviridae. *J Gen Virol* (2014) **95**:1055–66. doi:10.1099/vir.0.061309-0

14. Aguilar PV, Barrett AD, Saeed MF, Watts DM, Russell K, Guevara C, et al. Iquitos virus: a novel reassortant orthobunyavirus associated with human illness in Peru. *Plos Negl Trop Dis* (2011) **5**:e1315. doi:10.1371/journal.pntd.0001315

15. McGregor BL, Connelly CR, Kenney JL. Infection, dissemination, and transmission potential of north american culex quinquefasciatus, culex tarsalis, and culicoides sonorensis for oropouche virus. *Viruses* (2021) **13**:226. doi:10.3390/v13020226

16. Pinheiro FP, Hoch AL, Gomes Md LC, Roberts DR. Oropouche virus. IV. Laboratory transmission by Culicoides paraensis. *The Am J Trop Med Hyg* (1981) **30**:172–6. doi:10.4269/ajtmh.1981.30.172

17. Nunes MR, Martins LC, Rodrigues SG, Chiang JO, Azevedo Rdo S, da Rosa AP, et al. Oropouche virus isolation, Southeast Brazil. *Emerg Infect Dis* (2005) **11**:1610–3. doi:10.3201/eid1110.050464

18. Batista PM, Andreotti R, Almeida PSde, Marques AC, Rodrigues SG, Chiang JO, et al. Detection of arboviruses of public health interest in free-living New World primates (Sapajus spp.; *Alouatta caraya*) captured in Mato Grosso do Sul, Brazil. *Rev Soc Bras Med Trop* (2013) **46**:684–90. doi:10.1590/0037-8682-0181-2013

19. Gibrail MM, Fiaccadori FS, Souza M, Almeida TNV, Chiang JO, Martins LC, et al. Detection of antibodies to oropouche virus in non-human primates in goiânia city, goiás. *Rev Soc Bras Med Trop* (2016) **49**:357–60. doi:10.1590/0037-8682-0425-2015

20. Dégallier N, Rosa ATda, da Silva JMC, Rodrigues SG, Vasconcelos PFC, Rosa JTda, et al. As aves como hospedeiras de arbovírus na amazônia brasileira. *Bol Mus Para Emílio Goeldi* **8**. Available online at: https://patua.iec.gov.br/handle/iec/2623.

21. Dias HG, Familiar-Macedo D, Garrido IO, dos Santos FB, Pauvolid-Corrêa A. Exposure of domestic animals to Mayaro and Oropouche viruses in urban and peri-urban areas of West-Central Brazil. *One Health Outlook* (2024) **6**:12. doi:10.1186/s42522-024-00104-w

22. de Mendonça SF, Rocha MN, Ferreira FV, Leite THJF, Amadou SCG, Sucupira PHF, et al. Evaluation of aedes aegypti, aedes albopictus, and culex quinquefasciatus mosquitoes competence to oropouche virus infection. *Viruses* (2021) **13**:755. doi:10.3390/v13050755

23. Feitoza LHM, Gasparelo NWF, Meireles ACA, Rios FGF, Teixeira KS, da Silva MS, et al. Integrated surveillance for Oropouche Virus: molecular evidence of potential urban vectors during an outbreak in the Brazilian Amazon. *Acta Tropica* (2025) **261**:107487. doi:10.1016/j.actatropica.2024.107487

24. Saeed MF, Wang H, Suderman M, Beasley DWC, Travassos da Rosa A, Li L, et al. Jatobal virus is a reassortant containing the small RNA of Oropouche virus. In: *Virus research* (2001). doi:10.1016/S0168-1702(01)00262-3

25. PAHO. *Epidemiological alert - Oropouche in the Americas region - 13 december 2024*. Pan American Health Organization.

26. Dixon KE, Travassos da Rosa APA, Travassos da Rosa JF, Llewellyn CH. Oropouche virus: II. Epidemiological observations during an epidemic in santarém, parã, Brazil in 1975. *The Am J Trop Med Hyg* (1981) **30**:161–4. doi:10.4269/ajtmh.1981.30.161

27. Roberts DR, Hoch AL, Dixon KE, Llewellyn CH. Oropouche virus. III. Entomological observations from three epidemics in Para, Brazil, 1975. *The Am J Trop Med Hyg* (1981) **30**:165–71. doi:10.4269/ajtmh.1981.30.165

28. Romero-Alvarez D, Escobar LE, Auguste AJ, Del Valle SY, Manore CA. Transmission risk of oropouche fever across the Americas. *Infect Dis Poverty* (2023) **12**:47. doi:10.1186/s40249-023-01091-2

29. das Neves Martins FE, Chiang JO, Nunes BTD, Ribeiro Bd FR, Martins LC, Casseb LMN, et al. Newborns with microcephaly in Brazil and potential vertical transmission of Oropouche virus: a case series. *The Lancet Infect Dis* (2025) **25**:155–65. doi:10.1016/S1473-3099(24)00617-0

30. Garcia Filho C, Lima Neto AS, Maia AMPC, da Silva LOR, Cavalcante RC, Monteiro HS, et al. A case of vertical transmission of oropouche virus in Brazil. *New Engl J Med* (2024) **391**:2055–7. doi:10.1056/nejmc2412812

31. Schwartz DA, Dashraath P, Baud D. Oropouche virus (OROV) in pregnancy: an emerging cause of placental and fetal infection associated with stillbirth and microcephaly following vertical transmission. *Viruses* (2024) **16**:1435. doi:10.3390/v16091435

32. Brazilian Ministry of Health. Ministério da Saúde informa caso de anomalia congênita associada a Oropouche (2024). Available online at: https://www.gov.br/saude/pt-br/canais-de-atendimento/sala-de-imprensa/notas-a-imprensa/2024/ministerio-da-saude-informa-caso-de-anomalia-congenita-associada-a-oropouche (Accessed March 18, 2025).

33. Castilletti C, Huits R, Mantovani RP, Accordini S, Alladio F, Gobbi F. Replication-competent oropouche virus in semen of traveler returning to Italy from Cuba, 2024. *Emerg Infect Dis* (2024) **30**:2684–6. doi:10.3201/eid3012.241470

34. Durango-Chavez HV, Toro-Huamanchumo CJ, Silva-Caso W, Martins-Luna J, Aguilar-Luis MA, del Valle-Mendoza J, et al. Oropouche virus infection in patients with acute febrile syndrome: is a predictive model based solely on signs and symptoms useful? *PLoS One* (2022) **17**:e0270294. doi:10.1371/journal.pone.0270294

35. Vernal S, Martini CCR, da Fonseca BAL. Oropouche virus–associated aseptic meningoencephalitis, Southeastern Brazil. *Emerging Infect Dis* (2019) **25**:380–2. doi:10.3201/eid2502.181189

36. Bandeira AC, Pereira FM, Leal A, Santos SPO, Barbosa AC, Souza MSPL, et al. Fatal oropouche virus infections in nonendemic region, Brazil, 2024. *Emerg Infect Dis* (2024) **30**:2370–4. doi:10.3201/eid3011.241132

37. Mourão MPG, Bastos MS, Gimaque JBL, Mota BR, Souza GS, Grimmer GHN, et al. Oropouche fever outbreak, Manaus, Brazil, 2007-2008. *Emerging Infect Dis* **15**. doi:10.3201/eid1512.090917

38. Pinheiro F, Rocha A, Freitas R, Ohana B, Travassos da Rosa A, Rogério JS, et al. Meningitis associated with Oropouche virus infections. *Rev Inst Med Trop Sao Paulo* (1982) **24**:246–51.

39. Bastos MDS, Figueiredo LTM, Naveca FG, Monte RL, Lessa N, Pinto de Figueiredo RM, et al. Short report: identification of oropouche Orthobunyavirus in the cerebrospinal fluid of three patients in the Amazonas, Brazil. *The Am Soc Trop Med Hyg* (2012) **86**:732–5. doi:10.4269/ajtmh.2012.11-0485

40. Ribeiro Amorim M, Cornejo Pontelli M, Fabiano de Souza G, Primon Muraro S, Toledo-Teixeira DA, Forato J, et al. Oropouche virus infects, persists and induces IFN response in human peripheral blood mononuclear cells as identified by RNA PrimeFlow™ and qRT-PCR assays. *Viruses* (2020) **12**:785. doi:10.3390/v12070785

41. Proenca-Modena JL, Hyde JL, Sesti-Costa R, Lucas T, Pinto AK, Richner JM, et al. Interferon-regulatory factor 5-dependent signaling restricts orthobunyavirus dissemination to the central nervous system. *J Virol* (2016) **90**:189–205. doi:10.1128/jvi.02276-15

42. de Souza Luna LK, Rodrigues AH, Santos RIM, Sesti-Costa R, Criado MF, Martins RB, et al. Oropouche virus is detected in peripheral blood leukocytes from patients. *J Med Virol* (2017) **89**:1108–11. doi:10.1002/jmv.24722

43. Geddes VEV, Brustolini OJB, Cavalcante LTd F, Moreira FRR, de Castro FL, Guimarães APd C, et al. Common dysregulation of innate immunity pathways in human primary astrocytes infected with chikungunya, Mayaro, oropouche, and Zika viruses. *Front Cell Infect Microbiol* (2021) **11**:641261. doi:10.3389/fcimb.2021.641261

44. Almeida GM, Souza JP, Mendes ND, Pontelli MC, Pinheiro NR, Nogueira GO, et al. Neural infection by oropouche virus in adult human brain slices induces an inflammatory and toxic response. *Front Neurosci* (2021) **15**:674576. doi:10.3389/fnins.2021.674576

45. Santos RI, Almeida MFP, Paula FE, Rodrigues AH, Saranzo AM, Paula AE, et al. Experimental infection of suckling mice by subcutaneous inoculation with Oropouche virus. *Virus Res* (2012) **170**:25–33. doi:10.1016/j.virusres.2012.07.006

46. Araújo R, Dias LB, Araújo MT, Pinheiro F, Oliva OF. Ultrastructural changes in the hamster liver after experimental inoculation with Oropouche arbovirus (type BeAn 19991). *Rev Inst Med Trop Sao Paulo* (1978) **20**:45–54.

47. Rodrigues AH, Santos RI, Arisi GM, Bernardes ES, Silva ML, Rossi MA, et al. Oropouche virus experimental infection in the golden hamster (Mesocrisetus auratus). *Virus Res* (2011) **155**:35–41. doi:10.1016/j.virusres.2010.08.009

48. Proenca-Modena JL, Sesti-Costa R, Pinto AK, Richner JM, Lazear HM, Lucas T, et al. Oropouche virus infection and pathogenesis are restricted by MAVS, IRF-3, IRF-7, and type I interferon signaling pathways in nonmyeloid cells. *J Virol* (2015) **89**:4720–37. doi:10.1128/jvi.00077-15

49. Tilston-Lunel NL, Acrani GO, Randall RE, Elliott RM. Generation of recombinant oropouche viruses lacking the nonstructural protein NSm or NSs. *J Virol* (2016) **90**:2616–27. doi:10.1128/jvi.02849-15

50. Sakkas H, Bozidis P, Franks A, Papadopoulou C. Oropouche fever: a review. *Viruses* (2018) **10**:175. doi:10.3390/v10040175

51. Wesselmann KM, Postigo-Hidalgo I, Pezzi L, de Oliveira-Filho EF, Fischer C, de Lamballerie X, et al. Emergence of Oropouche fever in Latin America: a narrative review. *The Lancet Infect Dis* (2024) **24**:e439–e452. doi:10.1016/s1473-3099(23)00740-5

52. Cain M, Ly H. Oropouche virus: understanding 'sloth fever' disease dynamics and novel intervention strategies against this emerging neglected tropical disease. *Virulence* (2024) **15**:2439521. doi:10.1080/21505594.2024.2439521

53. Okesanya OJ, Amisu BO, Adigun OA, Ahmed MM, Agboola AO, Kab T, et al. Addressing the emerging threat of Oropouche virus: implications and public health responses for healthcare systems. *Trop Dis Trav Med Vaccin* (2025) **11**:1. doi:10.1186/s40794-024-00236-x

54. Travassos da Rosa JF, de Souza WM, Pinheiro Fd P, Figueiredo ML, Cardoso JF, Acrani GO, et al. Oropouche virus: clinical, epidemiological, and molecular aspects of a neglected orthobunyavirus. *The Am Soc Trop Med Hyg* (2017) **96**:1019–30. doi:10.4269/ajtmh.16-0672

55. Chen T, Ding Z, Lan J, Wong G. Advances and perspectives in the development of vaccines against highly pathogenic bunyaviruses. *Front Cell Infect Microbiol* (2023) **13**:1174030. doi:10.3389/fcimb.2023.1174030

56. Stubbs SH, Cornejo Pontelli M, Mishra N, Zhou C, de Paula Souza J, Mendes Viana RM, et al. Vesicular stomatitis virus chimeras expressing the oropouche virus glycoproteins elicit protective immune responses in mice. *mBio* (2021) **12**: e0046321. doi:10.1128/mbio.00463-21

57. Wernike K, Nikolin VM, Hechinger S, Hoffmann B, Beer M. Inactivated Schmallenberg virus prototype vaccines. *Vaccine* (2013) **31**:3558–63. doi:10.1016/j.vaccine.2013.05.062

58. Wernike K, Aebischer A, Roman-Sosa G, Beer M. The N-terminal domain of Schmallenberg virus envelope protein Gc is highly immunogenic and can provide protection from infection. *Sci Rep* (2017) **7**:42500. doi:10.1038/srep42500

59. Guerra GS, Barriales D, Lorenzo G, Moreno S, Anguita J, Brun A, et al. Immunization with a small fragment of the Schmallenberg virus nucleoprotein highly conserved across the Orthobunyaviruses of the Simbu serogroup reduces viremia in SBV challenged IFNAR-/- mice. *Vaccine* (2023) **41**:3275–84. doi:10.1016/j.vaccine.2023.04.027

60. Gräf T, Delatorre E, do Nascimento Ferreira C, Rossi A, Santos HGG, Pizzato BR, et al. Expansion of Oropouche virus in non-endemic Brazilian regions: analysis of genomic characterisation and ecological drivers. *Lancet Infect Dis* (2025) **25**: 379–89. doi:10.1016/S1473-3099(24)00687-X

61. Naveca FG, Nascimento VAdo, Souza VCde, Nunes BTD, Rodrigues DSG, Vasconcelos PFd C. Multiplexed reverse transcription real-time polymerase chain reaction for simultaneous detection of Mayaro, Oropouche, and Oropouche-like viruses. *Mem Inst Oswaldo Cruz* (2017) **112**:510–3. doi:10.1590/0074-02760160062

62. Saeed MF, Nunes M, Vasconcelos PF, Travassos Da Rosa AP, Watts DM, Russell K, et al. Diagnosis of Oropouche virus infection using a recombinant nucleocapsid protein-based enzyme immunoassay. *J Clin Microbiol* (2001) **39**: 2445–52. doi:10.1128/jcm.39.7.2445-2452.2001

63. Andreolla AP, Borges AA, Nagashima S, Vaz de Paula CB, de Noronha L, Zanchin NIT, et al. Development of monoclonal antibodies against oropouche virus and its applicability to immunohistochemical diagnosis. *Virol J* (2024) **21**:81. doi:10.1186/s12985-024-02323-z

64. Tilston-Lunel NL. Oropouche virus: an emerging orthobunyavirus. *The J Gen Virol* (2024) **105**:002027. doi:10.1099/jgv.0.002027

65. Pastula DM, Beckham JD, Tyler KL. Oropouche virus: an emerging neuroinvasive arbovirus. *Ann Neurol* (2025) **97**:28–33. doi:10.1002/ana.27139

66. Tilston-Lunel N, Shi X, Elliott R, Acrani G. The potential for reassortment between oropouche and Schmallenberg orthobunyaviruses. *Viruses* (2017) **9**:220. doi:10.3390/v9080220

67. Brazilian Ministry of Health. Arbovirus monitoring panel (2025). Available online at: https://www.gov.br/saude/pt-br/assuntos/saude-de-a-a-z/a/aedes-aegypti/monitoramento-das-arboviroses (Accessed April 14, 2025).

68. Sciancalepore S, Schneider MC, Kim J, Galan DI, Riviere-Cinnamond A. Presence and multi-species spatial distribution of oropouche virus in Brazil within the one health framework. *Trop Med Infect Dis* (2022) **7**:111. doi:10.3390/tropicalmed7060111

EBM Experimental Biology and Medicine

EBM is the official journal of the Society for Experimental Biology and Medicine

Experimental Biology and Medicine (EBM) is a global, peer-reviewed journal dedicated to the publication of multidisciplinary and interdisciplinary research in the biomedical sciences.

Discover more of our Special Issues

See more →

Contact

development@ebm-journal.org

See more

ebm-journal.org

publishingpartnerships.frontiersin.org/our-partners